A novel mechanism for the anaerobic degradation of non-methane hydrocarbons in archaea

Dissertation

zur Erlangung des Doktorgrades

der Naturwissenschaften

- Dr. rer. nat. -

dem Fachbereich Geowissenschaften

der Universität Bremen

vorgelegt von

Rafael Laso Pérez

October 2018

Die vorliegende Arbeit wurde in der Zeit von August 2015 bis Oktober 2018 am Max Planck Instiut für marine Mikrobiologie angefertigt.

1. Gutachterin: Prof. Dr. Antje Boetius

2. Gutachterin: Prof. Dr. Ida Helene Steen

1. Prüfer: Prof. Dr. Kai-Uwe Hinrichs

2. Prüfer: Dr. Tristan Wagner

Tag des Promotionskolloquiums: 19.12.2018

Dedicated to my biggest supporters: mamá, papá, Juan y Pablo

"Life did not take over the world by combat, but by networking"

Lynn Margulis

Table of contents

Summary

Crude oil and natural gas are formed due to the degradation of the organic matter in deep subsurface layers. From there, they can migrate towards the sediment surface, where they represent an energy source for microbial communities. Anaerobic methanotrophic archaea (ANME) are the main responsible of anaerobic oxidation of methane in anoxic environments. For methane oxidation, they use a reversal of the methanogenesis, whose key enzyme is the methyl-coenzyme M reductase (MCR). However, little is known about the role of archaea in the anaerobic oxidation of other hydrocarbons. Apart from ANME, only three archaea are described as anaerobic hydrocarbons degraders, although the three use mechanisms of bacterial origin. The **aim of my thesis** is to shed light on the role of archaea in anaerobic hydrocarbon degradation.

In **Chapter II**, we describe a new pathway to degrade butane and propane in two archaeal strains of the newly described clade *Candidatus* Syntrophoarchaeum, which we cultivated in consortia with syntrophic partner bacteria. Using meta-omics approaches, we discovered that *Ca.* Syntrophoarchaeum use before uncharacterized divergent MCRs to activate butane and propane. The produced alkyl-CoM units are then fully oxidized using a combination of different pathways and the reducing equivalents are transferred to the partner bacteria for sulfate reduction. **Chapter III** reports about archaea harbouring similar *mcr* genes in oil seeps of the Gulf of Mexico. Archaea of the D-C06 clade were especially abundant in these environments and we could visualize them in oil droplets without any associated bacteria. Metagenomic analyses revealed that D-C06 had a machinery for alkane degradation similar to *Ca.* Syntrophoarchaeum, including a divergent *mcr* gene. Strikingly they also contained a complete methanogenesis pathway with a canonical *mcr* copy. Therefore, we hypothesize that D-C06 are degrading hydrocarbons coupled to methane production in a single cell. **Chapter IV** focuses on the physiology of *Ca.* Syntrophoarchaeum using different substrate incubations, temperature growth studies and transcriptomics. Growth was detected only on butane and propane. While two *Ca.* Syntrophoarchaeum strains were found in butane enrichments, only one was detected in the propane cultures. Analysis of the expression of *mcr* genes revealed certain links between substrates and MCR enzymes. The knowledge for culturing these anaerobic hydrocarbon-degrading organisms is summarized in a detailed protocol in **Chapter V**, which may help in the cultivation of similar archaeal clades in the future.

In summary, my thesis describes a novel pathway in archaea to degrade hydrocarbons anaerobically. The key element is highly divergent MCRs that are capable to activate multi-carbon alkanes. This constitutes a genuine archaeal mechanism, previously unknown. Genomic analyses have revealed that this pathway can be found in different archaeal clades like *Ca.* Syntrophoarchaeum or D-C06 with different lifestyles. These archaea are detected in diverse hydrocarbon-rich environments like oil and gas seeps and deep reservoirs. This indicates a so far unexplored role of these groups in hydrocarbon degradation that should be addressed in future research.

Zusammenfassung

Erdöl und Erdgas entstehen durch den Abbau organischer Stoffe in tiefen unterirdischen Schichten. Von dort können sie ins Oberflächensediment diffundieren, wo sie eine Energiequelle für mikrobielle Gemeinschaften darstellen. Anaerob methan-oxidierende Archaeen (ANME) sind die wichtigsten Abbauer von Methan in sauerstofffreien Milieus. Sie benutzen die umgekehrte Methanogenese, deren Schlüsselenzym das Methyl-Coenzym-M-Reduktase (MCR) ist. Trotzdem ist wenig bekannt über die Rolle von Archaeen in der anaeroben Oxidierung von anderen Kohlenwasserstoffen. Abgesehen von ANME werden nur drei Archaeen als Kohlenwasserstoffabbauer beschrieben, obwohl diese drei Mechanismen bakteriellen Ursprungs benutzen. Das **Ziel meiner Doktorarbeit** ist, die Rolle von Archaeen im anaeroben Kohlenwasserstoffabbau zu untersuchen.

In **Kapitel II** beschreiben wir einen neuen Stoffwechselweg für den Abbau von Butan und Propan in zwei Archaeen der neu beschriebenen Klade *Candidatus* Syntrophoarchaeum, die wir im Konsortium mit Partnerbakterien kultivierten. Mittels Meta-Omics-Verfahren entdeckten wir, dass *Ca.* Syntrophoarchaeum ungewöhnlich divergente MCRs benutzen, um Butan und Propan zu aktivieren. Die erzeugten Alkyl-CoM Einheiten werden dabei durch eine Kombination der verschiedenen Stoffwechselwege vollständig oxidiert und die Elektronen werden zur Sulfatreduktion auf die Partnerbakterien übertragen. **Kapitel III** berichtet von Archaeen aus Erdölquellen im Golf von Mexico, die ähnliche *mcr* Gene aufweisen. Archaeen der D-C06 Gruppe waren in diesem Umfeld besonders reichlich vorhanden, und wir konnten sie in Öltröpfen ohne dazugehörige Bakterien visualisieren. Metagenomische Analysen zeigten, dass D-C06 ähnliche Mechanismen für den Alkanabbau hatten wie *Ca.* Syntrophoarchaeum, wozu auch ein divergentes *mcr* Gen gehörte. Auffälligerweise enthielten sie auch einen kompletten Methanogenese-Stoffwechselweg mit einem kanonischen *mcr* Gen. Deshalb vermuten wir, dass D-C06 Kohlenwasserstoffe bei gleichzeitiger Methanproduktion in einer einzigen Zelle abbauen. **Kapitel IV** behandelt die Physiologie von *Ca.* Syntrophoarchaeum durch verschiedene Substratinkubationen-Experimenten und Transcriptomics. Wachstum wurde nur bei Butan und Propan detektiert. Während zwei Arten von *Ca.* Syntrophoarchaeum in Butan-Anreicherungen gefunden wurden, wurde in den Propan-Kulturen nur eine detektiert. Analysen der Expression von *mcr* Genen offenbarten bestimmte Verbindungen zwischen Stoffen und MCR Enzymen. Die Art der Kultivierung dieser anaerob kohlenwasserstoffabbauenden Organismen wird in einem ausführlichen Protokoll in **Kapitel V** zusammengefasst. Dieses Protokoll könnte bei der Kultivierung von ähnlichen Archaeen in der Zukunft helfen.

Zusammenfassend beschreibt meine Doktorarbeit einen neuen Stoffwechselweg in Archaeen für den anaeroben Abbau von Kohlenwasserstoffen. Das Schlüsselelement dieses Abbaus sind hoch divergente MCRs, die Alkane aktivieren können. Deshalb ist dieser Mechanismus eindeutig archaeeller Herkunft. Genomanalysen deckten auf, dass unterschiedliche archaeelle Gruppen mit

vielfältigen Lebensweisen diesen Stoffwechselweg haben, zum Beispiel *Ca.* Syntrophoarchaeum oder D-C06. Diese Archaeen sind in verschiedenen kohlenwasserstoffreichen Milieus wie Erdöl- und Erdgasquellen und in tiefen Reservoirs zu finden. Das weist auf eine bisher unerforschte Rolle dieser Gruppen im Kohlenwasserstoffabbau hin, mit der sich die zukünftige Forschung beschäftigen sollte.

Abbreviations

Acc	Acetyl-CoA Carboxylase
ACDS/CODH	Acetyl-CoA Decarbonylase:Synthase/Carbon monoxide DeHydrogenase
ANME	ANaerobic MEthanotrophic archaea
AOM	Anaerobic Oxidation of Methane
AQDS	9,10-AnthraQuinone-2,6-DiSulfonate
Ass	AlkylSuccinate Synthase
Bad	Benzoyl-CoA reductase (originally Benzoic Acid Degradation)
BES	BromoEthaneSulfonate
Bss	BenzylSuccinate Synthase
(CARD-)FISH	(CAtalysed Reporter Deposition-)Fluorescence In Situ Hybridization
CLR	Centered-Log Ratio
CoA	Coenzyme A
CoM	Coenzyme M
CoM-CoB	Coenzyme M-Coenzyme B
DAPI	4′,6′-DiAmino-2-PhenylIndole
DIET	Direct Interspecies Electron Transfer
DSS	*DesulfoSarcina/DeSulfococcus*
EBDH	EthylBenzene DeHydrogenase
Fmd	FormylMethanofuran Dehydrogenase
FPKM	Fragments Per Kilobase of transcript per Million mapped reads
Ftr	Formylmethanofuran:H_4MPT formylTRansferase
H_4MPT	tetraHydroMethanoPTerin
Hmd	methylene- H_4MPT Dehydrogenase
HRP	HorseRadish Peroxidase
MAG	Metagenome-Assembled genome
Mas	MethylAlkylsuccinate synthase
Mch	Methenyl- H_4MPT CycloHydrolase
MCM	Methylmalonyl-CoA Mutase
MCR	Methyl-Coenzyme M Reductase
Mer	MEthylene-H_4MPT Reductase
Met	MEthylenetetrahydrofolate Reductase
MMO	Methane MonoOxygenase
Mta/Mtt/Mtb	Methylcobalamin:coenzyme M methyltransferase
Mtr	Methyl-H_4MPT:CoM methylTRansferase
PCR	Polymerase Chain Reaction
pMMO	Particulate Methane MonoOxygenase
SAG	Single-cell Amplified Genome
sMMO	Soluble Methane MonoOxygenase
SMTZ	Sulfate-Methane Transition Zone
SRB	Sulfate-Reducing Bacteria

Chapter I

Introduction

1.1 Hydrocarbons: chemistry, formation and occurrence

Hydrocarbons are molecules formed exclusively by carbon and hydrogen atoms linked with covalent bonds (Wilkes and Schwarzbauer, 2010). Depending on the kind of bonds between the carbon atoms, hydrocarbons can be classified as aliphatic or aromatic. Aliphatic hydrocarbons include alkanes, alkenes and alkynes. They may be linear, branched or cyclic, but are non-aromatic Alkanes are hydrocarbons where all atoms are linked through single bonds. The carbon atoms are connected by hybrid orbitals sp^3 linked with σ bonds (Morrison and Boyd, 1992). They are also referred to as saturated hydrocarbons, since each carbon cannot accept more hydrogen atoms. When alkanes are linear, they are noted as *n*-alkanes. By contrast, alkenes and alkynes are unsaturated hydrocarbons that contain at least one double or triple carbon-carbon bond respectively, which can accept additional hydrogen atoms. Double bonds are formed by one hybrid orbital sp^2 and one p orbital per carbon atom, while triple bonds consist of one hybrid orbital sp and two p orbitals per carbon atom. While the hybrid orbitals are linked with σ bonds, the p orbitals are associated with π bonds (Morrison and Boyd, 1992).

Aromatic hydrocarbons are characterized by a ring of resonance bonds, which confers additional properties, termed as aromaticity (Morrison and Boyd, 1992, Wilkes and Schwarzbauer, 2010). They have at least one planar cycle, where the carbon atoms are connected by σ bonds of the hybrid orbitals sp^2, while the p orbitals form π bonds that are delocalized in the ring (Morrison and Boyd, 1992). The simplest aromatic compound is benzene (C_6H_6), which consists of only one aromatic ring. Polycyclic aromatic hydrocarbons are formed by the union of several aromatic rings and the simplest molecule is naphthalene formed by two (Wilkes and Schwarzbauer, 2010). Aromatic compounds can possess additionally branched chains of aliphatic compounds like in the cases of toluene (or methylbenzene) and ethylbenzene.

The different hydrocarbon groups have different properties derived from their bonding and structure. Because of their covalent bonds, hydrocarbon molecules interact with each other through van der Waals forces, or in some cases trough dipole-dipole interactions, but these forces are relatively weak (Morrison and Boyd, 1992, Wilkes and Schwarzbauer, 2010). This causes that hydrocarbons are

hydrophobic, nonpolar and relatively inert molecules. However, there are differences among the various groups. Alkanes, alkenes and alkynes have low melting and boiling points, which increase with the molecular size (Morrison and Boyd, 1992). Under standard conditions, short-chain alkanes (C_1-C_4) are gases, medium-chain alkanes (C_5-C_{17}) are in liquid state and longer alkanes appear as solids (Morrison and Boyd, 1992). Alkanes are the most inert hydrocarbons, as they only have σ bonds, while alkenes and alkynes have a higher reactivity due to the π bond(s). The reason is that these bonds have an elevated electron density more susceptible of electrophilic attacks (Morrison and Boyd, 1992). Aromatic hydrocarbons are more stable as expected due to their planar structure with resonance bonds, which confers them a really low reactivity, because the π electrons are delocalized in their ring (Morrison and Boyd, 1992, Wilkes and Schwarzbauer, 2010). They have a higher melting and boiling point compared to the equivalent hydrocarbons of similar molecular mass (Morrison and Boyd, 1992).

Geological formation of hydrocarbons

Hydrocarbons are estimated to be among the most abundant organic compounds on Earth, with estimates of up to 10^{12} tons of C in subsurface deep reservoirs (Tissot and Welte, 1984) and 10^{12}-10^{13} tons of C as gas hydrates (Reeburgh, 2007). Some of this carbon pool can be from a biological origin, for example large amounts of methane are generated as metabolic product by methanogenic archaea in anoxic environments (Reeburgh, 2007). Hydrocarbons are also formed through geological processes due to the degradation of the organic matter forming petroleum, coal or natural gas. These processes are based on the degradation, burial and transformation of the organic matter by high pressure and temperatures (Tissot and Welte, 1984).

Petroleum forms in the seabed from organic matter deposits, which are formed due to the accumulation over geological timescales of organic material exported from the surface ocean. According to Tissot and Welte (1984), there are three stages in petroleum formation: diagenesis, catagenesis and metagenesis. Diagenesis starts with the burial and microbial degradation of the deposited organic matter (Tissot and Welte, 1984). In the upper sediment layers microorganisms use oxygen as final electron acceptor, while in deeper anoxic layers the degradation is coupled to reduction of nitrate, iron (III), manganese (IV), sulfate and finally CO_2 (Canfield, 1993, Canfield and Thamdrup, 2009). Many complex organic molecules cannot be mineralized and will become kerogen by condensation and expulsion of water (Tissot and Welte, 1984). Kerogen is a complex mixture of organic polymers present in the sedimentary rock. Catagenesis starts as burial depth increases. High pressures and elevated temperatures (50-150 °C) provoke a degradation of the kerogen that will generate most of the hydrocarbons, first in the form of oil and then as natural gas (Tissot and Welte, 1984). Petroleum may migrate from the source rock until reaching an impermeable rock layer, where it accumulates. Due to its lower density, natural gas is located over the oil in these reservoirs. Metagenesis only occurs at greater depths where the residual organic matter undergoes

transformations prior to metamorphism. Methane is the only hydrocarbon produced at this stage (Tissot and Welte, 1984).

Petroleum (or crude oil) consists of different components, mainly hydrocarbons with a relatively small fraction of resins, asphaltenes and other low weight compounds. Hydrocarbons represent 86% of the crude oil on average. The majority are alkanes (roughly 33% *n*- and *iso*-alkanes, and 32% cycloalkanes) and the rest are almost exclusively aromatic hydrocarbons (around 34-35%) (Tissot and Welte, 1984). Alkenes have been detected in some oils but represent usually a minor share of the total composition (Curiale and Frolov, 1998). Resins and asphaltenes are complex mixtures of large organic molecules formed by polyaromatic units that include nitrogen, oxygen and/or sulfur atoms (Tissot and Welte, 1984). There are several classifications of crude oil depending on their composition, commercial interest or geological aspects. Crude oils with high content (>50%) of alkanes are named paraffinic or naphthenic oils depending on the predominance of acyclic alkanes or cycloalkanes respectively. They are non- or little degraded and have low sulfur content. Aromatic oils are those with alkane content lower than 50%. The lower the alkane content, especially for *n*-alkanes, the more degraded is the oil. In heavy-degraded oils, aromatic hydrocarbons are also degraded and the share of resins and asphaltenes increases. Sulfur is also much more abundant in these degraded crude oils (Tissot and Welte, 1984). Natural gas produced during the catagenesis is mostly composed of methane. However, other components might be present like short-chain gaseous alkanes (C_2-C_4), CO_2, N_2, H_2 or H_2S. These substances are present in different proportions depending on the original material, the catagenesis conditions and the migration process (Tissot and Welte, 1984).

Marine hydrocarbon-rich environments

Deep reservoirs located in the oceanic and continental crust harbour enormous amounts of oil and gas (**Figure 1**). Conditions in these reservoirs are usually more favourable for microorganisms compared to the original source rock, for instance temperatures are much lower (Tissot and Welte, 1984). Therefore, microbial hydrocarbon degradation can become an important factor influencing the composition of the accumulated crude oil. Methanogenic degradation of hydrocarbons is thought to be the main microbial process, since sulfate and other electron acceptors are usually not available in these environments (Aitken*, et al.*, 2004, Dolfing*, et al.*, 2007, Jones*, et al.*, 2007). As a consequence, some reservoirs contain heavy degraded oil deposits largely depleted of alkanes and aromatic compounds. In fact, such reservoirs, like the Orinoco oil belt (Venezuela), are the largest petroleum deposits on Earth (Dolfing*, et al.*, 2007).

Hydrocarbons produced in deep layers can migrate into surface sediments and be introduced into the water column in different ways. Cold seeps are nature oil and gas seepage sites primarily found along continental margins (**Figure 1**). Globally, cold seeps are estimated to emit around 6×10^5 tons of oil per year, which accounts for 47% of the total crude oil that enters the ocean (Kvenvolden

and Cooper, 2003). The source of their hydrocarbon-rich fluids is diverse: from dozens of meters to reservoirs several kilometres deep (Suess, 2010). There are different types of cold seeps; some result from the instability of gas hydrates, which are crystalline solids where gas is trapped inside water molecules (Suess, 2010). Asphalt volcanoes are another seep example characterized by eruptions of molten asphalt, which solidifies forming large lava sheet-like deposits on the seafloor (MacDonald, *et al.*, 2004). Also mud volcanoes emit hydrocarbons, however mostly gas in the form of methane (Niemann and Boetius, 2010). Unlike "normal" volcanism, they do not erupt magmatic material, but discharge mud mixed with other fluids and gases.

Hydrocarbons are also present in the hot fluids of hydrothermal vent systems (**Figure 1**). In these systems seawater circulates through the oceanic crust under high temperatures, resulting in the discharge of hot fluids, which are enriched in reduced metals and gases (Koschinsky, 2014). Methane is the most abundant hydrocarbon in the fluids, although other alkanes might reach important concentrations owing to the thermal degradation of organic matter, as has been observed in the Guaymas Basin (Simoneit, *et al.*, 1988).

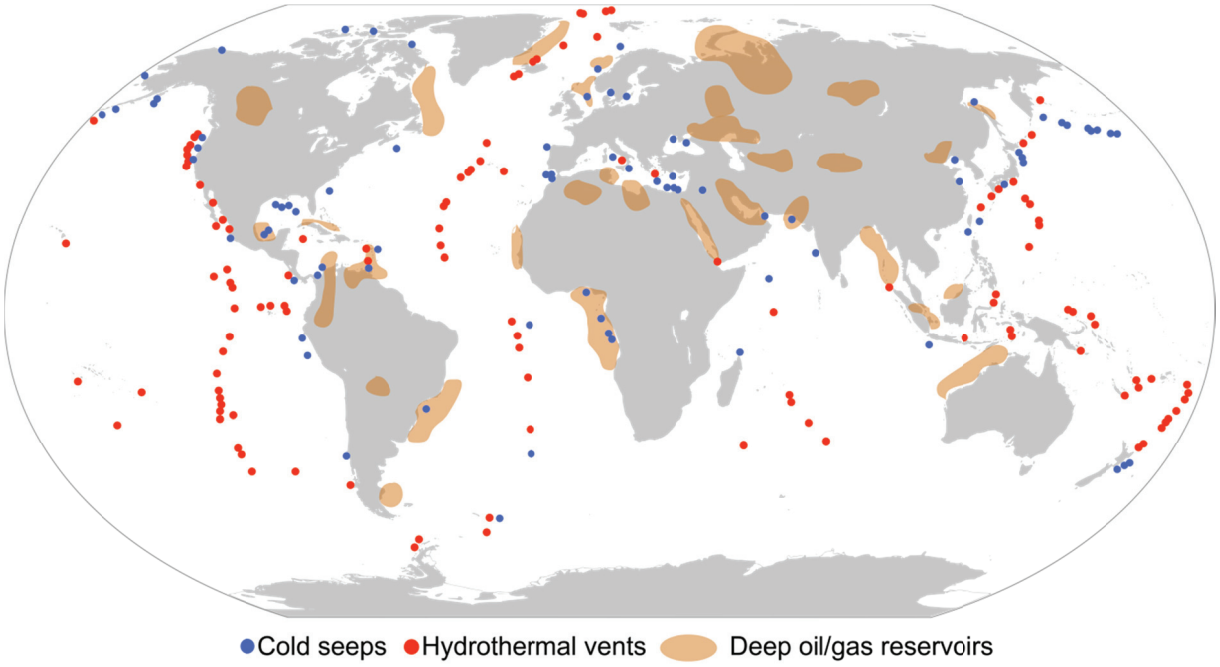

Figure 1. Global distribution of some hydrocarbon-rich environments. Cold seeps (blue circles), hydrothermal vents (red circles) and deep oil/gas reservoir areas (brown shapes) are indicated. For some hydrothermal vents, activity has only been inferred but not confirmed. Sources: US Geological Service, InterRidge Vents Database and Kleindienst (2012).

The outflowing hydrocarbons of all these systems represent a valuable energy source for different microorganisms in the deep-sea including free-living species and animal symbionts (Sibuet and Olu, 1998, Van Dover, 2000, Suess, 2010, Rubin-Blum, *et al.*, 2017). In anoxic sediments, different bacteria and archaea metabolize these hydrocarbons coupled to the reduction of diverse

electron acceptors, but mainly sulfate (Teske, *et al.*, 2002, Joye, *et al.*, 2004, Orcutt, *et al.*, 2010, Kleindienst, *et al.*, 2012, Ruff, *et al.*, 2015, Dowell, *et al.*, 2016). This results in the formation of large amounts of sulfide, which fuels microbial mats in the sediment surface (Nelson, *et al.*, 1989, Gundersen, *et al.*, 1992, Suess, 2010).

Importance of hydrocarbons in the current society

As fossil fuels, hydrocarbons have been the primary energy source for modern society in the last centuries, still representing the main energy commodity (World Energy Council, 2016). Additionally, many products such as plastics, solvents, waxes and oil are produced from petroleum derivatives. Since hydrocarbons are a finite resource, numerous studies tried to optimize or improve the different steps during hydrocarbon drilling, transport and management. For instance, understanding of the degradation of crude oil in the *in situ* reservoirs could help to increase the recovery during petroleum drilling (Dolfing, *et al.*, 2007, Head, *et al.*, 2010). Bioremediation using hydrocarbon-degrading organisms is also intensively studied to reduce the environmental impacts of oil spills (Röling, *et al.*, 2004, Head, *et al.*, 2006). Hydrocarbons also have an important impact in the global climate, as atmospheric methane has a warming effect 25 times higher than CO_2 (IPCC, 2014). Microbial degradation of hydrocarbons can also contribute in the mitigation of these problems. For example, natural microbial communities quickly consumed large amounts of methane that were released after the Deepwater Horizon accident (Kessler, *et al.*, 2011). Methanotrophic-oxidizing archaea play also a fundamental role in the anaerobic oxidation of methane (AOM) in marine sediments, consuming up to 80-90% of the 8.5×10^7 tons of CH_4 produced annually in this environment (Hinrichs and Boetius, 2003, Reeburgh, 2007). Therefore, it is essential to understand the microbial mechanisms for hydrocarbon degradation. Aerobic degradation has been studied since the beginning of the 20th century, while the systematic research on anaerobic processes started at the end of the 20th century. Most of this research has focused on bacteria. With the exception of AOM, the role and mechanisms of archaea in anaerobic hydrocarbon degradation remain largely unknown.

1.2 Aerobic hydrocarbon degradation

Aerobic degradation of hydrocarbons is known since the beginning of the 20th century (Söhngen, 1913) with reports of this process not only in bacteria (Watkinson and Morgan, 1991, Van Hamme, *et al.*, 2003, Abbasian, *et al.*, 2015), but also in archaea (Tapilatu, *et al.*, 2010) and eukaryotes like some fungi (Iida, *et al.*, 2000, Schmitz, *et al.*, 2000, Duetz, *et al.*, 2003). Research has focused mostly on *n*-alkanes and aromatic compounds but microbial degradation of branched alkanes, cycloalkanes and alkenes has also been shown (Fuchs, *et al.*, 2011, Abbasian, *et al.*, 2015).

Microorganisms involved in aerobic hydrocarbon degradation

Numerous microorganisms can degrade hydrocarbons under aerobic conditions, most of them bacteria, where this potential is widespread among diverse phyla such as *Proteobacteria, Bacteroidetes*, *Firmicutes* or *Actinobacteria* (Engelhardt, *et al.*, 2001, Syutsubo, *et al.*, 2001, Head, *et al.*, 2006, Toda, *et al.*, 2012). The majority of the described hydrocarbon-degrading organisms belong to the phylum *Proteobacteria*. For instance, different obligate hydrocarbon-degraders are present within *Gammaproteobacteria* like *Alkanivorax*, *Cycloclasticus* or *Oleophilus* (Dyksterhouse, *et al.*, 1995, Golyshin, *et al.*, 2002, Yakimov, *et al.*, 2007). Moreover, *Gammaproteobacteria* class includes also members of *Pseudomonas* that served as model organism in aerobic hydrocarbon degradation (van Beilen, *et al.*, 1994, van Beilen, *et al.*, 1994) and type I methanotrophs like *Methylococcus* and *Methylomona* (Hanson and Hanson, 1996, Murrell, *et al.*, 2000). Instead, type II methane-oxidizers like *Methylocistis* or *Methylosinus* affiliate to the class *Alphaproteobacteria* (Hanson and Hanson, 1996, Murrell, *et al.*, 2000). Other groups of *Alphaproteobacteria* can degrade longer alkanes or aromatic compounds like certain species of *Sphingomonas* (Zylstra and Kim, 1997, Story, *et al.*, 2001). Among the hydrocarbon-degrading genera of *Betaproteobacteria* stand out *Burkholderia* (Kim, *et al.*, 2003), *Alcaligenes* (Foss, *et al.*, 1998) or *Polaromonas* (Pumphrey and Madsen, 2007). Besides, some aerobic hydrocarbon-degrading archaea have been isolated from hypersaline environments. They are halophilic members from the genera *Haloferax, Haloarcula, Halobacterium* and *Halococcus* within the *Halobacteria* class (Bertrand, *et al.*, 1990, Al-Mailem, *et al.*, 2010, Tapilatu, *et al.*, 2010, Fathepure, 2014). They are able to degrade *n*-alkanes and aromatic compounds (Bertrand, *et al.*, 1990, Al-Mailem, *et al.*, 2010, Tapilatu, *et al.*, 2010).

Enzymes and mechanisms involved in the aerobic degradation of hydrocarbons

The key aspect in aerobic hydrocarbon degradation is the incorporation of oxygen into the hydrocarbon molecule yielding an alcohol (Watkinson and Morgan, 1991, Fuchs, *et al.*, 2011, Abbasian, *et al.*, 2015). This step is catalysed by monooxygenases or dioxygenases, which incorporate one or two oxygen atoms into the hydrocarbon molecules (Fuchs, *et al.*, 2011). The resulting alcohol is then transformed for further oxidation or biomass formation (Watkinson and Morgan, 1991, Fuchs, *et al.*, 2011).

Alkanes

Aerobic degradation is demonstrated for *n*-alkanes (Abbasian, *et al.*, 2015), branched substrates (Nhi-Cong, *et al.*, 2009) and cycloalkanes (Kostichka, *et al.*, 2001, Cheng, *et al.*, 2002). The degradation of *n*-alkanes is a well-studied process with three main mechanisms relying on monooxygenases. In the terminal oxidation, the monooxygenase hydroxylates the terminal carbon producing a primary alcohol that will be stepwise oxidized to the corresponding fatty acid, which then is metabolized in the

β-oxidation pathway (Watkinson and Morgan, 1991, Van Hamme, *et al.*, 2003, Abbasian, *et al.*, 2015). The biterminal oxidation or ω-oxidation is a variant from the previous one in which the produced fatty acid is subsequently hydroxylated by monooxygenases in the other terminal end, ω-position (Watkinson and Morgan, 1991, Coon, 2005). Further oxidation yields a dicarboxylic acid that enters the β-oxidation as well. The third pathway is the subterminal oxidation, in which the subterminal carbon is activated forming a secondary alcohol (Forney and Markovetz, 1970, Kotani, *et al.*, 2003).

There are several enzymes catalysing the initial activation step. AlkB is a terminal monooxygenase of the well characterized Alk system present in *Pseudomonas oleovorans* (Baptist, *et al.*, 1963, van Beilen, *et al.*, 1994), which activates C_3-C_{13} alkanes at the terminal position (van Beilen, *et al.*, 1994, Johnson and Hyman, 2006). Homologues of this enzyme are found in other bacteria, where they seem to preferentially oxidize alkanes larger than C_{10} (Van Beilen, *et al.*, 2004, Throne-Holst, *et al.*, 2007, Rojo, 2010). Some cytochromes P450 act as terminal monooxygenases responsible for the activation of medium-chain alkanes in bacteria like in some members of the genera *Acinetobacter* (Asperger, *et al.*, 1981, Maier, *et al.*, 2001) or *Mycobacterium* (Funhoff, *et al.*, 2006). For longer alkanes, an alkane monooxygenase (LadA) was isolated from *Geobacillus thermodenitrificans* (Wang, *et al.*, 2006, Li, *et al.*, 2008). LadA is able to activate C_{15}-C_{36} alkanes Another enzyme, AlmA, has also been reported in some *Acinetobacter* degrading long-chain alkanes (C_{20}-C_{32}) (Throne-Holst, *et al.*, 2007). In other *Acinetobacter* strains, a novel pathway was discovered involving dioxygenases instead of monooxygenases (Sakai, *et al.*, 1996, Ji, *et al.*, 2013). Here, long-chain alkanes (C_{13}-C_{44}) are oxidized to hydroperoxides by dioxygenases and then further transformed to fatty acids (Sakai, *et al.*, 1994, Sakai, *et al.*, 1996, Ji, *et al.*, 2013).

A special mention must be done for aerobic oxidation of methane. The main enzyme is the methane monooxygenase (MMO), which oxidizes methane to methanol (Hanson and Hanson, 1996, Murrell, *et al.*, 2000). Subsequently, methanol can be fully oxidized or assimilated as formaldehyde (Hanson and Hanson, 1996, Murrell, *et al.*, 2000). MMO is classified in two main groups: particulate MMO (pMMO) that is membrane-bound and soluble MMO (sMMO) that is cytoplasmic (Hanson and Hanson, 1996, Murrell, *et al.*, 2000). pMMO is present in all aerobic methanotrophic bacteria and can also oxidize short-chain alkanes like propane, butane and pentane (Elliott, *et al.*, 1997, Murrell, *et al.*, 2000, Chan, *et al.*, 2004). For organisms containing both enzymes, the concentration of copper ions in the medium was proposed to regulate their expression (Stanley, *et al.*, 1983, Prior and Dalton, 1985, Murrell, *et al.*, 2000).

Other hydrocarbons

Aerobic degradation has been reported for many aromatic hydrocarbons including benzene, naphthalene, phenanthrene or anthracene (Cao, *et al.*, 2009). The process starts with the hydroxylation with O_2 by mono- or dioxygenases and a further conversion to central intermediates like catechol (Van Hamme, *et al.*, 2003, Cao, *et al.*, 2009, Fuchs, *et al.*, 2011, Pérez-Pantoja, *et al.*, 2016). Afterwards,

ring cleavage is carried out by dioxygenases producing a dicarboxylic acid or hydroxyl semialdehydes, which are transformed into metabolites of the central metabolism (Fuchs, *et al.*, 2011, Pérez-Pantoja, *et al.*, 2016). Alkenes are often degraded by the action of a monooxygenase that introduces an oxygen atom into the double bond producing an epoxide (Abbasian, *et al.*, 2015). Two types of monooxygenases are described depending on their active centers: those with di-iron centres (Smith, 2009) and those with flavin centres (Toda, *et al.*, 2012, Abbasian, *et al.*, 2015).

Environmental role of aerobic hydrocarbon-degrading microorganisms

A lot of interest in the ecology of aerobic hydrocarbon-degrading organisms has been raised because of their potential use in bioremediation strategies (Atlas and Bartha, 1972, MacNaughton, *et al.*, 1999, Röling, *et al.*, 2002, Head, *et al.*, 2006). Studies have shown that these organisms are usually not abundant or detectable in certain habitats, but they become dominant members of the community after a hydrocarbon pollution event. For instance, *Alcanivorax* dramatically increased its relative abundance in seawater amended with oil or in microcosms experiments (Syutsubo, *et al.*, 2001, Kasai, *et al.*, 2002, Röling, *et al.*, 2002). They are the first colonizers in the oil-affected substrates and play a central role in the degradation of alkanes in oil-polluted beaches (Röling, *et al.*, 2002, Röling, *et al.*, 2004). By contrast, *Cycloclasticus* degrades aromatic hydrocarbons (Geiselbrecht, *et al.*, 1998, Kasai, *et al.*, 2002) and tends to appear later than *Alcanivorax,* when the alkane fraction is already largely depleted (Kasai, *et al.*, 2002, Kasai, *et al.*, 2002). The degradation process is not only dependent on single species but also on a complex network of interactions that includes production of surfactants to increase the oil readiness (Iwabuchi, *et al.*, 2002) or predation for nutrient recycling (Mattison and Harayama, 2001, Head, *et al.*, 2006). Additionally, nitrogen and phosphorus can be critical limiting factors during the degradation process (Atlas and Bartha, 1972, Kasai, *et al.*, 2002, Röling, *et al.*, 2002).

Based on laboratory studies, archaea are negatively affected by oil contamination in beaches, and they are not considered to play a major role in the hydrocarbon degradation (Röling, *et al.*, 2004). Consequently, they were proposed as biomarkers for ecosystem recovery (Head, *et al.*, 2006). Nonetheless, several halophilic hydrocarbon-degrading archaea have been isolated from hypersaline environments (Bertrand, *et al.*, 1990, Al-Mailem, *et al.*, 2010, Tapilatu, *et al.*, 2010), where they might carry out most of the oil mineralization after oil seepage according to some studies (Al-Mailem, *et al.*, 2012, Fathepure, 2014).

The disaster of the *Deepwater Horizon* represented a unique example to study the environmental function of these microorganisms (Hazen, *et al.*, 2010, Mason, *et al.*, 2012, King, *et al.*, 2015). Interestingly, the different studies showed that *Alcanivorax* was a dominant clade in the oil-affected sands (Kostka, *et al.*, 2011) but not in the planktonic environments where an oil plume was present (King, *et al.*, 2015), even though it was detected in water samples before the spill (King, *et al.*,

2013). Instead, the plume was dominated by members of *Oleospira, Cyloclasticus* and *Colwellia* (Hazen, *et al.*, 2010, Mason, *et al.*, 2012, King, *et al.*, 2015). Moreover, there was a strong response of the aerobic methanotrophic community that consumed almost all the released methane (Kessler, *et al.*, 2011).

1.3 Anaerobic hydrocarbon degradation

Anaerobic degradation of hydrocarbons in bacteria

Anaerobic degradation of hydrocarbon was already suggested based on environmental observations more than 70 years ago (Zobell, 1946, Muller, 1957, Kuhn, *et al.*, 1985). However, the process was not systematically studied, since the low reactivity of hydrocarbons favoured the view that hydrocarbons are not biodegradable under anoxic conditions (Gibson, 1984, Widdel and Rabus, 2001). By contrast, two organisms performing anaerobic oxidation of toluene were finally isolated in 1990: the denitrifying *Pseudomonas* sp. strain T later renamed as *Azoarcus* (Dolfing, *et al.*, 1990, Krieger, *et al.*, 1999) and the iron-reducing bacterium GS-15 (Lovley and Lonergan, 1990) later classified as *Geobacter metallireducens* (Lovley, *et al.*, 1993).

The deltaproteobacterium strain Hxd3 was the first bacterium shown to degrade alkanes, concretely *n*-hexadecane (Aeckersberg, *et al.*, 1991). Afterwards, more anaerobic bacteria have been reported to degrade *n*-alkanes with carbon chains between C_3-C_{20} (Aeckersberg, *et al.*, 1991, So and Young, 1999, Davidova, *et al.*, 2005, Callaghan, *et al.*, 2006, Kniemeyer, *et al.*, 2007) and also branched and cyclic alkanes (Bregnard, *et al.*, 1997, Grossi, *et al.*, 2000, Musat, *et al.*, 2010, Jaekel, *et al.*, 2015).

Bacteria can perform alkane degradation under nitrate-reducing (Bregnard, *et al.*, 1997, Ehrenreich, *et al.*, 2000, Musat, *et al.*, 2010), sulfate-reducing (Aeckersberg, *et al.*, 1991, So and Young, 1999, Callaghan, *et al.*, 2006) or methanogenic conditions (Zengler, *et al.*, 1999, Cheng, *et al.*, 2013). Methane is not metabolized by bacteria under anoxic conditions with the exception of *Candidatus* Methylomirabilis oxyfera, an anaerobic nitrite-reducing bacterium that presumably uses intracellular oxygen, produced during nitrite reduction, to oxidize methane in the canonical aerobic pathway (Ettwig, *et al.*, 2010). In the anaerobic degradation of aromatic compounds, alkyl-substituted compounds are considered easier to degrade than their unsubstituted counterparts (Widdel, *et al.*, 2010). Anaerobic degradation is described for several alkyl-substituted aromatic hydrocarbons like the model substrate toluene (Dolfing, *et al.*, 1990, Lovley and Lonergan, 1990, Rabus, *et al.*, 1993), ethylbenzene (Rabus and Widdel, 1995) or methylnaphthalene (Annweiler, *et al.*, 2000). Nonetheless, degradation of unsubstituted aromatic compounds is also described, like in the cases of benzene (Wilson, *et al.*, 1986, Edwards and Grbić-Galić, 1992, Botton and Parsons, 2007), naphthalene (Coates, *et al.*, 1996, Chang, *et al.*, 2006, Mouttaki, *et al.*, 2012) and phenanthrene (Zhang

and Young, 1997, Chang, *et al.*, 2006). Degradation of these compounds is coupled to the reduction of nitrate (Dolfing, *et al.*, 1990, Coates, *et al.*, 2001), iron (III) (Lovley and Lonergan, 1990, Zhang, *et al.*, 2013), manganese (IV) (Villatoro-Monzón, *et al.*, 2008) and sulfate (Rabus, *et al.*, 1993, Zhang and Young, 1997, Annweiler, *et al.*, 2000) as well as to syntrophic methanogenesis (Wilson, *et al.*, 1986, Edwards and Grbić-Galić, 1994, Chang, *et al.*, 2006).

Fewer studies have investigated anaerobic bacteria degrading alkenes or alkynes. They revealed that bacteria can degrade alkenes like squalene and hexadecane under sulfate-reducing, nitrate-reducing and methanogenic conditions (Schink, 1985, Aeckersberg, *et al.*, 1991, Rontani, *et al.*, 2002, Grossi, *et al.*, 2011). For alkynes, acetylene degradation under anaerobic conditions has been demonstrated for *Pelobacter acetylenicus* (Schink, 1985).

Phylogenetic affiliation of anaerobic hydrocarbon-degrading bacteria

Most anaerobic hydrocarbon-degrading bacteria are affiliated to the classes *Beta-* and *Deltaproteobacteria* (Widdel, *et al.*, 2010). The hydrocarbon-degrading *Betaproteobacteria* are denitrifiers, usually degrading aromatic compounds (Widdel, *et al.*, 2010). They are classified in two closely related genera within the family *Rhodocyclaceae*: *Azoarcus* (Krieger, *et al.*, 1999) and *Thauera* (Rabus and Widdel, 1995). Hydrocarbon-degrading *Deltaproteobacteria* usually couple the process to sulfate reduction, although coupling to iron reduction and methanogenesis with syntrophic archaea has been observed too (Widdel, *et al.*, 2010). They are distributed in different clades including genera like *Desulfosarcina* (Harms, *et al.*, 1999), *Desulfatiferula* (Grossi, *et al.*, 2011), *Desulfatibacillum* (Cravo-Laureau, *et al.*, 2004), *Desulfobacula* (Rabus, *et al.*, 1993), *Pelobacter* (Schink, 1985), *Desulfoglaeba* (Davidova, *et al.*, 2006) and *Geobacter* (Lovley, *et al.*, 1993).

More rarely anaerobic hydrocarbon degradation has been reported for members of *Gammaproteobacteria*, *Alphaproteobacteria* or *Firmicutes*. For these clades, mostly enrichments are described (Widdel, *et al.*, 2010), although some members have been isolated such as the gammaproteobacteria *Pseudomonas* sp. NAP-3-1 and *Vibrio pelagicus* (NAP-4) (Rockne, *et al.*, 2000), *Desulfotomaculum* sp. (OX39) affiliated to *Firmicutes* (Morasch, *et al.*, 2004) or the alphaproteobacterium *Blastochloris sulfoviridis* strain ToP1 (Zengler, *et al.*, 1999). The unique oxygenic methane-oxidizing bacterium *Candidatus* Methylomirabilis oxyfera is affiliated to the phylum NC10 (Ettwig, *et al.*, 2010).

Enzymatic mechanisms in the anaerobic degradation of hydrocarbons in bacteria

Among the different bacterial pathways for anaerobic degradation of hydrocarbons (**Figure 2**), fumarate addition is the most studied. It is also the most widespread, present in denitrifying and sulfate-reducing bacteria and used for the activation of alkanes and alkyl-substituted aromatic hydrocarbons like toluene or methylnaphthalene (Rabus, *et al.*, 2016, Wilkes, *et al.*, 2016). In this pathway, a fumarate molecule is added to the hydrocarbon molecule forming an alkylsuccinate (for

alkanes) or an arylalkylsuccinate (for aromatic compounds). This reaction was originally characterized for the activation of toluene by the identification of the corresponding product benzylsuccinate (Beller, *et al.*, 1992, Evans, *et al.*, 1992) and the isolation of responsible enzyme, benzylsuccinate synthase (Bss) (Leuthner, *et al.*, 1998). Afterwards, similar mechanisms and enzymes were identified for other aromatic compounds like 2-methylnaphthalene (Annweiler, *et al.*, 2000, Selesi, *et al.*, 2010) as well as for activation of alkanes (C_3-C_{16}) (Kropp, *et al.*, 2000, Rios-Hernandez, *et al.*, 2003, Cravo-Laureau, *et al.*, 2004, Kniemeyer, *et al.*, 2007). For alkanes, the responsible enzymes are called methylalkylsuccinate synthases (Mas) (Grundmann, *et al.*, 2008) or alkylsuccinate synthase (Ass) (Callaghan, *et al.*, 2008) and they usually perform the addition at the subterminal carbon atom (Kropp, *et al.*, 2000, Grundmann, *et al.*, 2008), although addition at the terminal carbon has been observed as well (Kniemeyer, *et al.*, 2007).

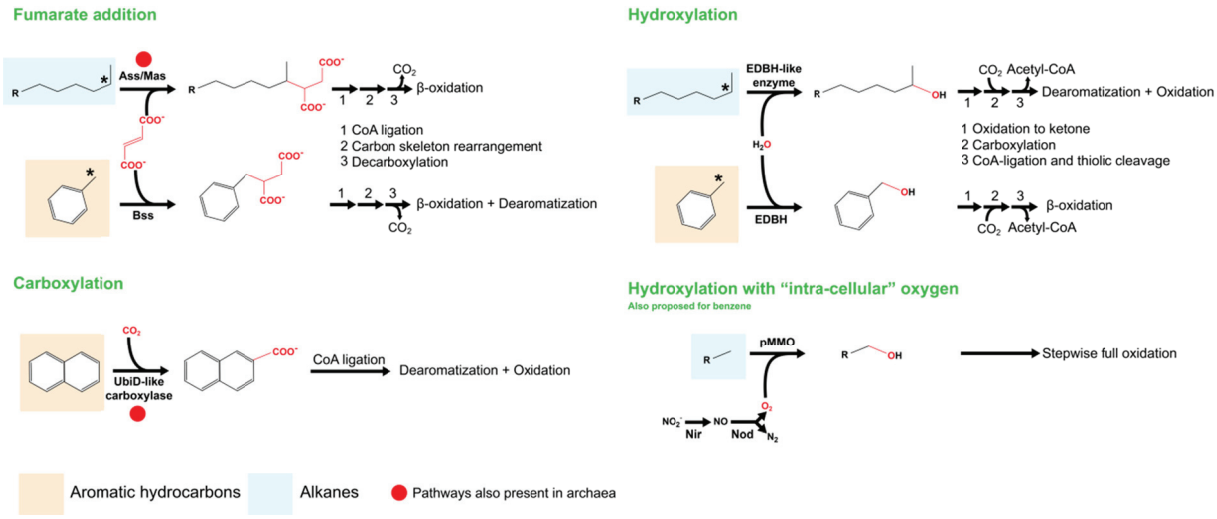

Figure 2. Pathways for anaerobic hydrocarbon degradation present in bacteria. Only pathway for alkanes (blue background) and aromatic hydrocarbons (orange background) are shown. Chemical formulas in red indicate the compounds or atoms involved in the activation. The asterisks indicate the preferential carbon for the activation. The red circles indicate which of these pathways have also been found in archaea. Hydroxylation with "intra-cellular" aerobic has been shown for methane in *Ca.* M. oxyfera and suggested for degradation of hexadecane in HdN1 bacterium and of benzene in *Dechloromonas*.

All identified succinate synthase enzymes belong to the family of glycyl radical enzymes and can be poorly distinguished based on sequence identity (Leuthner, *et al.*, 1998, Grundmann, *et al.*, 2008, Selesi, *et al.*, 2010). In genomic analyses, they are often annotated as pyruvate-formate lyase, another glycyl radical enzyme. Succinate synthase enzymes are formed by two heterotrimers. All catalytic subunits, like BssA, MasD or AssA, harbour a common amino acid motif RVXG, where G represents a conserved glycine and X can be any amino acid (Callaghan, *et al.*, 2008, Grundmann, *et al.*, 2008, Selesi, *et al.*, 2010, Funk, *et al.*, 2014). The glycine (G) generates an organic (gycyl) radical that is thought to carry out the activation step with a close cysteine residue (Funk, *et al.*, 2015, Rabus, *et al.*, 2016). After the activation, the produced alkyl-/arylalkylsuccinates are further processed.

Alkanes are proposed to be degraded in the β-oxidation pathway after coenzyme A (CoA) ligation, epimerization and decarboxylation (Wilkes, *et al.*, 2002, Davidova, *et al.*, 2005, Callaghan, *et al.*, 2006, Kniemeyer, *et al.*, 2007). Arylalkylsuccinates are further metabolized to the corresponding CoA-ligated fatty acid via a β-oxidation-resembling pathway producing benzoyl-CoA (Leuthner and Heider, 2000) or naphthoyl-CoA (Selesi, *et al.*, 2010), which are then dearomatized (Harwood, *et al.*, 1998, Selesi, *et al.*, 2010, Meckenstock, *et al.*, 2016, Rabus, *et al.*, 2016).

Hydroxylation is an alternative mechanism for the anaerobic degradation of alkyl-substituted aromatic hydrocarbons like ethylbenzene, which is present in some bacteria (Ball, *et al.*, 1996). Interestingly, ethylbenzene is also degraded through fumarate addition by sulfate-reducing deltaproteobacteria (Kniemeyer, *et al.*, 2003), whereas the hydroxylation pathway is used by denitrifying betaproteobacteria (Ball, *et al.*, 1996, Rabus and Heider, 1998). The hydroxylation pathway starts with an oxygen-independent activation of ethylbenzene to 1-phenylethanol by an ethylbenzene dehydrogenase (EBDH) using the oxygen atom from water (Ball, *et al.*, 1996). EBDH is a periplasmic enzyme formed by three subunits αβγ, being the α subunit responsible of the hydroxylation (Kniemeyer and Heider, 2001, Kloer, *et al.*, 2006). The produced 1-phenylethanol is oxidized to a ketone, carboxylated and ligated to CoA, yielding acetyl-CoA and benzoyl-CoA, which enter the corresponding metabolic pathways (Kniemeyer and Heider, 2001, Rabus, *et al.*, 2002, Jobst, *et al.*, 2010). A similar hydroxylation pathway has also been suggested for the oxidation of *n*-alkanes in the sulfate-reducing deltaproteobacterium *Desulfococcus oleovorans* Hxd3 (So, *et al.*, 2003) based on the identification of an EDBH-like complex in its genome (Callaghan, 2013).

Unsubstituted aromatic compounds can be degraded via carboxylation as shown in stable isotope experiments for naphthalene (Zhang and Young, 1997, Meckenstock, *et al.*, 2000). Candidate genes for this pathway have been identified in an operon in naphthalene- and benzene-degrading organisms, including a gene encoding a carboxylase in charge of the activation step (Abu Laban, *et al.*, 2010, DiDonato, *et al.*, 2010, Bergmann, *et al.*, 2011, Bergmann, *et al.*, 2011). This carboxylase, formed by two subunits, belongs to the UbiD family, responsible of the decarboxylation step in ubiquinone biosynthesis in *E. coli* (Cox, *et al.*, 1969). After carboxylation, the corresponding acids naphthoate and benzoate would be ligated to CoA (Abu Laban, *et al.*, 2010, Bergmann, *et al.*, 2011) and further oxidized in the corresponding dearomatizing pathways (Harwood, *et al.*, 1998, Meckenstock, *et al.*, 2016, Rabus, *et al.*, 2016).

Hydroxylation with "intra-cellular" oxygen is a recently proposed pathway, in which oxygen is produced during nitrite dismutation under anaerobic conditions and used by canonical aerobic enzymes for the degradation of an alkane molecule (Ettwig, *et al.*, 2010, Zedelius, *et al.*, 2011). This pathway was first proposed for methane oxidation by the already mentioned *Ca.* M. oxyfera (Ettwig, *et al.*, 2010). This bacterium degrades methane coupled to nitrite reduction, but lacks genes for the anaerobic methane oxidation. Instead, its genome encodes for the aerobic methane oxidation pathway including *pmo* genes (Ettwig, *et al.*, 2010). Later, the same mechanism was proposed for the

degradation of *n*-hexadecane by the denitrifying gammaproteobacterium HdN1, as this bacterium lacks genes for fumarate addition, but contains several genes encoding monooxygenases (Zedelius*, et al.*, 2011). This mechanism was also hypothesised for the degradation of benzene in *Dechloromonas* due to the lack of genes for anaerobic degradation of aromatic compounds (Salinero*, et al.*, 2009).

The mechanisms for the anaerobic degradation of alkenes are much less studied. Activation occurs (Widdel*, et al.*, 2010) either by hydration of the double bond (Schink, 1985) or by addition of an organic carbon (Grossi*, et al.*, 2007). Both are demonstrated for *Desulfatibacillum aliphaticivorans* strain CV2803, where hydration was observed in the double bond at C_1, while an unknown carbon compound was added at C_2, C_3 or at the subterminal carbon of the saturated end. The resulting compounds were further oxidized yielding linear or branched fatty acids respectively (Grossi*, et al.*, 2007).

Environmental role of anaerobic hydrocarbon-degrading bacteria

Hydrocarbons are abundant compounds in different anoxic environments including marine sediments, terrestrial soils and subsurface reservoirs. Here, anaerobic microorganisms can be main agents in hydrocarbon mineralization, as shown by various anoxic hydrocarbon-degrading enrichments established from samples derived from these habitats (Bregnard*, et al.*, 1997, Kniemeyer*, et al.*, 2007, Berdugo-Clavijo and Gieg, 2014, Jaekel*, et al.*, 2015). Bacteria have been considered the key players in this process and consequently most research has focused on them. For instance, several deltaproteobacteria from the cluster *Desulfosarcina*/*Desulfococcus* (DSS) are described as sulfate-reducing hydrocarbon degraders (Harms*, et al.*, 1999, Kniemeyer*, et al.*, 2007, Jaekel*, et al.*, 2015). Bacteria of the DSS cluster are dominant in different seeps distributed around the globe (Orphan*, et al.*, 2001, Knittel*, et al.*, 2003, Orcutt*, et al.*, 2010, Kleindienst*, et al.*, 2012) and according to stable isotope experiments, they are the main alkane degraders in marine seeps (Kleindienst*, et al.*, 2014). Other deltaproteobacteria from the family *Syntrophaceae* are proposed to play a major role in the degradation of crude oil under methanogenic conditions (Zengler*, et al.*, 1999, Kasai*, et al.*, 2005, Gray*, et al.*, 2011).

Recent studies aimed on linking ecological niche with metabolism, looking for functional marker genes in the environment. Specific primers for anaerobic hydrocarbon-degrading genes like *bssA* (Beller*, et al.*, 2002, Winderl*, et al.*, 2007, Beller*, et al.*, 2008, von Netzer*, et al.*, 2013), *assA* (Callaghan*, et al.*, 2010) and *masD* (Stagars*, et al.*, 2016) have been designed. The first study using this approach in the environment was carried out for the *bssA* gene in a tar oil-contaminated aquifer in Germany, where an unknown diversity of anaerobic toluene degraders was revealed (Winderl*, et al.*, 2007). Later studies have discovered both high and low diversity for *bssA* in different hydrocarbon-impacted sites (Callaghan*, et al.*, 2010). The search of *masD* genes in natural and contaminated marine environments discovered diverse microbial communities and suggested the existence of few cosmopolitan *masD* groups coexisting with a variety of endemic *masD* representatives depending on

the site conditions (Gittel, *et al.*, 2015, Johnson, *et al.*, 2015, Stagars, *et al.*, 2016). Interestingly, these genes have even been detected in non-hydrocarbon related environments like in a pristine lake in Sweden. Here, a novel lineage of *bssA* genes was found, what points out that the potential for hydrocarbon degradation could be more widespread as previously thought (Osman, *et al.*, 2014). In line with this idea, recent research evaluated the microbial response to petroleum seepage in Caspian Sea sediments revealing that *masD* genes could only be amplified in oil-treated sediments (Stagars, *et al.*, 2017).

Anaerobic oxidation of methane in archaea

Organisms involved in the anaerobic oxidation of methane

Anaerobic oxidation of methane (AOM) is performed by anaerobic methanotrophic archaea (ANME) of the phylum *Euryarchaeota,* which are clustered in three different groups: ANME-1, ANME-2 and ANME-3 (Knittel and Boetius, 2009). ANME-1 forms a distinct cluster close to the *Methanomicrobiales* (Hinrichs, *et al.*, 1999), while ANME-2 and -3 are located within the *Methanosarcinales* (Orphan, *et al.*, 2001, Knittel, *et al.*, 2005). Distinct subgroups are described for ANME-1 (a, b) and ANME-2 (a, b, c and d) (Orphan, *et al.*, 2001, Mills, *et al.*, 2003, Knittel, *et al.*, 2005). ANME are usually forming syntrophic consortia with partner sulfate-reducing bacteria (SRB) typically related to the *Deltaproteobacteria* (Boetius, *et al.*, 2000, Orphan, *et al.*, 2001, Michaelis, *et al.*, 2002, Knittel, *et al.*, 2005). ANME-1 and ANME-2 have been detected in psychrophilic and mesophilic environments associated to bacteria of the groups Seep-SRB-1a and Seep-SRB-2, both within the DSS cluster (Knittel, *et al.*, 2003, Knittel, *et al.*, 2005, Kleindienst, *et al.*, 2012, Krukenberg, *et al.*, 2018). Instead, ANME-3 was mostly found in consortia with *Desulfobulbus* bacteria at cold temperatures (Niemann, *et al.*, 2006). Additionally, thermophilic ANME-1 are reported in association with SRB of the HotSeep-1 cluster (Holler, *et al.*, 2011), a sister lineage of the *Deltaproteobacteria* (Krukenberg, *et al.*, 2016). Occasionally, other bacteria, like *Sphingomonas* (*Alphaproteobacteria*) and *Burkholderia* (*Betaproteobacteria*), have been discovered in consortia with ANME (Pernthaler, *et al.*, 2008). Besides ANME-1 have been detected without apparent partner bacteria as single cells, cell chains or monospecies consortia (Orphan, *et al.*, 2002). ANME-2d, also referred to as *Candidatus* Methanoperedens, represents the only ANME clade performing AOM coupled to the reduction of nitrate (Haroon, *et al.*, 2013, Hu, *et al.*, 2015), iron (Ettwig, *et al.*, 2016, Cai, *et al.*, 2018) or manganese (Ettwig, *et al.*, 2016), without an apparent need of a partner. However, they are frequently detected in association with nitrite-reducing or anammox bacteria like *Ca.* M. oxyfera and *Candidatus* Kuenenia stuttgartiensis (Haroon, *et al.*, 2013, Hu, *et al.*, 2015).

Reverse methanogenesis pathway

All ANME archaea catalyse the complete oxidation of methane to CO_2 through a reversal of the methanogenesis pathway (**Figure 3**) as suggested by metagenomic and metatranscriptomic studies (Hallam*, et al.*, 2004, Meyerdierks*, et al.*, 2010, Stokke*, et al.*, 2012, Haroon*, et al.*, 2013, Wang*, et al.*, 2013, Krukenberg*, et al.*, 2018). The key enzyme of the pathway is the methyl-coenzyme M reductase (MCR), which is a 300 kDa hexameric enzyme, consisting in two equal heterotrimers ($\alpha_2\beta_2\gamma_2$) and two non-covalently bound molecules of a nickel porphinoid coenzyme F_{430} (Ermler*, et al.*, 1997). Two coenzymes F_{430} have been found in ANME: one of 905 kDa present in ANME-2 and similar to the one of methanogens, and a modified one of 951 kDa exclusive of ANME-1 (Krüger*, et al.*, 2003). In AOM, MCR binds methane as a methyl group to coenzyme M (CoM) by reducing the heterodisulfide coenzyme M-coenzyme B (CoM-CoB)(Shima*, et al.*, 2011). The catalytic mechanism of MCR is not completely understood, although a recent study reported that the Ni atom of the cofactor F_{430} plays a fundamental role in the methane formation reaction by generation of a Ni(II)-thiolate with the CoM (Wongnate*, et al.*, 2016). Crystal structures of different MCRs have revealed several posttranslational modifications that are considered essential for the MCR functioning (Ermler*, et al.*, 1997, Shima*, et al.*, 2011). One of them is a thioglycine present in the active site of the MCR and proposed to be implicated in the catalytic mechanism because it is conserved among all MCRs (Grabarse*, et al.*, 2001, Horng*, et al.*, 2001, Goenrich*, et al.*, 2005).

In AOM, after the methane activation, the methyl group is transferred from CoM to tetrahydromethanopterin (H_4MPT) by a methyl-H_4MPT-CoM methyltransferase (Mtr). This is a membrane-bound Na^+-translocating enzyme composed of eight subunits (Hippler and Thauer, 1999). The released CoM is used to regenerate the disulfide CoM-CoB by heterodisulfide reductase complexes. Afterwards, the methyl-H_4MPT is oxidized to 5,10-methylene-H_4MPT. In ANME-2, this step is performed by a methylene-H_4MPT reductase (Mer) (Haroon*, et al.*, 2013, Wang*, et al.*, 2013), which catalyses the same step in methanogens, but in the opposite direction. However, neither the enzyme nor its encoding gene is found in ANME-1. A bypass of this enzymatic step via formation of free methanol and formaldehyde was first proposed (Meyerdierks*, et al.*, 2010), but genomic studies have suggested that Mer is replaced by a methylenetetrahydrofolate reductase (MetFV) enzyme, which catalyses a similar step in other organisms (Stokke*, et al.*, 2012, Krukenberg*, et al.*, 2018). The product 5-10-methylene-H_4MPT is then subsequently oxidized to 5,10-methenyltetrahydromethanopterin and to 5-formyl-H_4MPT by methylene-H_4MPT dehydrogenase (Hmd) and a methenyl-H_4MPT cyclohydrolase (Mch) respectively. Afterwards, the formyl group is transferred from H_4MPT to methanofuran by a formylmethanofuran:H_4MPT formyltransferase (Ftr). Formylmethanofuran is finally oxidized to CO_2 by a formylmethanofuran dehydrogenase (Fmd).

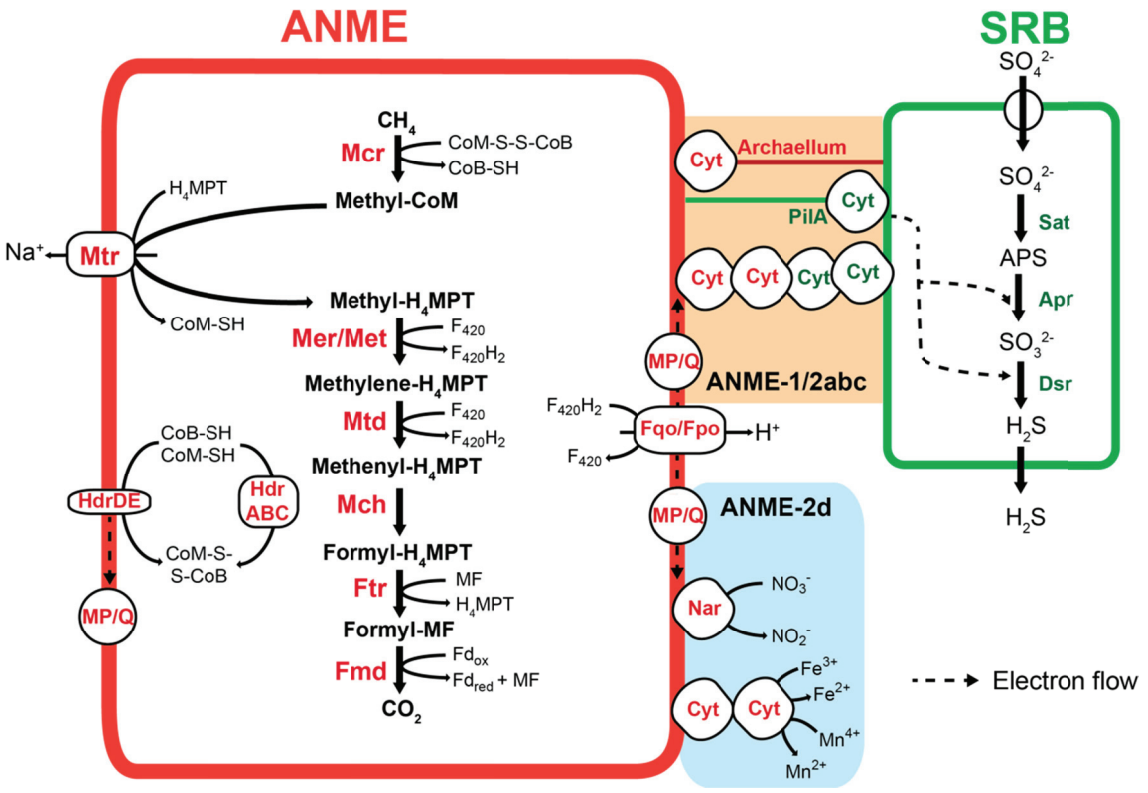

Figure 3. Metabolic model for AOM in ANME based on the current literature. ANME cells (red rectangle) performs AOM using a reversal of the methanogenesis. This process has been demonstrated for the clades ANME-1 and ANME-2. AOM is coupled to nitrate, iron and manganese in ANME-2d (blue background). In ANME-1 and ANME-2abc, AOM is coupled to sulfate reduction by syntrophic partner bacteria (SRB, green rectangle). The current models propose that reducing equivalents are transferred from ANME to the SRB through conductive extracellular structure. ANME-3 are supposed to perform sulfate-dependent AOM associated with SRB, yet their physiology and interaction has not been studied *in vitro*. For ANME-2abc, decoupling of the syntrophic interaction with artificial electron acceptors has also been demonstrated (Scheller, *et al.*, 2016).

Electron acceptors in AOM

The oxidation of methane in ANME requires an electron sink for the released reducing equivalents. As mentioned above, ANME-2d couples AOM to the reduction of nitrate, iron (III) or manganese (IV) (**Figure 3**). The proposed enzymes responsible of these reactions are a nitrate reductase (Haroon, *et al.*, 2013) and multiheme *c*-type cytochromes and cytochrome *c* oxidoreductases (Ettwig, *et al.*, 2016, Cai, *et al.*, 2018). Therefore, ANME-2d organisms could potentially live without a partner, although they have been detected in enrichment cultures in close association with organisms potentially thriving on their end-products (Haroon, *et al.*, 2013, Hu, *et al.*, 2015).

By contrast, coupling of AOM to sulfate reduction requires a syntrophic interaction of ANME archaea and SRB partner bacteria (**Figure 3**). In this case, reducing equivalents released in the oxidation of methane are transferred to bacteria, which carry out the sulfate reduction (Hoehler, *et al.*, 1994, Boetius, *et al.*, 2000, Nauhaus, *et al.*, 2002). The nature of the reducing equivalent and, thus of the syntrophic interaction, has been object of research for many years. Organic molecules or hydrogen

were first proposed as intermediates between both partners (Hoehler, *et al.*, 1994, Valentine and Reeburgh, 2000, Moran, *et al.*, 2008), yet none of these proposals could be supported by experimental evidence (Nauhaus, *et al.*, 2002, Nauhaus, *et al.*, 2005, Moran, *et al.*, 2008, Meulepas, *et al.*, 2010). Later, a new model proposed that ANME were able to reduce sulfate to zero-valent sulfur, which would be disproportionated by the partner bacteria to sulfate and sulfide (Milucka, *et al.*, 2012). However, there is little support for the ability of ANME to perform dissimilatory sulfate reduction (Nauhaus, *et al.*, 2005, Meyerdierks, *et al.*, 2010, Krukenberg, *et al.*, 2018).

Recently, researchers have favoured the interspecies electron transfer hypothesis that was already proposed before (Thauer and Shima, 2008, Summers, *et al.*, 2010). In this model, the archaea transfer directly electrons to the bacterial partner using conductive structures. Support to this hypothesis was already given by the presence of genes encoding for extracellular cytochromes in several ANME genomes (Meyerdierks, *et al.*, 2010, Wang, *et al.*, 2013). Then, several research groups showed the existence of potential mechanisms mediating the direct interspecies electron transfer (DIET) in different AOM consortia (McGlynn, *et al.*, 2015, Wegener, Krukenberg, *et al.*, 2015, Krukenberg, *et al.*, 2018). Wegener, Krukenberg and colleagues (2015) reported the existence of a network of nanowire-like pili in different consortia of ANME-1 and -2 as well as the presence of cytochromes in the extracellular matrix that could mediate DIET (Wegener, Krukenberg, *et al.*, 2015, Krukenberg, *et al.*, 2018). The genes encoding these complexes showed high levels of expression according to transcriptomic analysis. More evidence in favour of the DIET hypothesis came from McGlynn *et al*, who visualized cytochromes in the extracellular matrix of AOM consortia and reported genes encoding multiheme cytochromes in ANME-2 genomes (McGlynn, *et al.*, 2015). The DIET hypothesis was strongly supported with the decoupling of the syntrophy between ANME-2 and SRB using the artificial electron acceptor 9,10-anthraquinone-2,6-disulfonate (AQDS), iron(III)-citrate and humic acids (Scheller, *et al.*, 2016). In this study, incubations with electron-accepting compounds, but without sulfate, showed that methane oxidation was maintained in ANME, while SRB were not anymore active. The ANME extracellular conductive structures were suggested to transfer the reducing equivalents to the alternative electron acceptors.

Environmental role and ecology of anaerobic oxidation of methane

AOM has been reported in many environments like terrestrial mud volcanoes (Alain, *et al.*, 2006, Chang, *et al.*, 2012), landfills (Grossman, *et al.*, 2002) and freshwater systems (Raghoebarsing, *et al.*, 2006, Crowe, *et al.*, 2011, Deutzmann and Schink, 2011, Timmers, *et al.*, 2015) but it is especially relevant in marine sediments (Knittel and Boetius, 2009). Here, large amounts of methane are produced as a result of the degradation of the accumulated organic matter; however it is estimated that AOM consumes up to 90% of the produced methane (Hinrichs and Boetius, 2003, Reeburgh, 2007). Therefore, AOM is an important biogeochemical process preventing the release of great quantities of methane to the water column and finally to the atmosphere, where it could have a considerable impact in the global climate, as methane is a greenhouse gas 25 times more powerful than CO_2 (IPCC, 2014).

In marine sediments, AOM mostly occurs in the sulfate-methane transition zone (SMTZ), where methane migrating from lower depths co-occurs with sulfate coming downwards from the water column (Reeburgh, 1980, Iversen and Jorgensen, 1985, Knittel and Boetius, 2009). Here, methane can be completely oxidized to CO_2 coupled to sulfate reduction (Regnier, *et al.*, 2011). Moreover, AOM has also been described coupled to electron acceptors different than sulfate like nitrate (Haroon, *et al.*, 2013), iron and manganese (Beal, *et al.*, 2009, Ettwig, *et al.*, 2016). AOM can as well be a relevant process in other marine habitats like cold seeps (Joye, *et al.*, 2004, Knittel, *et al.*, 2005, Omoregie, *et al.*, 2008, Beal, *et al.*, 2009), hydrothermal vents (Holler, *et al.*, 2011) and the marine water column under anoxic conditions (Durisch-Kaiser, *et al.*, 2005, Schubert, *et al.*, 2006).

Anaerobic degradation of non-methane hydrocarbons in archaea

Few other anaerobic archaea have been described as hydrocarbon degraders. The first one was *Thermococcus sibiricus*, a hyperthermophilic archaeon isolated from a Siberian oil reservoir (Mardanov, *et al.*, 2009). *T. sibiricus* was reported to grow on hexadecane coupled to the reduction of zero-valent sulfur. Fumarate addition was suggested as the responsible pathway, since the genome of *T. sibiricus* encodes for a pyruvate:formate lyase that resembles the *masD* gene. However, the growth medium contained yeast extract as additional carbon source and hexadecane-dependent growth was only determined based on an increase of cell counts. Additionally, a β-oxidation pathway for further degradation of the activated hexadecane was not encoded (Mardanov, *et al.*, 2009). Therefore, the hexadecane-degrading capacity of *T. sibiricus* has to be validated in future studies.

The hyperthermophilic archaeon *Archaeoglobus fulgidus* was shown to degrade *n*-alk-1-enes (C_{12}-C_{21}) (Khelifi, *et al.*, 2010) and long-chain alkanes (C_{10} to C_{21}) (Khelifi, *et al.*, 2014) coupled to the reduction of thiosulfate or sulfate. For alkene degradation, the activation is still not resolved, although hexadecene-derived fatty acids were detected (Khelifi, *et al.*, 2010). The activation of alkanes seems to proceed as in *T. sibiricus* through the fumarate addition. A gene encoding a pyruvate:formate lyase was found in the genome, being highly expressed during growth on hexadecane. Phylogenetic analysis showed that this was more closely related to the *ass* and *bss* from hydrocarbon-degrading bacteria than to pyruvate:formate lyase, suggesting a gene lateral transfer from bacteria to *A. fulgidus* (Khelifi, *et al.*, 2014).

The last anaerobic archaeon that has been proven to degrade hydrocarbons was the hyperthermophilic *Ferroglobus placidus,* which degrades benzene using Fe(III) as the final electron acceptor (Holmes, *et al.*, 2011). For that, benzene is carboxylated to benzoate, which is further degraded through the canonical pathways of benzoate degradation. The carboxylation is presumably catalysed by an UbiD-like carboxylase. Its encoding gene is upregulated like the genes for the benzoate degradation pathway. All these genes seem to have a bacterial origin (Holmes, *et al.*, 2011).

In the three above cases, the mechanisms for anaerobic hydrocarbon degradation have a bacterial origin. Thus, the only archaeal pathway for anaerobic hydrocarbon degradation is the reverse

methanogenesis in AOM (Widdel and Rabus, 2001, Widdel, *et al.*, 2010). Despite this fact, archaea are also involved in the syntrophic methanogenic degradation of hydrocarbons with bacteria as shown by numerous enrichments degrading alkanes (Zengler, *et al.*, 1999, Anderson and Lovley, 2000, Mbadinga, *et al.*, 2012, Cheng, *et al.*, 2014), alkenes (Schink, 1985) and aromatic compounds (Edwards and Grbić-Galić, 1994, Chang, *et al.*, 2006, Sakai, *et al.*, 2009, Noguchi, *et al.*, 2014). Here, bacteria metabolize the hydrocarbons to different intermediates, which are consumed by the methanogenic archaea.

Two main routes have been proposed: complete oxidation to H_2 and CO_2, and incomplete oxidation to acetate linked to syntrophic acetate oxidation and methanogenesis. In the complete oxidation, a single bacterium metabolizes the hydrocarbons completely to CO_2 and H_2, which are used by archaea to perform hydrogenotrophic methanogenesis (Dolfing, *et al.*, 2007). In the incomplete oxidation, bacteria are proposed to degrade alkanes to acetate, which is used by acetoclastic methanogens producing CO_2 and CH_4 and by syntrophic acetate-oxidizing bacteria that produce H_2 and CO_2, which are used by hydrogenotrophic methanogens to produce methane (Dolfing, *et al.*, 2007, Jones, *et al.*, 2007, Gray, *et al.*, 2011, Cheng, *et al.*, 2014). Both routes are thermodynamically feasible in deep oil reservoirs (Dolfing, *et al.*, 2007), although more evidence has been found for the one involving acetate as intermediate. Methanogenic oxidation of hydrocarbons could have a fundamental role in the degradation of petroleum in deep oil reservoirs since these environments are often depleted of alternative electron acceptors (Aitken, *et al.*, 2004, Dolfing, *et al.*, 2007, Jones, *et al.*, 2007). Thus, several studies have aimed to establish methanogenic hydrocarbon-degrading enrichments from these environments and other contaminated sites (Townsend, *et al.*, 2003, Jones, *et al.*, 2007, Gieg, *et al.*, 2008, Cheng, *et al.*, 2014).

Additionally, there is growing evidence that archaea play a bigger role in the global hydrocarbon cycle. Several studies have shown the presence of archaeal groups with unknown function in cold seeps (Lloyd, *et al.*, 2006, Orcutt, *et al.*, 2010, Ruff, *et al.*, 2015) and other hydrocarbon-rich environments (Schulze-Makuch, *et al.*, 2011, Elsaied, 2014). For instance, sequences of the D-C06 group (also referred to as GoM-Arc2), a deep branching clade of the *Methanomicrobia*, were found in oil seeps of the Gulf of Mexico (Orcutt, *et al.*, 2010). In the same study, sequences of the previously described GoM-Arc1 group were also detected. This clade is phylogenetically related to the ANME-2d and was previously described in hypersaline sediments of the Gulf of Mexico (Lloyd, *et al.*, 2006). GoM-Arc1 was also reported in oil samples from an asphalt lake in Trinidad and Tobago, where several other archaeal groups classified as Tar ARC I-IV were found without knowing their role in the environment (Schulze-Makuch, *et al.*, 2011). Furthermore, incubations with C_1-C_4 alkanes from samples derived from hydrothermal sediments showed the proportional enrichment of certain archaea like *Archaeoglobi*, although a conclusive link between these archaea and sulfate-dependent alkane oxidation could not be established (Adams, *et al.*, 2013).

1.4 Research questions of the thesis

Researchers have started only recently to study the role of microorganisms in the anaerobic degradation of hydrocarbons, yet we began to understand their potential in bioremediation or their implication in the alteration of oil in deep reservoirs. Most studies have focused on the implication of bacteria in this process, with the exception of AOM and the role of methanogens in syntrophic hydrocarbon degradation. However, diverse archaeal groups with unknown function have been repeatedly detected in anoxic hydrocarbon-rich environments like oil seeps and deep reservoirs, and thus they might be important agents in the hydrocarbon degradation.

The aim of this thesis is to study the role of archaea in anaerobic oxidation of hydrocarbons with three main objectives: 1) identification of archaeal clades involved in the anaerobic degradation of hydrocarbons (**Chapters II and III**); 2) cultivation of these clades (**Chapters II, IV and V**) and 3) unravelling the molecular basis of the anaerobic oxidation of hydrocarbons by archaea using genomic, transcriptomic and physiological experiments (**Chapters II, III and IV**). Based on these objectives, the following research hypotheses are proposed:

Archaea can use different mechanisms than bacteria for the anaerobic oxidation of hydrocarbons

So far, the only described hydrocarbon-degrading archaea use mechanism from bacterial origin with the exception of anaerobic methane-oxidizing archaea that use a reversal of the methanogenesis. The **Chapter II** focuses on a novel archaeal group *Candidatus* Syntrophoarchaeum capable of anaerobic oxidation of butane and propane and how these archaea metabolize alkanes.

Diverse archaeal groups with genomic potential for anaerobic degradation of hydrocarbons can be detected in oil and gas seeps of the Gulf of Mexico

Oil seeps have shown diverse archaeal communities, although the function of many of them is unknown. In **Chapter III,** the abundance and distribution of different archaeal clades is studied in oil seeps from the Gulf of Mexico and their potential for hydrocarbon degradation is evaluated.

Hydrocarbon-degrading archaea use different, specifically adapted enzymes to activate different hydrocarbons

Candidatus Syntrophoarchaeum can activate butane and propane via coenzyme M activation. The presence of four MCR gene sets per genome raises the question about their potential to activate different substrates. The **Chapter IV** explores the substrate range and expression profile of these archaea during growth with different substrates through physiological experiments and transcriptomic analysis.

Novel hydrocarbon-degrading archaea can be enriched under anaerobic conditions

The advances of –omics approaches have revolutionized the study of microbial ecology allowing the discovery of novel clades with potential new metabolisms. Nevertheless, cultivated representatives are essential to understand and confirm the hypothetical lifestyles. The **Chapter V** is a detailed protocol for cultivating anaerobic hydrocarbon-degrading organisms based on previous knowledge (**Chapter II and IV**) that can be adapted for different conditions and settings.

1.5 Material and methods

This section gives an overview of the materials and methods used in this thesis to test the hypothesis proposed in the previous sections. As materials, I worked with enrichments derived from hydrothermally-heated sediments and with samples from cold oil seeps. Owing to the different nature of these materials, diverse approaches were employed for their study including culture-dependent and -independent methods such as physiological experiments and meta-omics, respectively. The combination of both kinds of methods helped to collect more evidences for our hypothesis. For instance, metagenomics-driven postulates can be supported by the physiological response of enrichment cultures. As a result of the experience in the cultivation of anaerobic hydrocarbon-degrading organisms, one of the chapters (**Chapter V**) is a detailed protocol about how to enrich these organisms and recommended methods for further analysis.

Materials

In my research project I worked with samples of two different origins. In **Chapters II** and **IV**, enrichment cultures were used to study the metabolic capabilities and physiology of a syntrophic consortia degrading butane, focusing on the archaeal partner. Both chapters are based on culture-dependent techniques, which allowed the realization of physiological and metabolic experiments. By contrast, **Chapter III** is exclusively based in environmental sediment samples. Therefore, hypothesis about the role of archaea in these sediments were proposed based on culture-independent approaches.

Enrichment cultures

Microbial enrichments can become a fundamental tool in the current –omics era, since they represent a valuable resource to confirm hypothesis derived from culture-independent methods. The enrichment technique is based on increasing the number and/or proportion of targeted organisms in a laboratory culture. Unlike pure cultures that consist of a clonal strain of a single organism, enrichment cultures contained a more or less diverse microbial community that develops when a natural sample with a certain microbial community is incubated with a specific combination of substrates, electron acceptors and physicochemical conditions depending on a final goal. For instance, if the enrichment of specific hydrocarbon-degraders is desired, determined substrates like butane or benzene are provided as unique energy sources. Of course, the enrichment success is highly dependent on the selection of the proper inoculum that should contain the target microorganisms. The main advantage of enrichment cultures versus pure cultures is that they allow the study of the physiology of the targeted organisms circumventing problems like syntrophic growth, ecosystem relationships or slow growth.

My research included two microbial enrichment cultures: Butane-50 and its derived culture Propane-50, which was established from Butane-50. Both cultures harbour microorganisms that oxidize alkanes (butane and propane respectively) coupled to the reduction of sulfate to sulfide.

Butane and propane are the single energy source and sulfate was the only electron acceptor. Organisms of these cultures are moderate thermophiles, since cultures were incubated at 50 °C.

The source material for the Butane50 enrichment culture was collected in the Guaymas Basin, which is a deep basin between the North American and the Pacific plates in the Gulf of California. Its formation and geochemical features are linked to the tectonic activity of the seafloor spreading centres and transform faults of the San Andreas system (Einsele*, et al.*, 1980, Lonsdale and Becker, 1985). The basin is characterized by a thick layer of sediment, 100 m deep on average, mainly formed due to the deposition of organic material, mostly diatoms, from the productive photic zone (Simoneit*, et al.*, 1979). As a result of basaltic intrusions, intense hydrothermal activity is produced and steep temperature gradients are found in the subsurface sediment, what stimulates a rapid degradation of the deposited organic matter (Einsele*, et al.*, 1980, Simoneit and Lonsdale, 1982, Lonsdale and Becker, 1985). Consequently, large amounts of methane are produced as well as other small and medium hydrocarbons, and organic molecules (Simoneit*, et al.*, 1979, Simoneit and Lonsdale, 1982). These compounds mix with the hydrothermal fluids and migrate towards the sediment surface sustaining a diverse microbial community that degrades them coupled to methanogenesis, methanotrophy (for methane) and sulfate reduction (Teske*, et al.*, 2002, Dowell*, et al.*, 2016). Therefore, considerable amounts of sulfide are diffusing through the sediments to the surface, where they are the energy source at the surface for sulfide-oxidizing microbial mats, indicating hotspots for sulfate reduction and organic matter biodegradation (Nelson*, et al.*, 1989, Gundersen*, et al.*, 1992).

The Butane-50 enrichment culture derived from sediment samples collected with the submersible *Alvin* in a hydrothermal vent site in Guaymas Basin (27°00.437 N, 111°24.548 W) during the *Atlantis* cruise AT15-56 in November/December 2009 (Holler*, et al.*, 2011). Sediment cores of 45 cm were retrieved at a site covered by bacterial mats and with steep temperature gradients (4-85°C). Using the material from the horizon B (14-25 cm, 30-60 °C), a methane-oxidizing enrichment culture was established under sulfate-reducing conditions at 50°C (Holler*, et al.*, 2011). The analysis of its microbial composition revealed the dominance of two microorganisms in consortia: methane-oxidizing archaea from the ANME-1 clade and bacteria from the HotSeep-1 cluster that is related to *Deltaproteobacteria* (Holler*, et al.*, 2011, Krukenberg*, et al.*, 2016, Wegener*, et al.*, 2016).

Previously, HotSeep-1 bacteria were thought to be butane degraders, as they appeared to be the main bacteria in a butane-degrading enrichment (Kniemeyer*, et al.*, 2007). To test this hypothesis, an aliquot of the thermophilic AOM culture was incubated at 50 °C with butane headspace (0.101 MPa) instead of methane as sole energy source. Artificial seawater was used as medium and prepared according to Widdel and Bak (1992) with sulfate (28 mM) as electron acceptor. Under the new condition, it took a long lag phase of half a year until a slow increase in sulfide concentration was detected. The growth of the established culture was monitored by measuring sulfide production via the Cord-Ruwisch method (Cord-Ruwisch, 1985). The culture was maintained for years by transferring it when sulfide concentrations exceeded 12 mM. This procedure resulted in a sediment-free culture

named Butane-50, which was provided to me for my research. In a physiological experiment, I tested the substrate range of Butane-50 providing several alkanes. Most substrates did not sustain microbial activity, yet growth was detected in propane incubations resulting in the establishment of a new enrichment culture named Propane-50. The maintenance of Propane-50 was similar to Butane-50 with the only difference that propane was provided as energy source instead of butane.

Butane- and Propane-50 are highly enriched cultures harbouring consortia of archaea and bacteria. The archaea belong to the clade *Candidatus* Syntrophoarchaeum (previously named GoM-Arch87 group) within the class *Methanomicrobia* and are responsible of the alkane degradation, while the bacteria are affiliated to *Candidatus* Desulfofervidus auxilii, belonging to the HotSeep-1 clade, and performed sulfate reduction. Based on sequencing analysis, two *Ca.* Syntrophoarchaeum strains were detected: *Candidatus* Syntrophoarchaeum butanivorans and *Candidatus* Syntrophoarchaeum caldarius. Both strains are present in the Butane-50 culture but only *Ca.* S. caldarius is detected in Propane-50. Additionally, there is a minor flanking community consisting of some *Thermoplasmata* archaea and deltraproteobacteria. The optimum temperature of both cultures based on highest sulfate reduction rates are between 50-55 °C with a temperature range of 37-60 °C. Samples from both cultures were subject of different molecular and sequencing analysis as well as physiological studies.

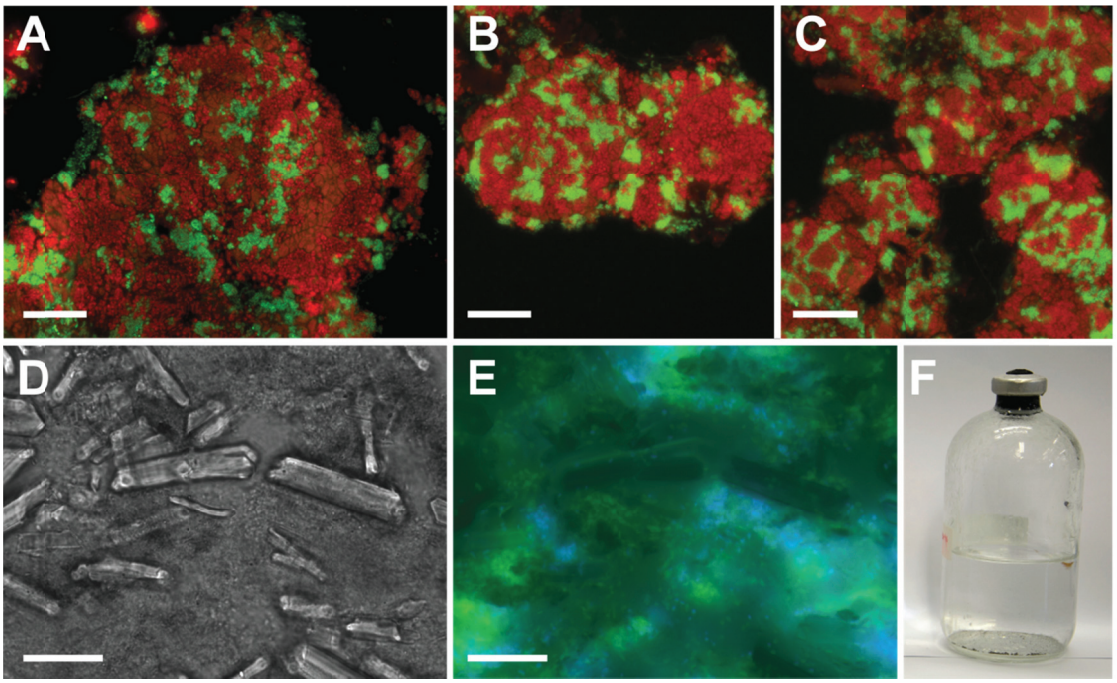

Figure 4. Visualization of the butane-degrading enrichment Butane-50. **A-C**: FISH micrographs of thin sections of the consortia present in Butane-50 formed by *Ca.* Syntrophoarchaeum (red) and *Ca.* D. auxilii (here only identified in green with the general bacterial probe). Pictures obtained in the Orphan lab (CalTech, California, USA). **D**: Bright field image of a Butane-50 sample. Large crystals can be appreciated. **E**: Fluorescence image from (**D**) showing the autofluorescence of *Ca.* Syntrophoarchaeum due to the cofactor F_{420} (blue) and the autofluorescence of *Ca.* D. auxilii (green). **F**: Butane-50 cultures. Large particles and iron precipitates can be distinguished at the bottom of the bottle. All scale bars are equal to 20 µm.

Visualization of the microbial community of Butane-50 with specific oligonucleotides probes showed high abundance of consortia formed by *Ca.* Syntrophoarchaeum archaea and *Ca.* D. auxilii (**Figure 4A-C**). They are forming mixed consortia with clusters of archaea and bacteria with similar proportions of both partners. Both organisms showed distinct autofluorescence when excited with a certain wavelength, in the case of the archaea due to the presence of the cofactor F_{420} (**Figure 4E**). *Ca.* Syntrophoarchaeum cells appear mostly as coccoid cells with a diameter of 1-1.5 μm, although they appear in some occasions as larger cells with a round-squared morphology and with a lighter staining signal. The bacterial partner presents a rod shape (1-2 μm × 0.5-1 μm). A more detailed study of the bacterial partner has already been published (Krukenberg*, et al.*, 2016). The flanking community of the cultures has different morphologies including coccoid and filamentous cells. Besides, the enrichments contain large spike-shaped crystals and iron sulfur precipitates observable under the bright field objective (**Figure 4D**).

Environmental samples

Environmental samples can be studied with culture-independent approaches. In this case, the proposed conclusions are based on the results and on the physicochemical conditions of the sampling sites and their ecology. During my thesis research, I studied environmental samples collected from the Campeche Knolls (southern Gulf of Mexico) during the *RV Meteor* cruise M114-2 (March, 2015). I focused on four sediment cores retrieved from the Chapopote asphalt volcano area and from the Mictlan asphalt field. The samples were used for different molecular analysis, for instance 16S rRNA gene sequencing, metagenomics and microscopy visualization as well as certain geochemical parameters.

The Chapopote asphalt volcano is characterized by extensive lava-like asphalt fields produced by subsurface materials containing heavy-degraded oil originated from organic matter of the Jurassic period (Magoon*, et al.*, 2001). Numerous active oil and gas seeps are localized in the area, resulting in high concentrations of hydrocarbons in the sediment and the water column (MacDonald*, et al.*, 2004, Sahling*, et al.*, 2016). Diverse microbial communities inhabit the oil-containing sediments thriving on the different hydrocarbons, especially anaerobic microorganisms since oxygen is quickly consumed in the upper sediment. Additionally, there is a rich fauna around the seep that comprises animals with chemosynthetic symbionts thriving on the reduced compounds of the seep fluids (MacDonald*, et al.*, 2004, Sahling*, et al.*, 2016, Rubin-Blum*, et al.*, 2017). Two push cores of 10 cm were retrieved from this area at around 2900 m water depth. The first one was collected next to the asphalt volcano (21°53.993'N; 93°26.112'W). The sediment core was covered by microbial mats indicating high sulfate reduction rates in the sediment likely due to the oil and gas degradation in the sediment. By contrast, the second push core was sampled near the asphalt field (21°53.954'N; 93°26.261'W) but this area was not affected by the oil. Besides, a gravity core (40 cm) was used to sample the fresh and unaltered asphalt close to the massive deposits of the volcano (21°53.964'N; 93°26.226'W).

Mictlan Knoll is an asphalt volcano with a distinct crater-like structure. Like Chapopote, there are extensive asphalt deposits and a diverse biological community. However, no oil and gas seepage was observed in the asphalt field unlike in Chapopote sites (Sahling*, et al.*, 2016). The sample from the Mictlan asphalt field (22°01.354'N; 93°14.809'W) was retrieved by a gravity core (0-135 cm). The core consists of homogenous pelagic sediment sample with asphalt pieces and oil at the bottom.

Methods to investigate the physiology of the microorganisms

Physiological methods are usually culture-dependent techniques employed to study the metabolism, growth and other capabilities of microorganisms in cultures. During this thesis, physiological methods were applied to subcultures of Butane- and Propane-50 in order to investigate different metabolic aspects, substrate range and optimum growth conditions.

Incubations with metabolic and inhibitory substrates

One way to study the physiology of microorganisms in an enrichment culture is to see their response during incubation with different substrates. Depending on the nature of the substrate, this response can be evaluated differently. For instance, the response to the addition of organic substrates potentially supporting growth of microbial community members can be measured by tracking the substrate concentration (for instance butane) or the formation of metabolic products like sulfide over time. In cases where there are positive indications for the consumption of the provided substrate, further analysis must be performed to identify the responsible organisms, as the addition of new substances can change the microbial community composition of the enrichment. Other substrates are provided to inhibit specific microbial reactions in the culture such as molybdate to stop sulfate reduction. The success of the inhibition can be determined by measuring the consumption of the substrate provided as energy source (like butane) or the formation of the normal or alternatives end-products (like sulfide and hydrogen respectively). During my research, I performed incubations in Butane-50 subcultures with both kinds of substrate, supporting growth or inhibiting microbial reactions.

On the one hand, I evaluated the metabolic substrate range by incubating Butane-50 subcultures with different hydrocarbons (C_1-C_6). In each of the incubations, only one substrate was supplied and the measurement of sulfide concentration over time was used to evaluate the response. An increase of sulfide concentration was considered as a sign that the microbial enrichment can metabolize that substrate and was followed by further analysis to identify the responsible organisms and mechanisms. By contrast, no increase of sulfide concentration was interpreted as an inability of the microorganisms present in the culture to use that substrate.

On the other hand, I performed two experiments with inhibitory substrates. In one of them, I added bromoethanesulfonate (BES) to Butane-50 subcultures. BES is an analogue of coenzyme M and functions as an inhibitor of the (reverse) methanogenesis pathway (Gunsalus*, et al.*, 1978, Nauhaus*, et*

al., 2005). The success of the inhibition was evaluated measuring sulfide production. The second substrate was sodium molybdate, which was employed to inhibit the sulfate reduction pathway (Oremland and Capone, 1988). In this case, the inhibition was evaluated by tracking sulfide concentration after the addition of sodium molybdate as well as by measuring the production of H_2 as alternative end-product.

Temperature growth optimum

Defining the growth conditions of microorganisms, such as temperature, pH or salinity, is necessary to improve the cultivation success as well as a requisite to define new species. For that, microorganisms are cultured under different ranges of the selected factors and the growth is evaluated based on the biomass yield or the efficiency of key metabolic processes. Microbial enrichments can also be tested with similar approaches, although the existence of different organisms in the culture can result in the selection of different species or strains, especially if the enrichment was recently established or lacks a dominant microbial species. Butane-50 and Propane-50 were used for a temperature growth experiment during my thesis research. The optimum temperature for growth was determined by calculating the sulfate reduction rate under a range of nine temperatures (from 28 °C to 75 °C).

Methods to investigate the microbial community composition

The study of the microbial community composition of environmental samples and enrichment cultures is essential to connect function/processes and identity of organisms. The methods employed for that are usually based on the 16S rRNA gene, which acts as marker gene due to its nature as "molecular clock". There are two main techniques to study community composition based on this marker gene: 16S rRNA gene sequencing and microscopy based on fluorescence *in situ* hybridization with oligonucleotide specific probes.

16S rRNA gene amplicon sequencing

The study of the 16S rRNA gene has been essential to understand the phylogenetic diversity and relationships between different organisms (Woese, 1987, Yarza*, et al.*, 2014). As a result, 16S rRNA gene sequencing has become a key tool to study microbial diversity in the environment. Nowadays, the most common technique for this purpose, known as amplicon or tag sequencing, is based on high throughput sequencing, mostly with Illumina machines. They are used to sequence partial 16S rRNA gene sequences, previously amplified by polymerase chain reaction (PCR) from the extracted total DNA extracted of a sample.

I used this method to analyse the microbial community composition of sediment samples from the Gulf of Mexico (**Chapter III**). The general procedure of Illumina 16S library preparation and sequencing is as follows: total DNA is firstly extracted from a sample and the 16S rRNA gene is

amplified by PCR using specific primer targeting phylogenetically significant regions of the gene. In my research, general primers for bacteria (Bact 341F/785R) and archaea (Arch 349F/915R) were used. Subsequently, Illumina adapters including sequencing barcodes are attached to the amplified sequences to generate the amplicon library, which is loaded on a flow cell in the Illumina machine for sequencing. Via the attached adapters, the amplified 16S library fragments are bound to the flow cell channel surface, where a dense lawn of primers allows the "bridge" amplification of individual fragments generating dense clusters of DNA copies around each original amplicon fragment. Afterwards, these clusters are sequenced using the stepwise incorporation of fluorescently labelled nucleotides, complementary to the bases of the library fragments in each cluster (sequencing by synthesis). After nucleotide incorporation, laser excitation of the fluorescent labels causes the emission of a specific signal for each cluster. In every sequencing cycle, only one base is incorporated per cluster and therefore only one signal is recorded.

The sequencing results must then be processed: primers and adapters must be removed, reads must be quality-trimmed and, if both ends of the library fragments were sequenced (paired end sequencing), they should be merged to obtain the original length of the amplified fragment. Afterwards, the processed reads can be subjected to different methods for dereplication (to correct for sequencing errors), clustering and classification. In our research, I used Swarm as clustering-dependent algorithm (Mahé*, et al.*, 2014) and SINA aligner (Pruesse*, et al.*, 2012) as classification method using the SILVA database as reference.

Catalysed reporter deposition fluorescence in situ hybridization (CARD-FISH)

CARD-FISH is a technique where microorganisms are identified by specific probes that hybridize with the 16S rRNA present in the ribosomes (Amann and Fuchs, 2008). It is also used to quantify microbial abundances and evaluate 16S tag sequencing results, since these are PCR-biased (Schirmer*, et al.*, 2015). CARD-FISH probes are oligonucleotides tagged with horseradish peroxidase (HRP) that exactly match the 16S rRNA sequence of the targeted organisms. Unlike FISH probes, CARD-FISH probes are not fluorescently labelled. Instead, they hybridize the targeted 16S rRNA and then the HRP catalyses the deposition of fluorescently labelled tyramide after its activation with hydrogen peroxide. The main advantage is that CARD-FISH increases the sensitivity compared to FISH, which allows the visualization of cells with low ribosome content or with low activity (Amann and Fuchs, 2008). However, probes are much larger due to the HRP and consequently cells walls must be permeabilized. The standard protocol of CARD-FISH is described in Pernthaler*, et al.* (2002). During this thesis, modifications of this protocol were used both with enrichment cultures and environmental samples to visualize, identify and quantify different microorganisms. In short, samples were fixed with formaldehyde and sonicated, if necessary. The sonication was performed to disrupt large aggregates and detach cells from sediment samples. Afterwards, cells were embedded in agarose and their walls were permeabilized using different reagents like lysozyme, proteinase K and/or achromopeptidase.

After inactivation of endogenous peroxidases with hydrogen peroxide, the hybridization step took place using specific probes with the stringent temperature and formamide concentration. Different probes were used during this step including general ones for *Archaea* (Stahl and Amann, 1991) and *Bacteria* (Amann*, et al.*, 1990, Daims*, et al.*, 1999) and specific probes for targeted organisms like *Ca*. Syntrophoarchaeum, GoM-Arc1, D-C06 and *Ca.* D. auxilii. For the latter one, an already designed probe was used (Krukenberg*, et al.*, 2016), while for the rest specific probes were designed during this thesis research. In some cases, helpers and competitors were also applied to increase the probe efficiency. After the indicated washing steps, the fluorochromes Alexa Fluor 594 and/or 488 were added for the amplification step by the HRP. In case of double hybridization, HRP of the first amplification were inactivated before. Finally, cells were stained with DAPI (4′,6′-diamino-2-phenylindole) and visualized with epifluorescence microscopy or confocal microscopy for image acquisition.

Methods to investigate genomic potential and gene expression

The variety of techniques that are catalogued as "-omics" represent important tools in microbial ecology and physiology. They include a diverse group of disciplines including genomics, transcriptomics, proteomics or metabolomics; each of them based on a different biological molecule. For example, genomics deals with the study of the function and evolution of the information contained in the DNA, the hereditary material of the cell; while transcriptomics and proteomics analyse the expression of the genes at the RNA and protein level, respectively. Finally, metabolomics looks into the functioning of the cell through the metabolic molecules present in a biological system. Recent advances in these techniques have improved their resolution and performance, expanding their use for high-throughput study of biological communities and not only for single organisms. These new approaches are called metaomics standing out metagenomics and metatranscriptomics. Both have become widely used techniques in microbial ecology, because they make possible to study yet non-cultivated organisms. These two methods rely on the production of large amounts of DNA and RNA sequence data with several times coverage by high-throughput sequencing. These massive amounts of data allow later for genome reconstruction and the study of gene expression.

Genomic potential: metagenomics and single cell sequencing

The study of the genomic potential of an organism was made possible by the development of sequencing technologies. Initially, only small fragments of a genome could be produced by Sanger sequencing due to the high cost. The emergence of new sequencing technologies known as next-generation sequencing as well as the dramatic reduction of the sequencing costs has opened an era of massive sequencing, where huge amounts of DNA can be easily sequenced for every sample with little cost. In this regard, one of the most widely used technologies is Illumina sequencing, which I used for the study of both enrichment cultures and environmental samples during the course of my research.

For both samples, metagenomes from the whole microbial community were produced in order to investigate the genomic potential of organisms of interest. Additionally, single cell sequencing was also carried out for one of the environmental samples of the Gulf of Mexico. For that, cells from the sediment sample had to be sorted into a well plate using fluorescence-activated cell sorting (FACS). Only one cell was sorted per well. After DNA extraction, 16S rRNA tag sequencing was performed to identify organisms of interest, which were subject to whole genome sequencing.

The process of Illumina whole genome sequencing can be shortly described as follows (**Figure 5**). First, extracted DNA from a sample is sheared into smaller fragments to which adapters are attached creating a sequencing library. Two kinds of libraries can be produced: paired-end or mate pair. In paired-end libraries, adapters are directly attached to the ends of the fragments generated by the shearing. Fragments are relatively small, thus generating short inserts. Insert is defined as the fragment of original DNA sample between the sequencing adapters. Two reads will be produced during sequencing: one in the forward direction and a second one in the reverse direction. These reads can have overlapping regions due to the small insert size. In contrast, a different shearing technique produces larger fragments for mate pair libraries, to which biotinylated linker sequences are attached. The large fragments are then circularized, connecting two distant genomic areas, marked by the biotinylated ends. A second fragmentation of the circularized DNA takes place, followed by selection of biotinylated fragments. As a result, only fragments with biotinylated tags (which now are not at the end of the fragments) are enriched. At this point, adapters are ligated and the library is ready for sequencing. Mate pair libraries produce sequences with a known distance between them in the original DNA strand (usually 5-10kb), providing information about the vicinity and connectivity of different genomic areas.

Prepared libraries are then loaded on a flow cell for sequencing in an Illumina machine. The sequencing process is as described for 16S tag sequencing. The fragments are attached to the surface of the flow cells lanes where bridge amplification takes place generating clusters of copies of the same DNA fragment. Then, sequencing occurs by the incorporation of fluorescently-labelled nucleotides, one per cycle. Each nucleotide emits a distinct light signal used to record the sequence information. As a result, large amounts of short DNA reads are produced. Afterwards, these reads are quality-controlled and then subjected to an assembly using informatics tools (**Figure 5**). The assembly consist of the reconstruction of large DNA segments based on the sequence overlap of the short reads. These reconstructed segments are called contigs. For metagenomes, the assembly process is more challenging due to the presence of genomic reads from different organisms. In the case of single cell sequencing, the assembly results in a group of contigs that can be considered a single-cell amplified genome (SAG).

For metagenomes, the resulting assemblies are further processed with a binning software to generate genomic bins that represent draft genomes of single organisms (**Figure 5**). These bins are also called metagenome-assembled genome (MAG). Different criteria are used during this process

such as sequencing coverage, tetranucleotide frequency or GC content (guanine-cytosine content). Moreover, the quality of the bins is assessed with different parameters such as completeness, contamination, N50 value or other metrics (contig number, assembly number…). N50 represents the contig length at 50% of the total assembly length. Extracted bins from an assembly can be used for targeted reassembly to improve the quality of the bin. For that, the metagenomic reads are mapped to the extracted bin and the mapped ones are used for a reassembly and subsequent binning. The process can be repeated until the quality does not increase, resulting in a (high-quality) draft genome. This binning and reassembly process is not necessary for single cell sequencing, where all the generated contigs belong to a single organism and can be directly analysed. The generated draft genomes are then used to predict genes and function using different bioinformatics tools, permitting the inference of potential proteins and the study of the hypothetical metabolism of the organism. Predicted genes can be used to calculate phylogenetic trees in order to understand the relation of the gene of interest with similar genes of other organisms.

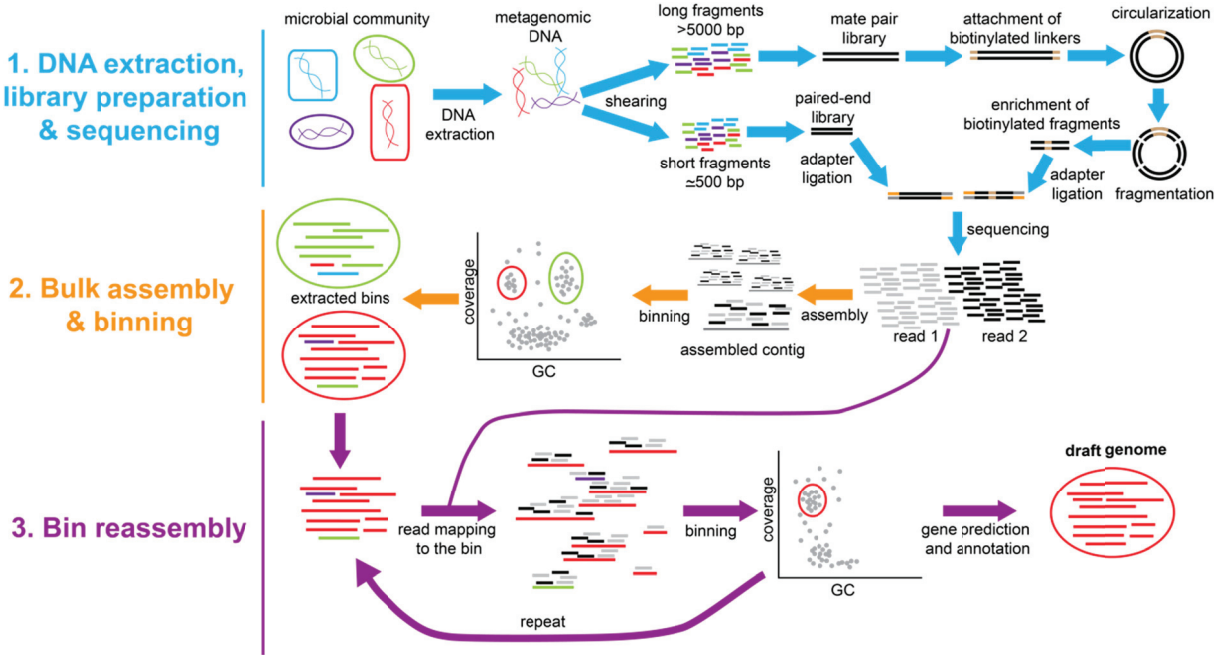

Figure 5. Workflow of a metagenomic analysis. The process starts with the DNA extraction and library preparation (in blue). Two libraries can be produced: paired-end or mate pair. After sequencing, the generated reads are assembled and the resulting contigs are binned using different bioinfomatic tools (orange). Targeted reassembly can be performed in bins of interest to increase the quality of the bin (purple). As a result, high-quality draft genomes are obtained.

Gene expression: metatranscriptomics

Similarly to DNA, RNA can also be sequenced nowadays in a high-throughput manner. Illumina sequencing was also used in this thesis to obtain metatranscriptomic reads from enrichment cultures. RNA differs from DNA in two main aspects. First, RNA is a much more fragile molecule, which makes more difficult its extraction and handling. The fact that Butane- and Propane-50 are

thermophilic cultures caused the establishment of a different approach to obtain RNA. RNA was first fixed inside the cells with RNAlater, a stabilization solution, at the *in situ* temperature of 50°C and under the normal growth atmosphere. This step was critical according to results obtained from other thermophilic AOM enrichment cultures, since it avoided the degradation of the RNA as well as a change in the gene expression pattern during extraction. Afterwards, cells were sonicated and RNA extracted using conventional kits. The second difference is that RNA library preparation requires an additional step. It consists on the synthesis of a double stranded cDNA (complementary DNA) from the original RNA fragments. First, a cDNA strand is synthesized using RNA fragments as templates. Then, the second cDNA strand is produced using the first cDNA as template. This double-stranded cDNA is then ligated to adaptors, loaded on a flow cell and used for sequencing in an Illumina machine similarly as described before. In our case, libraries with cDNA inserts of circa 150 bp length were generated.

The resulting transcriptomic reads are quality controlled. The messenger RNA (mRNA) sequences can then be mapped to reference genomes to evaluate the expression levels of the different genes, for what different methods exist. In this thesis, gene expression was evaluated using two transformations. On the one hand, absolute fragment counts per gene were normalized per length and per absolute read number obtaining a value known as fragment per kilobase of transcript per million mapped reads (FPKM) (Trapnell*, et al.*, 2010). On the other hand, a centered-log ratio transformation (CLR) was applied (Fernandes*, et al.*, 2014), where absolute fragment counts per gene were normalized per length and per the geometric mean of the transformed CLR values of the total sample or organism. While FPKM normalize the gene expression based on length and sample size, CLR intends to reduce the compositionality effect in the samples and estimates if a gene is enriched or depleted in a dataset.

1.6 Overview of enclosed manuscripts

Chapter II: Thermophilic archaea activate butane via alkyl-CoM formation

Rafael Laso-Pérez, Gunter Wegener, Katrin Knittel, Friedrich Widdel, Katie J. Harding, Viola Krukenberg, Dimitri V. Meier, Michael Richter, Halina E. Tegetmeyer, Dietmar Riedel, Hans-Hermann Richnow, Lorenz Adrian, Thorsten Reemtsma, Oliver J. Lechtenfeld and Florin Musat

*Published in Nature **539:** 396-401 (17/11/2016). doi:10.1038/nature20152*

This manuscript studies the thermophilic enrichment culture Butane-50. It is dominated by consortia of archaea and bacteria that couple the degradation of butane to sulfate reduction. Using microscopy, physiology and metaomics, we show that the newly described *Ca*. Syntrophoarchaeum archaea oxidize butane with a mechanism resembling those present in ANME. *Ca*. Syntrophoarchaeum activate butane with highly divergent MCRs enzymes and then fully oxidize the produced butyl-CoM using the fatty acid oxidation pathway, the Wood-Ljungdahl pathway and the downstream part of the methanogenesis. The reducing equivalents are transferred via conductive pili to the bacterial partner for sulfate reduction. This is the first demonstration of a CoM activation for a multi-carbon compound and represents a novel mechanism for hydrocarbon degradation in archaea.

The study was initiated by G.W. who retrieved the original samples. R.L.-P., G.W. and F.M. designed research and performed cultivation. R.L.-P. performed CARD-FISH microscopy with the support of K.K, K.J.H and V.K. Physiological experiments were performed by R.L.-P., G.W. and F.M. R.L.-P. performed the metagenomics and transcriptomic analyses with the supervision of V.K., D.V.M. and M.R. R.L.-P. carried out the phylogenetic analyses. R.L.-P. developed the metabolic model and wrote the first version of the manuscript under the supervision of G.W. and with contribution of F.W., F.M. and other co-authors.

Chapter III: Coupling of alkane degradation to methane formation in a single archaeon

Rafael Laso-Pérez, Cedric Hahn, Dann M. van Vliet, Halina E. Tegetmeyer, Florence Schubotz, Nadine T. Smit, Heiko Sahling, Gerhard Bohrmann, Antje Boetius, Katrin Knittel and Gunter Wegener

Manuscript ready for submission

This manuscript investigates the role of archaea in the anaerobic degradation of hydrocarbon in cold seeps from the Gulf of Mexico. Combining 16S rRNA gene sequencing and microscopy visualization, we identify the most dominant archaea in oil-rich sediments. Apart from ANME, archaea of the unknown clades D-C06 and GoM-Arc1 were especially abundant, the fist as single cells in oil droplets and the second forming consortia with bacteria. We were able to obtain two draft genomes affiliated to D-C06 using metagenomics. Based on their metabolic potential, we propose that D-C06 archaea represent novel hydrocarbon-degrading organisms that couple the process to methanogenesis in a

single cell. We based this hypothesis on the existence of two MCRs sets in their genome: one similar to the divergent MCRs of *Ca.* Syntrophoarchaeum and another one related to methane metabolism.

Research was planned and initiated by R.L.-P. and G.W. R.L.-P. performed 16S tag sequencing analysis and conducted metagenomics analyses. R.L.-P. designed the metabolic model and wrote the manuscript under the supervision of G.W. and A.B. with contributions of all co-authors.

Chapter IV: Substrate and gene expression patterns of different alkane-degrading strains of *Ca.* Syntrophoarchaeum

Provisional author list: Rafael Laso-Pérez, David Benito Merino, Pier L. Buttigieg, Halina E. Tegetmeyer, Antje Boetius and Gunter Wegener

Manuscript in preparation

In this study, the physiology of *Ca.* Syntrophoarcheum is investigated using cultivation techniques and transcriptomics analysis. During incubations with different short-chain alkanes, growth of *Ca.* Syntrophoarchaeum was only possible with propane and butane. Interestingly, *Ca.* Syntrophoarchaeum strains show substrate specificity. While one strain grows on both alkanes, another one only grows on butane. Transcriptomic analysis revealed that some genes are expressed differently depending on the growth substrate.

R.L.-P. and G.W. designed experiments and research. R.L.-P. performed cultivation and physiological experiments with the help of D.B.M. R.L.-P. carried out transcriptomic analysis with the support of P.L.B. R.L.-P. wrote the initial version of the manuscript and R.L.-P. and G.W. are working on the manuscript with contribution of all co-authors.

Chapter V: Establishing anaerobic hydrocarbon-degrading enrichment cultures of microorganisms under strictly anoxic conditions

Rafael Laso-Pérez, Viola Krukenberg, Florin Musat and Gunter Wegener

*Published in Nature Protocols **13:** 1310-1330 (17/05/2018). doi:10.1038/nprot.2018.030*

This manuscript represents a comprehensive protocol for the preparation and establishment of hydrocarbon-degrading enrichment cultures under anoxic conditions. It includes a detailed explanation of all materials, reagents and steps needed as well as a troubleshooting guide to solve possible problems that appear during the procedures. Moreover, graphic material in the form of pictures and videos is included facilitating the understanding of the most complicated steps.

All the authors contributed equally to the validation and optimization of the protocol and wrote cooperatively the manuscript. R.L.-P. wrote the initial version of the manuscript. All authors edited later the version of the manuscript. Figures were prepared by R.L.-P., V.K. and G.W. Supplementary videos were produced by R.L.-P. and G.W.

This thesis was funded by the Leibniz Grant of the Deutsche Forschungsgemeinschaft (DFG) awarded to Antje Boetius. Additional resources came from the Max Planck Society and the Excellence Cluster MARUM of the University Bremen.

Chapter II

Thermophilic archaea activate butane via alkyl-coenzyme M formation

Rafael Laso-Pérez[1,2], Gunter Wegener[1,2,3], Katrin Knittel[1], Friedrich Widdel[1], Katie J. Harding[1]†, Viola Krukenberg[1,2], Dimitri V. Meier[1], Michael Richter[1], Halina E. Tegetmeyer[2,4], Dietmar Riedel[5], Hans-Hermann Richnow[6], Lorenz Adrian[6], Thorsten Reemtsma[6], Oliver Lechtenfeld[6] & Florin Musat[1,6]

[1]Max-Planck Institute for Marine Microbiology, 28359 Bremen, Germany.
[2]Alfred Wegener Institute Helmholtz Center for Polar and Marine Research, 27570 Bremerhaven, Germany. [3]MARUM, Center for Marine Environmental Sciences, University Bremen, 28359 Bremen, Germany.
[4]Center for Biotechnology, Bielefeld University, 33615 Bielefeld, Germany.
[5]Max Planck Institute for Biophysical Chemistry, 37077 Göttingen, Germany.
[6]Helmholtz Centre for Environmental Research, UFZ, 04318 Leipzig, Germany.
†Present address: University of California at Santa Cruz, Ocean Sciences Department, Santa Cruz, California 95064, USA.

Nature ***539****, 396-401*
Received 6 June; accepted 11 October 2016.
Published online 17 October 2016.

Correspondence to Gunter Wegener (gwegener@mpi-bremen.de) or Florin Musat (florin.musat@ufz.de)

https://www.nature.com/articles/nature20152
DOI: 10.1038/nature20152
Running title: *Butane activation via alkyl-CoM formation*

Abstract

The anaerobic formation and oxidation of methane involve unique enzymatic mechanisms and cofactors, all of which are believed to be specific for C_1-compounds. Here we show that an anaerobic thermophilic enrichment culture composed of dense consortia of archaea and bacteria apparently uses partly similar pathways to oxidize the C_4 hydrocarbon butane. The archaea, proposed genus '*Candidatus* Syntrophoarchaeum', show the characteristic autofluorescence of methanogens, and contain highly expressed genes encoding enzymes similar to methyl-coenzyme M reductase. We detect butyl-coenzyme M, indicating archaeal butane activation analogous to the first step in anaerobic methane oxidation. In addition, *Ca.* Syntrophoarchaeum expresses the genes encoding β-oxidation enzymes, carbon monoxide dehydrogenase and reversible C_1 methanogenesis enzymes. This allows the complete oxidation of butane. Reducing equivalents are seemingly channelled to HotSeep-1, a thermophilic sulfate-reducing partner bacterium known from the anaerobic oxidation of methane. Genes encoding 16S rRNA and MCR similar to those identifying *Ca.* Syntrophoarchaeum were repeatedly retrieved from marine subsurface sediments, suggesting that the presented activation mechanism is naturally widespread in the anaerobic oxidation of short-chain hydrocarbons.

Etymology. *Syntrophoarchaeum*, *syn* (Greek): together; *trophae* (Greek): nourishment; *archae* (Greek): origin, beginning, *butanivorans*, *butanum* (Latin): butane; *vorans* (Latin): eating, devouring. The name implies an organism capable of butane oxidation, however demanding syntrophic electron sinks. A second strain is named '*Candidatus* S. caldarius'. *caldarius* (Latin): warm or hot. Refers to the strain's thermophilic growth condition.

Locality. Enriched from hydrothermally heated, hydrocarbon-rich marine sediments of the Guaymas Basin at 2000 m water depth, Gulf of California, Mexico.

Diagnosis. Anaerobic, butane-oxidizing archaeon, variable morphology, 1.5 × 1 μm, dependent on syntrophic support by the sulfate-reducing partner bacterium '*Candidatus* Desulfofervidus auxilii'.

Main text

Massive amounts of natural gas migrate from deep-seated reservoirs towards the sea floor[1-3]. Most of this gas is consumed in the anoxic zone by microorganisms coupling oxidation of the hydrocarbons to the reduction of the abundant electron acceptor, sulfate. Research on the anaerobic oxidation of natural gas has largely been focused on methane as the most abundant constituent[2-4]. The anaerobic oxidation of methane (AOM) is carried out by anaerobic methanotrophic archaea (ANME) forming consortia with sulfate-reducing bacteria (SRB); ANME activate methane to methyl-coenzyme M by methyl-CoM reductase (MCR)[4,5]. The CoM-bound methyl group is further oxidized to CO_2 by reversing the enzymatic chain of methanogenesis[6,7], while reducing equivalents are channelled to the partner SRB[8,9].

However, natural gas generated by thermogenic decomposition of organic matter contains considerable amounts (up to 20%) of short-chain alkanes, including mostly ethane (up to 15%), but also propane, *iso*-butane and *n*-butane (hereafter butane)[10,11]. Although these gases are potential growth substrates for microorganisms, the anaerobic oxidation of the non-methane hydrocarbons became of interest only recently. All cultures known so far to oxidize short-chain hydrocarbons anaerobically are bacteria that couple complete substrate oxidization to CO_2 and sulfate reduction in one organism[12-16]. The only pure culture available so far is strain BuS5, a deltaproteobacterium[12]. Strain BuS5 and related organisms activate propane and butane via addition to fumarate yielding alkyl-substituted succinates, to date the most-studied anaerobic activation mechanism for hydrocarbons[12,17-19]. A recent study, however, suggests that this mechanism is not always involved in short-chain hydrocarbon oxidation[20]. Here we combined physiological experiments, community sequencing, microscopy, omics approaches and metabolite analyses to provide evidence for an alternative anaerobic activation reaction of butane in a highly enriched thermophilic culture of archaeal–bacterial consortia.

Archaea catalyse thermophilic butane oxidation

Thermophilic anaerobic methanotrophic archaea (ANME-1) were previously found to be associated with a deltaproteobacterial phylotype, HotSeep-1[9,21] that had been detected independently in thermophilic enrichment cultures with short-chain alkanes[12,15]. This prompted us to attempt again thermophilic enrichments with a short-chain hydrocarbon, butane. For these, we used inocula from Guaymas Basin sediment samples that had already been incubated with methane and developed thermophilic AOM activity. After two months, butane-dependent sulfate reduction became obvious. Further cultivation and subsequent transfers to new medium with butane yielded a sediment-free culture, hereafter called Butane50. This culture reduced 10 mM sulfate within approximately 14 weeks of incubation. Quantitative growth experiments showed that the amount of butane degraded was coupled to the reduction of sulfate to sulfide almost in a 1:3.25 ratio (**Fig. 1a**; **Supplementary Table 1**), as demonstrated also for strain BuS5, yielding the net reaction

$$4C_4H_{10} + 13SO_4^{2-} + 26H^+ \rightarrow 16CO_2 + 13H_2S + 20H_2O$$

In this culture the ANME-1 phylotype was no longer detectable by molecular analysis. Instead, archaea closely related to *Methanosarcinales* had become dominant owing to the change to butane as substrate; they were members of the GoM-Arch87 clade[22] (**Extended Data Table 1**). Like ANME-1, GoM-Arch87 also forms densely packed consortia with the HotSeep-1 partner bacterium (**Fig. 1b,c**). These consortia show strong blue-green autofluorescence (maximum at approximately 475 nm; **Fig. 1d**), which is characteristic of cofactor F_{420}, a hydrogen carrier typical for methanogenic and ANME archaea[6,23]. Phylotype GoM-Arch87 was originally detected in cold-seep areas of the Gulf of Mexico[22], and since then was also found in other marine environments, especially seep and vent areas (see SILVA database release SSU 119; http://www.arb-silva.de). The environmental role of these archaea has been so far unknown.

From the metagenome assembly we retrieved two bins of contigs indicating genomes of two different GoM-Arch87 (**Supplementary Table 2** and **Extended Data Table 2**). The two GoM-Arch87 bins have sizes of 1.46 Mb (GoM-Arch87-1) and 1.66 Mb (GoM-Arch87-2). On the basis of their tRNA content, archaeal-specific single-copy gene numbers and lineage-specific marker gene sets (*Euryarchaeota*) the draft genomes cover an estimated 85–89% of the complete genome of GoM-Arch87-1 and 95–97% of GoM-Arch87-2, indicating genome sizes of 1.64 to 1.71 Mb. According to their 16S rRNA gene identity of 96% and whole genome identity of 74–90% (**Fig. 1e**; **Extended Data Table 2**), the two bins probably represent different species of one genus. Hence we propose to name the more abundant (according to genome coverage) strain GoM-Arch87-1, *Candidatus* Syntrophoarchaeum butanivorans and the less abundant strain GoM-Arch87-2, *Candidatus* Syntrophoarchaeum caldarius. The two strains have largely similar gene content, and are further discussed together as *Ca.* Syntrophoarchaeum.

Ca. Syntrophoarchaeum genomes encode a fatty acid oxidation pathway, two complete acetyl-CoA decarbonylase/synthase:CO dehydrogenase (ACDS/CODH) complexes, and an almost complete methanogenesis-related pathway. Each of the two draft genomes contains four complete *mcr* gene sets, of which three (*Ca.* S. butanivorans) or all four (*Ca.* S. caldarius) are organized in operons (**Extended Data Fig. 1**). The correct assembly and the unusually high number of *mcr* genes in a single genome were confirmed by cloning and resequencing 7 of the 8 *mcrA* genes. Metatranscriptome and metaproteome analyses (only studied on *Ca.* S. butanivorans) showed that all these gene/protein sets were highly expressed/abundant (**Extended Data Tables 3-5**). Neither the metagenomic assembly nor the draft genomes of *Ca.* Syntrophoarchaeum contain genes encoding the otherwise widespread glycyl radical enzymes (*assA/masD*, *bssA*) for anaerobic hydrocarbon activation. Accordingly, these genes could not be amplified from extracted DNA using specific primers (see Methods). These results strongly indicated that the activation of butane in *Ca.* Syntrophoarchaeum proceeds via mechanisms different from those described for bacteria. An appealing hypothesis was that butane in *Ca.* Syntrophoarchaeum is activated by the distinct variants of MCR in a reaction analogous to that of

methane at 'reverse' MCR in ANME. The expected first metabolite would thus be butyl-coenzyme M rather than methyl-coenzyme M.

***Ca.* Syntrophoarchaeum forms butyl-coenzyme M**

Analysis of cell extracts of active Butane50 cultures by direct infusion ultra-high resolution mass spectrometry indeed provided direct evidence for butane-dependent formation of butyl-coenzyme M. A mass peak of m/z = 197.03116 was detected, which corresponded exactly to the hypothesized butyl-CoM ($C_6H_{13}S_2O_3^-$). Following quadrupole isolation and collision-induced fragmentation this compound yielded two major fragments representing a butylthiol (m/z = 89.0430, $C_4H_9S^-$) and an apparently CoM-derived bisulfite (m/z = 80.9652, HSO_3^-; **Fig. 2** and **Extended Data Fig. 2a**). Use of synthesized authentic standards showed that the two isomers, 1-butyl-CoM and 2-butyl-CoM, were present and separated by liquid chromatography, with apparently higher amounts of the latter (**Fig. 2c**). The presence of two butyl-CoM isomers offers, in principle, two explanations. First, one could be the initial product whereas the other is the subsequently formed intermediate. Second, only one isomer may be the genuine, directly metabolized activation product, whereas the other is formed as a by-product owing to relaxed catalytic specificity of the activating enzyme; this would be similar to the anaerobic activation of propane by strain BuS5, where both *n*- and *iso*-propylsuccinate have been detected as activation products[12,24]. Because the different amounts of the detected isomers reflect steady-state concentrations (dynamic pools), they cannot offer clues as to their metabolic significance. To further corroborate butyl-CoM formation as a specific activation reaction, that is, exclude that it can be accomplished 'accidentally' by other means, we added butane to a methane-oxidizing ANME-1 enrichment. Neither butyl-CoM nor its derived fragments were detected. Moreover, these compounds were not detected in sterile controls, in substrate-starved Butane50 cultures, or in cultures of the bacterial butane-oxidizer strain BuS5 (**Fig. 2** and **Extended Data Fig. 2a**).

Mechanistic relatedness between butane activation at the MCR variant and methane activation at MCR of methanotrophic archaea was demonstrated using an inhibition experiment. The coenzyme M analogue, bromoethanesulfonate, which inhibits methanogenesis as well as anaerobic methane oxidation[25] also inhibited butane-dependent sulfate reduction (**Extended Data Fig. 3**). Inhibition must occur in the archaeal metabolism, because bromoethanesulfonate did not affect the partner bacterium, HotSeep-1 (*Ca.* Desulfofervidus auxilii) when separately grown with hydrogen and sulfate; the tested partner originated from the thermophilic AOM culture[26].

Aliquots of the Butane50 culture were also tested with other hydrocarbons. After approximately two months of incubation with propane, sulfate reduction became obvious. The rate increased and became similar as with butane. A possible shift in the microbial composition or gene expression upon incubation with propane has yet not been assessed. However, a mass peak exactly corresponding to that of propyl-CoM was analysed (m/z = 183.0155; **Extended Data Fig. 2c**). This further corroborates the formation of alkyl-CoM as the apparent initial product in short-chain alkane

activation. So far, no sulfate reduction was detectable with added methane, ethane, *iso*-butane, *n*-pentane or *n*-hexane.

This is the first demonstration, to our knowledge, of coenzyme M acting *in vivo* as a carrier of alkyl moieties other than the methyl group. The closest known precedent is the *in vitro* reduction of the homologous substrate ethyl-CoM to ethane by MCR from methanogenic archaea[27,28]. Turnover rates of ethyl-CoM in these assays were two orders lower than of methyl-CoM, which was explained by a steric hindrance of the larger ethyl-CoM molecule in the MCR enzyme[28]. This suggests that an efficient activation of butane to butyl-CoM may require highly adapted MCR-like enzymes. Analysis of the deduced amino acid sequences of the eight *mcr* genes detected in *Ca.* Syntrophoarchaeum revealed low similarity, with an identity similarity of only 29–82%. Two different MCR enzymes encoded in the genome of *Ca.* S. butanivorans were highly abundant in protein extracts of the culture, qualifying them as likely candidates for butane activation (**Extended Data Table 3**).

A high substrate specificity of the MCR type apparently involved in butane oxidation was also indicated in an incubation experiment with both, butane and methane. In the active culture, butyl-CoM but no methyl-CoM was detected (**Extended Data Fig. 2b**). Hence, there was no evidence for co-activation of methane, even though alone by its molecular size the latter should not encounter any steric binding hindrance. One may speculate that reaction at the enzyme requires substrate 'fixation' by binding of an alkyl chain of a minimum length. Understanding as to which extent the slightly weaker C–H bond in higher alkanes in comparison to that in methane could play a role may need refined theoretical consideration. Furthermore, the population and abundant MCR type in the recent propane-adapted subculture will have to be analysed. Currently, it is unknown whether propane and butane are activated by the same organism and enzyme or cause selection of different ones with respective substrate preference.

Notably three of the McrA subunits of *Ca.* S. butanivorans have a related equivalent in *Ca.* S. caldarius. The fourth McrA subunit (SBU_000314) forms a cluster with McrA sequences of the recently described *Bathyarchaeota*[29], whereas the fourth sequence of *Ca*. S. caldarius (SCAL_000352) has a distant phylogenetic position (**Fig. 3**; for further phylogenetic analysis see Methods and **Supplementary Fig. 1**). Together, McrA sequences of *Ca*. Syntrophoarchaeum and *Bathyarchaeota* form a cluster that is highly divergent from methanogens or methanotrophs. This probably reflects the evolution of genes that encode enzymes able to accommodate larger alkanes such as butane.

Complete oxidation of butane

The measured stoichiometric balance shows that the CoM-bound butyl moiety must be completely degraded to CO_2. Only a minor fraction is expected to enter biosynthesis, as in other strict anaerobes[30]. Complete oxidation requires four basic metabolic features, the conversion of the butyl-thioether to the butyryl-thioester (presumably butyryl-CoA), oxidation of butyryl-CoA to acetyl-CoA, terminal oxidation of acetyl-CoA to CO_2, and channelling of the reducing equivalents (electrons) into sulfate

reduction. Our proteogenomic analysis provides explanations for all of these processes, with the exception of the first.

The role and significance of the butyl-CoM isomers and their subsequent processing steps could not be clarified on the basis of our present analyses. Also, there are no precedent cases of natural pathways involving non-methyl CoM-thioethers that could suggest particular reactions. Still, one may argue that 1-butyl-CoM is the genuine and directly metabolized activation product. Because MCR in AOM activates a primary C–H bond, its variant in culture Butane50 may also attack butane at the primary carbon. In this way, first oxidation and functionalization would occur at the same carbon atom which in a subsequent β-oxidation would become the activated carboxyl group (thioester). In such case, 2-butyl-CoM would be a by-product; it is presently unknown whether an isomerase converts it to 1-butyl-CoM.

In methyl-CoM oxidation in AOM and in the oxidative branch in methanol-utilizing *Methanosarcina*, the subsequent steps would be transfer of the methyl group to tetrahydromethanopterin (H_4MPT) or tetrahydrosarcinapterin (H_4SPT) and oxidation via the bound formaldehyde and formate states to CO_2. None of the genes encoding methyl-H_4MPT:coenzyme M methyltransferase were found in the genome. We can only speculate about an analogous transfer of the butyl-moiety by the abundant, presumably modified methyltransferase (**Fig. 4**; **Extended Data Table 3**), because the postulated butyl-cobalamin intermediate would be unprecedented. Furthermore, tetrahydropterins and methanofuran are, to our knowledge, exclusive C_1-carriers. Hence, the enzymatic reactions converting 1-butyl-CoM to the butyryl (bound acid) level are presently puzzling, even though transfer and oxidation reactions of higher carbon compounds can be theoretically formulated with most C_1-carriers.

The predicted β-oxidation enzymes of *Ca.* Syntrophoarchaeum (**Fig. 4**; **Extended Data Table 3**) are highly related to those of deltaproteobacterial sulfate reducers and syntrophic partners of methanogens[31-32] (**Extended Data Table 6**). This suggests horizontal gene transfer across the two domains of life. The gene encoding the most abundantly formed acyl-CoA dehydrogenase of *Ca.* Syntrophoarchaeum is located in an operon with genes for an electron transfer flavoprotein (*etf*) complex and a [FeS]-oxidoreductase. Hence, these gene products probably act as electron acceptors in the oxidation of butyryl-CoA (**Fig. 4**), as previously shown for bacterial butyrate oxidizers[33,34].

The key enzyme for the metabolism of acetyl-CoA from β-oxidation is the detected acetyl-CoA decarbonylase/synthase:CO dehydrogenase (ACDS/CODH). The carboxyl group-derived bound CO can be oxidized to free CO_2 and yield reduced ferredoxin as shown previously for methanogens[23]. The methyl group is probably oxidized via the reverse methanogenesis pathway, of which almost all genes are present and their corresponding transcripts and proteins were detected (**Fig. 4**; **Extended Data Table 4**). The N5,N10-methylene-tetrahydromethanopterin (methylene-H4MPT) reductase *(mer*) gene is absent in *Ca.* Syntrophoarchaeum. However, as in ANME-1, Mer could be substituted by the highly abundant putative methylenetetrahydrofolate reductase complex as previously

suggested[35]. The genes encoding the Met complex of *Ca.* Syntrophoarchaeum have a similar operon structure to those of *Moorella thermoacetica*[36]. In conclusion, the combination of enzymes in *Ca.* Syntrophoarchaeum results in the archaeal version of the oxidative Wood–Ljungdahl pathway, as originally shown for the sulfate-reducing *Archaeoglobus fulgidus*[37].

Ca. Syntrophoarchaeum does not have the genes for canonical sulfate reduction (that is, *dsrAB*, *aprAB*), and hence depends on an external electron sink. This role is apparently fulfilled by the partner bacterium. We tested for the production of hydrogen as a canonical intermediate in syntrophic associations. Although *Ca.* Syntrophoarchaeum encodes for a cytoplasmic [NiFe] hydrogenase (**Extended Data Table 5**), only minor amounts of hydrogen were produced in active or molybdate-treated Butane50 cultures, which cannot explain the required reducing equivalent transfer (**Fig. 5a**). To study how reducing equivalents are transferred to the partner bacterium further, the draft genome of the Butane50 HotSeep-1 strain was retrieved from the metagenome. On the basis of different marker genes, this HotSeep-1 strain is basically identical to *Ca.* D. auxilii, the partner in thermophilic AOM[26] (**Supplementary Table 3**). *Ca.* D. auxilii is a lithoautotrophic sulfate reducer that in thermophilic AOM thrives on electrons directly supplied by the ANME via pili-based nanowires and cytochromes[9,26]. Also, in the Butane50 culture HotSeep-1 expresses genes encoding pili assembly proteins, especially the main component of type IV pilus (PilA), and many different potential cytochromes including extracellular ones (**Extended Data Table 7**). Using transmission electron microscopy we found a similarly dense, apparently pili-based, nanowire network in the intercellular space of the Butane50 consortia (**Fig. 5b**). On the basis of these results we propose that nanowire-based direct interspecies electron transfer[38] also mediates electron exchange in the butane-oxidizing consortia. From a thermodynamic point of view, the interspecies transfer of reducing equivalents would be also possible via H_2; its measured partial pressure of approximately 1 Pa would allow energy conservation in both partners, albeit with quite unequal energy sharing (calculation in Supplementary Discussion; **Supplementary Fig. 2**). However, the extremely slow rate of H_2 formation (**Fig. 5a**) is difficult to reconcile with the observed rate of sulfate reduction.

Channelling of the reducing equivalents to the sulfate-reducing partner bacterium requires electrons with redox potentials below the average potential of sulfate reduction ($E^{\circ\prime}$ = -220 mV), which is reached by most proposed redox reactions. However, the oxidation of butyryl-CoA to crotonyl-CoA (**Fig. 4**) releases electrons with far higher potentials ($E^{\circ\prime}$ = -125/-10 mV[33]). A shift in the redox potential of these electrons can be achieved by different mechanisms, including energy-driven reverse electron transport[33] or electron confurcation[39], both demonstrated for syntrophic bacteria. Two of the required genes, encoding EtfAB and FeS oxidoreductase, were identified in *Ca.* Syntrophoarchaeum. Other genes with products involved in electron transport have been identified, including different heterodisulfide reductases (**Extended Data Table 5**) such as one complex of HdrABC (SBUT_000297-299) followed by the genes encoding the β-subunit of formate dehydrogenase (FdhB) and the δ-subunit of methylviologen-reducing hydrogenase (MvhD) (**Extended**

Data Table 5). This complex was already identified in ANME-1 genomes and was hypothesized to act as an electron-accepting complex[7].

Evolutionary and environmental aspects

The analysis of the anaerobic consortia enriched with butane provides first insights into an additional mechanism for the oxygen-independent activation and use of non-methane saturated hydrocarbons in archaea. Saturated hydrocarbons belong to the chemically least reactive compounds. In anaerobic bacteria, the radical-catalysed addition of alkanes to fumarate yielding substituted succinates is regarded as common[40,41], even though alternative mechanisms have been proposed[42,43]. The MCR-like proteins produced by *Ca.* Syntrophoarchaeum and formation of butyl-coenzyme M in the culture suggest that the mechanistic principle for the activation of methane, the most stable hydrocarbon, was evolutionarily adapted to also use short-chain alkanes. Another requirement for metabolic processing was, apart from the yet unsolved subsequent reaction step of the alkyl-thioether, the acquisition of enzymes for β-oxidation, which has been demonstrated previously in other archaea[44]. The subsequent reactions leading to CO_2 are enabled by steps which in principle are well-documented in methanogens.

The presently suggested pathway for anaerobic oxidation of non-methane alkanes might not be limited to *Ca.* Syntrophoarchaeum. The recently detected uncultivated *Bathyarchaeota* contain genes for MCR types highly similar to those of *Ca.* Syntrophoarchaeum (**Fig. 3**). Furthermore, the draft genomes of *Bathyarchaeota*[29] as well as the pan-genome of uncultivated *Hadesarchaea*[46] encode most enzymes of the methanogenesis pathway, for short-chain fatty acid oxidation and for acetyl-CoA oxidation via ACDS/CODH. On the basis of these predicted features, *Bathyarchaeota* were described as heterotrophic methanogens. Our results indicate that at least some of these uncultivated archaea may be also viewed as alkane oxidizers.

In conclusion, anaerobic microorganisms thriving on non-methane alkanes may be phylogenetically and metabolically even more diverse than previously thought[47,48]. Such diversity may reflect a long-existing presence of saturated hydrocarbons in the biosphere and their exploitation as growth substrates through various evolving pathways, long before the oxygen-dependent pathways. The factors which in modern anoxic environments select for consortial, archaeal hydrocarbon oxidation over oxidation by a single bacterial species[12,41] are still unknown and require more comprehensive *in situ* studies.

METHODS

Origin of inoculum and cultivation of the Butane50 enrichment culture

Gas-rich hydrothermally-heated sediments covered with dense mats of *Beggiatoa* were obtained in the Guaymas Basin vent area (27° 00.437′ N, 11° 24.548′ W; 2,000 m water depth). Samples were collected by push coring using the submersible Alvin (dive 4570) on RV Atlantis during

November/December 2009. The sediments were stored anaerobically in butyl rubber stopper-sealed glass vials. In the laboratory sediments were 1:4 diluted with anoxic artificial seawater (ASW) medium[49], initially provided with methane as a substrate, and incubated at 50°C. These incubations showed immediate methane-dependent sulfate reduction. After 3 months a subsample was incubated with butane (0.2 MPa). Initially, we did not detect butane-dependent sulfide production, however after 2 months of incubation sulfide production set in. When sulfide concentrations exceeded 15 mM the culture was diluted (1:5) in fresh ASW medium (semi-continuous cultivation) and resupplied with butane. This procedure was repeated several times and resulted in a virtually sediment-free culture after 2 years of cultivation. For quantitative growth experiments, cultures were set up in 150 ml serum bottles containing 80 ml ASW medium, and inoculated with a 20 ml aliquot of a grown culture. Parallel cultures with different starting amounts of butane (5 and 7.5 ml butane in the culture headspace) were prepared. As controls, we used sterile cultures receiving butane, and inoculated cultures lacking butane. All cultures were incubated at 50°C without shaking. Measurements of sulfide production and butane were performed in triplicate.

Chemical analyses of sulfide and butane

Sulfide concentrations were determined by transferring 0.1 ml culture into 4 ml acidified copper sulfate (5 mM) solution. The formation of colloidal copper sulfide was determined photometrically at 480 nm (ref. 50). To quantify butane concentration, volumes of 0.1 ml headspace gas were withdrawn using N_2-flushed, gas-tight syringes. The gas samples were injected without a split into a Shimadzu GC-14B gas chromatograph, equipped with a Supel-Q PLOT column (30 m × 0.53 mm, 30 μm film thickness; Supelco, Bellefonte, USA) and a flame ionization detector. The oven temperature was maintained at 140°C, and the injection and detection temperatures were maintained at 150°C and 280°C, respectively. The carrier phase was N_2 at a flow rate of 3 ml min^{-1}. Samples were analysed in triplicates. Butane concentrations were calculated based on an external calibration curve.

Detection of autofluorescence in Butane50 culture

Consortia from the Butane50 culture were visualized by Confocal Laser Scanning Microscopy (LSM 780, Zeiss, Germany) with an excitation light of 405 nm and an emission filter >463 nm, and by recording the maximum autofluorescence at 470 nm wavelength.

Amplification, sequencing and phylogenetic classification of 16S rRNA and functional genes

Total DNA was extracted from 10 ml of the Butane50 culture pelleted via centrifugation (4,000 r.p.m. for 15 min; Eppendorf Centrifuge 5810R) using the FastDNA Spin Kit for Soil (MP Biomedicals) following the manufacturer's protocols. Bacterial and archaeal 16S rRNA gene fragments were amplified using the primer pairs GM3/GM4[51] and Arch20F[52]/1492R[53]. Furthermore genes encoding canonical anaerobic hydrocarbon-activating enzymes including *assA/masD* (primer pairs 7757F-1,

7757F-2/8543R[54]) and *bssA* (primer pair 1213F/1987R[55]) were targeted for amplification. For amplification of *assA*, a mixture of forward primers was applied to improve diversity coverage[54]. Polymerase chain reactions (PCR) were performed in 20-µl volumes containing 0.5 µM of each primer solution, 7.5/6 µg bovine serum albumin solution, 250 µM deoxynucleoside triphosphate (dNTP) mixture, 1 × PCR reaction buffer (5Prime, Germany), 0.25U Taq DNA polymerase (5Prime) and 1 µl DNA template (25–50 ng). PCR reactions (Mastercycler; Eppendorf) included an initial denaturation step of 95°C for 5 min followed by 34 cycles of denaturation (95°C for 1 min.), annealing (1.5 min at 44°C for bacterial 16S primers, or at 58°C for archaeal 16S primers), and extension (72°C for 3 min) and a final 72°C step for 10 min. For amplification of genes encoding canonical hydrocarbon-activating enzymes, the protocol consisted of an initial denaturation step (95°C for 5 min) followed by 34 cycles of denaturation (96°C for 1 min), annealing (58°C for *assA* primers and 55°C for *bssA* primers, both for 1 min) and extension (72°C for 2 min) ending with a final extension (72°C for 10 min). All products were checked on 1% agarose gels, stained with ethidium bromide and visualized with UV light. Amplicons (archaeal and bacterial 16S rRNA gene) were purified (QIAquick PCR Purification Kit; Qiagen) and cloned in *Escherichia coli* (TOPO TA cloning Kit for sequencing; Invitrogen). Clones were screened by standard PCR procedure and positive inserts were sequenced using Taq cycle sequencing with ABI BigDye Terminator chemistry and an ABI377 sequencer (Applied Biosystems, Foster City, CA, USA). Representative full-length sequences were used for phylogenetic analysis using the ARB software package[56] and the SSURef_NR99_115 SILVA database[57]. Phylogenetic trees of 16S rRNA genes were constructed with RAxML (version 7.7.2) using a 50% similarity filter and the GTRGAMMA model. An extended phylogenetic tree is provided as **Supplementary Fig. 3.** Branch support values were determined using 100 bootstrap replicates. From the Butane50 culture no *masD*/*assA* and *bssA* genes could be amplified.

Catalysed reported deposition fluorescence *in situ* hybridization (CARD-FISH)

Cell aliquots were fixed for 2 h in 2% formaldehyde, washed and stored in phosphate buffered saline (PBS; pH = 7.4): ethanol 1:1. Samples were sonicated (30 s; Sonoplus HD70; Bandelin) and incubated in 0.1 M HCl (1 min) to remove potential carbonate precipitates. Aliquots were filtered on GTTP polycarbonate filters (0.2 µm pore size; Millipore, Darmstadt, Germany). CARD-FISH was performed according to Pernthaler *et al.*[58] including the following modifications: cells were permeabilized with a lysozyme solution (0.5 M EDTA pH 8.0, 1 M Tris-HCl pH 8.0, 10 mg ml^{-1} lysozyme; Sigma-Aldrich) at 37°C for 30 min and with a proteinase K solution (0.5 M EDTA, 1 M Tris/HCl, 5 M NaCl, 7.5 µM of proteinase K; Merck, Darmstadt, Germany) for 5 min at room temperature; endogenous peroxidases were inactivated by incubation in a solution of 0.15% H_2O_2 in methanol for 30 min at room temperature. Specific 16S rRNA-targeting oligonucleotide probes used were SYNA-407 and HotSeep-1-1456[26], both applied at 20% formamide concentration. SYNA-407 was developed during this project using the probe design tool within the ARB software package to specifically detect *Ca*.

Syntrophoarchaeum. The probe is highly specific for *Ca.* Syntrophoarchaeum and has at least one mismatch to non-target group sequences in the current database. The stringency of probe SYNA-407 was experimentally tested on the Butane50 culture using 10% to 40% formamide in the hybridization buffer. The sequence of the probe is: 5′-AGTCGACACAGGTGCCGA-3′. Three helpers were necessary: hSYNA-388 (5′-ACTCGGAGTCCCCTTATC-3′), hSYNA-369 (5′-CACTTGCGTGCATTGTAA-3′) and hSYNA-426 (5′-TATCCGGACAGTCGACAC-3′). Probes were purchased from Biomers (Ulm, Germany). In case of double hybridization, the peroxidases from the first hybridization were inactivated by incubating the filters in 0.30% H_2O_2 in methanol for 30 min at room temperature. The hybridized archaeal and bacterial cells were stained by addition of the fluorochromes Alexa Fluor 594 and Alexa Fluor 488 for the two target organisms. Finally the filters were stained with DAPI (4′,6′-diamino-2-phenylindole) and analysed by epifluorescence microscopy (Axiophot II Imaging, Zeiss, Germany). Selected filters were analysed by Confocal Laser Scanning Microscopy (LSM 780, Zeiss, Germany).

Extraction of genomic DNA, library construction and sequencing

Genomic DNA was extracted from 15 ml of the Butane50 culture using the FastDNA Spin Kit for Soil (MP Biomedicals, Illkirch, France). For paired-end library preparation the TruSeq DNA PCR-Free Sample Prep Kit (Illumina) was used including the following modifications of the manufacturer's guidelines. A total amount of 700 ng DNA (in 50 µl volume) was fragmented in 500 µl nebulization buffer (50% glycerol v/v, 35 mM Tris-HCl, 5 mM EDTA), using a Nebulizer (Roche), with a fragmentation time of 3 min, and applied pressure of 32 p.s.i. The fragmented DNA was purified via a MinElute purification column (Qiagen). Following end repair, the first size-selection step (removal of large DNA fragments) was done with a sample purification bead/H_2O mixture of 6/5 (v/v).

For mate-pair library construction, genomic DNA was extracted from 35 ml Butane50 culture following the protocol after Zhou *et al.*[59] with the following modifications: cells were collected by centrifugation of the culture aliquot (3,000*g* for 5 min). The pellet was resuspended in 450 µl of extraction buffer, homogenized in a tissue grinder and the mixture was freeze–thawed three times. Subsequently 1,350 µl of fresh extraction buffer and 60 µl of Proteinase K were added. In total, 1,370 ng of DNA were obtained and used for mate-pair library construction with the Illumina Nextera Mate Pair Sample Preparation Kit following the manufacturer's guidelines with the following modifications: a total amount of 1.3 µg DNA was used and the fragmentation time was reduced to 15 min. Fragments of lengths between 4 kb and 9 kb were obtained on an agarose gel which were then used for further library preparation. Sequencing of both libraries was performed on a MiSeq 2500 instrument (Illumina; 2 × 300 cycles) using v3 sequencing chemistry. In total 4,460,548 and 21,182,518 reads were obtained for the paired-end and mate-pair library respectively.

Read processing, bin assembly and data analysis

The paired-end Illumina reads were quality-trimmed after adaptor and contaminant removal using the bbduk tool in BBMap (version 34, http://sourceforge.net/projects/bbmap; minimum quality value of 20; minimum read length ≥50 bp). Overlapping paired-end reads were merged using bbmerge when overlap exceeded 20 bases without mismatches for reads ≥150 bp. The 16S rRNA based phylogenetic composition of the paired-end library was estimated using the software phyloFlash (https://github.com/HRGV/phyloFlash), which classifies reads taxonomically by mapping reads against the SSU SILVA 119 database using bbmap. For quantification, only unambiguously mapped reads were counted. For the mate-pair library, junctions, contaminants and external adaptors were removed using bbduk. Afterwards, the reads were quality trimmed (quality value ≥20 and minimum sequence length 50 bp). Bulk assembly of processed libraries was done with SPAdes (version 3.5.0 (ref. 60)) including the BayesHammer error correction step and using default *k*-mer size recommended for the read length (21, 33, 55, 77, 99, 127). The resulting scaffolds were analysed and binned using the Metawatt software (version 2.1 (ref. 61)), which analyses the GC content, coverage, open reading frames (ORF) and tetranucleotide pattern for each scaffold. The subsequent binning of the scaffolds was based on three different criteria: highly similar tetranucleotide frequency (98% confidence level), coherent taxonomic classification according to BlastP search of the translated ORFs and similar GC content and read coverage in the metagenome. Using the software RNAmmer[62], the 16S rRNAs present in the bulk assembly were extracted to classify the different bins of the bulk assembly phylogenetically. Bins corresponding to the GoM-Arch87 group were selected and refined. The refinement started with a mapping of the raw reads (from complete libraries) to the selected bins (with a minimum identity of 90% the first time and 97% the next ones) using the bbmap tool from the BBMap package. The mapped reads were reassembled using SPAdes (same settings as for the bulk assembly), followed by binning in Metawatt. Contigs smaller than 1 kb were removed from the bin. The mate-pair read mapping information of the bin was used to create connectivity graphs using Cytoscape[63,64] and to remove poorly connected contigs. After bin refinement, its completeness was checked using AMPHORA2[65], which screens for 104 archaeal single copy genes; CheckM[66], which analyses completeness and contamination based on lineage-specific marker sets, in our case *Euryarchaeota* and tRNAscan[67], which screens for the different tRNA sequences. The final bins were used as draft genome of *Ca.* S. butanivorans and *Ca.* S. caldarius for automated gene annotation in RAST[68] and genDB[69] after gene prediction using Glimmer3.02[70]. After selecting the best annotation for each ORF using the automated annotation tool MicHanThi[71], the GenDB results were visualized using the JCoast frontend[72]. All presented genes were manually curated afterwards.

Analysis of species identity and bacterial electron transfer mechanisms

A HotSeep-1 bin was retrieved and annotated as described above for *Ca.* Syntrophoarchaeum. To compare our HotSeep-1 bin and the published draft genome of *Ca.* D. auxilii (CP013015),

JSpecies1.2.1 (ref. 73) was used, which analyses the average nucleotide identity and the tetranucleotide frequency between two genomes. This method was also used to compare the two genome bins of *Ca.* Syntrophoarchaeum. Furthermore, the two HotSeep-1 strains were compared by checking the identity of the following genes: 16S rRNA, 23S rRNA, sulfate adenylyltransferase (*sat*), adenylylsulfate reductase subunit alpha (*apr* alpha), adenylylsulfate reductase subunit beta (*apr* beta) and dissimilatory sulfite reductase subunit alpha (*dsr* alpha) and of the internal transcribed spacer (ITS) region. To study genes encoding pili and cytochromes of HotSeep-1, genes of interest were identified. This selection was manually curated using Blastp and Pfam search. The subcellular localization of cytochromes was predicted using PSORTb (version 3.0.2 (ref. 74)).

Search for canonical alkyl succinate synthase genes

To search for canonical genes of hydrocarbon oxidation in the metagenome and the bins of *Ca.* S. butanivorans and *Ca.* S. caldarius, a protein database of anaerobic hydrocarbon oxidation genes was constructed. Full-length sequences from hydrocarbon degrading enzymes present in the Uniprot database were combined with recently published *masD* sequences[47]. These enzymes were AssA, BssA, MasD, the alpha subunit from naphtylmethylsuccinate synthase (Nms), the alpha subunit from a ring cleaving hydrolase (BamA), and pyruvate formate lyase (Pfl). The bulk assembly and the *Ca.* Syntrophoarchaeum draft genomes were searched against this database using Blastx with an E-value of 10^{-5}.

Treatment of Butane50 culture with bromoethanesulfonate

Triplicate Butane50 cultures and duplicates of *Ca.* D. auxilii cultures were grown on their respective substrates (butane or hydrogen). Two active Butane50 cultures were incubated with bromoethanesulfonate (BES, 5 mM final concentration) and as growth control, one culture remained untreated. To check the effect of BES on the bacterial partner alone, hydrogenotrophic grown *Ca.* D. auxilii cultures were also treated with 5 mM of BES. Sulfate-reducing activity was determined by sulfide measurements as described above.

Phylogenetic analysis of methyl-CoM reductases in *Ca.* Syntrophoarchaeum draft genomes

The McrA amino acid sequences in the genomes of *Ca.* S. butanivorans and *Ca.* S. caldarius were extracted from the genomic data, and used for a phylogenetic reconstruction. 124 reference McrA protein sequences longer than 450 amino acids from public databases were aligned with Muscle3.7[75], accession numbers of these sequences are provided in the **Supplementary Table 4**. After manual refinement of the alignment a masking filter accounting the alignment ambiguity of each column was designed using the ZORRO software[65]. Phylogenetic trees were calculated using maximum likelihood algorithm RAxML (version 8.2.6 (ref. 76)) with the masking filter and the PROTGAMMA model with LG as amino acid substitution model and empirical base frequencies. These were the best-fitting

conditions according to RAxML using both Akaian and Bayesian information criterion. To find the optimal tree topology 149 bootstraps were calculated according to the bootstrap convergence criterion of RAxML. To verify results of the presented phylogenetic affiliation, the phylogenetic analyses were repeated using IQ-TREE[77] with LG+I+F+C20 as substitution model on the same alignment (**Supplementary Fig. 1a**).

To avoid the possibility of long branch attraction, further partial McrA sequences of *Bathyarchaeota* (**Supplementary Table 4**) were included and only the McrA sequence regions common between the partial McrAs of *Bathyarchaeota* and our previous set of full-length sequences (>300 residues) was considered for phylogenetic analysis. First, it was confirmed that using these regions for phylogenetic analysis resulted in similar tree topology as using the full-length sequences by calculating a phylogenetic tree using RAxML (PROTGAMMALG+I+F) with the respective parts of all full-length sequences (the data set used in the previous phylogenetic analysis; **Supplementary Fig. 1b**). Then the partial sequences of *Bathyarchaeota* were included into the set to perform phylogenetic analysis of the common McrA sequence parts using both RAxML (PROTGAMMALG+I+F, **Supplementary Fig. 1c**) and IQ-tree (LG+I+F+C20, **Supplementary Fig. 1d**). Finally, to check if the overall tree topology was influenced by the deeply-branching SCAL_000352 sequence, a tree using RAxML (PROTGAMMALG+I+F) with only full-length sequences but excluding the SCAL_000352 sequence was constructed (**Supplementary Fig. 1e**). All resulting trees were plotted using the iTol webserver[78].

Verification of different *mcrA* subunits

To test the correct genome assembly and to confirm the presence of four *mcrA* genes per bin, a *mcrA* clone library was constructed. For each of the eight *mcrA* genes found in the two *Ca.* Syntrophoarchaeum bins primer sets were developed, which were used for PCR amplification from Butane50 culture DNA (**Supplementary Table 5**). PCR reactions (20 µl volume) were performed containing 1 µM primer each, 200 µM dNTPs, 1 × PCR buffer, and 0.5 U DNA polymerase (TaKaRa Taq, TaKaRa Bio Europe, France) under the following conditions: initial denaturation at 95°C for 5 min, followed by 39 cycles of denaturation (96°C, 1 min), annealing for 1 min, elongation (72°C, 2 min), and a final elongation step (72°C, 10 min). For two primer sets, amplification was done with Phusion High-Fidelity DNA Polymerase (Thermo Fischer Scientific, Germany) using 50 µl reactions containing 1.5 mM $MgCl_2$, 3% (v/v) DMSO, 0.4 µM primer each, 50 µM dNTPs, 1 × PCR buffer, and 1 U DNA polymerase under the following conditions: initial denaturation at 98°C for 30 s, followed by 39 cycles of denaturation (98°C, 10 s), annealing for 30 s, elongation (72°C, 50 s), and a final elongation step (72°C, 10 min). For annealing temperatures for the individual primer sets see **Supplementary Table 5**. PCR resulted in multiple bands, therefore amplicons of expected size were excised from an 1% agarose gel and purified using the MinElute Gel extraction kit (Qiagen, Germany). DNA was ligated in a pGEM T-Easy vector (Promega, Madison, WI) and transformed into

E. coli TOP10 cells (Invitrogen, Carlsbad, CA) according to the manufacturer's recommendations. Sequencing was performed by *Taq* cycle sequencing using a vector-specific primer (M13F or M13R) with a model ABI377 sequencer (Applied Biosystems). Sequence data were analysed with the ARB software package[56].

Extraction of RNA, library construction and data analysis

Total RNA was extracted from 100 ml of an active Butane50 culture, which was kept at 50°C during the whole procedure: first most medium (>90%) was replaced by butane gas, whereas the biomass remained at the bottom of the bottle. Then RNA was preserved by adding 90 ml preheated RNAlater (Sigma-Aldrich; 10:1 RNAlater vs sample) for 1 h. Subsequently this mixture was filtered through an RNA-free cellulose nitrate filter (pore size 0.45 µm; Sartorius; Göttingen, Germany). The filter was extracted in an RNase-free tube with glass beads and 600 µl of RNA Lysis Buffer (Quick-RNA MiniPrep, Zymoresearch, USA) applying bead beating (2 cycles of 6 m s^{-1} for 20 s). The lysate was cleared by centrifugation (10,000*g*; 1 min) and the supernatant was used for RNA extraction with the Quick-RNA MiniPrep Kit (Zymoresearch, Irvine, CA, USA) according to the manufacturer's guidelines but omitting the on-column DNase treatment step. The RNA extract was cleaned from DNA by incubating it at 37 °C for 40 min with 10 µl of DNase I (DNase I recombinant, RNA-free; Roche Diagnostics, Mannheim, Germany), 7 µl of 10 × incubation buffer (Roche) and 2 µl of RNase-Inhibitor (Protector RNase Inhibitor, Roche Diagnostics, Mannheim, Germany). DNases were inactivated by heating for 10 min to 56 °C. Subsequently the RNA was purified with the RNeasy MinElute Cleanup Kit (QIAGEN, Hilden, Germany). In total 450 ng of high-quality RNA was obtained.

The TruSeq Stranded Total RNA Kit (Illumina) was used for RNA library preparation. The rRNA depletion step was omitted. 80 ng of the total RNA (in 5 µl volume) was combined with 13 µl of 'Fragment, Prime and Finish mix', for the RNA fragmentation step according to the Illumina TruSeq stranded mRNA sample preparation guide. Subsequent steps were performed as described in the sample preparation guide. The library was sequenced on a MiSeq instrument; with v3 sequencing chemistry in 2 × 75 cycles paired-end runs. The resulting reads were pre-processed including removal of adaptors and contaminants and quality trimming to Q10 using bbduk v34 from the BBMAP package. Trimmed reads were used to quantify the 16S rRNA gene based phylogenetic composition of the library by phyloFlash as described above for the DNA paired-end library. Trimmed reads were also mapped to the bins of interest (*Ca.* S. butanivorans, HotSeep-1) using bbmap with a minimum identity of 97%. The expression level of each gene was quantified by counting the number of unambiguously mapped reads per gene using featureCount[79] with the –p option to count fragments instead of reads. To compare expression levels between genes, absolute fragment counts per genes were converted into fragments per kilobase of transcript per million mapped reads (FPKM[80]) as follows:

$$\mathrm{FPKM}_i = \frac{C_i}{L_i \sum_j C_j} \times 10^9$$

where i = any specific gene, j = sum of all the transcribed genes, C = counts and L = length (bp).

Protein analysis by nanoLC-MS/MS

For total protein analysis, the cells from 50 ml of grown (approximately 10 mM sulfide) Butane50 enrichment culture were harvested by centrifugation, frozen in liquid nitrogen and stored at -20°C until analysis. The cell pellets were suspended in 30 µl of 50 mM ammonium bicarbonate buffer, and lysed by three 60 s freeze–thaw cycles between liquid nitrogen and +40°C (thermal shaker, 1,400 r.p.m.). The cell lysate was incubated with 50 mM dithiothreitol at 30°C for 1 h, followed by alkylation with 200 mM iodacetamide for 1 h at room temperature, in the dark, and trypsin digestion (0.6 µg trypsin, Promega) overnight at 37°C. Peptides were desalted using C18 Zip Tip columns (Millipore), and analysed by nLC-MS/MS using an LTQ-Orbitrap mass spectrometer (Thermo Fisher Scientific) equipped with a nanoUPLC system (nanoAquity, Waters) as described previously[81].

Peptide identification was conducted by Proteome Discoverer (version 1.4.1.14, Thermo Fisher Scientific) using the Mascot search engine with the annotated metagenome of *Ca.* Syntrophoarchaeum as a database[81]. Peptides were considered to be identified by Mascot when a probability of 0.05 (probability-based ion score threshold of 40) was achieved. emPAI values calculated by Mascot for identified proteins were used as semi-quantitative measure to estimate the abundance of proteins in the analysed sample[82]. The mass spectrometry proteomics data have been deposited to the ProteomeXchange Consortium[83] via the PRIDE partner repository[84].

Synthesis of authentic standards

To synthesize 1-butyl-CoM and 2-butyl-CoM, 5 g of coenzyme M (Na 2-mercaptoethanesulfonate, purity 98%; Sigma Aldrich) were dissolved in 40 ml of a 30% (v/v) ammonium hydroxide solution, in serum vials. Twice the molar amount of 1-bromobutane (purity 99%; Sigma Aldrich) or 2-bromobutane (purity 98%; Sigma Aldrich) were added, the serum bottles were closed with butyl rubber septa and incubated at room temperature with vigorous shaking (500 r.p.m.) for 4 h. The aqueous phase was separated from the excess hydrophobic 1- or 2-bromobutane via separatory funnels. Residual, dissolved 1- or 2-bromobutane was removed by bubbling with nitrogen. The solutions were analysed for the presence of 1-butyl-CoM or 2-butyl-CoM by FT-ICR-MS analysis without further purification. Both solutions contained a major m/z peak at 197.0311; no m/z peaks were indicative of free CoM, CoM dimers, 1- or 2-bromobutane being detected. Both standards were stable and no interconversion of isomers was observed.

Metabolite extraction

For preparation of cell extracts, volumes of 20 ml were collected from grown Butane50 cultures (sulfide concentrations of 14–15 mM) under anoxic conditions. The cells were harvested by centrifugation (10 min, 10,000 r.p.m., 4 °C), washed twice with a 100 mM ammonium bicarbonate solution, and finally suspended in 1 ml of acetonitrile/methanol/water solution (40:40:20 v/v). Glass beads (0.1 mm diameter, Roth) were added (0.3 g per tube), and the cells were lysed with a PowerLyzer 24 bench top bead-based homogenizer (MO BIO Laboratories, Carlsbad, CA) using 5 cycles of 2,000 r.p.m. for 50 s, with a 15 s pause between cycles. Prior to use, the glass beads were treated with 1N HCl solution and washed twice with deionized water. Glass beads and cell debris were removed by centrifugation, and the aqueous cell extracts were stored in glass vials at 4 °C until analysis.

Mass spectrometry of cell extracts and standards

Authentic standards and cell extract samples were measured with ultra-high resolution mass spectrometry (SolariX XR 12T Fourier transform ion cyclotron resonance mass spectrometer, Bruker Daltonics Inc., Billerica, MA) with negative electrospray ionization (capillary voltage: 4.5 kV) in direct infusion mode (4 µl min^{-1} and 0.1 s accumulation time). Spectra were recorded with a 2 MWord time domain (0.42 s transient length) between *m*/*z* 74 and 3,000 resulting in a mass resolution of approximately 250,000 at *m*/*z* 200. Instrument mass accuracy was linearly calibrated with low-molecular mass fatty acids (C4–C12) between 88 and 199 Da, resulting in an average root-mean square error of the calibration masses of 39 p.p.b. ($n = 7$). For each measurement, 64 (Butane50 samples), or 128 (controls) spectra were co-added (lock mass: 143.10775 *m*/*z*) and internally recalibrated with naturally present fatty acids. Collision induced fragmentation of *m*/*z* 197 was carried out after quadrupole isolation (10 Da window) with 12 V collision energy and 128 scans per measurement (lock mass: 199.17035 *m*/*z*). The 1-butyl-CoM and 2-butyl-CoM standards were diluted to approximately 10 µg ml^{-1} and checked for appropriate collision energy and fragment pattern. Fragment masses 89.0430 ($C_4H_9S^-$) and 80.9652 (HSO_3^-) were then used as indicative fragment for butyl-CoM in the cell extracts. The formation of an even-electron fragment HSO_3^- from bisulfite is favoured when a beta H atom is present[85]. However, $SO_3^{-\bullet}$ (*m*/*z* = 79.9674) was also produced upon fragmentation of the standards.

Fragmentation information of the butyl-CoM standards was used to implement a UPLC-MS/MS method to validate the isomeric form of *m*/*z* 197.031 in the samples. A triple quadrupole mass spectrometer (Xevo TQ-S, Waters Cooperation, Manchester, UK) in negative electrospray ionization mode was used in multiple reaction monitoring (MRM) mode. Indicative butyl-CoM transitions (*m*/*z* 197 > 89 and *m*/*z* 197 > 81) were initially optimized (cone voltage and collision energy) by direct infusion of standard solutions into the mass spectrometer. The mass spectrometer was coupled to a

UPLC (ACQUITY I-Class, Waters Cooperation Milford, MA, USA) equipped with a reversed phase column (HSS T3, 25 cm, Waters) and run with a binary gradient (1% methanol in water to 90% methanol) at a flow rate of 0.3 ml min^{-1}. For each analysis, 10 µl were injected into the UPLC. Retention time, presence of both MRM transitions and relative ion ratios as compared to the standards were used as quality criteria.

Quantification of hydrogen production in experiment

Hydrogen production in the Butane50 culture was measured by analysing the headspace of replicate incubations which were constantly agitated on a shaking table in a 50°C incubator. The butane-dependent sulfide production (and therefore potential hydrogen production) was determined from tracking the sulfide production (as above) for 4 weeks. Gas phase (1 ml) was sampled with a gas-tight syringe to determine hydrogen concentrations (i) before changing the headspace, (ii) after exchanging the headspace in 30 min intervals for 6 h (iii) the next day, before and after addition of sodium molybdate solution (10 mM final concentration) to the culture to stop potential hydrogen-dependent sulfate reduction. Gas phase was immediately injected into a Peak Performer 1 gas chromatograph (Peak Laboratories, Palo Alto, CA) equipped with a reducing compound photometer. Development of hydrogen concentrations were converted into hydrogen production rates and compared with potential hydrogen production rates according to a stoichiometry of 4:1 (H_2 production vs sulfate reduction).

Transmission electron microscopy

A 100 ml grown Butane50 culture was concentrated by centrifugation at 2,000 r.p.m. using a Stat Spin Microprep 2 table-top centrifuge. Aliquots were placed in aluminium platelets of 150 µm depth containing 1-hexadecen[86]. The platelets were frozen using a Leica EM HPM100 high pressure freezer (Leica Mikrosysteme, Wetzlar, Germany). The frozen samples were transferred to an Automatic Freeze Substitution Unit (Leica EM AFS2) and substituted at -90°C in a solution containing anhydrous acetone, 0.1% tannic acid for 24 h and in anhydrous acetone, 2% OsO_4, 0.5% anhydrous glutaraldehyde (Electron Microscopy Sciences, Ft. Washington, USA) for additional 8 h. After a further incubation over 20 h at -20°C samples were warmed up to +4 °C and washed with anhydrous acetone subsequently. The samples were embedded at room temperature in Agar 100 (Epon 812 equivalent) at 60°C over 24 h. Thin sections (80 nm) were examined using a Philips CM 120 BioTwin transmission electron microscope (Philips Inc. Eindhoven, The Netherlands). Images were recorded with a TemCam F416 CMOS camera (TVIPS, Gauting, Germany), for additional images see **Supplementary Fig. 4**.

Data availability

All sequence data are archived in NCBI database under the BioSample number SAMN05004607. Representative full-length 16S rRNA gene sequences of the clone library of the Butane50 culture have

been submitted to NCBI under accession numbers KX812780–KX812802. Draft genomes of the *Ca.* Syntrophoarchaeum organisms can be found under the BioProject accession numbers PRJNA318983 (*Ca.* S. butanivorans) and PRJNA319143 (*Ca.* S. caldarius). Metagenomic and metatranscriptomic reads have been submitted to the short read archive under accession number SRS1505411. The mass spectra of the proteomic data set have been deposited to the ProteomeXchange Consortium with the data set identifier PXD005038.

Acknowledgements

We thank R. Appel, K. Büttner, I. Kattelmann and S. Menger for assistance in cultivation and molecular work, B. Scheer for proteomic analyses, and M. Sickert, J. Then Bergh and K. Dürkop for support in standard synthesis and LC-MS/MS analyses. We thank as well A. Férnandez-Guerra, H. Gruber-Vodicka and P. Offre for supporting us with bioinformatics and biochemistry. We thank A. Boetius for discussions and financial support provided by her Leibniz Grant of the Deutsche Forschungsgemeinschaft (DFG). Research was further financed by the DFG Research Center and Cluster of Excellence MARUM and the Deep Carbon Observatory (Deep Life grant 11121/6152-2121-2329-9973-CC to G.W.), the Max Planck Society and the Helmholtz Society. We are indebted to A. Teske and the shipboard party, the crew and pilots of research expedition AT15-16 Research Vessel Atlantis and Research Submersible Alvin (NSF Grant OCE-0647633). We acknowledge the Centre for Chemical Microscopy (ProVIS) at the Helmholtz Centre for Environmental Research supported by European regional Development Funds (EFRE – Europe funds Saxony) for using their analytical facilities.

Author Contributions

G.W. and F.M. retrieved the original samples and performed cultivation. R.L.-P., G.W. and F.M. designed research. R.L.-P., K.K., K.J.H. and V.K. designed the CARD-FISH probes and performed microscopy. R.L.-P., G.W. and F.M. performed physiological experiments. H.E.T. prepared and sequenced the DNA and RNA libraries. R.L.-P., V.K., D.V.M. and M.R. performed metagenomic and transcriptomic analyses. R.L.-P., K.K. and K.J.H. performed phylogenetic analysis. D.R. performed thin-sectioning and electron microscopy. H.-H.R., L.A. and F.M. performed proteome analyses. T.R., O.L. and F.M. analysed metabolic intermediates. R.L.-P., G.W., F.W. and F.M. developed the metabolic model, and wrote the manuscript with contributions of all co-authors.

Reviewer Information

Nature thanks T. Ettema, M. Jetten, S. Ragsdale and R. Thauer for their contribution to the peer review of this work.

References

1. Simoneit, B. R. T., Kawka, O. E. & Brault, M. Origin of gases and condensates in the Guaymas Basin hydrothermal system (Gulf of California). *Chem. Geol.* **71,** 169–182 (1988).

2. Reeburgh, W. S. Oceanic methane biogeochemistry. *Chem. Rev.* **107,** 486–513 (2007).

3. Boetius, A. & Wenzhofer, F. Seafloor oxygen consumption fuelled by methane from cold seeps. *Nat. Geosci.* **6,** 725–734 (2013).

4. Orphan, V. J., House, C. H., Hinrichs, K. U., McKeegan, K. D. & DeLong, E. F. Methane-consuming archaea revealed by directly coupled isotopic and phylogenetic analysis. *Science* **293,** 484–487 (2001).

5. Boetius, A. *et al.* A marine microbial consortium apparently mediating anaerobic oxidation of methane. *Nature* **407,** 623–626 (2000).

6. Hallam, S. J. *et al.* Reverse methanogenesis: testing the hypothesis with environmental genomics. *Science* **305,** 1457–1462 (2004).

7. Meyerdierks, A. *et al.* Metagenome and mRNA expression analyses of anaerobic methanotrophic archaea of the ANME-1 group. *Environ. Microbiol.* **12,** 422–439 (2010).

8. McGlynn, S. E., Chadwick, G. L., Kempes, C. P. & Orphan, V. J. Single cell activity reveals direct electron transfer in methanotrophic consortia. *Nature* **526,** 531–535 (2015).

9. Wegener, G., Krukenberg, V., Riedel, D., Tegetmeyer, H. E. & Boetius, A. Intercellular wiring enables electron transfer between methanotrophic archaea and bacteria. *Nature* **526,** 587–590 (2015).

10. Claypool, G. E. & Kvenvolden, K. A. Methane and other hydrocarbon gases in marine sediment. *Annu. Rev. Earth Planet. Sci.* **11,** 299–327 (1983).

11. Tissot, B. P. & Welte, D. H. *Petroleum Formation and Occurrence*. (Springer-Verlag, 1984).

12. Kniemeyer, O. *et al.* Anaerobic oxidation of short-chain hydrocarbons by marine sulphate-reducing bacteria. *Nature* **449,** 898–901 (2007).

13. Savage, K. N. *et al.* Biodegradation of low-molecular-weight alkanes under mesophilic, sulfate-reducing conditions: metabolic intermediates and community patterns. *FEMS Microbiol. Ecol.* **72,** 485–495 (2010).

14. Jaekel, U. *et al.* Anaerobic degradation of propane and butane by sulfate-reducing bacteria enriched from marine hydrocarbon cold seeps. *ISME J.* **7,** 885–895 (2013).

15. Adams, M. M., Hoarfrost, A. L., Bose, A., Joye, S. B. & Girguis, P. R. Anaerobic oxidation of short-chain alkanes in hydrothermal sediments: potential influences on sulfur cycling and microbial diversity. *Front. Microbiol.* **4,** 110 (2013).

16. Kleindienst, S. *et al.* Diverse sulfate-reducing bacteria of the Desulfosarcina/Desulfococcus clade are the key alkane degraders at marine seeps. *ISME J.* **8,** 2029–2044 (2014).

17. Kropp, K. G., Davidova, I. A. & Suflita, J. M. Anaerobic oxidation of n-dodecane by an addition reaction in a sulfate-reducing bacterial enrichment culture. *Appl. Environ. Microbiol.* **66,** 5393–5398 (2000)

18. Rabus, R. *et al.* Anaerobic initial reaction of n-alkanes in a denitrifying bacterium: evidence for (1-methylpentyl)succinate as initial product and for involvement of an organic radical in n-hexane metabolism. *J. Bacteriol.* **183,** 1707–1715 (2001).

19. Heider, J. *et al.* Structure and function of benzylsuccinate synthase and related fumarate-adding glycyl radical enzymes. *J. Mol. Microbiol. Biotechnol.* **26,** 29–44 (2016).

20. Gittel, A. *et al.* Ubiquitous presence and novel diversity of anaerobic alkane degraders in cold marine sediments. *Front. Microbiol.* **6,** 1414 (2015)

21. Holler, T. *et al.* Thermophilic anaerobic oxidation of methane by marine microbial consortia. *ISME J.* **5,** 1946–1956 (2011).

22. Orcutt, B. N. *et al.* Impact of natural oil and higher hydrocarbons on microbial diversity, distribution, and activity in Gulf of Mexico cold-seep sediments. *Deep Sea Res. Part II Top. Stud. Oceanogr.* **57,** 2008–2021 (2010).

23. Thauer, R. K. Biochemistry of methanogenesis: a tribute to Marjory Stephenson. 1998 Marjory Stephenson Prize Lecture. *Microbiology* **144,** 2377–2406 (1998)

24. Jaekel, U., Vogt, C., Fischer, A., Richnow, H.-H. & Musat, F. Carbon and hydrogen stable isotope fractionation associated with the anaerobic degradation of propane and butane by marine sulfate-reducing bacteria. *Environ. Microbiol.* **16,** 130–140 (2014).

25. Nauhaus, K., Treude, T., Boetius, A. & Krüger, M. Environmental regulation of the anaerobic oxidation of methane: a comparison of ANME-I and ANME-II communities. *Environ. Microbiol.* **7,** 98–106 (2005)

26. Krukenberg, V. *et al. Candidatus* Desulfofervidus auxilii, a hydrogenotrophic sulfate-reducing bacterium of the HotSeep-1 cluster involved in the thermophilic anaerobic oxidation of methane. *Environ. Microbiol.* **18,** 3073–3091 (2016).

27. Ahn, Y., Krzycki, J. A. & Floss, H. G. Steric course of the reduction of ethyl coenzyme M to ethane catalyzed by methyl coenzyme M reductase from Methanosarcina barkeri. *J. Am. Chem. Soc.* **113,** 4700–4701 (1991).

28. Scheller, S., Goenrich, M., Thauer, R. K. & Jaun, B. Methyl-coenzyme M reductase from methanogenic archaea: isotope effects on label exchange and ethane formation with the homologous substrate ethyl-coenzyme M. *J. Am. Chem. Soc.* **135,** 14985–14995 (2013).

29. Evans, P. N. *et al.* Methane metabolism in the archaeal phylum Bathyarchaeota revealed by genome-centric metagenomics. *Science* **350,** 434–438 (2015).

30. Nauhaus, K., Albrecht, M., Elvert, M., Boetius, A. & Widdel, F. *In vitro* cell growth of marine archaeal-bacterial consortia during anaerobic oxidation of methane with sulfate. *Environ. Microbiol.* **9,** 187–196 (2007).

31. McInerney, M. J., Bryant, M. P., Hespell, R. B. & Costerton, J. W. *Syntrophomonas wolfei* gen. nov. sp. nov., an anaerobic, syntrophic, fatty acid-oxidizing bacterium. *Appl. Environ. Microbiol.* **41,** 1029–1039 (1981).

32. Schmidt, J. E. & Ahring, B. K. Effects of hydrogen and formate on the degradation of propionate and butyrate in thermophilic granules from an upflow anaerobic sludge blanket reactor. *Appl. Environ. Microbiol.* **59,** 2546–2551 (1993).

33. Schmidt, A., Müller, N., Schink, B. & Schleheck, D. A proteomic view at the biochemistry of syntrophic butyrate oxidation in *Syntrophomonas wolfei*. *PLoS One* **8,** e56905 (2013).

34. Wasmund, K. *et al.* Genome sequencing of a single cell of the widely distributed marine subsurface *Dehalococcoidia*, phylum *Chloroflexi*. *ISME J.* **8,** 383–397 (2014).

35. Stokke, R., Roalkvam, I., Lanzen, A., Haflidason, H. & Steen, I. H. Integrated metagenomic and metaproteomic analyses of an ANME-1-dominated community in marine cold seep sediments. *Environ. Microbiol.* **14,** 1333–1346 (2012).

36. Mock, J., Wang, S., Huang, H., Kahnt, J. & Thauer, R. K. Evidence for a hexaheteromeric methylenetetrahydrofolate reductase in *Moorella thermoacetica*. *J. Bacteriol.* **196,** 3303–3314 (2014).

37. Möller-Zinkhan, D. & Thauer, R. K. Anaerobic lactate oxidation to 3 CO_2 by *Archaeoglobus fulgidus* via the carbon monoxide dehydrogenase pathway: demonstration of the acetyl-CoA carbon-carbon cleavage reaction in cell extracts. *Arch. Microbiol.* **153,** 215–218 (1990).

38. Summers, Z. M. *et al.* Direct exchange of electrons within aggregates of an evolved syntrophic coculture of anaerobic bacteria. *Science* **330,** 1413–1415 (2010).

39. Weghoff, M. C., Bertsch, J. & Müller, V. A novel mode of lactate metabolism in strictly anaerobic bacteria. *Environ. Microbiol.* **17,** 670–677 (2015) .

40. Callaghan, A. V. Metabolomic investigations of anaerobic hydrocarbon-impacted environments. *Curr. Opin. Biotechnol.* **24,** 506–515 (2013).

41. Musat, F. The anaerobic degradation of gaseous, nonmethane alkanes – from in situ processes to microorganisms. *Comput. Struct. Biotechnol. J.* **13,** 222–228 (2015).

42. So, C. M., Phelps, C. D. & Young, L. Y. Anaerobic transformation of alkanes to fatty acids by a sulfate-reducing bacterium, strain Hxd3. *Appl. Environ. Microbiol.* **69,** 3892–3900 (2003).

43. Heider, J., Szaleniec, M., Sünwoldt, K. & Boll, M. Ethylbenzene dehydrogenase and related molybdenum enzymes involved in oxygen-independent alkyl chain hydroxylation. *J. Mol. Microbiol. Biotechnol.* **26,** 45–62 (2016).

44. Klenk, H.-P. *et al.* The complete genome sequence of the hyperthermophilic, sulphate-reducing archaeon *Archaeoglobus fulgidus*. *Nature* **390,** 364–370 (1997).

45. Ferry, J. G. Biochemistry of methanogenesis. *Crit. Rev. Biochem. Mol. Biol.* **27,** 473–503 (1992).

46. Baker, B. J. *et al.* Genomic inference of the metabolism of cosmopolitan subsurface Archaea, Hadesarchaea. *Nat. Microbiol.* **1,** 16002 (2016).

47. Stagars, M. H., Ruff, S. E., Amann, R. & Knittel, K. High diversity of anaerobic alkane-degrading microbial communities in marine seep sediments based on (1-methylalkyl)succinate synthase genes. *Front. Microbiol.* **6,** 1511 (2016).

48. Rabus, R., Boll, M., Golding, B. & Wilkes, H. Anaerobic degradation of *p*-alkylated benzoates and toluenes. *J. Mol. Microbiol. Biotechnol.* **26,** 63–75 (2016).

References Methods

49. Widdel, F. & Bak, F. in *The Prokaryotes* Vol. 4 (ed Trüper HG Balows A, Dworkin M, Harder W, Schleifer KH) 3352–3378 (Springer, 1992).

50. Cord-Ruwisch, R. A quick method for the determination of dissolved and precipitated sulfides in cultures of sulfate-reducing bacteria. *J. Microbiol Methods* **4,** 33–36 (1985).

51. Muyzer, G., Teske, A., Wirsen, C. O. & Jannasch, H. W. Phylogenetic relationships of *Thiomicrospira* species and their identification in deep-sea hydrothermal vent samples by denaturing gradient gel electrophoresis of 16S rDNA fragments. *Arch. Microbiol.* **164,** 165–172 (1995).

52. Massana, R., Murray, A. E., Preston, C. M. & DeLong, E. F. Vertical distribution and phylogenetic characterization of marine planktonic Archaea in the Santa Barbara Channel. *Appl. Environ. Microbiol.* **63,** 50–56 (1997).

53. Teske, A. *et al.* Microbial diversity of hydrothermal sediments in the Guaymas Basin: evidence for anaerobic methanotrophic communities. *Appl. Environ. Microbiol.* **68,** 1994–2007 (2002).

54. von Netzer, F. *et al.* Enhanced gene detection assays for fumarate-adding enzymes allow uncovering of anaerobic hydrocarbon degraders in terrestrial and marine systems. *Appl. Environ. Microbiol.* **79,** 543–552 (2013).

55. Callaghan, A. V. *et al.* Diversity of benzyl- and alkylsuccinate synthase genes in hydrocarbon-impacted environments and enrichment cultures. *Environ. Sci. Technol.* **44,** 7287–7294 (2010).

56. Ludwig, W. *et al.* ARB: a software environment for sequence data. *Nucleic Acids Res.* **32,** 1363–1371 (2004).

57. Quast, C. *et al.* The SILVA ribosomal RNA gene database project: improved data processing and web-based tools. *Nucleic Acids Res.* **41,** D590–D596 (2013).

58. Pernthaler, A., Pernthaler, J. & Amann, R. Fluorescence *in situ* hybridization and catalyzed reporter deposition for the identification of marine bacteria. *Appl. Environ. Microbiol.* **68,** 3094–3101 (2002).

59. Zhou, J., Bruns, M. A. & Tiedje, J. M. DNA recovery from soils of diverse composition. *Appl. Environ. Microbiol.* **62,** 316–322 (1996).

60. Bankevich, A. *et al.* SPAdes: a new genome assembly algorithm and its applications to single-cell sequencing. *J. Comput. Biol.* **19,** 455–477 (2012).

61. Strous, M., Kraft, B., Bisdorf, R. & Tegetmeyer, H. E. The binning of metagenomic contigs for microbial physiology of mixed cultures. *Front. Microbiol.* **3,** 410 (2012).

62. Lagesen, K. *et al.* RNAmmer: consistent and rapid annotation of ribosomal RNA genes. *Nucleic Acids Res.* **35,** 3100–3108 (2007).

63. Shannon, P. *et al.* Cytoscape: a software environment for integrated models of biomolecular interaction networks. *Genome Res.* **13,** 2498–2504 (2003).

64. Albertsen, M. *et al.* Genome sequences of rare, uncultured bacteria obtained by differential coverage binning of multiple metagenomes. *Nat. Biotechnol.* **31,** 533–538 (2013).

65. Wu, M. & Scott, A. J. Phylogenomic analysis of bacterial and archaeal sequences with AMPHORA2. *Bioinformatics* **28,** 1033–1034 (2012).

66. Parks, D. H., Imelfort, M., Skennerton, C. T., Hugenholtz, P. & Tyson, G. W. CheckM: assessing the quality of microbial genomes recovered from isolates, single cells, and metagenomes. Report No. 2167-9843, (PeerJ PrePrints, 2014)

67. Schattner, P., Brooks, A. N. & Lowe, T. M. The tRNAscan-SE, snoscan and snoGPS web servers for the detection of tRNAs and snoRNAs. *Nucleic Acids Res.* **33,** W686–W689 (2005).

68. Aziz, R. K. *et al.* The RAST Server: rapid annotations using subsystems technology. *BMC Genomics* **9,** 75 (2008).

69. Meyer, F. *et al.* GenDB–an open source genome annotation system for prokaryote genomes. *Nucleic Acids Res.* **31,** 2187–2195 (2003).

70. Delcher, A. L., Bratke, K. A., Powers, E. C. & Salzberg, S. L. Identifying bacterial genes and endosymbiont DNA with Glimmer. *Bioinformatics* **23,** 673–679 (2007).

71. Quast, C. *MicHanThi-design and Implementation of a System for the Prediction of Gene Functions in Genome Annotation Projects*. Diploma Thesis, Universität Bremen (2006).

72. Richter, M. *et al.* JCoast - a biologist-centric software tool for data mining and comparison of prokaryotic (meta)genomes. *BMC Bioinformatics* **9,** 177 (2008).

73. Richter, M. & Rosselló-Móra, R. Shifting the genomic gold standard for the prokaryotic species definition. *Proc. Natl Acad. Sci. USA* **106,** 19126–19131 (2009).

74. Yu, N. Y. *et al.* PSORTb 3.0: improved protein subcellular localization prediction with refined localization subcategories and predictive capabilities for all prokaryotes. *Bioinformatics* **26,** 1608–1615 (2010).

75. Edgar, R. C. MUSCLE: multiple sequence alignment with high accuracy and high throughput. *Nucleic Acids Res.* **32,** 1792–1797 (2004).

76. Stamatakis, A. RAxML-VI-HPC: maximum likelihood-based phylogenetic analyses with thousands of taxa and mixed models. *Bioinformatics* **22,** 2688–2690 (2006).

77. Letunic, I. & Bork, P. Interactive Tree Of Life (iTOL): an online tool for phylogenetic tree display and annotation. *Bioinformatics* **23,** 127–128 (2007).

78. Nguyen, L.-T., Schmidt, H. A., von Haeseler, A. & Minh, B. Q. IQ-TREE: a fast and effective stochastic algorithm for estimating maximum-likelihood phylogenies. *Mol. Biol. Evol.* **32,** 268–274 (2015).

79. Liao, Y., Smyth, G. & Shi, W. featureCounts: an efficient general-purpose read summarization program. *Bioinformatics* **30,** 923–930 (2013).

80. Mortazavi, A., Williams, B. A., McCue, K., Schaeffer, L. & Wold, B. Mapping and quantifying mammalian transcriptomes by RNA-seq. *Nat. Methods* **5,** 621–628 (2008).

81. Wagner, A., Cooper, M., Ferdi, S., Seifert, J. & Adrian, L. Growth of *Dehalococcoides mccartyi* strain CBDB1 by reductive dehalogenation of brominated benzenes to benzene. *Environ. Sci. Technol.* **46,** 8960–8968 (2012).

82. Ishihama, Y. *et al.* Exponentially modified protein abundance index (emPAI) for estimation of absolute protein amount in proteomics by the number of sequenced peptides per protein. *Mol. Cell. Proteomics* **4,** 1265–1272 (2005).

83. Vizcaíno, J. A. *et al.* ProteomeXchange provides globally coordinated proteomics data submission and dissemination. *Nat. Biotechnol.* **32,** 223–226 (2014).

84. Vizcaíno, J. A. *et al.* 2016 update of the PRIDE database and its related tools. *Nucleic Acids Res.* **44** (D1), D447–D456 (2016).

85. Jariwala, F. B., Wood, R. E., Nishshanka, U. & Attygalle, A. B. Formation of the bisulfite anion (HSO_3^-, *m*/*z* 81) upon collision-induced dissociation of anions derived from organic sulfonic acids. *J. Mass Spectrom.* **47,** 529–538 (2012).

86. Studer, D., Michel, M. & Müller, M. High pressure freezing comes of age. *Scanning Microsc. Suppl.* **3,** 253–268, discussion 268–269 (1989).

Figures and Tables

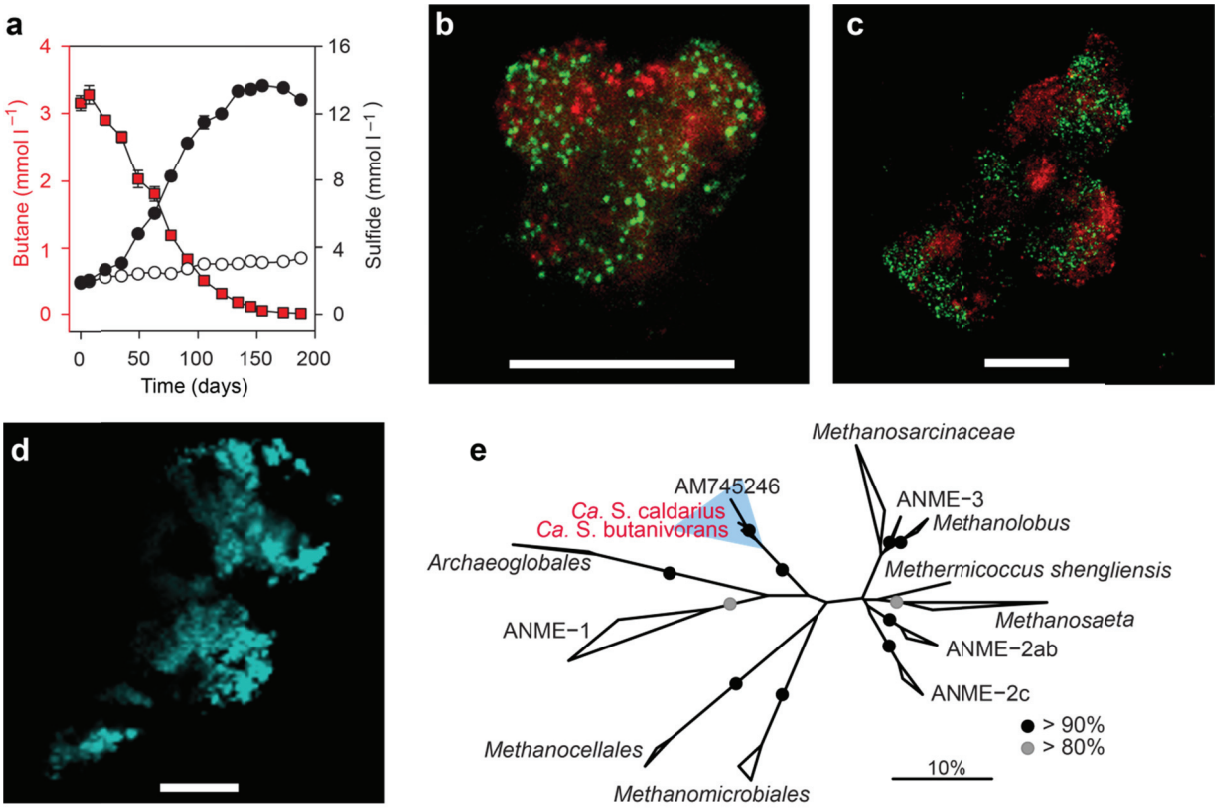

Figure 1 Characterization of the Butane50 culture. a, The Butane50 culture consumed butane (red squares) coupled to the reduction of sulfate to sulfide (black circles); no sulfide was produced in cultures without butane (white circles). Error bars, standard deviation; $n = 3$. **b**, **c**, Fluorescence micrographs of Butane50 consortia stained with specific probes for GoM-Arch87 (red) and HotSeep-1 (green); representative for 20 recorded images. Scale bar, 10 μm. **d**, Autofluorescence of microbial consortia visualized using excitation light at 405 nm and a long-pass emission filter (>463 nm). The autofluorescence maximum at 470 nm is indicative of the presence of the cofactor F_{420}; representative for 10 recorded images. Scale bar, 10 μm. **e**, Phylogenetic affiliation of the 16S rRNA gene sequences from the studied *Ca.* Syntrophoarchaeum strains (in red) within the *Euryarchaeota.* The GoM-Arch87 cluster is indicated with blue background; bar = 10% estimated sequence divergence; bootstraps values >80% and >90% are indicated by grey and black circles, respectively.

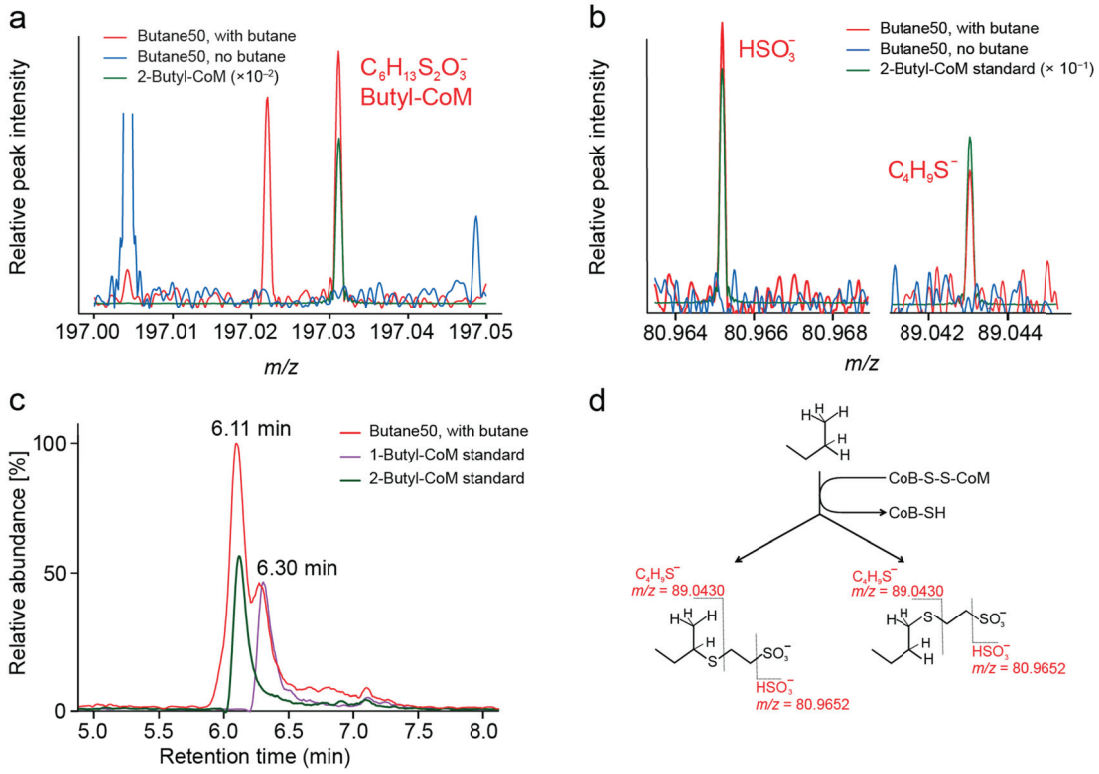

Figure 2 Butyl-CoM as initial metabolic intermediate in butane oxidation a, Full scan mass spectrum of Butane50 culture extracts (Butane50, with butane; $n = 6$ at different time points) revealed a peak at $m/z = 197.0312$, which matches the butyl-CoM standard (mass accuracy +0.18 p.p.m.). This mass peak was absent in control incubations without butane (Butane50, no butane; for more controls see **Extended Data Fig. 2**). **b**, Isolation and collision induced fragmentation of this mass peak yielded bisulfite (mass accuracy +0.03 p.p.m.) and butylthiol (mass accuracy +0.01 p.p.m.), which are likewise produced by fragmentation of the butyl-CoM standards. **c**, Liquid chromatography resolved the presence of the two isomers: 1- and 2-butyl-CoM in the culture ($n = 4$ at different sulfide concentrations). **d**, Interpretation of these analyses. Butane is activated by ligation to coenzyme M by MCR-like enzymes, yielding both 1- and 2-butyl-CoM with identical fragmentation patterns.

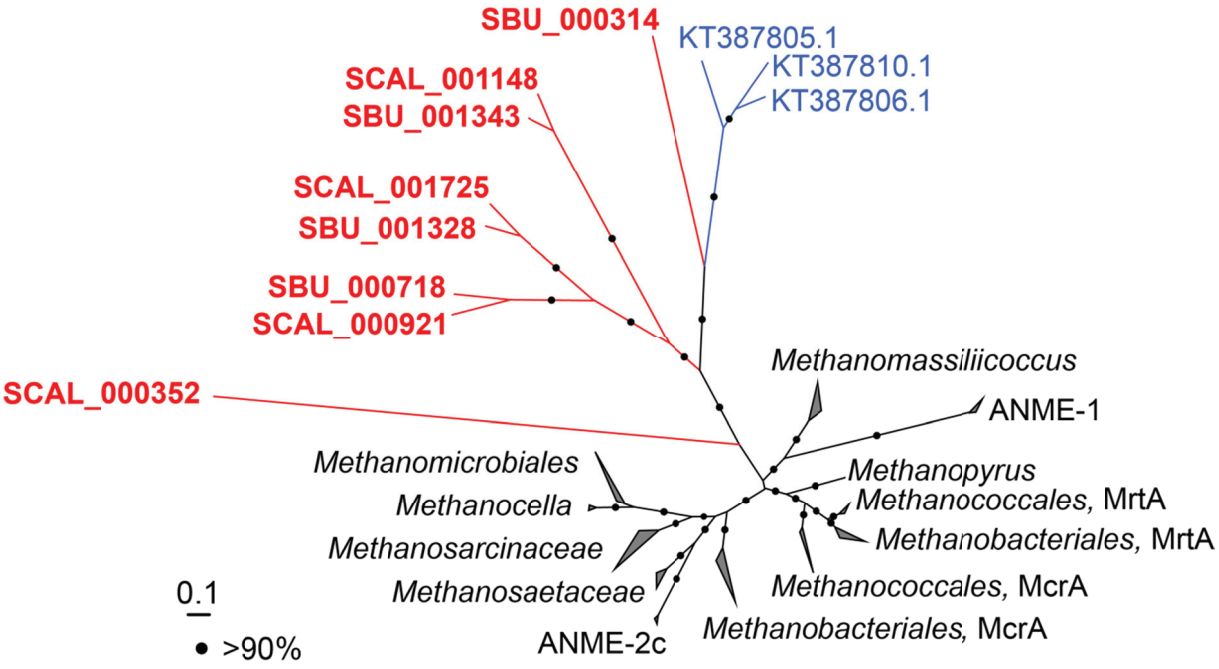

Figure 3 Phylogenetic affiliation of McrA amino acid sequences present in *Ca.* S. butanivorans and *Ca.* S. caldarius. The phylogenetic tree was constructed based on a maximum likelihood algorithm considering more than 450 amino acid positions. Red branches, sequences from *Ca.* Syntrophoarchaeum; SBU, *Ca.* S. butanivorans; SCAL, *Ca.* S. caldarius; the identifiers refer to the locus tag of the gene sequences in the draft genomes. Blue branches indicate *Bathyarchaeota*-related sequences from Evans *et al.*[29]. The scale bar indicates the number of amino acid substitutions per site. Bootstrap values higher than 90% are indicated by filled circles on the corresponding branch. MrtA is synonymous to McrA II in the corresponding groups.

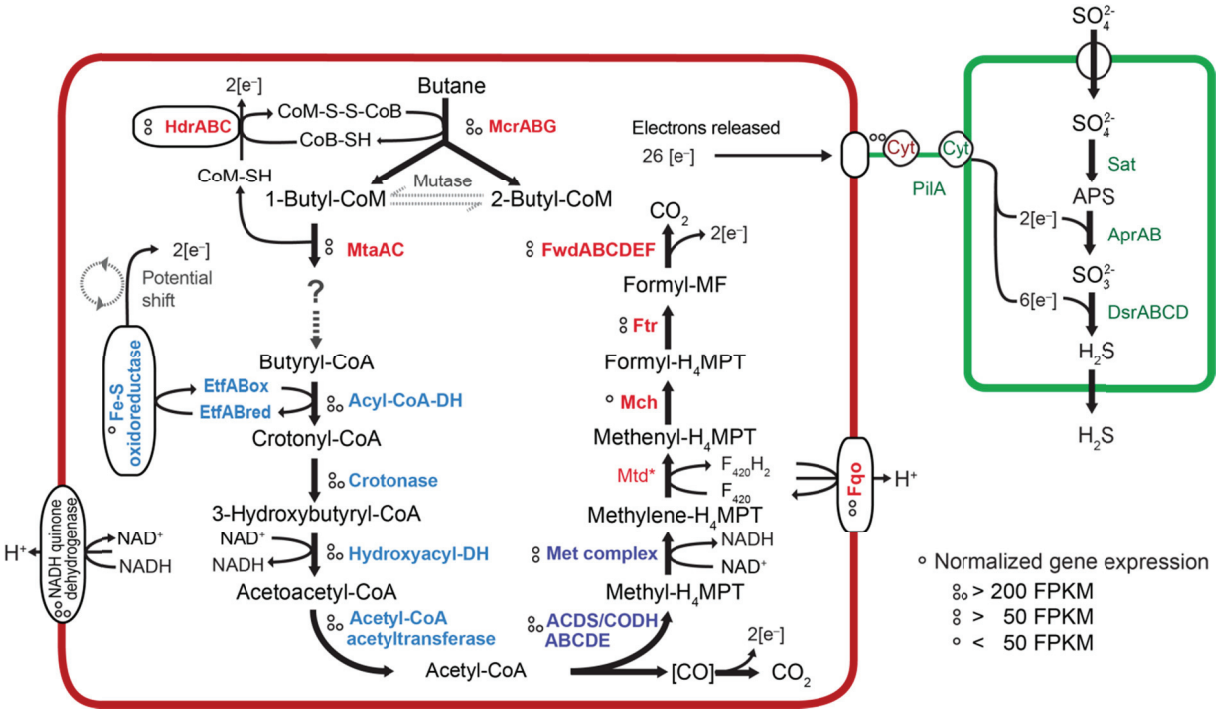

Figure 4 Metabolic scheme proposed for butane oxidation with sulfate based on molecular analyses. *Ca.* Syntrophoarchaeum (red cell) uses steps of the methanogenesis pathway (red labels) to activate butane and to oxidize methylene-tetrahydromethanopterin to CO_2. Butyryl-CoA oxidation is catalysed by enzymes shared with syntrophic bacteria (blue labels). Acetyl-CoA is oxidized by a reverse Wood–Ljungdahl pathway (violet labels). Reducing equivalents are transferred via cytochromes (produced by both organisms) and pili-based nanowires to the sulfate-reducing HotSeep-1 partner bacterium (green cell and labels). Normalized gene expression for *Ca.* S. butanivorans is indicated as FPKM (fragments per kilobase of transcript per million mapped reads) according to the legend code; enzyme names in bold indicate their detection in protein extracts; dotted arrows mark hypothetical pathways without detected genes; **mtd* has only been detected in the more complete genome of *Ca.* S. caldarius. Symbol [e^-] indicates electrons bound to haem or [FeS] clusters in proteins, or to unknown or non-specified carriers. H_2O, energy conservation and biosynthesis are not indicated.

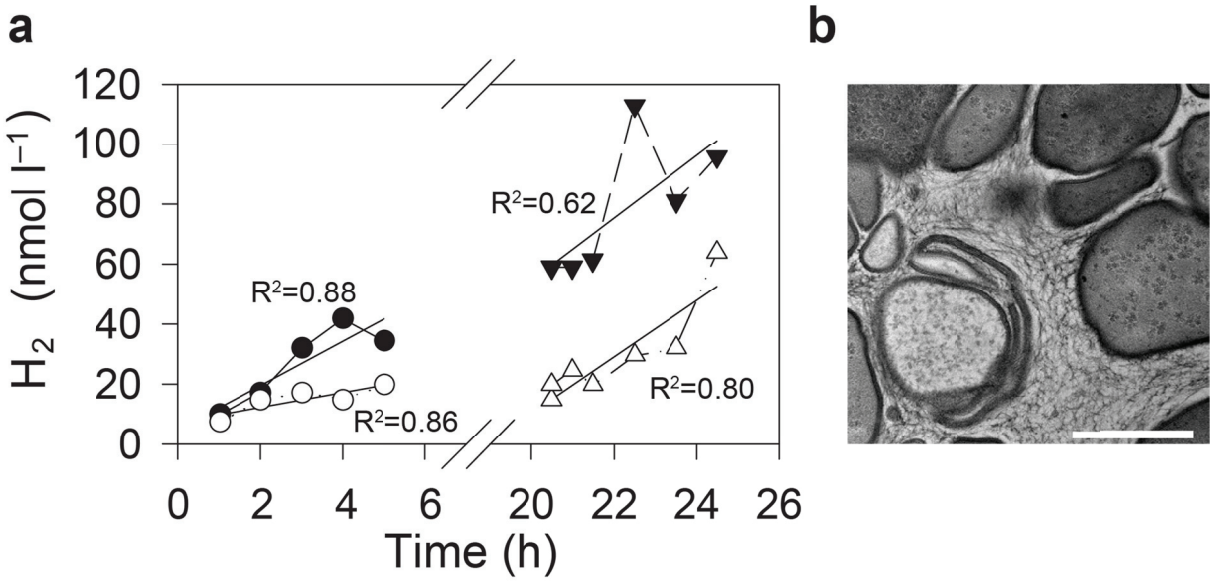

Figure 5 Testing metabolic interaction of *Ca.* Syntrophoarchaeum and *Ca.* D. auxilii in Butane50 cultures. **a**, Development of hydrogen concentration in active Butane50 cultures ($n = 2$) without molybdate (circles), and with 10 mM molybdate (triangles) added the next day to inhibit sulfate reduction. H_2 production was 3–7 nmol l^{-1} h^{-1} and therefore four orders of magnitude below 46,000 nmol l^{-1} h^{-1} needed to account for the observed butane-dependent sulfate reduction rate of 11,500 nmol l^{-1} h^{-1} via H_2 as the intermediate. **b**, Transmission electron micrograph of a thin-section of an EPON 812 embedded consortium. The intercellular space in the consortium contains abundant nanowire-like structures. Scale bar, 0.5 μm; representative for >30 recorded images.

Extended Data

Extended Data Figures

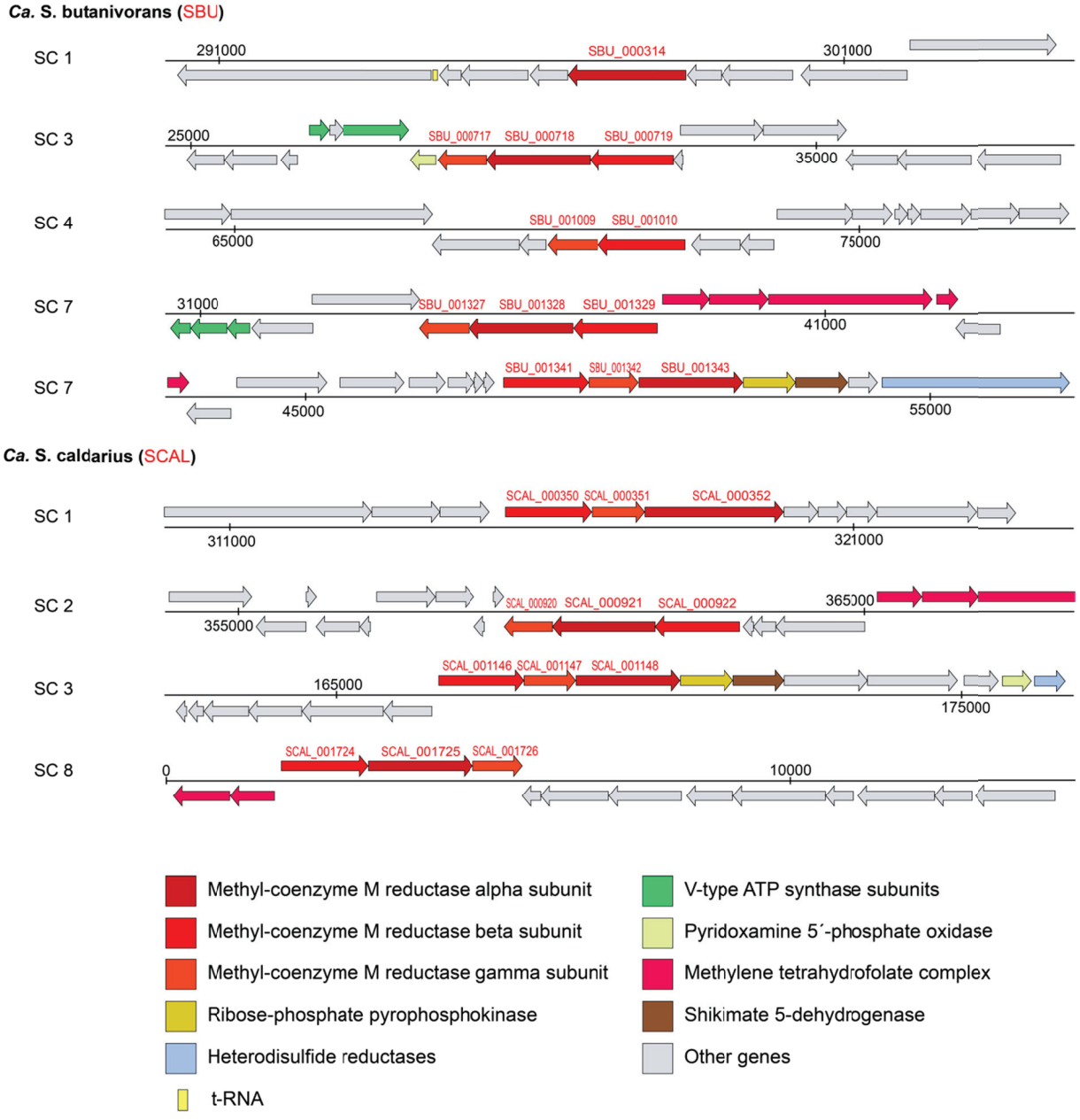

Extended Data Figure 1 | Genetic structure of *mcr* genes in *Ca.* Syntrophoarchaeum. In *Ca*. S. butanivorans one *mcr* gene set is separated, with the *mcrA* subunit in scaffold 1, and *mcrB* and *mcrG* in scaffold 4.

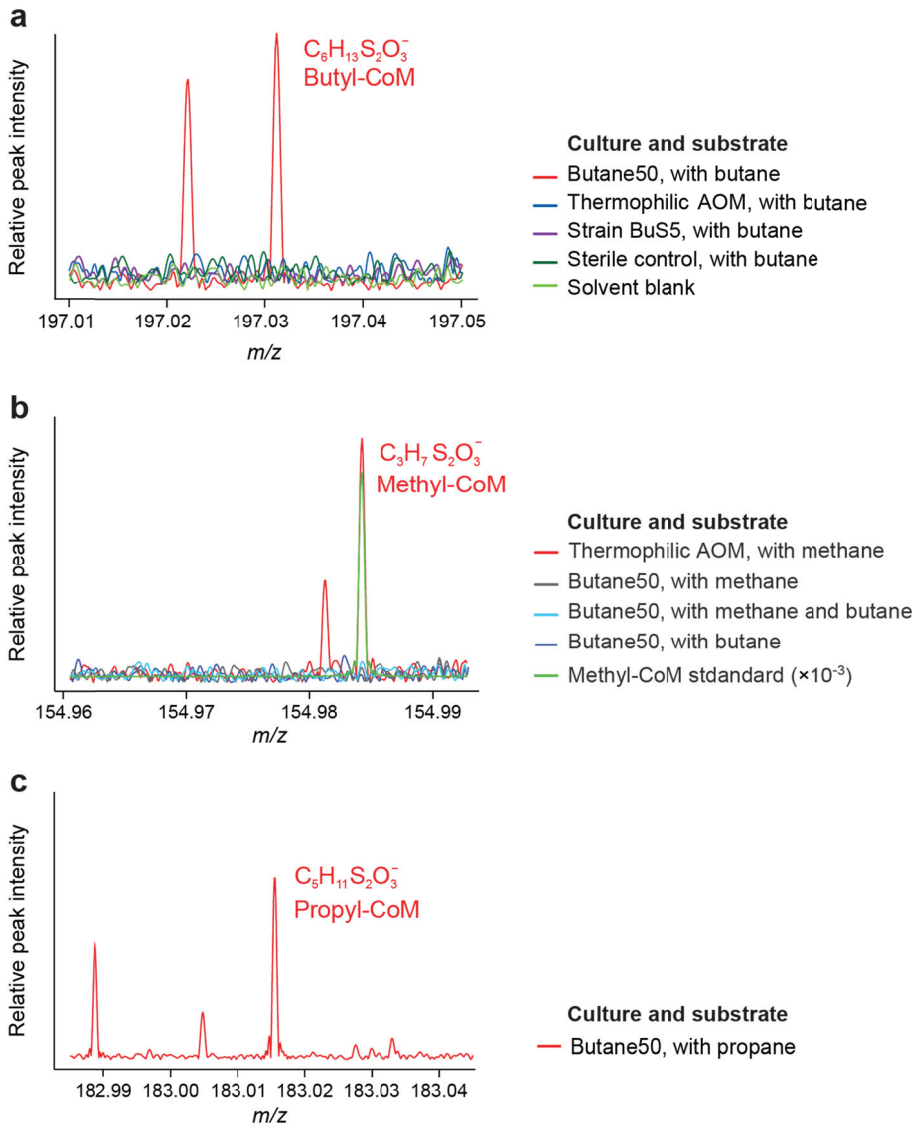

Extended Data Figure 2 | Experiments validating production of alkyl-CoM compounds in anaerobic cultures. a, Screening for butyl-CoM in Butane50, in a thermophilic AOM culture supplied with butane ($n = 2$ with 2 different sampling time points), in BuS5 cultures ($n = 3$) and in controls. The mass peak of butyl-CoM ($m/z = 197.0312$) was only found in the Butane50 culture. **b**, Screening for methyl-CoM ($m/z = 154.984$; mass accuracy –0.15 p.p.m.) in the thermophilic AOM culture supplied with methane ($n = 3$) and in the Butane50 culture ($n = 2$). Methyl-CoM was only found in the thermophilic AOM culture. These analyses (**a**, **b**) indicate high specificity for either butane or methane in the corresponding cultures. **c**, Screening for propyl-CoM ($m/z = 183.016$; mass accuracy –0.21 p.p.m.) in the propane-degrading culture ($n = 1$) showing activation of this substrate with CoM.

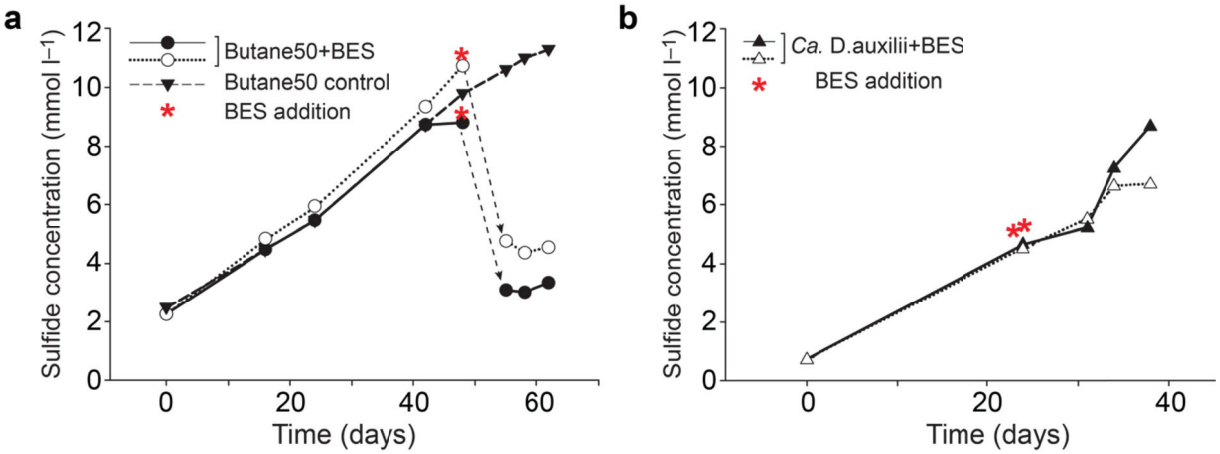

Extended Data Figure 3 | Effect of bromoethanesulfonate (BES, 5 mM final concentration) on Butane50 and *Ca.* D. auxilii cultures. a, Upon addition of BES, butane-dependent sulfate reduction in Butane50 cultures (circles, $n = 2$) was immediately inhibited compared to a control without BES (triangles, $n = 1$). **b**, By contrast, BES addition had no influence on hydrogen-dependent sulfate reduction in *Ca.* D. auxilii cultures (triangles, $n = 2$).

Extended Data Tables

Extended Data Table 1 | Microbial diversity in the AOM enrichment[21] used as inoculum and in the Butane50 culture.

Phylogenetic group	Clones	Clones	Metagenome reads	Metatranscriptome reads
Archaea				
Euryarchaeota				
Methanomicrobia				
GoM-Arch87		46	596	32009
Methermicoccus				2316
ANME-1	46			1465
Thermoplasmata	6			
19c-33 cluster		38	199	
pMC2A24 cluster		1	30	
20c-4 cluster			132	
Halobacteria	4			
Sum	**56**	**85**	**957**	**35790**
Bacteria				
Proteobacteria				
Deltaproteobacteria				
HotSeep-1 cluster	53	63	575	4780
Syntrophobacteraceae	1	5		626
Others	3	3		
Spirochaete				
Kazan-3B-09		1		
TA06		8	44	
Candidate division OP3	3	6	36	
Candidate division KB1			159	827
Candidate division WS3			33	
BHI80-139		1		
Chloroflexi	3			
Anaerolineaceae		3	138	
Others	17			
Sum	**80**	**92**	**985**	**6233**

*Based on 16S rRNA gene sequences retrieved by clone library approach from the Butane50 culture, and found in the metagenome and metatranscriptome libraries using the phyloFlash software. Taxa which account for ≥1% of all 16S rRNA gene sequences are shown.

Extended Data Table 2 | Draft genome information and pairwise comparison of whole genome identity of *Ca.* S. butanivorans and the *Ca.* S. caldarius.

	***Candidatus* Syntrophoarchaeum butanivorans**	***Candidatus* Syntrophoarchaeum caldarius**
Size (base pairs)	1,456,963	1,666,081
Scaffolds/Contigs	16/21	10/15
Scaffold N50 (bp)	219,218	410,601
Coverage (times)	360	134
GC content (%)	48.7	45.5
Number of ORFs	1,604	1,790
rRNAs	3	3
tRNAs	39	44
Genome completeness (%)	85[1]; 88[2]; 89[3]	95[1]; 97[2]; 96[3]
Contamination[3] (%)	0.97	0.32
Duplication of single copy genes[3]	2	1
Strain heterogeneity[3] (%)	0	0

	Average nucleotide identity (Blast)	**Average nucleotide identity (MUMmer)**	**Tetranucleotide frequency**
Ca. S. butanivorans/*Ca.* S. caldarius	73.57	89.57	88.19
Ca. S. caldarius/*Ca.* S. butanivorans	73.56	89.03	88.19

[1]Based on tRNA completeness, using tRNAscan.

[2]Based on archaea-specific single-copy genes, using AMPHORA2.

[3]Based on lineage-specific marker genes of *Euryarchaeota*, using CheckM.

Extended Data Table 3 | Genes encoding enzymes for butane activation, candidates for further conversion reactions and butyryl-CoA oxidation in *Ca.* S. butanivorans.

Gene	Feature	Locus tag	Transcriptome		Proteome
			Absolute reads	FPKM	emPAI
Butane activation					
mcrA	Methyl coenzyme M reductase subunit alpha	SBU_000314	8320	491.4	0.15
mcrA	Methyl coenzyme M reductase subunit alpha	SBU_000718	1640	108.9	0.05
mcrA	Methyl coenzyme M reductase subunit alpha	SBU_001328	514	34.1	0.07
mcrA	Methyl coenzyme M reductase subunit alpha	SBU_001343	1077	70.5	0.11
mcrB	Methyl coenzyme M reductase subunit beta	SBU_000719	5047	418.0	0.07
mcrB	Methyl coenzyme M reductase subunit beta	SBU_001010	2628	210.1	0.46
mcrB	Methyl coenzyme M reductase subunit beta	SBU_001329	311	25.7	
mcrB	Methyl coenzyme M reductase subunit beta	SBU_001341	602	49.0	0.3
mcrG	Methyl coenzyme M reductase subunit gamma	SBU_000717	689	97.7	
mcrG	Methyl coenzyme M reductase subunit gamma	SBU_001009	1787	243.0	0.5
mcrG	Methyl coenzyme M reductase subunit gamma	SBU_001327	642	91.4	
mcrG	Methyl coenzyme M reductase subunit gamma	SBU_001342	366	52.3	0.37
hdrA	CoB--CoM heterodisulfide reductase subunit A	SBU_000296	2586	94.9	0.12
hdrB	CoB--CoM heterodisulfide reductase subunit B	SBU_000294	222	27.4	
hdrC	CoB--CoM heterodisulfide reductase subunit C	SBU_000295	127	36.3	0.35
hdrA	Heterodisulfide reductase subunit A	SBU_001347	459	16.9	
hdrA	Heterodisulfide reductase subunit A	SBU_001502	903	60.7	0.05
hdrA	Heterodisulfide reductase subunit A	SBU_001503	995	56.9	0.14
Candidates for conversion to butyryl-CoA					
mtaA	Methyltransferase corrinoid activation protein	SBU_000376	1503	83.6	0.36
mtaA	Methylcobamide:CoM methyltransferase	SBU_000378	583	61.7	0.09
mtaA	Methylcobamide:CoM methyltransferase	SBU_000450	988	101.7	0.61
mtaA	Methylcobamide:CoM methyltransferase	SBU_001175	274	28.4	
mtaA	Methylcobamide:CoM methyltransferase	SBU_001379	133	13.6	
mtaA	Methylcobamide:CoM methyltransferase	SBU_001480	553	57.7	0.08
mtaC	Corrinoid protein	SBU_000377	1016	156.7	1.33
mtaC	Corrinoid methyltransferase	SBU_001174	95	16.0	
Butyryl-CoA oxidation					
	Acyl-CoA dehydrogenase domain-containing protein	SBU_000172	1751	168.5	1.43
	Acyl-CoA dehydrogenase	SBU_000399	2844	205.1	0.55
	Acyl-CoA dehydrogenase domain-containing protein	SBU_000724	449	42.9	0.25
	Acyl-CoA dehydrogenase	SBU_001146	177	12.4	0.11
crt	Crotonase	SBU_000400	1745	236.4	1.65
	3-Hydroxyacyl-CoA dehydrogenase	SBU_000288	2425	312.5	0.81
	3-Hydroxyacyl-CoA dehydrogenase	SBU_000843	1151	162.5	0.12
	Acetyl-CoA acetyltransferase	SBU_000329	103	9.8	
	Acetyl-CoA acetyltransferase	SBU_000402	3198	295.4	0.34
	Acetyl-CoA acetyltransferase	SBU_000404	1644	152.6	0.16
	Acetyl-CoA acetyltransferase	SBU_001291	161	15.5	
etfA	Electron transfer flavoprotein subunit alpha	SBU_000173	557	63.6	0.10
etfB	Electron transfer flavoprotein subunit beta	SBU_000174	506	69.8	0.58
	Fe-S Oxidoreductase	SBU_000175	402	38.8	0.55

Expression as absolute read counts and as fragments per kilobase of transcript per million mapped reads (FPKM) is shown, as well as the corresponding protein abundance as emPAI index.

Extended Data Table 4 | Genes encoding enzymes of C-1 pathway in *Ca.* S. butanivorans

Gene	Feature	Locus_tag	Transcriptome		Proteome
			Absolute reads	FPKM	emPAI
cdhA	Acetyl-CoA decarbonylase/synthase complex alpha	SBU_000891	3756	172.8	0.65
cdhA	Acetyl-CoA decarbonylase/synthase complex alpha	SBU_001568	1518	70.5	0.05
cdhB	Acetyl-CoA decarbonylase/synthase complex epsilon	SBU_000890	557	120.8	0.64
cdhB	Acetyl-CoA decarbonylase/synthase complex epsilon	SBU_001569	325	65.1	0.35
cdhC	Acetyl-CoA decarbonylase/synthase complex beta	SBU_000889	4798	350.2	0.96
cdhC	Acetyl-CoA decarbonylase/synthase complex beta	SBU_001570	2738	212.9	0.09
cdhD	Acetyl-CoA decarbonylase/synthase complex delta	SBU_000887	3183	232.8	3.03
cdhD	Acetyl-CoA decarbonylase/synthase complex delta	SBU_001572	940	79.6	1.41
cdhE	Acetyl-CoA decarbonylase/synthase complex gamma	SBU_000886	3419	266.4	0.52
cdhE	Acetyl-CoA decarbonylase/synthase complex gamma	SBU_001573	1503	118.6	1.21
metV	5,10-Methylenetetrahydrofolate reductase, C-terminal	SBU_000428	220	36.2	
metF	5,10-Methylenetetrahydrofolate reductase	SBU_000429	487	59.8	0.01
hdrA	Heterodisulfide reductase subunit A	SBU_000430	1435	80.5	
hdrB	Heterodisulfide reductase subunit B	SBU_000431	703	45.3	
hdrC	Heterodisulfide reductase subunit C	SBU_000432	1259	81.5	
mvhD	Methyl-viologen-reducing hydrogenase delta subunit	SBU_000433	356	53.9	
hdrA	Heterodisulfide reductase subunit A	SBU_000434	839	47.2	
mvhD	Methyl-viologen-reducing hydrogenase delta subunit	SBU_000435	585	154	
metV	5,10-Methylenetetrahydrofolate reductase, C-terminal	SBU_001330	263	39.4	0.25
metF	5,10-Methylenetetrahydrofolate reductase	SBU_001331	711	83.9	0.20
hdr	Heterodisulfide reductase	SBU_001332	392	16.5	
mvhD	Methyl-viologen-reducing hydrogenase delta subunit	SBU_001333	170	57.4	
mch	N(5)N(10)-MethenylH4MPT cyclohydrolase	SBU_000838	197	22.6	0.10
ftr	FormylMF-H4MPT formyltransferase	SBU_001141	416	51.4	0.10
fwdA	Formylmethanofuran dehydrogenase subunit A	SBU_000443	1215	79.2	0.11
fwdB	Formylmethanofuran dehydrogenase subunit B	SBU_000444	555	47.3	
fwdB	Formylmethanofuran dehydrogenase subunit B	SBU_000048	226	21.4	
fwdC	Formylmethanofuran dehydrogenase subunit C	SBU_000442	567	81.3	0.12
fwdD	Formylmethanofuran dehydrogenase subunit D	SBU_000047	75	20.6	
fwdD	Formylmethanofuran dehydrogenase subunit D	SBU_000445	151	43.8	
fwdE	Formylmethanofuran dehydrogenase subunit E	SBU_000903	23	3.8	
fwdF	Formylmethanofuran dehydrogenase subunit F	SBU_001540	91	8.7	

Expression as absolute read counts and as fragments per kilobase of transcript per million mapped reads (FPKM) is shown, as well as the corresponding protein abundance as emPAI index.

Extended Data Table 5 | Genes encoding proteins related to electron cycling and energy transfer in *Ca.* S. butanivorans

Gene	Feature	Locus_tag	Transcriptome		Proteome
			Absolute reads	FPKM	emPAI
	[Ni-Fe]-Hydrogenase large subunit	SBU_000461	5409	343.7	0.28
	[Ni-Fe]-Hydrogenase small subunit	SBU_000462	1702	196.6	
	Cytochrome c-type protein	SBU_000189	324	73.2	
	Cytochrome c	SBU_000960	1161	125.5	0.17
	Cytochrome C	SBU_001187	184	15.3	
	Cytochrome c	SBU_001594	62	5.0	0.21
	Multiheme cytochrome	SBU_000341	196	25.4	
	Multiheme cytochrome	SBU_000342	148	13.1	
	Multiheme cytochrome	SBU_000614	646	83.2	
	Multiheme cytochrome	SBU_000694	4224	659.7	
	Multiheme cytochrome	SBU_000777	3660	571.6	
	Multiheme cytochrome	SBU_000778	3189	395.7	
	Multiheme cytochrome	SBU_001337	1953	389.1	0.61
hdrA	Heterodisulfide reductase, subunit A*	SBU_000297	646	27.0	0.40
hdrB	Heterodisulfide reductase, subunit B*	SBU_000298	1146	146.1	
hdrC	Heterodisulfide reductase, subunit C*	SBU_000299	503	91.7	0.31
fdhB	Formate dehydrogenase subunit beta	SBU_000300	838	86.2	0.89
mvhD	Methyl-viologen-reducing hydrogenase	SBU_000301	205	53.9	0.78
fqoJ	F420H2:quinone oxidoreductase subunit J	SBU_000209	3	0.6	
fqoK	F420H2:quinone oxidoreductase subunit K	SBU_000210	12	4.1	
fqoL	F420H2:quinone oxidoreductase subunit L	SBU_000211	133	9.7	
fqoM	F420H2:quinone oxidoreductase subunit M	SBU_000213	166	10.6	
fqoN	F420H2:quinone oxidoreductase subunit N	SBU_000214	142	12.7	
fqoA	F420H2:quinone oxidoreductase subunit A	SBU_000215	85	26.7	0.26
fqoBCD	F420H2:quinone oxidoreductase subunit	SBU_000216	323	15.5	0.04
fqoH	F420H2:quinone oxidoreductase subunit H	SBU_000217	171	17.3	
fqoI	F420H2:quinone oxidoreductase subunit I	SBU_000218	112	16.9	
fqoF	F420H2:quinone oxidoreductase subunit F	SBU_000219	94	10.0	
nuoH	NADH:quinone oxidoreductase subunit H	SBU_000563	446	47.5	0.18
nuoD	NADH:quinone oxidoreductase subunit D	SBU_000564	458	45.7	0.26
nuoC	NADH:quinone oxidoreductase subunit C	SBU_000565	236	56.8	0.69
nuoB	NADH:quinone oxidoreductase subunit B	SBU_000566	345	34.2	
nuoA	NADH:quinone oxidoreductase subunit A	SBU_000567	30	9.4	
nuoI	NADH:quinone oxidoreductase subunit I	SBU_000874	119	34.2	0.23
nuoJ	NADH:quinone oxidoreductase subunit J	SBU_000875	67	30.4	
nuoK	NADH:quinone oxidoreductase subunit K	SBU_000877	69	24.4	
nuoL	NADH:quinone oxidoreductase subunit L	SBU_000878	950	54.5	
nuoM	NADH:quinone oxidoreductase subunit M	SBU_000879	802	57.6	
nuoN	NADH:quinone oxidoreductase subunit N	SBU_000880	994	74.9	

Expression as absolute read counts and as fragments per kilobase of transcript per million mapped reads (FPKM) is shown, as well as the corresponding protein abundance as emPAI index.

*Submitted as CoB-CoM heterodisulfide reductases.

Extended Data Table 6 | BLASTP search of proteins involved in butyrate oxidation. Best results according to the E-value are shown

Gene product	Locus tag	Blast annotation	Accession number	Organism	Coverage /Identity	E-value
Acyl-CoA dehydrogenase domain-containing protein	SBU_000172	Acyl-CoA dehydrogenase	WP_028324559.1	*Desulfatirhabdium butyrativorans*	100/66	0.0
Acyl-CoA dehydrogenase	SBU_000399	Acyl-CoA dehydrogenase	WP_028321791.1	*Desulfatiglans anilini*	99/51	6e-175
Acyl-CoA dehydrogenase domain-containing protein	SBU_000724	Acyl-CoA dehydrogenase	WP_028319806.1	*Desulfatiglans anilini*	98/62	8e-175
Acyl-CoA dehydrogenase	SBU_001146	Hypothetical protein	WP_036734863.1	*Peptococcaceae bacterium* SCADC1_2_3	97/58	0.0
Crotonase	SBU_000400	Hypothetical protein	WP_029475295.1	Dehalococcoidia bacterium SCGC AB-539-J10	96/69	7e-128
3-Hydroxyacyl-CoA dehydrogenase	SBU_000288	3-hydroxybutyryl-CoA dehydrogenase Hbd	EMS78924.1	*Desulfotignum phosphitoxidans* DSM 13687	100/65	8e-134
3-Hydroxyacyl-CoA dehydrogenase	SBU_000843	3-hydroxy-2-methylbutyryl-CoA dehydrogenase	WP_007907297.1	*Ktedonobacter racemifer*	98/61	5e-98
Acetyl-CoA acetyltransferase	SBU_000329	Acetyl-CoA acetyltransferase	WP_014407007.1	*Methanocella conradii*	99/67	0.0
Acetyl-CoA acetyltransferase	SBU_000402	Conserved hypothetical protein, thiolase family	CBH39006.1	uncultured archaeon	100/70	0.0
Acetyl-CoA acetyltransferase	SBU_000404	Conserved hypothetical protein, thiolase family	CBH39006.1	uncultured archaeon	100/57	6e-159
Acetyl-CoA acetyltransferase	SBU_001291	Acetyl-CoA acetyltransferase	WP_010917519.1	*Thermoplasma volcanium*	98/43	4e-103

Extended Data Table 7 Genes encoding Type IV pili and 10 most expressed cytochromes identified in the HotSeep-1 genome bin from the Butane50 culture

Gene	Best Blast Hit			Pfam hits	RNA expression	
	Feature	Accession number	Coverage/ identity	Domain ID/ accession	Absolute reads	FPKM
PilA	Type IV pilus assembly protein	AMM41792.1	100/99	N_methyl_3/ PF13633.3	8	3
PilA	Pilus assembly protein PilA	AMM39924.1	100/88	N_methyl_3/ PF13633.3	1780	582
Peptidase A24	Peptidase A24	AMM42236.1	100/100	Dis_P_Dis/ PF06750; Peptidase_A24/ PF01478	31	9
PilQ	Pilus modification protein PilQ	AMM40410.1	100/99	AMIN/ PF11741; STN/ PF07660; Secretin_N/ PF03958; Secretin/PF00263	116	12
PilP	Type IV pilus assembly protein PilP	AMM40409.1	100/99	T2SSC/ PF11356; PilP/PF04351	8	4
PilO	Pilus assembly protein PilO	AMM40408.1	100/100	PilO/PF04350	7	2
PilN	Type IV pilus assembly protein PilN	AMM40407.1	100/98	PilN/PF05137	13	5
PilM	Pilus assembly protein PilM	AMM40406.1	100/99	Pil_2/PF11104	32	6
PilW	Putative pilus assembly protein PilW	AMM39834.1	100/99	N_methyl_2/PF13544	53	10
PilY1	Type IV pilus assembly protein	AMM41700.1	100/98	-	247	12
PilY1	Putative pilus assembly protein PilY	AMM41699.1	100/99	Neisseria_PilC/ PF05567	91	16
PilL	Type IV pilus assembly protein pilL	AMM41701.1	100/93	-	3	2
PilC	Type IV pilus assembly protein PilC	AMM42043.1	97/99	T2SSF/PF00482 (x2)	50	9

Cytochrome c type based on PfamA domain prediction	Best Blast Hit			Cellular localization (PSORTb)	Heme groups	RNA expression	
	Feature	Accession number	Coverage/ identity			Absolute reads	FPKM
Cytochrom_CIII	Class III cytochrome C	AMM42051.1	100/97	Periplasmic	4	505	238
Paired_CXXCH_1	Doubled CXXCH cytochrome C	AMM40456.1	99/46	Extracellular	5	1244	232
Paired_CXXCH_1	Doubled CXXCH cytochrome C	AMM40456.1	100/94	Unknown (CM,P,OM,E)	6	768	143
Paired_CXXCH_1	Doubled CXXCH cytochrome C	AMM39976.1	100/94	Unknown (CM,P,OM,E)	7	471	94
Paired_CXXCH_1	Cytochrome C	AMM40455.1	96/95	Extracellular	6	483	96
Cytochrom_CIII	Class III cytochrome C	AMM41048.1	100/99	Periplasmic	4	69	31
Paired_CXXCH_1	Cytochrome C	AMM40346.1	100/99	Cytoplasmic	10	135	28
Paired_CXXCH_1	Cytochrome C	AMM40455.1	99/46	Periplasmic	7	105	21
Cytochrom_c3_2	Cytochrome C	AMM40350.1	100/100	Unknown (CM,P,E)	12	72	17
Cytochrom_c3_2	Cytochrome C	AMM40349.1	100/99	Periplasmic	12	53	14

[1]For unknown cellular localization of cytochromes, potential locations are indicated according to the score value.

CM, cytoplasmic membrane; P, periplasmic; OM, outer membrane; E, extracellular.

Supplementary Information

Supplementary Discussion

Calculation of the energetic feasibility of H_2 formation and consumption during butane oxidation

Literature data[1]

Compound		$\Delta_f G°_{298K}$ (kJ mol^{-1})	$\Delta_f H_{298K}$ (kJ mol^{-1})
H_2 (g)		0	0
H^+ (aq)		0	0
pH = 7	($\Delta_f G°'$)	–40.0	0
H_2O (lq)		–237.18	–285.83
n-C_4H_{10} (g)		–17.20	–125.60
CO_2 (g)		–394.36	–393.51
H_2S (aq)		–27.87	–39.8
SO_4^{2-} (aq)		–744.6	–909.3

[1]From Dean, J.A., Lange's Handbook of Chemistry. McGraw-Hill, New York (1992); and Thauer, R.K., Jungermann, K., Decker, K., Energy conservation in chemotrophic anaerobic bacteria. Bacteriol. Rev. 41, 100–180 (1977).

a) Conversion of butane to hydrogen

$$C_4H_{10}\,(g) + 8\,H_2O\,(lq) \rightarrow 4\,CO_2\,(g) + 13\,H_2\,(g) \qquad (1)$$

At 298.15 K, and standard activities/fugacities:

$$\Delta G°_{298K} = +337.2\ \text{kJ mol}^{-1}{}_{\text{Butane}}$$

$$\Delta H_{298K} = +838.2\ \text{kJ mol}^{-1}{}_{\text{Butane}}$$

At 323.15 K (50 °C), but otherwise standard activities/fugacities:

$$\Delta G^{o}_{323K} = \frac{323}{298}\left(\Delta G^{o}_{298K} - \Delta H^{o}\right) + \Delta H^{o} \qquad (2)$$

(Derived from $\Delta G = \Delta H - T\Delta S$, and the assumption that ΔH and ΔS are the same at the lower and higher temperature.)

$$\Delta G^{o}_{323K} = +295.2\ \text{kJ mol}^{-1}{}_{\text{Butane}} \qquad (3)$$

Free energy depends on activity/fugacity according to:

$$\Delta G = \Delta G° + R\,T \ln \frac{\{CO_2\}^4\{H_2\}^{13}}{\{\text{Butane}\}\{H_2O\}^8} \qquad (4)$$

With the above ΔG^{o}_{323K}, R = 8.314 · 10^{-3} kJ mol^{-1} K^{-1}, T = 323 K and assuming for convenience {Butane} = 1, {H_2O} = 1, {CO_2} = 0.3 = $10^{-0.523}$, the free energy (in kJ) depends on H_2 fugacity according to

$$\Delta G = 295.2 + 6.18 \log (10^{-2.09} \cdot \{H_2\}^{13}) \qquad (5)$$

$$\Delta G = 282.3 + 80.34 \log\{H_2\} \qquad (6)$$

If, as a convenient approximation, H_2 fugacity is expressed via H_2 partial pressure in Pa:

$$\Delta G = 282.3 + 80.34 \log \frac{p_{H_2}}{10^{5.004}\ \text{Pa}} \quad (7)$$

$$\Delta G = -119.7 + 80.34 \log \frac{p_{H_2}}{1\ \text{Pa}} \quad \text{(kJ per mol butane)} \quad (8)$$

b) Consumption of hydrogen by sulfate reduction

$$4\ H_2\ (g) + SO_4^{2-}\ (aq) + 2\ H^+\ (aq) \rightarrow\ H_2S\ (aq) + 4\ H_2O\ (lq) \quad (9)$$

At 298.15 K, and standard activities/fugacities:

$\Delta G° = -232.0$ kJ mol$^{-1}_{\text{Sulfate}}$ (formal value for hypothetical $\{H^+\} = 1$, i.e. pH = 0)

$\Delta H° = -273.8$ kJ mol$^{-1}_{\text{Sulfate}}$

At 323.15 K (50 °C), but otherwise standard activities/fugacities, via eqn. 2:

$$\Delta G^{\circ}_{323K} = -228.5\ \text{mol}^{-1}{}_{\text{Sulfate}}$$

Free energy depends on activity/fugacity according to:

$$\Delta G = \Delta G° + R\ T \ln \frac{\{H_2S\}\ \{H_2O\}^4}{\{H_2\}^4\ \{SO_4^{2-}\}\ \{H^+\}^2} \quad (10)$$

With the above ΔG°_{323K}, $R = 8.314 \cdot 10^{-3}$ kJ mol^{-1} K^{-1}, $T = 323$ K and assuming for convenience $\{SO_4^{2-}\} = 0.0023 = 10^{-2.64}$ (from 0.023 M sulfate present after 50 days of incubation, and activity coefficient of approx. 0.1 M^{-1}), $\{H^+\} = 10^{-7}$, $\{H_2S\} = 0.005 = 10^{-2.3}$ (from 0.005 M sulfide formed after 50 days of incubation), and $\{H_2O\} = 1$, the free energy (in kJ) depends on H_2 fugacity according to (calculation analogous to eqn. 5):

$$\Delta G = -139.9 - 24.72 \log\{H_2\} \quad \text{(kJ per mol sulfate)} \quad (11)$$

If, as a convenient approximation, H_2 fugacity is expressed via H_2 partial pressure in Pa:

$$\Delta G = -139.9 - 24.72 \log \frac{p_{H_2}}{10^{5.004}\ \text{Pa}} \quad \text{(kJ per mol sulfate)} \quad (12)$$

$$\Delta G = -16.2 - 24.72 \log \frac{p_{H_2}}{1\ \text{Pa}} \quad \text{(kJ per mol sulfate)} \quad (13)$$

Per mol butane, 3.25 mol sulfate are reduced with 13 mol H_2, yielding the free energy change

$$\Delta G = -454.7 - 80.34 \log\{H_2\} \quad \text{(kJ per 3.25 mol sulfate)} \quad (14)$$

or with H_2 pressure in Pa

$$\Delta G = -52.7 - 80.34 \log \frac{p_{H_2}}{1\ \text{Pa}} \quad \text{(kJ per 3.25 mol sulfate)} \quad (15)$$

ΔG vs. p_{H_2} plots are shown in **Supplementary Figure 2**.

Supplementary Tables

Supplementary Table 1. Electron balance of the *n*-butane degradation coupled to sulfate reduction to sulfide by the thermophilic enrichment culture.

n-Butane, sulfate, electrons (mmol l^{-1})	Butane50 + 7% *n*-butane (v/v in headspace)	Butane50 + 12% *n*-butane (v/v in headspace)	Butane50 – *n*-butane	Abiotic control + 7% *n*-butane (v/v in headspace)
n-Butane supplied	2.1	3.2	-	2.1
n-Butane consumed	2.0	3.1	-	0.15
Electrons from *n*-butane [a]	48.1	76.7	-	-
Sulfate supplied	28.0	28.0	28.0	-
Sulfate consumed	7.8	11.8	1.2	-
Electrons for sulfate reduction [c]	52.8	84.8	-	-
Electron balance[d]	1.09	1.10	-	-

Quantitative growth experiments were carried out in serum bottles with 100 ml culture volume and different starting amounts of *n*-butane. The cultures were incubated for 155 days.

[a] Electrons from consumed *n*-butane were calculated considering the complete oxidation reaction: $C_4H_{10} + 8H_2O \rightarrow 4CO_2 + 26H^+ + 26e^-$. The amount of *n*-butane consumed was corrected for the amount of *n*-butane disappearing in the abiotic control.

[b] The amount of sulfate consumed was determined by quantification of produced sulfide, corrected for the concentration of sulfide at the start of the incubation experiments.

[c] Electrons for sulfate reduction were calculated considering: $SO_4^{2-} + 8e^- + 9H^+ \rightarrow HS^- + 4H_2O$. The sulfide produced in cultures with *n*-butane was corrected for the sulfide produced in *n*-butane-free bottles.

[d] Electrons consumed by sulfate reduction divided by electrons from *n*-butane consumed .

Supplementary Table 2. Basic information of the metagenome and the metatranscriptome of the Butane50 culture

Metagenome	**Mate-pair library**	Number of raw Illumina reads	21,182,518
		Number of reads after trimming	12,333,536
		Reads in metagenomic contigs	7,483,911
	Paired-end library	Number of raw Illumina reads	4,460,548
		Number of reads after trimming	4,187,678
		Reads in metagenomic contigs	2,172,844
	Bulk assembly	Reads from both libraries	9,656,755
		Assembled metagenome size (Mbp)	35.9
		N50 (bp)	3,014
		Maximum scaffold size (bp)	941,878
		Number of scaffolds	17,436
Metatranscriptome		Number of raw Illumina reads	48,444,528
		Number of reads after trimming	46,198,928

Supplementary Table 3. Pairwise comparison of nucleotide sequences and whole genome identity of the HotSeep-1 bin from the Butane50 culture vs. *Ca.* D. auxilii

	HotSeep-1 bin/*Ca.* D. auxilii			***Ca.* D. auxilii/HotSeep-1 bin**		
	Identity	Coverage	e-value	Identity	Coverage	e-value
16S RNA gene	99	100	0.00	99	100	0.00
23S RNA gene	99	100	0.00	99	100	0.00
Sat	99	100	0.00	99	100	0.00
***apr* alpha**	99	100	0.00	99	100	0.00
***apr* beta**	99	100	5e-113	99	100	5e-113
***dsr* alpha**	100	97	0.00	97	86	0.00
ITS	99	97	4e-144	99	100	4e-144

	Average Nucleotide Identity (Blast)	**Average Nucleotide Identity (MUMmer)**	**Tetranucleotide frequency**
HotSeep-1 bin/*Ca.* D. auxilii	98.38	98.45	99.48
Ca. D. auxilii/HotSeep-1 bin	98.48	98.24	99.48

sat, sulfate adenylyltransferase; *apr,* adenylylsulfate reductase; *dsr*, dissimilatory sulfite reductase; ITS, internal transcribed spacer

Supplementary Table 4. Accession numbers of published McrA sequences that have been included in the phylogenetic analyses of McrA subunits of *Ca.* Syntrophoarchaeum (Figure 3, Supplementary Figure 1).

P12971	CAE46369	YP_004004295	KT387808*
ABN56311	WP_011171503	YP_004520866	KT387809*
ABD41854	P07962	YP_003707758	KT387811*
ABN07237	NP_633264	WP_023845930	KT387813*
ABN07725	NP_988679	YP_007250108	KT387816*
CAJ37024	1MRO_D	YP_001549157	KT387817*
AAB98063	1E6Y_D	YP_003541782	KT387818*
AAB98851	1E6V_D	YP_008075839	
ABK14360	ZP_01702953	YP_007248437	
AAB85618	YP_001046528	WP_008513191	
AAB85653	YP_567018	WP_004079635	
ABE53268	CBH39484	YP_001403743	
CAA50044	AIJ05353	WP_004039455	
AAM01870	AHY86395	YP_006545377	
AAA73439	AHY86394	WP_004037742	
AAZ69867	AIJ05899	YP_004743325	
AAM07885	YP_007713068	YP_004291467	
AAM30936	YP_005919503	YP_006545160	
AAB02003	YP_005380187	YP_003457854	
AAQ63481	YP_007489939	YP_003424666	
ABO34334	YP_003355571	YP_008916519	
CAF31115	YP_004484839	WP_007044524	
AAA72598	YP_003246499	WP_004031277	
ABC56731	YP_686530	YP_004484066	
CAA30633	YP_004383383	WP_008514009	
CAE48306	YP_003615915	YP_001273475	
CAA30639	YP_003128256	WP_019264905	
AAA73445	YP_003458728	WP_018154763	
AAA72197	YP_006922405	WP_004035797	
AAQ63476	YP_002467317	YP_003895179	
ZP_01799689	WP_007043982	YP_004289577	
ZP_01799496	YP_007313393	YP_003895599	
CAA50044	WP_017981119	YP_003247534	
S43897	WP_018153522	YP_008072226	
AAU84252	YP_003726594	WP_019176774	
AAU83782	YP_003850404	Q58256.1	
AAU83544	YP_004004345	O27232.1	
AAU83007	YP_004576704	P11558.1	
AAU82960	YP_008916650	KT387810	
AAU82711	YP_004615938	KT387805	
AAU82276	WP_004029250	KT387806	
AAB98063			

* indicates partial sequences only used in some of the phylogenetic calculations (see Methods)

Supplementary Table 5. Primer sequences and PCR conditions used for amplification of *mcrA* genes from Butane50 enrichment.

Primer sets	Primer sequences (5' - 3')	Specificity	Polymerases[$]	Annealing-temp. [°C]	Expected amplicon length*	PCR product
McrA_1706F / McrA_1706R	CTTGACGACTTCAAGCGAATA/ CCCCTCCGGTGTAATTGGA	SCAL_001725	Phusion	52	1645	+
McrA_354F2 / McrA_354R	CGTGGAAGATGTACGCGAA/ ACGCTCACCTGCGGGCAT	SCAL_000352	TaKaRa Taq	52	1638	+
McrA_445F / McrA_445_1470R	GCCAGCGGGAGATGTACAA/ CGCTCACCKGCAGGCTCA	SBU_000314	TaKaRa Taq	54	1674	+
McrA_850_1455_F2 / McrA_850_915_1455R	GGAGATTTTCRGGGAGGA/ ACCTCCCWGGYTTTATYG	SBU_000718	Phusion	50	1632	+
McrA_915F / McrA_850_915_1455R	ACGATGCAACACGTGAGTA/ ACCTCCCWGGYTTTATYG	SCAL_000921	TaKaRa Taq	48	1614	+
McrA_1135F / McrA_1135R	AACATGGTGGAACACGCCA/ CTCTCACCCGCAGGCTCA	SCAL_001148	TaKaRa Taq & Phusion	52	1572	-
McrA_1455F / McrA_850_915_1455R	TGATCCCACCCGGAGAAA/ ACCTCCCWGGYTTTATYG	SBU_001328	TaKaRa Taq	48	1613	+
McrA_1470F / McrA_445_1470R	GACAGGACAAAGGAGCATAT / CGCTCACCKGCAGGCTCA	SBU_001343	TaKaRa Taq	52	1654	+

*according to *mcrA* genes retrieved from *Ca.* S. butanivorans and *Ca.* S. caldarius genomes; [$] Phusion: Phusion High-Fidelity DNA Polymerase (Thermo Fischer Scientific, Germany); TaKaRa Taq: TaKaRa Taq DNA Polymerase (TaKaRa Bio Europe, France)

Supplementary Figures

Supplementary Figure 1. Affiliation of the amino acid sequences of the *mcrA* genes of *Ca.* Syntrophoarchaeum (in red) obtained from the Butane50 culture. The *Ca.* Syntrophoarchaeum sequences are labelled with their locus tag in the draft genomes (SBU=*Ca.* S. butanivorans; SCAL=*Ca.* S. caldarius). In blue, *Bathyarchaeota* sequences from Evans et al., Science, 2015. Black dots represent bootstrap values >90; scale bar indicates the number of amino acids substitutions per site.

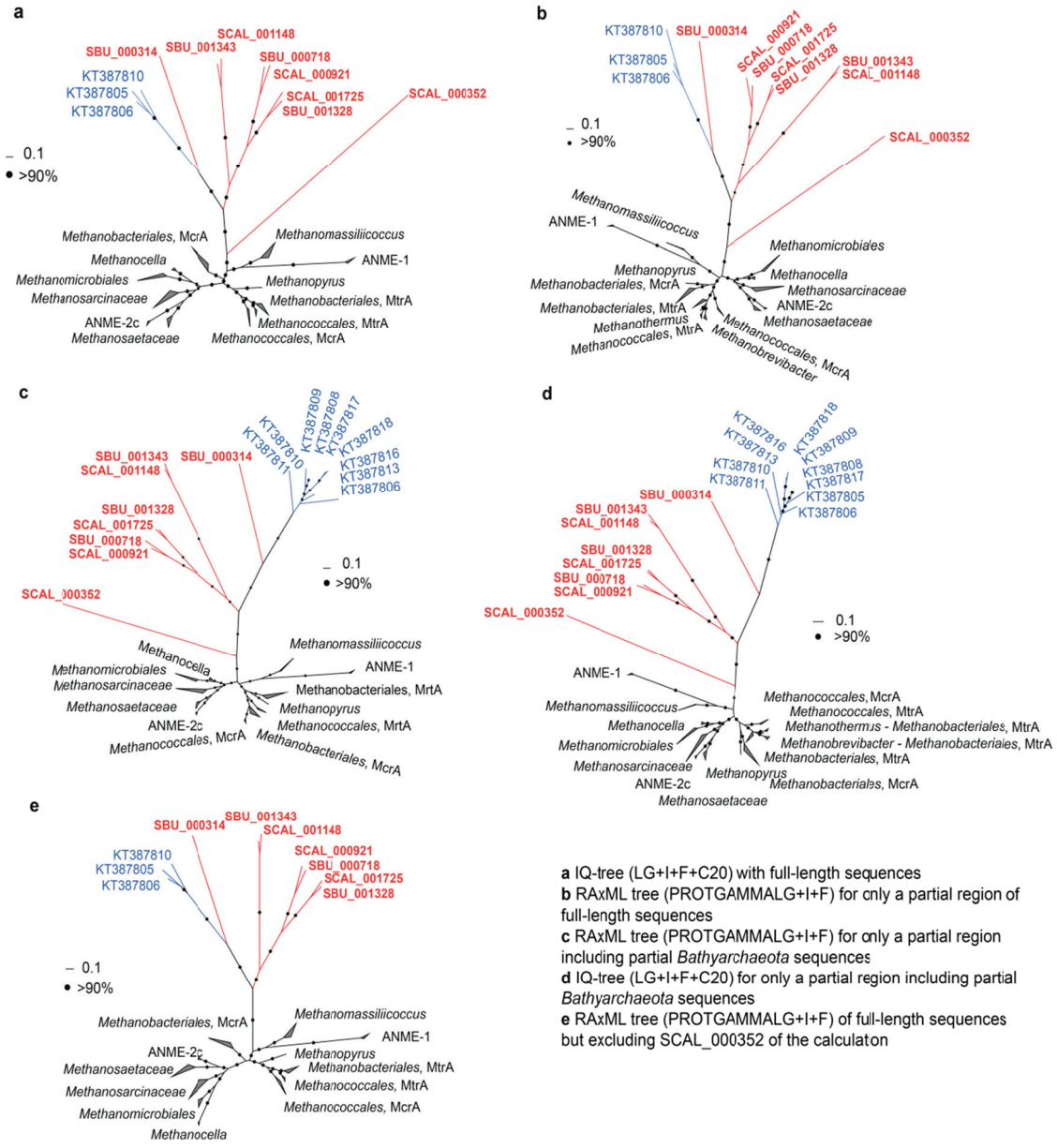

a IQ-tree (LG+I+F+C20) with full-length sequences
b RAxML tree (PROTGAMMALG+I+F) for only a partial region of full-length sequences
c RAxML tree (PROTGAMMALG+I+F) for only a partial region including partial *Bathyarchaeota* sequences
d IQ-tree (LG+I+F+C20) for only a partial region including partial *Bathyarchaeota* sequences
e RAxML tree (PROTGAMMALG+I+F) of full-length sequences but excluding SCAL_000352 of the calculaton

Supplementary Figure 2. Dependence of the free energy of butane oxidation (archaeal partner, red line) and sulfate reduction (bacterial partner, green lines) on the partial pressure of H_2 as an assumed intermediate (see Supplementary Discussion).

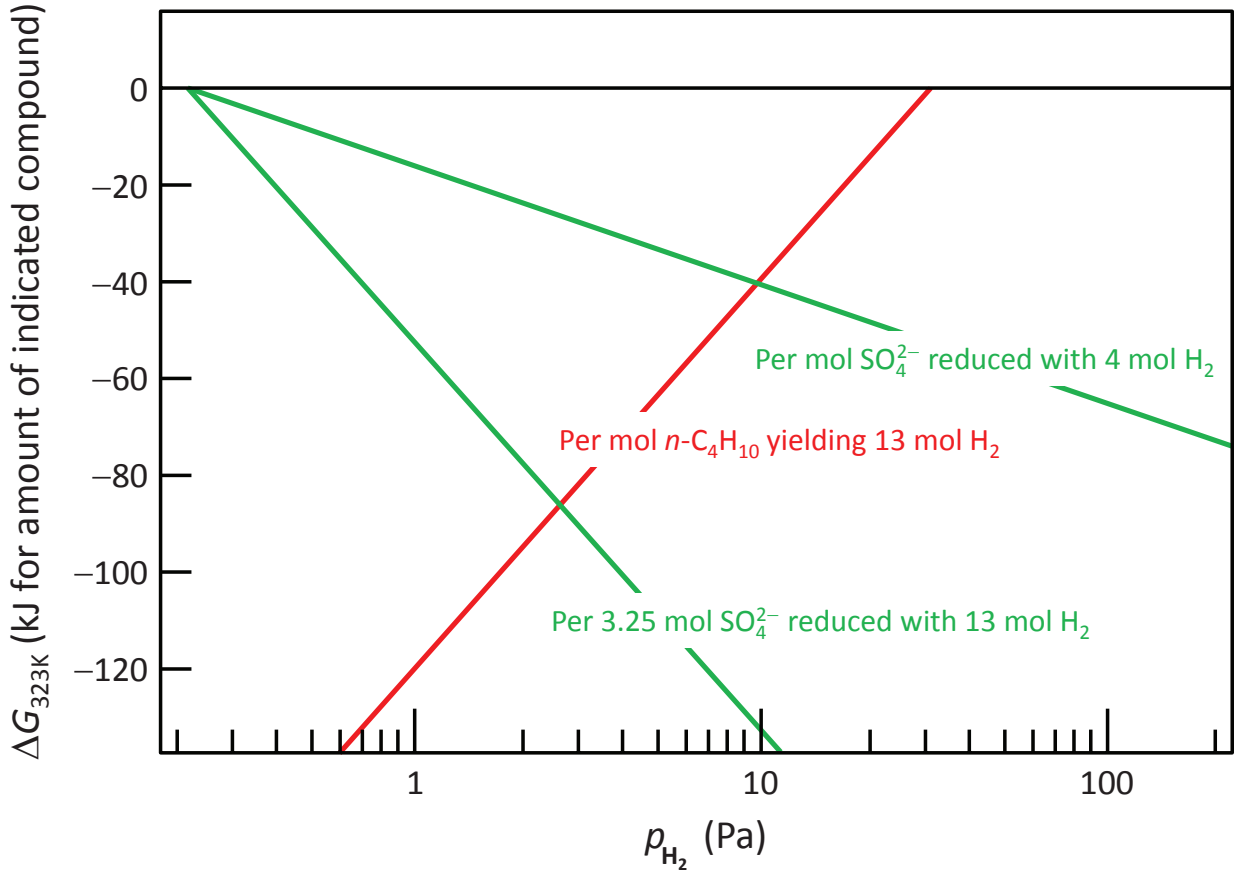

Supplementary Figure 3. Phylogenetic affiliation of the 16S rRNA gene sequences from the studied *Ca.* Syntrophoarchaeum strains (in red) and the *Thermoplasmata* sequence (blue) obtained from the Butane50 enrichment within *Euryarchaeota* (outgroup = *Thaumarchaeota*); bar = 10% estimated sequence divergence; bootstrap values > 90% and >70% are indicated by filled black and grey circles, respectively, on corresponding branch.

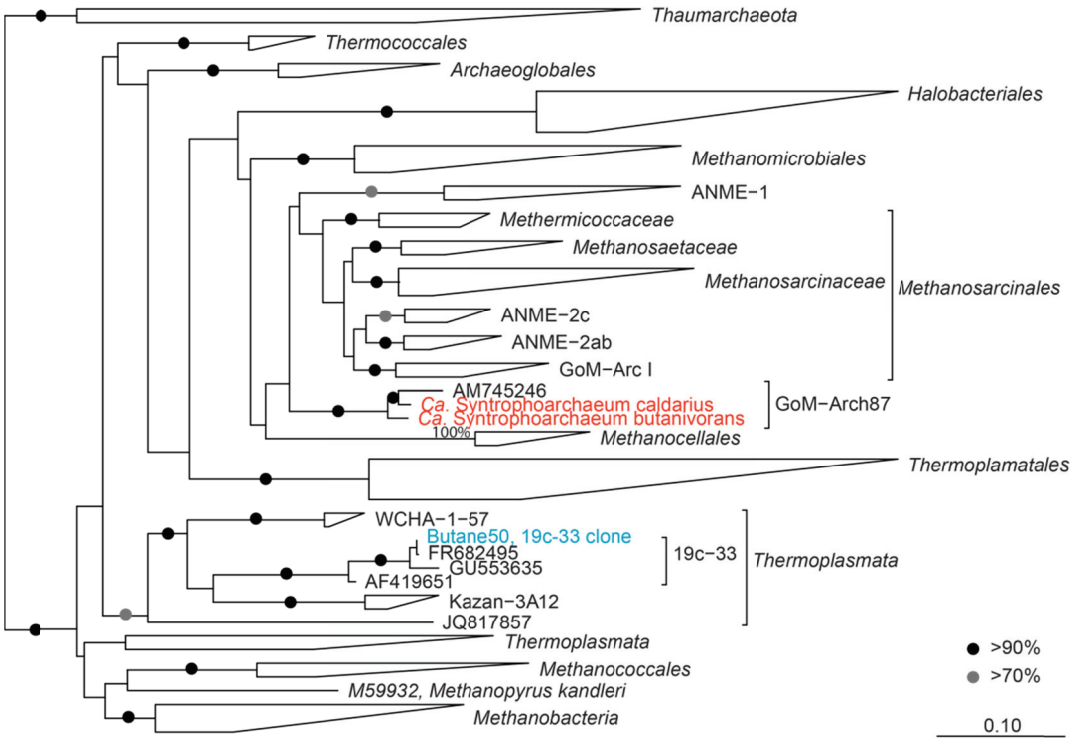

Supplementary Figure 4. Additional electron micrographs showing the abundant presence of pili-like nanowires in the intercellular space of archaeal bacterial aggregates collected from the Butane50 culture. Bar scales 1 µm.

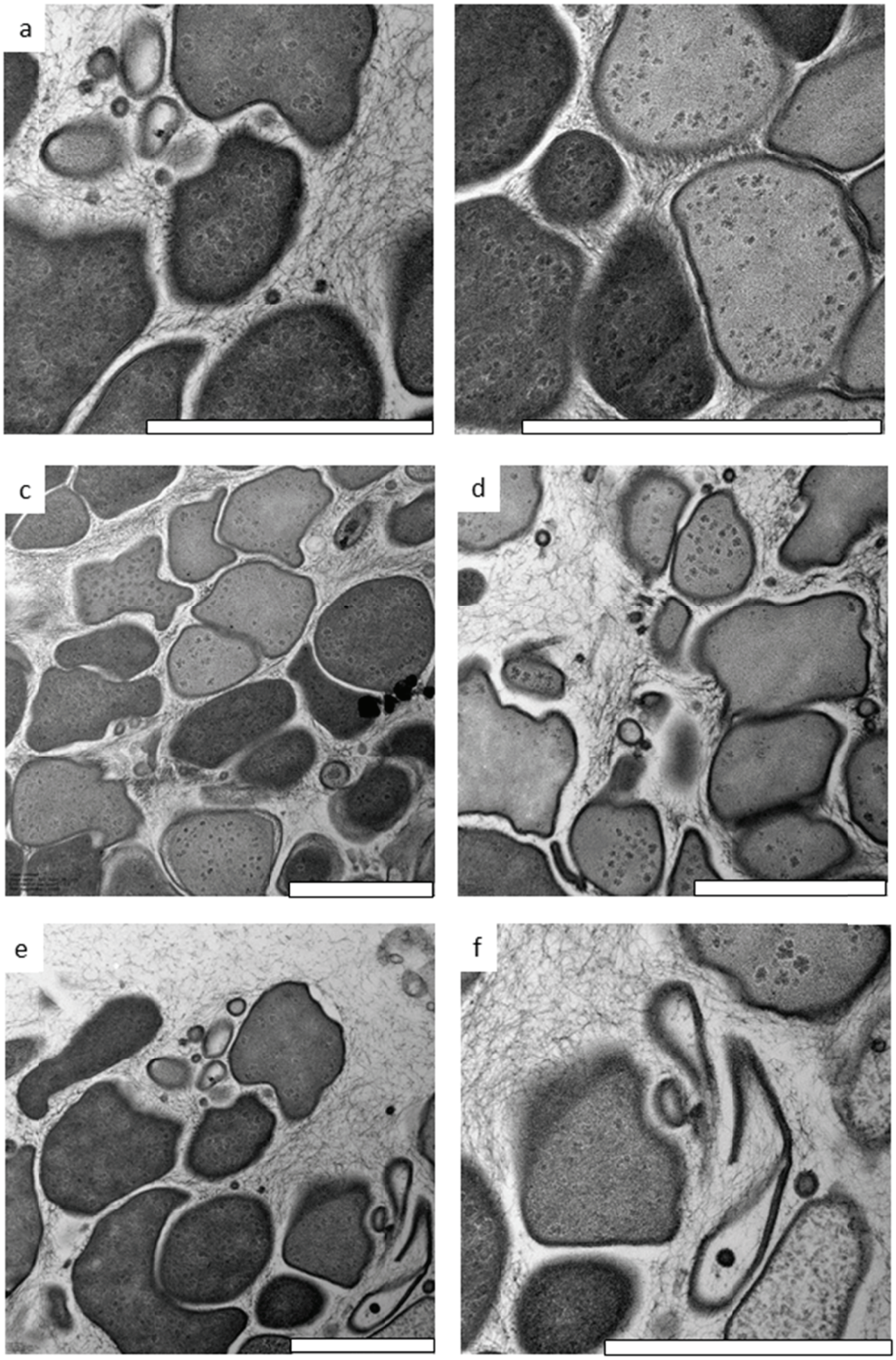

Continuation Supplementary Figure 4.

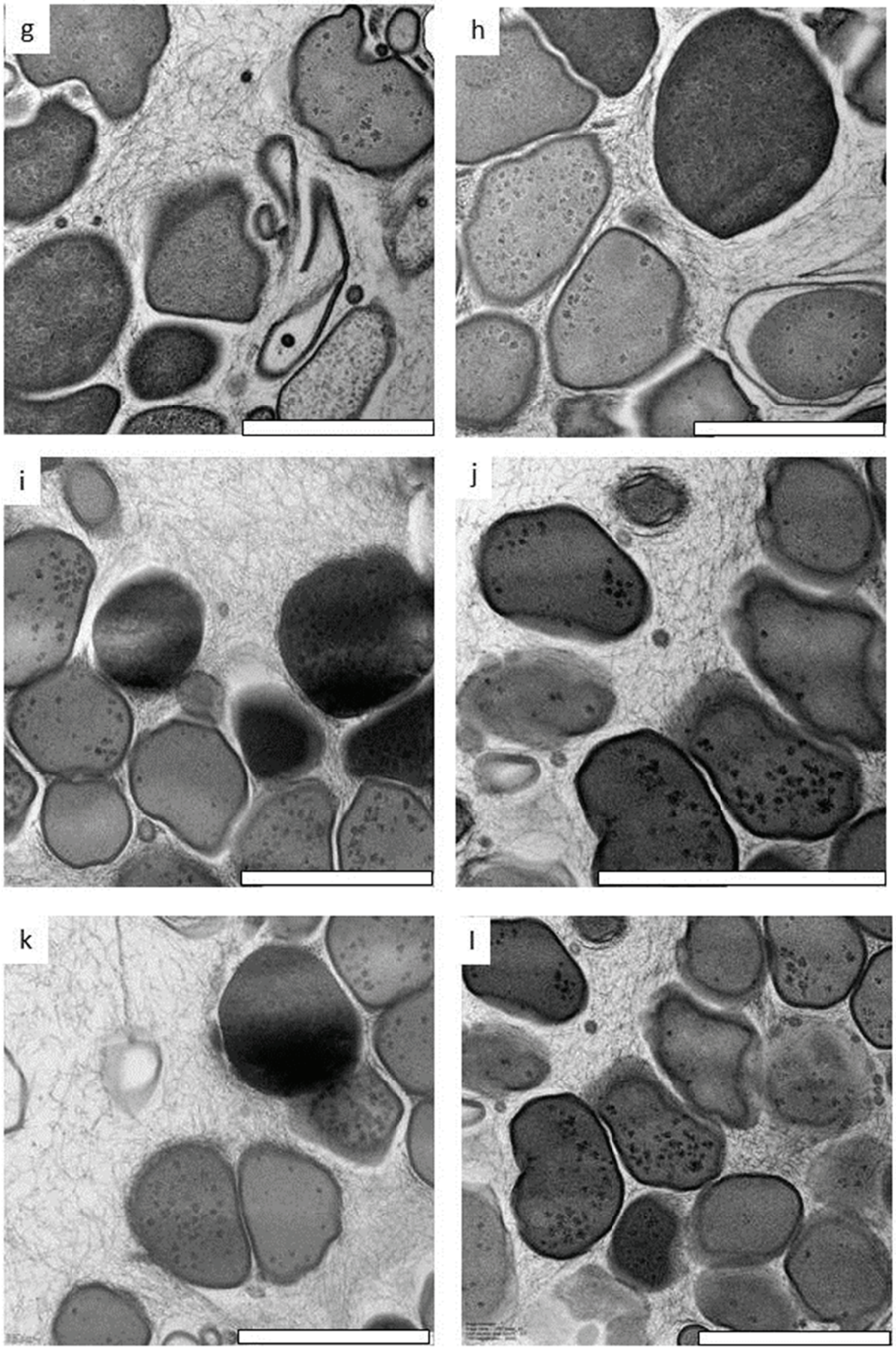

Chapter III

Coupling of alkane degradation to methane formation in a single archaeon

Rafael Laso-Pérez[1,2], Cedric Hahn[1], Daan M. van Vliet[3], Halina E. Tegetmeyer[2,4], Florence Schubotz[5], Nadine T. Smit[5], Heiko Sahling[5], Gerhard Bohrmann[5], Antje Boetius[1,2,5], Katrin Knittel[1], Gunter Wegener[1,2,5]

[1]Max-Planck Institute for Marine Microbiology, 28359 Bremen, Germany.
[2]Alfred Wegener Institute Helmholtz Center for Polar and Marine Research, 27570 Bremerhaven, Germany.
[3]Laboratory for Microbiology, Wageningen University and Research, 6708WE Wageningen, The Netherlands.
[4]Center for Biotechnology, Bielefeld University, 33615 Bielefeld, Germany.
[5]MARUM, Center for Marine Environmental Sciences, University Bremen, 28359 Bremen, Germany.

Manuscript ready for submission

Running title: *Coupling of alkane degradation to methane formation*

Abstract

Crude oil and gases in the seabed provide an important energy source for seabed microorganisms. We investigated the role of archaea in the anaerobic degradation of alkanes in deep-sea oil seeps from the Gulf of Mexico. The sediments contain a substantial diversity of hydrocarbon-dependent archaea such as anaerobic methanotrophs (ANME), *Candidatus* Syntrophoarchaeum and GoM-Arc1 archaea. These groups associate with partner bacteria to couple hydrocarbon oxidation to sulfate reduction. Here we also found oil-rich sediments dominated by archaea of the D-C06 clade, which occurred as single cells without bacterial partners. Metagenome-assembled genomes of D-C06 encode a complete methanogenesis pathway including a canonical MCR, but also highly divergent methyl-coenzyme M reductases (MCR) related to those of the alkane degrader *Ca.* Syntrophoarchaeum, and pathways for the oxidation of long-chain alkyl units. Based on its metabolic potential and its appearance in various hydrocarbon reservoirs, we propose that D-C06 is an important methanogenic alkane degrader in subsurface environments, producing methane by alkane disproportionation.

Introduction

Archaea are key players in the global carbon, nitrogen and sulfur cycle (Offre*, et al.*, 2013). In particular, methanogenic archaea have been important for the Earth's climate through time as their metabolic product, methane, is an important greenhouse gas that is 25 times more powerful than CO_2 (IPCC, 2014). All cultured methanogens belong to the *Euryarchaeota* phylum and produce methane either from the reduction of carbon dioxide with hydrogen or formate, the disproportionation of acetate or the use of methylated substrates. The key enzyme of this process is methyl-coenzyme M reductase (MCR) which catalyses the final step in methane formation.

In marine sediments, massive amounts of biogenic methane are generated as final product of the biodegradation of sedimented organic matter (Reeburgh, 2007). The thermogenic degradation of residual organic matter also produces methane but also other hydrocarbons, including gases such as ethane, propane and butane as well as liquid compounds (crude oil) (Tissot and Welte, 2012). These hydrocarbons tend to migrate from deep organic-rich source rocks towards the sediment surface. However, a large fraction, primarily alkanes, is already degraded within anoxic sediment layers (Joye*, et al.*, 2004, Kleindienst*, et al.*, 2014). The anaerobic oxidation of methane (AOM) is performed by different clades of anaerobic methanotrophic archaea (ANME), belonging to the phylum *Euryarchaeota* (Knittel and Boetius, 2009). They oxidize methane using a reversal of the methanogenesis pathway. AOM is mostly coupled to sulfate reduction performed by bacterial partners (Boetius*, et al.*, 2000, Hallam*, et al.*, 2004, Meyerdierks*, et al.*, 2010, Stokke*, et al.*, 2012, Wang*, et al.*, 2013, Wegener*, et al.*, 2015). However, some ANME may thrive without partners in presence of other electron acceptors such as iron, manganese and nitrate (Beal*, et al.*, 2009, Haroon*, et al.*, 2013, Ettwig*, et al.*, 2016, Cai*, et al.*, 2018).

The anaerobic degradation of other alkanes was for long exclusively assigned to bacteria. Several pathways have been proposed to activate these compounds, but the most widespread is the fumarate addition (Widdel*, et al.*, 2010, Rabus*, et al.*, 2016, von Netzer*, et al.*, 2016). Here, alkanes are added to a fumarate molecule by alkylsuccinate synthase enzymes. The now succinate-bound alkyl units are further oxidized through a fatty acid oxidation pathway (Kniemeyer*, et al.*, 2007, Rabus*, et al.*, 2016). Some of these bacteria degrade hydrocarbons in consortia with methanogens (Zengler*, et al.*, 1999). Elements of the bacterial alkane degradation pathway are also present in some archaea, including the hexadecane-degrading archaea *Thermococcus sibiricus* (Mardanov*, et al.*, 2009) and *Archaeoglobus fulgidus* (Khelifi*, et al.*, 2010, Khelifi*, et al.*, 2014).

In recent years, thermophilic archaea of the *Candidatus* Syntrophoarchaeum clade were shown to degrade short-chain alkanes using modified enzymes related to those of the methanogenesis pathway. *Ca.* Syntrophoarchaeum uses highly modified versions of the MCR to activate propane and butane with coenzyme M (CoM) forming CoM-bound alkyl units as primary intermediate (Laso-Pérez*, et al.*, 2016). The alkyl units are transformed to coenzyme A-bound fatty acids in unknown steps, and are then fully oxidized by the fatty acid oxidation pathway, the Wood-Ljungdahl pathway and the downstream part of the methanogenesis pathway. Similar to AOM, this process is coupled to sulfate reduction in partner bacteria.

Environmental studies from heated hydrocarbon-rich environments revealed the presence of highly modified MCR in metagenome-assembled genomes (MAG) of *Bathyarchaeota* (Evans*, et al.*, 2015) and GoM-Arc1 (Dombrowski*, et al.*, 2017). Gene sequences of *Ca.* Syntrophoarchaeum have also been found in cold seep sediments of the Gulf of Mexico (Orcutt*, et al.*, 2010). The same study reported on sequences of the uncultured methanomicrobal clades GoM-Arc1 and D-C06 (also named GoM-Arc2 in the Orcutt study). Yet, little is known about the environmental function of these microorganisms.

Here, we study oil and asphalt seeps of the Campeche Hydrocarbon province and combined geochemical data, metagenomics and in situ hybridization to decipher the potential role of archaea in the anaerobic degradation of hydrocarbons. Previous studies suggested that these oil and gas seeps host abundant archaeal clades with so far unknown function including *Ca.* Syntrophoarchaeum, GoM-Arc1 and D-C06 (Orcutt*, et al.*, 2010, Pachiadaki*, et al.*, 2010, Schulze-Makuch*, et al.*, 2011, Ruff*, et al.*, 2015). We hypothesize that under sulfate-reducing and methanogenic conditions these archaea play a central role in the anaerobic degradation of non-methane hydrocarbons.

Material and methods

Sampling of hydrocarbon-rich sediments. Sediment samples were collected during the RV METEOR cruise M114-2 in March 2015 at Campeche Knolls in the Gulf of Mexico (Sahling and Ohling, 2017). Sediment samples from the targeted gas and oil seeps (hereafter oil sediment) were collected at Chapopote asphalt volcano by push coring during ROV QUEST dive 362 (GeoB 19351-

14 21°53.993'N; 93°26.112'W at 2925 m water depth). The solid and fresh asphalt flow (40 cm deep) was sampled in the vicinity by gravity coring (GeoB 19345-1 21°53.964'N; 93°26.226'W, 2905 m water depth). A sediment sample without any oil or asphalt (hereafter ambient sediment) was also retrieved by push coring dive from a nearby location at the rim of the main asphalt field (GeoB 19351-5, 21°53.954'N; 93°26.261'W). The asphaltic sediment sample (hereafter asphalt sediments) was retrieved from the Mictlan asphalt field using a gravity corer (GC-5; 1-135 cm) at 3092 m water depth (GeoB 19331-1, 22°01.354'N; 93°14.809'W). On board sediment samples were sliced in different layers (oily sediments: 5 layers: 0-3 cm, 3-5cm, 5-7 cm, 7-9 cm and 9-10 cm; ambient sediments: 4 layers: 0-2 cm, 2-4 cm, 4-7 cm, 7-10 cm; asphalt sediments: 4 sections, 115 and 135 cm depth layers contained asphalt pieces and were used for further analysis). From all sections samples were fixed for cell counts, fluorescence in situ hybridization, nucleic acid extraction and geochemical parameters.

Measurement of gaseous hydrocarbons. For gas analysis, 2 ml sediment volume was sampled from the different core sections using tip-cut syringes immediately after sample recovery. Samples were transferred to 20 ml crimp vials filled with 5 ml sodium hydroxide solution and vials were closed with butyl rubber septa. Hydrocarbon concentrations in the headspace of these vials were determined by gas chromatography coupled to flame ionization mass spectrometry and converted to concentrations per liter of sediment.

Rates of methane oxidation and sulfate reduction. To determine rates of methane oxidation and sulfate reduction, specific depth horizons of the push cores from the oil sites were subsampled into small gas tight cylinders closed with septum and plungers. Radiolabelled (^{14}C)-methane and (^{35}S)-sulfate were added in three replicates and killed controls, respectively, and samples were incubated at 4°C for 24 hours. To stop the ^{14}C-incubations, samples were transferred to gas-tight bottles filled with sodium hydroxide solution (2.5%). To determine rates of methane oxidation, methane concentrations were measured in the samples by gas chromatography (Focus GC Thermo). Tracer content in methane and dissolved inorganic carbon were determined by methods described in Treude et al. (2003). To stop the ^{35}S-incubations, samples were transferred to zinc acetate (2%) solution. Tracer content in sulfate was determined from the supernatant. The product of the reaction, reduced sulfur, was released from the sample and collected using the cold chromium approach (Kallmeyer*, et al.*, 2004). Radioactivity in the samples was measured by scintillation counting (Scintillation cocktail Ultima gold; scintillation counter 2900TR LSA; Packard). Concentrations of sulfate (porewater samples from replicate cores) were determined using non-suppressed ion chromatography (Metrohm 760c). Rates were calculated as described previously (Holler*, et al.*, 2011).

Patterns of long-chain hydrocarbons in oily sediments and asphalt flow. The organic fraction of the oily sediments and the asphalt flows was extracted with dichloromethane (DCM) in an ultrasonic

bath for 10 minutes. Asphaltenes were precipitated in three steps by addition of cold *n*-hexane. The *n*-hexane fraction was subsequently subjected to silica gel column chromatography and saturated hydrocarbons were eluted with *n*-hexane. The saturated fraction was analysed on a ThermoFinnigan Trace GC equipped with a 30 m RTX-5MS fused silica column (0.25 mm, 0.25 μm) coupled to a ThermoFinnigan TraceMS. The MS was operated in electron impact mode at 70 eV with a full scan mass range of 40-800 *m/z*. The initial oven temperature was held at 60°C for 2 minutes and subsequently heated to 325°C at a rate of 4°C per min and held at 325°C for 20 minutes. The carrier gas was helium with a constant flow of 1.0 ml min^{-1}.

DNA extraction, amplification of 16S rRNA genes and tag sequencing. DNA was extracted according to (Zhou*, et al.*, 1996) with some modifications. For the asphalt sediments, extraction buffer was added and samples were freeze-thawed three times. Samples were sonicated for 10 minutes and placed in a water bath for 30 minutes at 65°C. Extraction continued according to Zhou et al., with the modification that proteinase K concentration was 20 mg ml^{-1} and the incubation temperature for this step was 65°C. Up to 12.5 ng of each DNA extract (ambient, oil and asphalt sediments) were used for the preparation of 16S rDNA amplicon libraries for Illumina sequencing, following the 16S Metagenomic Sequencing Library Preparation guide provided by Illumina. Amplicon libraries for both Archaea and Bacteria were sequenced on an Illumina MiSeq instrument (2x300 bp paired end run, v3 chemistry) at CeBiTec (Bielefeld, Germany). Arch 349F and Arch915R primers were used to amplify archaeal V3-V5 regions, while for Bacteria V3-V4 regions were amplified using Bact 341F and Bact 785R as primers (**Supplementary Table 5**). From the retrieved sequences, primer sequences and remaining adapters were clipped using Cutadapt v1.9.1 (Martin, 2011) with 0.16 as maximum allowed error rate (-e) and no indels allowed. For Archaea, clipped reads were merged using PEAR v0.9.6 (Zhang*, et al.*, 2014) setting 10 bp as the minimum overlap and 400 and 570 bp as minimum and maximum assembly length respectively. Afterwards, merged reads were trimmed using Trimmomatic v0.35 (Bolger*, et al.*, 2014) with 6:12 as sliding window and 450 bp as minimum length. For Bacteria, clipped reads were first trimmed (sliding window 4:15 and minimum length 100) and then merged (minimum overlap 10 bp, minimum length 350 bp and maximum length 500 bp) using similar software. Both bacterial and archaeal sequences were then dereplicated and were clustered into OTUs using Swarm v2.2.2 (Mahé*, et al.*, 2014) with the following parameters: -b 3, -d 1 and –f. Then, OTUs were classified against the SSURef_NR99_123 SILVA database using SINA aligner v1.2.11 (Pruesse*, et al.*, 2012). The classified OTUs were then analysed using the software R.

Catalysed reported deposition fluorescence in situ hybridization (CARD-FISH) analysis. Samples for CARD-FISH analysis were fixed on board for 2 hours in 2% formaldehyde, washed and stored in phosphate buffered saline (PBS; pH 7.4):ethanol 1:1 (v/v) at -20°C. Aliquots were sonicated (30 sec; 20% power; 20% cycle; Sonoplus HD70; Bandelin) and filtered on GTTP polycarbonate

filters (0.2 µm pore size; Millipore; Darmstadt; Germany). CARD-FISH reaction was performed as described in Pernthaler*, et al.* (2002) with following modifications: cells were permeabilised with a lysozyme solution (PBS; pH 7.4, 0.005 M EDTA pH 8.0, 0,02 M Tris-HCl pH 8.0, 10 mg ml^{-1} lysozyme; Sigma-Aldrich) at 37°C for 60 minutes and either achromopeptidase solution (0,01 M NaCl, 0,01 M Tris-HCl pH 8,0, 20 µg ml^{-1} achromopeptidase) at 37 °C for 30 minutes or proteinase K solution (PBS; pH=7.4, 0.005 M EDTA pH 8.0, 0,02 M Tris-HCl pH 8.0, 7.5 µM of proteinase K; Merck, Darmstadt, Germany) at room temperature for 5 minutes; endogenous peroxidases were inactivated by incubation in a solution of 0.15% H_2O_2 in methanol for 30 min at room temperature. 16S rRNA was targeted with the specific oligonucleotide probes EUB-338 I-III (Amann*, et al.*, 1990, Daims*, et al.*, 1999), ARCH-915 (Stahl and Amann, 1991), GOM-ARCI-660, DC06-735 and SYNA-666 (**Supplementary Table 1**). The probes EUB-338, ARCH-915 and GOM-ARCI-660 were applied at 35% formamide, the probe DC06-735 at 10% formamide and the probe SYNA-666 at 25% formamide. The probes GOM-ARCI-660, DC06-735 and SYNA-666 were designed in this project using the ARB software package to specifically detect GoM-Arc1, D-C06 and *Ca.* Syntrophoarchaeum, respectively. The probes have at least one mismatch to non-target groups in the current database. The stringency of the probes was experimentally tested with the Butane50 culture (Laso-Pérez*, et al.*, 2016) for the probe SYNA-666 and on environmental samples with the probes GOM-ArcI-660 and DC06-735 using 10-50% formamide. For probe SYNA-666, three helper probes (h1-h3SYNA-666) were applied to increase the performance of the probe together with an unlabelled competitor (c1SYNA-666) targeting the Marine Benthic Group E to avoid unspecific binding of the probe. Probe GOM-ARCI-660 was used with three competitors (c1-c3-GOM-ARCI-660). The probe DC06-735 was applied without helpers or competitors. All probes were purchased from Biomers.net (Ulm, Germany). For double hybridization, the peroxidases from the first hybridization were inactivated by repeating the inactivation step described above. The fluorochromes Alexa Fluor 488 and Alexa Fluor 594 were used. Filters were counterstained with DAPI (4',6'-diamino-2-phenylindole) and analyzed by epifluorescence microscopy (Axiophot II Imaging, Zeiss, Germany). Selected filters were analyzed by Confocal Laser Scanning Microscopy (LSM 780, Zeiss, Germany) including the Airyscan technology. Estimated cell abundances were determined by counting signals in 20 grids. For aggregates a sphere shape was assumed with coccoid cells and an average cell size of 1 µm in diameter.

Metagenomic library preparation and DNA sequencing. Previously extracted DNA was also used for metagenomics sequencing. For the oil site, DNA from the 9-10 cm depth sediment sample was used. 9 PCR-free DNA shotgun libraries were generated, with insert sizes between 350-750 bp. Libraries with the same insert size and sequenced on the same flow cell were merged, resulting in a final number of 6 libraries (**Supplementary Table 2**). DNA input amounts were 1 µg for libraries with up to 450bp insert sizes, and 2 µg for insert sizes larger than 450bp. Library preparation was done

following the Illumina TruSeq® DNA PCR-Free Sample Preparation Guide. The libraries were sequenced on MiSeq (2x300 PE run, v3 chemistry) and HiSeq 1500 (2x250 PE run, Rapid v2 SBS chemistry) instruments. For the asphalt sediments, one DNA shotgun library with an insert size between 550-600 bp was generated from 600 ng DNA from the 135 cm depth, following the Illumina TruSeq® Nano DNA Library Prep Guide. The library was sequenced on a MiSeq instrument (2x300 PE run, v3 chemistry). All Illumina sequencing was done at the CeBiTec (Bielefeld, Germany). After sequencing, primers and adapters were removed from all libraries and they were quality trimmed using the bbduk from the BBTools package (Bushnell, 2016) with a minimal Q-value of 20 and minimal length of 50 bp.

Metagenomic analysis. The 6 DNA shotgun library sequence data sets from the oil site were used to produce a bulk assembly using SPAdes v.3.9.0 (Bankevich*, et al.*, 2012) with default parameters. Afterwards, the bulk assembly was binned using Metawatt 3.5.3 (Strous*, et al.*, 2012) based on tetranucleotide identity, coverage mapping and coherence of the taxonomic affiliation of the predicted bin proteins. A bin with a 16S rRNA gene affiliated with the D-C06 clade was extracted. In order to improve the bin quality, targeted reassembly was performed consisting in read mapping to the contig and reassembly of the mapped reads. For mapping, the reads from the 6 oil site metagenomics libraries were mapped with 99% identity to the contigs of the extracted bin of each assembly round using bbmap from the BBTols package. Afterwards, the mapped reads were assembled with SPAdes with the flag –careful and the assembly was binned using Metawatt discarding contigs below 1000 bp. Finally, completeness and contamination of the bin was evaluated using checkM (Parks*, et al.*, 2015) with the *Euryarchaeota* marker genes set. To improve genome quality 16 reassembly rounds were carried out. The sequence data set obtained from the asphalt sediments library was used to produce a bulk assembly using SPAdes. Like for the oil site, the assembly was binned using Metawatt and a bin with a 16S rRNA gene affiliated to the D-C06 clade was extracted. As described before, 7 rounds of targeted reassembly were carried out in order to improve the quality of the bin.

Single cell sequencing of *Ca.* Syntrophoarchaeum. Anoxic aliquots of sediment samples from the 9-10 cm depth of the oil site were shipped at 5°C to the Bigelow Laboratory Single Cell Genomics Center (SCGC; https://scgc.bigelow.org). There, cells were separated from the sediment after dilution by centrifugation. Then, by high-speed fluorescence-activated and droplet-based cell sorting (FACS) single cells were sorted into a 384-well plate, where cell were lysed by five freeze-thaw cycles and KOH treatment. Multiple displacement amplification of the single cell genomic DNA was performed followed by phylogenetic identification of *Ca.* Syntrophoarchaeum cells and subsequent genome sequencing as previously described (Stepanauskas*, et al.*, 2017). Phylogenetic identification was performed by 16S rRNA gene tag sequencing. Only one cell affiliated with the *Ca.* Syntrophoarchaeum clade. For genome sequencing, libraries were constructed with Nextera XT

(Illumina) and then sequenced with NextSeq 500. Afterwards, reads were quality controlled using Trimmomatic v0.32 (Bolger, *et al.*, 2014) with the parameters '-phred33 LEADING:0 TRAILING:5 SLIDINGWINDOW:4:15 MINLEN:36' and then they were searched for human contamination. The quality-controlled reads were assembled using SPAdes with the parameters --careful --sc --phred-offset 33 after normalizing the read kmer coverage using kmernorm v1.05 with the flags -k 21 -t 30 -c 3. After assembly, contigs below 2200 bp were discarded. The final bin was screened for contamination and completeness using checkM.

Phylogenetic analyses of target organisms. 739 full-length 16S rRNA gene sequences from *Euryarchaeota* obtained from the SILVA_132_SSURef_NR99 database were used for phylogenetic analysis together with the three obtained 16S rRNA genes of the D-C06 and *Ca.* Syntrophoarchaeum bins obtained during this study. Ten trees were calculated with the ARB software (Ludwig, *et al.*, 2004) using the maximum likelihood algorithm RAxML with GTRGAMMA as model and a 50% similarity filter. 1000 bootstraps were performed to calculate branch support values. The tree with the best likelihood score was selected. For the D-C06 clade tree, short sequences were added to the calculated tree using the "Quick Add" option from the ARB package with the default filter for archaea excluding fast-evolving positions and reducing the filter to the 16S rRNA gene boundaries with the termini filter. To calculate phylogenetic affiliations of the methyl-coenzyme M reductase subunit alpha (*mcrA*), the methylcobalamin:coenzyme M methyltransferase (*mta)* and the methyl-H_4MPT:coenzyme M methyltransferase subunit H (*mtrH*) present in the bins of D-C06 and *Ca.* Syntrophoarchaeum, their respective protein sequences were aligned to protein sequences of the corresponding genes obtained from the NCBI database (305 McrA sequences, 504 Mta sequences and 152 MtrH sequences). Sequences were aligned using the software MUSCLE (Edgar, 2004) v3.7 followed by manual refinement. Afterwards, a masking filter over the common regions of every alignment was calculated using Zorro (Wu, *et al.*, 2012). Trees were calculated using the maximum likelihood algorithm RAxML (Stamatakis, 2014) v.8.2.11 using the masking filter with the automatic protein model assignment algorithm, PROTGAMAAUTO, which selected always LG as amino acid substitution model. Bootstraps were performed according to the convergence criterion of RAxML, performing 99 iterations for McrA, 149 for Mta and 100 for MtrH. The resulting trees were displayed with iTol webserver (Letunic and Bork, 2016).

Results and discussions

Hydrocarbon degradation in oil- and asphalt-rich sediments.

All samples of this study were obtained from marine sediments and asphalt deposits of the Campeche hydrocarbon province in the Gulf of Mexico (Sahling and Ohling, 2017). Samples from four sites were retrieved (**Table 1**). The main sample (hereafter oily sediment; **Supplementary Figure 1A**) was obtained from sediments in the direct vicinity of the Chapopote asphalt volcano (MacDonald, *et al.*,

2004, Marcon*, et al.*, 2018). Here, emerging oily gas bubbles and partly oil-coated gas hydrate outcrops showed the hydrocarbon-rich nature of this habitat. Abundant sulfide-dependent chemosynthetic seep fauna suggested intense hydrocarbon-dependent sulfate reduction in this sediment. The sample contained large amounts of oily hydrocarbons; gaseous alkanes such as methane (>2500 µmol per liter sediment), ethane (around 360 µM) and propane and butane (both around 50 µM) were particularly abundant in the deeper sediment horizons at 5-7 cm (**Figure 1A**). The anaerobic oxidation of methane in the sediments created a sulfate-methane transition zone at approximately 3-6 cm below seafloor. Measured rates of sulfate reduction exceeded methane oxidation rates by up to 4-fold, indicating that a fraction of the sulfate reduction was coupled to the oxidation of non-methane hydrocarbons. This imbalance of sulfate reduction to methane oxidation has been observed before in other Gulf of Mexico hydrocarbon seeps (Joye*, et al.*, 2004, Orcutt*, et al.*, 2010). In principle also long-chain alkanes could fuel sulfate reduction. However, these compounds were largely depleted in the oily sediments (here a mixed sample from 5-7 cm) compared to the asphalt flow (**Figure 1B**). This suggests that long-chain alkanes are largely consumed under methanogenic conditions in the sediments. Indeed, previous studies from the site have shown that methane isotopic compositions are highly depleted with $\delta^{13}C$ values down to -65‰ vs Vienna PeeDee Belemnite scale, suggesting intense biogenic methanogenesis based on hydrocarbon degradation (Schubotz*, et al.*, 2011, Sahling*, et al.*, 2016).

As second sample, the relatively fresh and unaltered asphalt (hereafter asphalt flow) was sampled at massive asphalt deposits of Chapopote asphalt volcano to compare the original composition of hydrocarbons. This sample contained gas hydrates in pores of the asphalt which bound most of the water in those samples. In contrast to the oily sediments, the asphalt flows contained a suite of *n*-alkanes (C_{12-38}) (**Figure 1B**). A third sample (hereafter ambient sediments) was retrieved from nearby sediment with no exposure to oil or other hydrocarbons (**Supplementary Figure 1B**). This sample was light-grey, non-sulfidic and contained only trace amounts of gaseous hydrocarbons and no oil. The sediment coloring suggested that oxygen penetrated several centimetres deep and sulfate was not consumed. The fourth sample (hereafter asphalt sediment) was retrieved using a gravity core from the Mictlan asphalt volcano situated northeast of Chapopote (Sahling*, et al.*, 2016, Sahling and Ohling, 2017). The upper part contained normal pelagic sediment. In the bottom, at 135 cm sediment depth, solid asphalt pieces were retrieved and further studied for their microbial communities.

Diverse archaeal and bacterial clades inhabit oil- and asphalt-rich sediments.

To characterize the microbial community compositions of three of the sites (oily, ambient and asphalt sediments), 16S rRNA gene amplicon libraries for *Bacteria* and *Archaea* were obtained and sequenced. The bacterial library from the ambient sediments contained mostly *Epsilonbacteria* and *Gammaproteobacteria,* while the one from the oily sediments contained mostly *Deltaproteobacteria*

affiliated with *Desulfobacterales* and *Syntrophobacterales* (**Supplementary Figure 2A**). Some of their members are considered to be important anaerobic alkane degraders (Knittel*, et al.*, 2003, Kleindienst*, et al.*, 2012, Kleindienst*, et al.*, 2014, Stagars*, et al.*, 2016). A large portion of sequences clustered with the Seep-SRB 1 and Seep-SRB 2 clades (**Figure 2A**), which are the most abundant sulfate-reducing partner bacteria of ANME archaea in AOM (Schreiber*, et al.*, 2010, Kleindienst*, et al.*, 2012). The asphalt sediments contained only small proportions of these Seep-SRB clades. Instead they were dominated by *Atribacteria*, which are heterotrophic anaerobes that have been repeatedly found in hydrocarbon-rich environments (Nobu*, et al.*, 2015).

The archaeal 16S rRNA gene libraries of the ambient sediments were dominated by *Thaumarchaeota* and *Woesearchaeota* with a small proportion of *Thermoplasmata* (Supplementary **Figure 2B**). By contrast, the libraries of the oily and asphalt sediments were dominated by the euryarchaeotal groups ANME-1 and D-C06. The oily sediments additionally contained considerable numbers of sequences affiliated to Marine Benthic Group B, ANME-2c, GoM-Arc1 and Marine Group II, the latter belonging to the *Thermoplasmatales* (**Figure 2B**). Sequences affiliated with the short-chain alkane degrader *Ca.* Syntrophoarchaeum were only found at the oil site, but in low relative abundances (<1%). The asphalt sediments were dominated by ANME-1 sequences with considerable proportions of D-C06 in both depths.

The high relative sequence abundance of ANME-1 and ANME-2c in the oily sediments underlines AOM as one of the main sulfate sinks in these sediments. Although in low abundance, *Ca.* Syntrophoarchaeum is likely degrading short-chain alkanes like propane and butane as seen before (Laso-Pérez*, et al.*, 2016). The environmental role of the other two groups, D-C06 and GoM-Arc1, has not been resolved so far, although *mcr* genes affiliated to the ones of *Ca.* Syntrophoarchaeum have been found in GoM-Arc1 MAGs (Dombrowski*, et al.*, 2017).

CARD-FISH analyses were performed to study the distribution of the three archaeal clades of interest (*Ca.* Syntrophoarchaeum, GoM-Arc1 and D-C06) in the sediment. For that purpose, specific probes were designed (see Material and methods, **Supplementary Table 1**). All three groups were detected in the oily sediments, while only GoM-Arc1 was found in the asphalt sediments and none of the three were present in the ambient sediments (**Figure 3**, **Supplementary Figure 3**). Up to 2.2% of archaeal cells belonged to *Ca.* Syntrophoarchaeum with a higher relative abundance closer to the surface and an estimated abundance of up to 6×10^6 cells per ml sediment. *Ca.* Syntrophoarchaeum appeared to form consortia with bacterial cells (**Figure 3**) as previously described (Laso-Pérez*, et al.*, 2016). GoM-Arc1 was also detected forming consortia with bacterial cells (**Figure 3**) with up to 35% of the total archaeal cells in deeper sediment (**Supplementary Figure 3**). Total estimated abundances for GoM-Arc1 ranged from 5×10^6 cells per ml in the upper sediment, up to 4×10^7 cells per ml sediment in the lower part of the core. D-C06 archaea were detected as single cells or as multicellular chains, representing up to 9% of archaeal cells (**Supplementary Figure 3**). Most D-C06 cells were found within oil droplets (**Figure 3**), which most likely had an impact on the total estimated cell

abundances. Light is scattered by oil in a way that only cells close to the surface of the oil droplets could be visualized with CARD-FISH. This is likely the cause of the differences between relative abundances in the 16S rRNA gene amplicon sequences (8-23%) and *in situ* counts. Hence, our estimates ranging from 7×10^6 cells to 1×10^7 cells per ml of sediment may underestimate the total abundance of D-C06 in these sediments. Most of the D-C06 cells were barrel-shaped and appeared to be surrounded by an extracellular sheath as shown for thermophilic ANME-1 archaea (Wegener*, et al.*, 2015). No associated bacterial cells were detected in the oil droplets. This suggests that D-C06 may perform oil degradation without the participation of a partner bacterium.

Metagenomic sequencing and phylogenetic analysis of assembled genomes.

To investigate the metabolic potential of the targeted archaea, total DNA metagenomic libraries were prepared and sequenced from the oil and asphalt sediments (**Supplementary Table 2**). A bulk assembly was performed for each sample. After contig binning, bins with 16S rRNA genes affiliated with D-C06 were extracted and further refined, yielding two high quality metagenome assembled genomes (MAG) from the oily (D-C06_oil) and the asphalt (D-C06_asphalt) sediments. The final MAGs have a size between 1.79-1.90 Mb with a completeness between 75% and 92% and a contamination lower than 5.5% (**Table 2**). No GoM-Arc1 and *Ca.* Syntrophoarchaeum MAGs were retrieved; however, a single amplified genome (SAG) affiliated to *Ca.* Syntrophoarchaeum (hereafter Syntropho_SAG) was recovered from the oil site. The SAG had a size of 0.81 Mb and a completeness of 42.7% and no contamination (**Table 2**). It represents a different, non-thermophilic species of *Ca.* Syntrophoarchaeum compared to the previously published SAGs (**Supplementary Table 3**), although they seem to have a largely similar metabolic potential (**Supplementary Figure 4**).

Both D-C06 MAGs and the Syntropho_SAG contained complete 16S rRNA genes that were used to construct a comprehensive phylogenetic tree using the RAxML algorithm (**Figure 4)** including all sequences of the target organisms longer than 1350 bp present in the SILVA database (Ref NR 99 v132). *Methanomicrobia* sequences cluster together in the tree, but they also include the class *Halobacteria*, as shown by phylogenetic analyses of single-copy genes (Adam*, et al.*, 2017). Sequences assigned by the SILVA database to D-C06 form two distinct groups. Five sequences form a cluster related to *Methanopyrus* and *Methanobacteria*. These sequences derived from a subsurface water sample of a mine in the Kalahari Shield and were named SAPMEG-1 group (Gihring*, et al.*, 2006). In this study, it was suggested that SAPMEG-1 could represent a new phylum. Our results indicate that sequences from this clade share only 73-79% identity with our and the original D-C06 sequences from the Gulf of Mexico (Orcutt*, et al.*, 2010), which we refer to as the D-C06 group. All sequences of the D-C06 group derive from environments rich in liquid alkanes such as marine oil-seeps or terrestrial oil reservoirs (**Figure 4**, **Table 3**). With identity values to 78-82% to the sister clades, D-C06 likely represents a distinct class within *Euryarchaeota*.

Ca. Syntrophoarchaeum (previously GoM-Arch 87) sequences form a distinct clade including the original sequence of the Gulf of Mexico (AM745246), the sequences related to the Guaymas Basin

strains, the 16S rRNA gene of the Syntropho_SAG and two sequences from the Gulf of Mexico and Taiwan subsurface sediment. *Ca.* Syntrophoarchaeum has ANME-1 and *Methanosarcinales* as sister groups. Our results indicate that *Ca.* Syntrophoarchaeum should be a separate order next to ANME-1 and *Methanosarcinales* based on the identity values to these groups of 81-86%. Recent phylogenetic analyses of protein marker genes support these results, placing *Ca.* Syntrophoarchaeum next to ANME-1 close to the *Methanomicrobia* (Adam*, et al.*, 2017).

Genomic potential of D-C06 archaea.

The two D-C06 MAGs retrieved from the asphalt and the oily sediments have a high average nucleotide identity (95%) and identical metabolic potential (**Supplementary Table 4**). Hence, they likely belong to the same species according to genomic standards (Goris*, et al.*, 2007) (**Supplementary Table 3**).

Methanogenesis pathway. D-C06 encodes for the complete methanogenesis pathway including two *mcr* operons in each genome (**Figure 5**, **Supplementary Table 4**). The protein sequences of the two *mcrA* genes per single MAG are highly divergent, sharing only 41% identity (**Figure 6**). One *mcrA* belongs to the canonical McrA type found in methanogens and methanotrophs and forms an independent cluster related to McrA sequences of *Methanomicrobiales* and *Methanobacteriales.* Genes encoding enzymes catalysing all further steps of the methanogenesis pathway are present in D-C06 (**Figure 5**), including the methyl-H_4MPT:coenzyme M methyltransferase (Mtr). Mtr catalyses the transfer of a methyl radical between CoM and tetrahydromethanopterin. A phylogenetic analysis of the MtrH (**Supplementary Figure 5A**) shows a close affiliation with MtrH units of methanogens (*Methanosarcinales*) and methanotrophs (ANME-1), suggesting that it catalyses the transfer of C_1-compounds and therefore it is most likely part of an intact (reverse) methanogenesis pathway. In contrast, *mtr* has not been found in the short-chain alkane degrading *Ca.* Syntrophoarchaeum (Laso-Pérez*, et al.*, 2016).

Alkane activation by MCR. From the second McrA present in D-C06, only one full copy was retrieved, since the one of D-C06_asphalt was truncated. This second McrA is affiliated to the divergent McrA types, which are found in *Bathyarchaeota* and *Ca.* Syntrophoarchaeum (Evans*, et al.*, 2015, Laso-Pérez*, et al.*, 2016). In *Ca.* Syntrophoarchaeum, these MCRs catalyse the activation of multi-carbon alkanes such as butane and propane (Laso-Pérez*, et al.*, 2016), forming alkyl-CoM as primary intermediate. Based on these findings, D-C06 might have the potential to activate multi-carbon alkanes but also to produce or oxidize methane.

Additionally, D-C06 harbours genes that encode several methylcobalamin:coenzyme M methyltransferases (related to the MtaA and the MtbA/MttBC). In *Ca.* Syntrophoarchaeum, these enzymes were suggested to transform the butyl-CoM into an intermediate, which after oxidation is converted to butyryl-CoA (Laso-Pérez*, et al.*, 2016). The cobalamin methyltransferase from D-C06_oil clusters in a deep-branching clade with one of the *mtaA* copies of *Ca.* Syntrophoarchaeum (**Supplementary Figure 5B**) suggesting a similar mechanism for the initial transformation of CoM-

bound alkanes in D-C06. Moreover, the D-C06 MAGs harbour genes that may encode the following steps towards a CoA-bound fatty acid (**Figure 5**): using the encoded cobalamin methyltransferase, the CoM-bound alkyl units could be released as free alcohol, which might then be sequentially oxidized by an alcohol and an aldehyde dehydrogenase, which are encoded in the MAGs. The produced fatty acid might be ligated to CoA using the encoded CoA-ligase. Interestingly, the D-C06 MAGs encode for several long-chain fatty-acid-CoA ligases and a 4-hydroxybutyrate-CoA transferase, which could indicate the potential to degrade a variety of different long- and short-chain alkanes. This proposed link between CoM bound alkyl units and the CoA bound fatty acid was not found in the genomes of *Ca.* Syntrophoarchaeum, which miss CoA-ligases (Laso-Pérez*, et al.*, 2016). This may indicate that *Ca.* Syntrophoarchaeum and D-C06 use different strategies to connect the CoM activation with the fatty acid degradation.

Fatty acid degradation. The CoA-bound fatty acids can be further degraded via the fatty acid degradation pathway, of which many steps are encoded in several copies per single MAG (**Figure 5**). The product of this pathway is acetyl-CoA. Several encoded enzymes in the MAGs could metabolize the acetyl-CoA including the acetyl-CoA decarbonylase/synthase complex (ACDS) and acetyl-CoA synthetase. The ACDS complex should work in the oxidative direction, cleaving the acetyl-CoA into CO_2 and methyl-H_4MPT. In *Ca.* Syntrophoarchaeum, the methyl-H_4MPT is fully oxidized with the downstream part of the methanogenesis. However, the presence of the *mtr* and two distinct *mcr* in D-C06 could be indications of a different metabolism.

Interestingly, the D-C06 MAGs contain several genes that indicate potential for degradation of aromatic compounds like benzene. Both MAGs contain an operon formed by genes encoding two subunits of the benzoyl-CoA reductase (BadEG) flanked by methylmalonyl-CoA mutase genes. The D-C06_oil operon includes a gene encoding a CoA-ligase, whereas the D-C06_asphalt operon contains another gene encoding another benzoyl-CoA reductase subunit (BadF). BadEGF genes have high similarity with the genes of the 2-hydroxymethylglutaryl-CoA dehydratase enzyme, which is involved in the degradation of L-glutamate, what could indicate a different role than degradation of aromatic compounds. Genes encoding enzymes that catalyse the following steps of benzoyl-CoA degradation (Harwood*, et al.*, 1998) (like cyclic dienoyl-CoA hydratase or dienoyl-CoA reducing enzyme) have not been detected, although they are similar to enzymes of the fatty acid degradation pathway (like acyl-CoA dehydrogenase or enoyl-CoA hydratase). Therefore, further studies are needed to elucidate the potential of D-C06 to degrade aromatic compounds.

Electron cycling. Genes encoding several electron cycling complexes are present in both MAGs including the complete electron transport complex Rnf, the CoB-CoM heterodisulfide reductase (HdrABC), several 4Fe-4S proteins associated to aldehydes oxidoreductases and a hydrogenase (Hyh) related to those of *Pyrococcus furiosus.* The Hyh enzymes of *P. furiosus* are formed by four subunits (Pedroni*, et al.*, 1995, Peters*, et al.*, 2015). However, only the beta and gamma subunits were present in both D-C06 MAGs, while the alpha catalytic subunit was absent. Although the absence could be

attributed to the incompleteness of the MAGs, it might also be possible that the Hyh of D-C06 is not involved in hydrogen metabolism but just in electron cycling. Associated to the *hdr* operon, the D-C06 MAGs contain electron transfer flavoproteins and a Fe-S oxidoreductase, which are probably involved in the electron flow in the fatty acid oxidation (Schmidt*, et al.*, 2013). Additionally, D-C06_oil MAG has an operon encoding several hydrogenases subunits resembling the ferredoxin hydrogenase (Mvh) and a NiFe hydrogenase which has been described to be involved in CoM regeneration in different methanogens (Peters*, et al.*, 2015). Genes encoding cytochromes c were only found associated to genes involved in the detoxification of reactive oxygen species. Therefore, they might play a different role compared to the cytochromes of ANME-1 or *Ca.* Syntrophoarchaeum, which are thought to be involved in the direct electron transfer (McGlynn*, et al.*, 2015, Laso-Pérez*, et al.*, 2016, Krukenberg*, et al.*, 2018). Genomic information is insufficient to predict the interplay of the encoded enzymes, and the direction of electron transfers. However, these complexes show that D-C06 has the machinery required for internal electron cycling and energy conservation. Similar to *Ca.* Syntrophoarchaeum and ANME, D-C06 lacks the machinery for a dissimilatory sulfate reduction pathway. D-C06_oil harbour genes encoding the phosphoadenosine phosphosulfate reductase, an adenylyl-sulfate kinase and a sulfate adenylyltransferase, but these genes encode enzymes for assimilatory purposes.

Metabolic model for D-C06.

We propose that the divergent MCR of D-C06 catalyses the alkane activation, forming a CoM-bound alkyl unit as primary intermediate, which would be degraded to CO_2 and methyl-H_4MPT (**Figure 5**). Two possibilities emerge for the role of the canonical MCR. D-C06 may either thrive on complete methane and/or hydrocarbon oxidation, or they disproportionate longer alkanes producing methane and CO_2 as products. In the first scenario, D-C06 would use both of its MCRs in the oxidative direction, defining D-C06 as a novel ANME clade with the additional capability to also oxidize higher hydrocarbons. It would fully oxidize the methane- and alkane-derived methyl-H_4MPT with the downstream part of the reverse methanogenesis pathways. D-C06 does not encode for a dissimilatory sulfate reduction pathway and lacks a bacterial partner. In principle, reducing equivalents might be used to form hydrogen or acetate, but under standard conditions such reactions are highly endergonic for alkanes (**Table 4**). Extremely low *in situ* intermediate concentrations would need to be maintained, and there are currently no indications for such a scenario. Moreover, according to prior studies, hydrogenases similar to those encoded in the D-C06 MAGs are rather used in the oxidative direction than for hydrogen production (Schut*, et al.*, 2012, Peters*, et al.*, 2015).

In the second scenario, D-C06 would degrade alkanes producing methane and CO_2 as products. In this case, the Mtr of D-C06 would transfer the methyl group from H_4MPT to CoM forming methyl-CoM, which is finally reduced to methane using the canonical MCR. The surplus reducing equivalents released during the cleavage would be used for the reduction of CO_2 forming additional methane. Based only on metagenomic data, we cannot define the range of alkanes that D-C06 could metabolize. Under standard conditions methanogenesis would be feasible for all multi-

carbon alkanes (Schink, 1985) and energy yields for methanogenic alkane degradation increase with alkane chain length (Dolfing*, et al.*, 2007). However experimental data with environmental samples showed alkane-dependent methanogenesis only for substrates with at least 6 carbon atoms (Siddique*, et al.*, 2006). In the following, we discuss alkane degradation with hexadecane, one of the most abundant compounds in the saturate fraction of the asphalt flows as example (**Table 4**). The overall reaction (without considering biosynthesis) would be:

$$C_{16}H_{34} + 7.5\ H_2O \rightarrow 12.25\ CH_4 + 3.75\ CO_2 \qquad \text{(Equation 1)}$$

This reaction is exergonic under standard conditions but also under a wide range of environmental conditions. The methanogenic degradation of hydrocarbons has already been described for several decades, but so far it was based in the syntrophic interaction of hydrocarbon-degrading bacteria with methanogenic archaea (Zengler*, et al.*, 1999, Sakai*, et al.*, 2009, Gray*, et al.*, 2011). In the case of D-CO6, the complete reaction may proceed in a single cell, which is an unprecedented finding. In a first step, the alkane oxidation (see metabolic model) would produce methyl groups bound to H_4MPT (-R) and CO_2 in equal amounts releasing 50 electrons.

$$C_{16}H_{34} + 16\ H_2O + 8\ RH \rightarrow 8\ R\text{-}CH_3 + 8\ CO_2 + 50H^+ + 50e^- \qquad \text{(Equation 2)}$$

Of these electrons, 16 would be used to reduce the methyl-H_4MPT to methane in an energy-conserving step including the translocation of sodium ions out of the membrane.

$$8\ R\text{-}CH_3 + 16\ e^- + 16H^+ \rightarrow 8\ CH_4 + 8\ RH \qquad \text{(Equation 3)}$$

The remaining 34 electrons would need an electron sink, likely in the form of methanogenic CO_2 reduction.

$$4.25\ CO_2 + 34\ H^+ + 34\ e^- \rightarrow 4.25\ CH_4 + 8.5\ H_2O \qquad \text{(Equation 4)}$$

Environmental data support alkane-dependent methanogenesis in D-C06.

Here we studied D-C06, a clade of yet uncultured anaerobic archaea that inhabit oil-rich and mostly sulfate-depleted environments. We propose that D-C06 archaea are able to disproportionate alkanes producing methane and CO_2 as final products in a sole cell. This is supported by microscopic observation. D-C06 cells appear within the oil droplets without any potentially partners (**Figure 3**).

The alkanes present in the oil droplets would be their sole energy source. D-C06 is evenly abundant throughout the sediment core including also the sulfate-depleted horizons (**Figure 2**, **Supplementary Figure 3**). In samples from the same environment, methane $\delta^{13}C$ values were with -60 to -64 ‰ strongly depleted compared to that of thermogenic methane rising from deep reservoirs (Schubotz*, et al.*, 2011). This pattern has been considered as evidence for biological methanogenesis in these shallow sediments. D-C06 could be the key organism for this process based on its overproportional abundance in the oily sediments (**Figure 2**, **Supplementary Figure 3**). With canonical methanogens being rare (**Figure 2**), it is unlikely that a significant proportion of the observed methane production and hydrocarbon degradation is via syntrophic methanogenesis (Zengler*, et al.*, 1999).

D-C06 archaea might also play an important role in other crude oil-rich environments. 16S rRNA gene sequences from D-C06 have mostly been recovered from oil-related places like deep petroleum reservoirs and oil seeps, but rarely from dry oil-lacking gas seeps (**Table 3**). A 16S rRNA gene phylogeny of the D-C06 clade including short sequences reveals the existence of two subgroups within the D-C06 clade (**Supplementary Figure 6**). The two 16S rRNA gene sequences from our MAGs cluster with others from marine oil-affected environments, while a second group includes sequences from terrestrial oil reservoirs, asphalt lakes and contaminated sites. This phylogeny includes short sequences affiliated to D-C06 detected in a hexadecane-degrading enrichment established from production water of an oil reservoir (Cheng*, et al.*, 2011). Moreover, D-C06 was detected in methanogenic enrichments degrading crude oil established from oil field sludge at 35 and 55°C (Cheng*, et al.*, 2014). The study assumed that the consumption of alkanes in the enrichments was performed by consortia of alkane-degrading bacteria and methanogenic archaea. However, our results suggest that D-C06 alone is responsible for methanogenic oil degradation.

Conclusions and implications

Many studies have shown that archaea play a key role in methane cycling at hydrocarbon-rich seeps and vents (Knittel and Boetius, 2009, Ruff*, et al.*, 2015). At the Campeche Knolls, we investigated alkane-degrading archaea based on ecological and genomic data. We show that the oil seeps contain a high diversity of archaea like *Ca.* Syntrophoarchaeum and potential alkane-degrading clades like GoM-Arc1 and D-C06. These organisms likely contribute to oil degradation using different strategies, substrates and reactions. *Ca.* Syntrophoarchaeum and GoM-Arc1 archaea form consortia with likely sulfate-reducing partner bacteria. These archaeal groups probably degrade gaseous substrates, as *Ca.* Syntrophoarchaeum has been shown to degrade butane and propane. In contrast, D-C06 archaea appear as single cells or monospecies aggregates mainly within oil droplets, thereby likely thriving on larger hydrocarbon compounds. D-C06 genomes encode for a complete methanogenesis pathway with a canonical MCR and a highly divergent MCR, which likely allows for alkane disproportion producing CO_2 and CH_4. This implies a before overlooked role of archaea in hydrocarbon degradation. Archaea could be solely responsible for oil and hydrocarbon degradation without the need of a bacterial partner in deep petroleum reservoirs, gas and oil seeps and other oil-related environments. The cultivation of D-C06 is a necessary future step to confirm this hypothesis.

Acknowledgements: We thank M. Meiners, E. Weiz-Bersch and S. Miksch for assistance and support in the CARD-FISH analysis. We are indebted to the crew, the MARUM ROV QUEST pilots and the shipboard party of RV METEOR research expedition M114. This research project was funded by the DFG Leibniz Grant of the Deutsche Forschungsgemeinschaft (DFG) to Antje Boetius, and the DFG Research Center and Cluster of Excellence MARUM, the University of Bremen and the Deep Carbon

Observatory (Deep Life grant 11121/6152-2121-2329-9973-CC to G.W.), the Max Planck Society and the Helmholtz Society.

Author contribution: G.W., G.B., H.S. and F.S. retrieved the original samples. R.L.-P. and G.W. designed research. G.W., F.S. and N.S. carried out the geochemical analysis. K.K. and C.H. designed the CARD-FISH probes and performed microscopy. H.E.T. prepared and sequenced the DNA libraries. R.L.-P. and D.M.V. performed 16S tag sequencing analysis. R.L-P. performed metagenomic analyses. R.L.-P., G.W. and A.B. developed the metabolic model, and wrote the manuscript with contributions from all co-authors.

Author information: The authors declare no competing financial interests. Readers are welcome to comment on the online version of the paper. Correspondence and requests for materials should be addressed to R.L-P. (rlperez@mpi-bremen.de) or G.W. (gwegener@mpi-bremen.de).

Figures and Tables

Figures

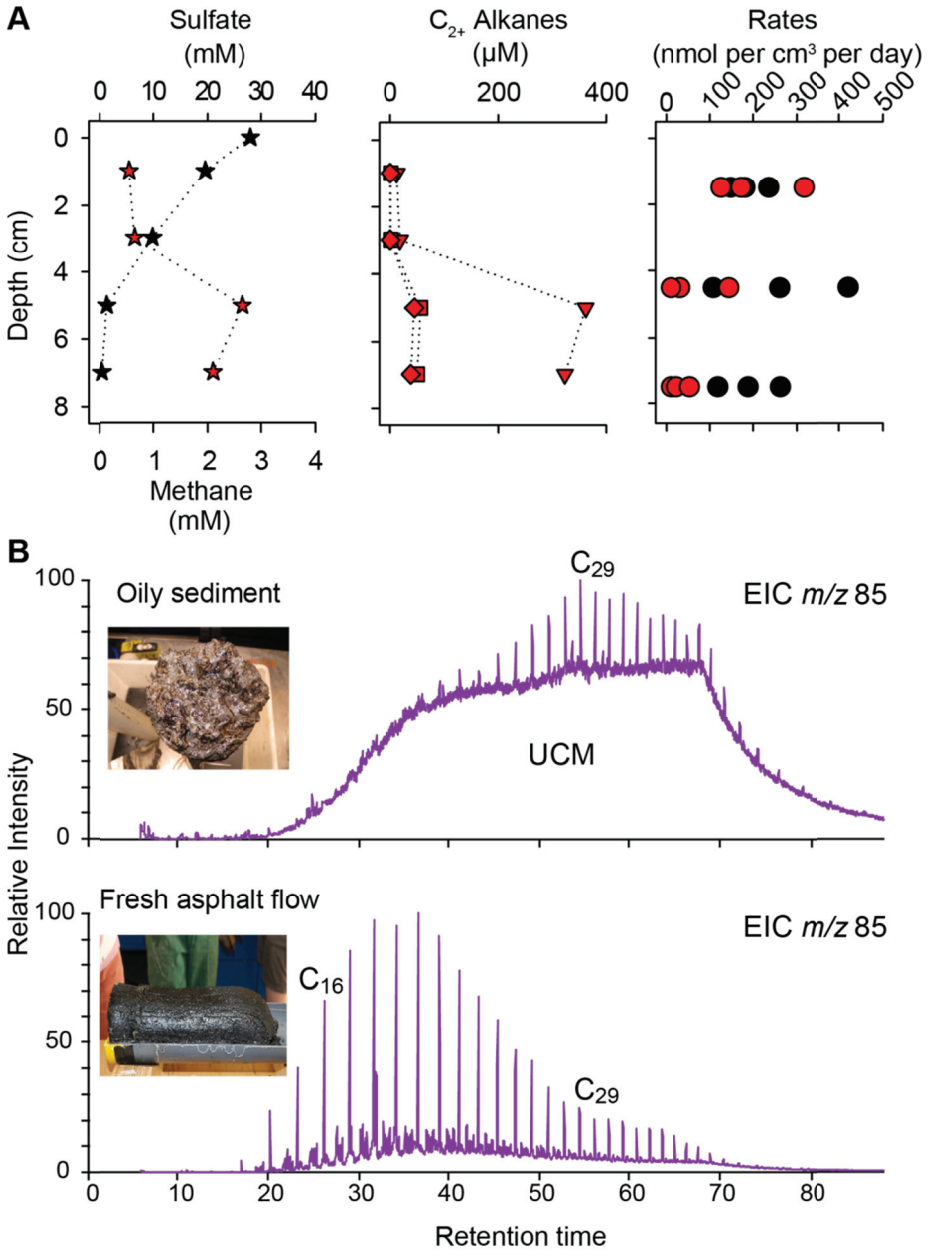

Figure 1. Geochemical analyses of the oily sediments (station 19351-14) and asphalts flows (station 19345-1). A, Concentrations of sulfate (black stars) and methane (red stars) in mM (left panel), short-chain alkanes (ethane=triangles, propane=squares, butane=diamond) in µM (middle panel) and rates of sulfate reduction (black circles) and methane oxidation (red circles) in nmol cm^{-3} of sediment day^{-1} (right panel) in oily sediments. **B**. Extracted mass chromatogram *m/z* 85 of the saturate fraction of the oily sediment at 5-7 cm depth (top) and fresh asphalt flow sample at circa 45 cm depth (bottom), showing *n*-alkane distributions and varying degrees of biodegradation. Note that the baseline in the oily sediment sample is elevated because most of the *n*-alkanes have been removed.

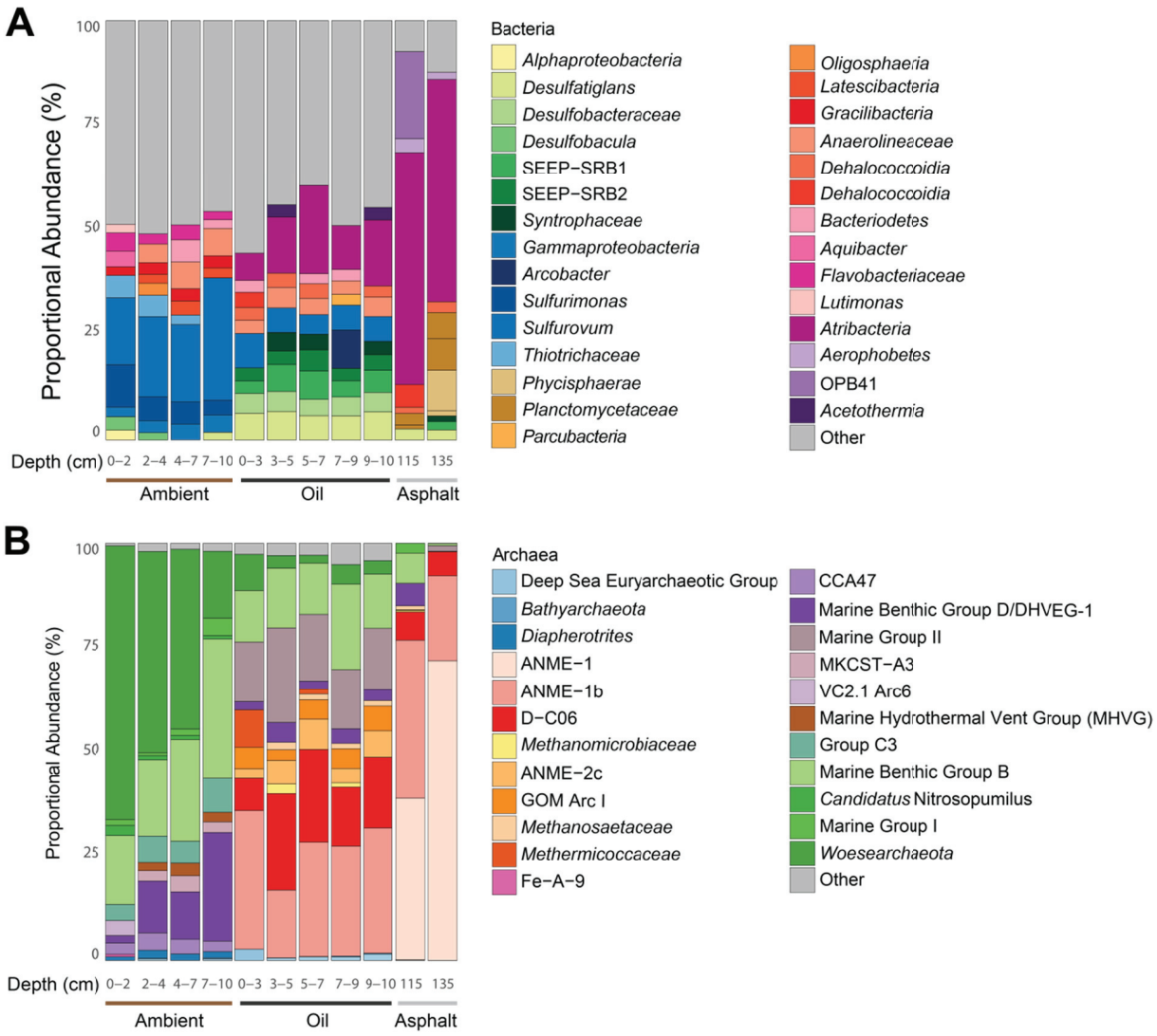

Figure 2. Relative abundance of 16S rRNA gene tags for (A) bacteria (genus level) and (B) archaea (family level) in the ambient, oily and asphalt sediments. For each sample and depth only the 10 most abundant clades are depicted. In the ambient sediments sequences of mostly aerobic and partly planktonic microorganisms were found. The oil site contained many archaeal sequences related to ANME-1, D-C06 and GoM-Arc1 as well as deltaproteobacteria described as oil degraders (*Desulfobacula, Syntrophaceae*) and syntrophic partner bacteria of ANME (SEEP-SRB1). In the asphalt sediments sequences of D-C06 were found only in the proximity of the asphalt chunks.

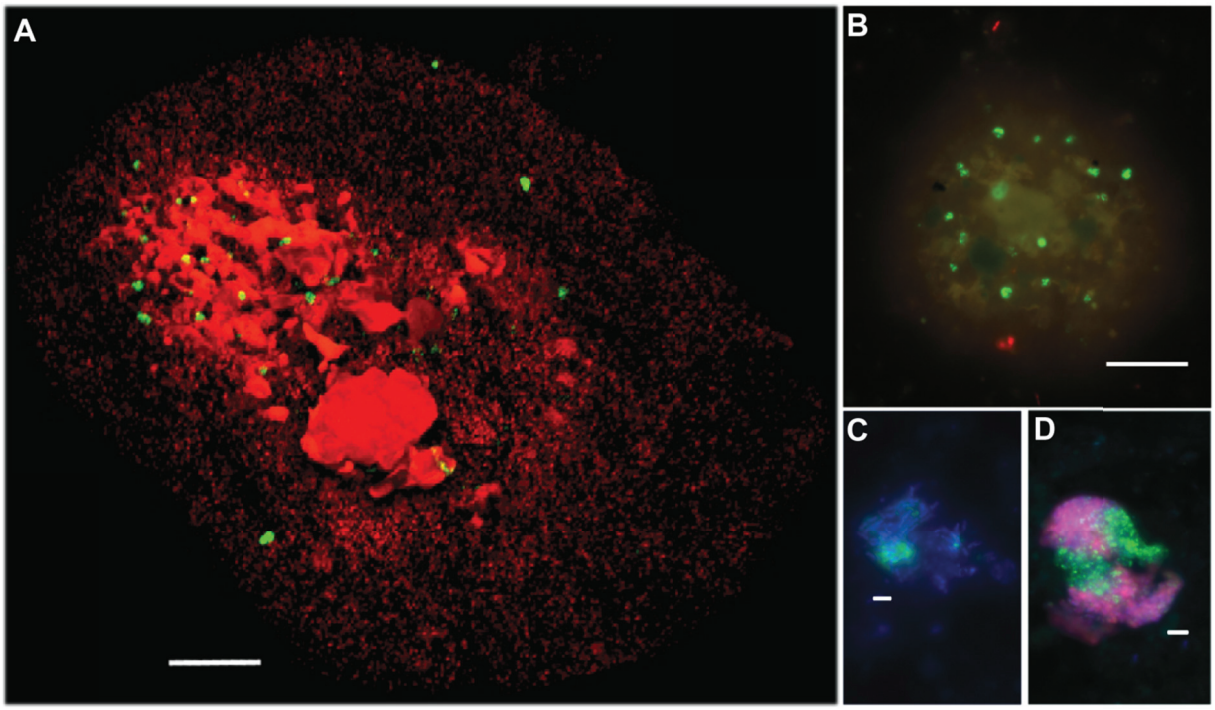

Figure 3. Epifluorescence micrograph of D-C06, GoM-Arc1 and *Ca.* Syntrophoarchaeum cells in oily sediments from the Gulf of Mexico. A. CARD-FISH staining of D-C06 with the DC06-735 probe (green) in an immersed oil droplet (autofluorescence in red). **B.** Dual CARD-FISH staining of D-C06 cells (green) and bacteria (red; targeted with probe EUB388 I-III). The autofluorescence of oil shows the contours of the oil droplet. **C.** CARD-FISH staining of *Ca.* Syntrophoarchaeum cells in consortia with the SYNA-666 probe (green) and DAPI counterstain (blue). **D.** CARD-FISH staining of GoM-Arc1 cells with the GOM-ARCI-660 probe (green), bacteria (red) and DAPI counterstain (blue). Scale bars in images: A-B = 10 µm; C-D = 2 µm.

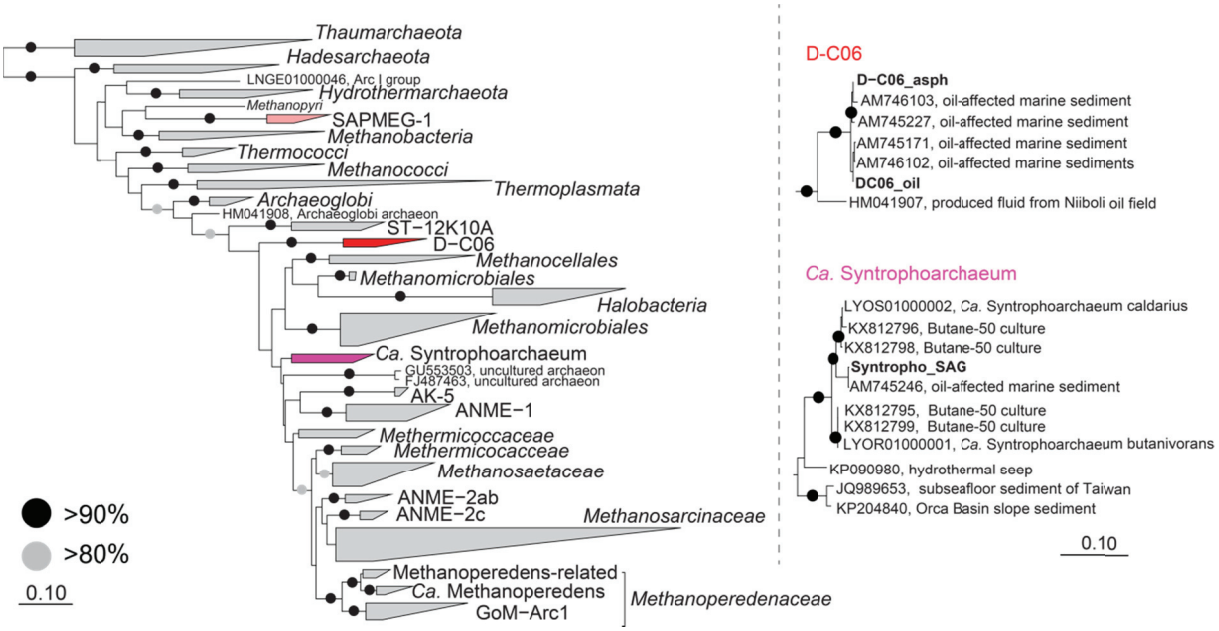

Figure 4. Phylogenetic affiliation of GoM-Arc1, *Ca.* Syntrophoarchaeum and D-C06. A. Phylogenetic tree for *Euryarchaeota* with a focus on the *Methanomicrobia*. Sequences of the D-C06 clade (according to ARB SILVA taxonomy**)** are clustered in two groups: SAPMEG-1 (light red) and D-C06 (red). *Ca.* Syntrophoarchaeum clade is shown in purple. **B.** Extended display of the clades of interest with 16S rRNA gene sequences of the D-C06 and *Ca.* Syntrophoarchaeum bins in bold. Bootstrap values > 80% and > 90% are indicated with grey and black circles. Scale bars represent the number of nucleotide substitutions per site.

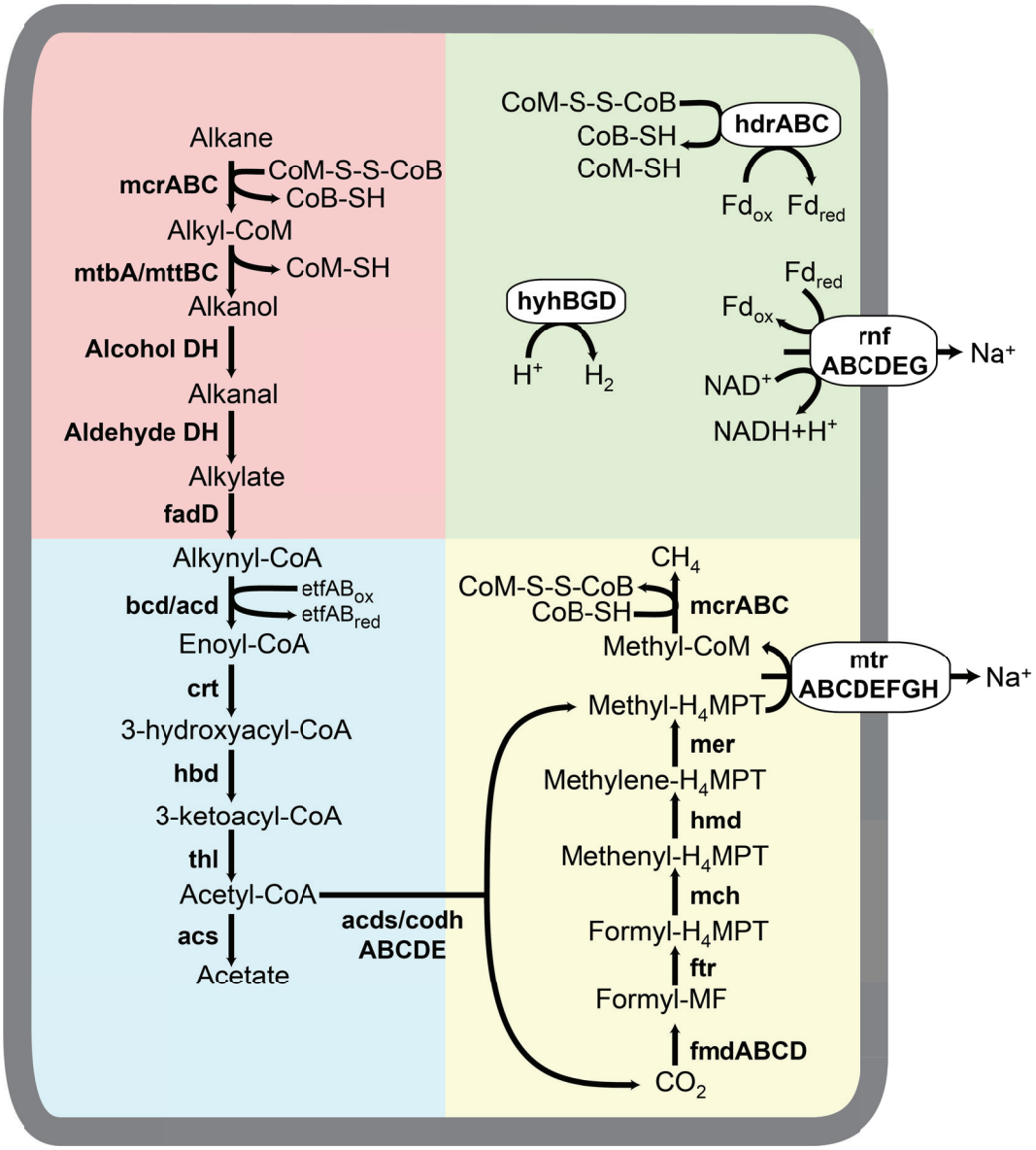

Figure 5. Metabolic model of alkane disproportionation proposed for D-C06. Genes for all the proposed steps were found in the MAGs. Background colours for the alkane activation and conversion to a CoA-bound fatty acid (red); fatty acid degradation and ACDS (blue); methanogenesis (yellow) and electron cycling (green). The alkanes are activated forming alkyl-CoM as primary intermediate. Then, free alcohols are formed that are sequentially oxidized to fatty acids, which are ligated to CoA and oxidized into acetyl-CoA. This molecule is split into CO_2 and H_4MPT-bound methyl groups. Methyl- H_4MPT is reduced to methane in an energy-conserving step (sodium translocation). The surplus reducing equivalents released during this alkane disproportionation are used for additional methane formation through CO_2 reduction. Additional energy conserving steps would be possible via the regeneration of CoM-S-S-CoB and the transfer of electrons from ferrodoxin to NADH. A hydrogenase could be present to balance additional electron gradients.

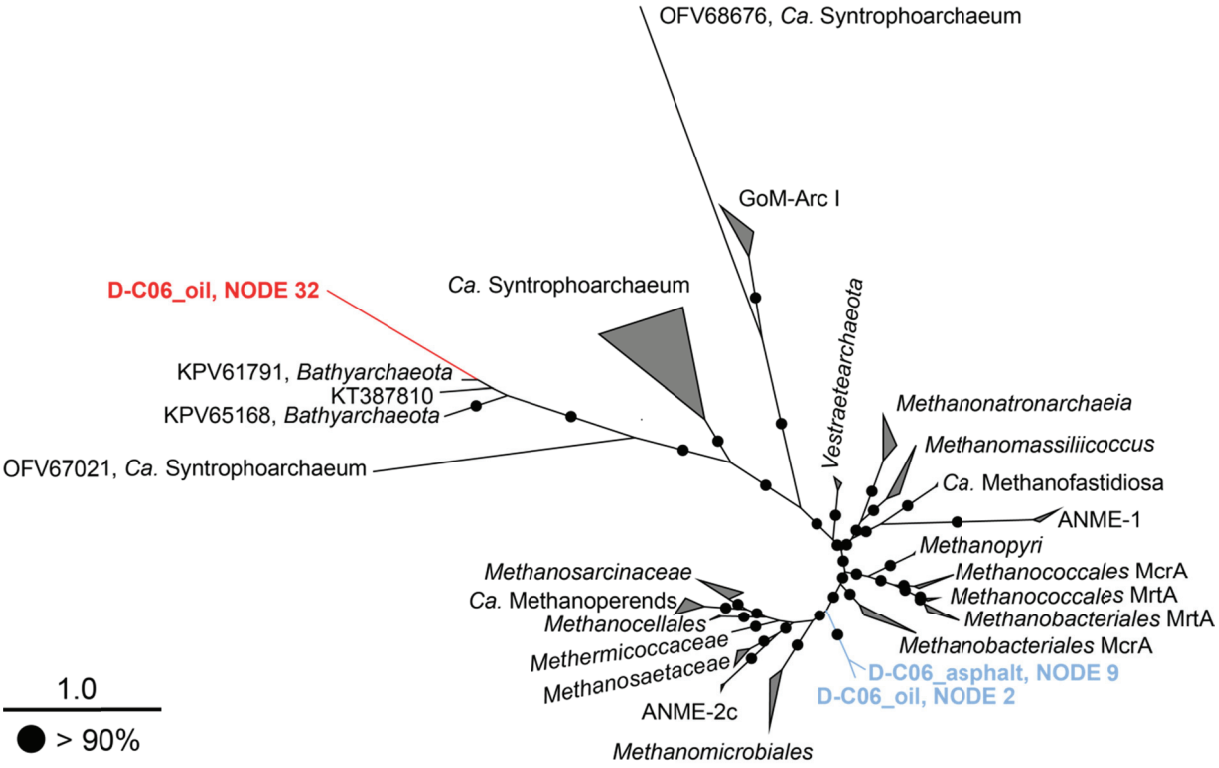

Figure 6. Phylogenetic tree of the amino acid sequences of the *mcrA* genes present in D-C06 MAGs. The tree was calculated based on a maximum likelihood algorithm using 305 amino acid sequences using over 450 amino acid positions for calculations. D-C06 *mcrA* genes are indicated in red (related to *Ca.* Syntrophoarchaeum and *Bathyarchaeota*) or blue (related to methane cycling) indicating the original bin and scaffold. Scale bar indicates the number of amino acid substitutions per site. Bootstrap values > 90% are indicated with black circles.

Table 1. Information about the samples used in this study. The most relevant data concerning sampling and location are provided as well as the analysis, where the different samples were used.

Sample name	Station name	Location	Sampling area	Sample description	Sampling method	Water depth (m)	Analysis performed
Oily sediments	GeoB 19351-14	21°53.964'N; 93°26.226'W	Chapopote	Oily sediments in the vicinity of the asphalt volcano	Push core (1-10 cm)	2925	Geochemistry, 16S gene tag sequencing, microscopy visualization, cell counting, metagenomics
Asphalt flow	GeoB 19345-1	21°53.964'N; 93°26.226'W	Chapopote	Solid and fresh asphalt from asphalt deposits	Gravity core (40 cm)	2926	Geochemical analysis
Ambient sediments	GeoB 19351-5	21°53.954'N; 93°26.261'W	Chapopote	Sediment elevation not affected by oil or gas	Push core (1-10 cm)	2905	16S gene tag sequencing, cell counting
Asphalt sediments	GeoB 19331-1	22°01.354'N; 93°14.809'W	Mictlan	Sediments with solid asphalt pieces	Gravity core (135 cm)	3092	16S gene tag sequencing, cell counting, metagenomics

Table 2. Genomic information from the extracted MAGs of D-C06 (D-C06_oil and D-C06_asphalt) and the SAG affiliated to *Ca.* Syntrophoarchaeum (Syntropho_SAG).

	D-C06_oil	**D-C06_asphalt**	**Syntropho_SAG**
Size (bp)	1796491	1905026	816919
Scaffolds/Contigs	247/247	390/391	46/46
GC content (%)	42.6	42.9	44.1
Scaffold N50 (bp)	10035	8058	33143
Number of ORFs	1737	2159	861
rRNAs	5S, 16S, 23S	5S, 16S, 23S	5S, 16S and 23S
tRNAs	30	54	23
Completeness (%)[1]	75.2	92.2	42.7
Contamination (%)[1]	5.5	3.7	0.0
Strain heterogeneity (%)[1]	22.2	25.0	0.0

[1]Based on lineage-specific marker genes of *Euryarchaeota* using CheckM.

Table 3. Environmental information from publically available 16S rRNA gene sequences affiliated to D-C06 present in the SILVA v132 database. A representative sequence from each study has been selected. Sequences have length range of 394-1451 bp.

Accession number	Isolation source	Environment	Comments	References
AM746103	Gulf of Mexico, Campeche Knolls region	Hydrocarbon-rich marine sediments close to an asphalt volcano (2902 m deep)	First study defining D-C06 clade as GoM-Arc2	Orcutt et al., 2010
AY454634	Brazil: Santos-Sao Vicente estuary	Brackish hydrocarbon exposed marine sediments with high concentrations of polycyclic aromatic hydrocarbons	This sequence belongs to the clone D_C06 after which the clade was renamed	Piza, 2004
AY542189	Gulf of Mexico, Green Canyon	Marine gas hydrates (575 m deep)	High percentage of short-chain alkanes	Mills et al., 2004
AJ556299	China: Jurong	Paddy soil		Wu et al., 2006
DQ521755	Gulf of Mexico, Green Canyon	Mud volcano with oil present (876 m deep)		Lloyd et al., 2006
EU735576	China: Jidong oilfield	Oil-contaminated soil		Liu et al., 2009
FM866673	Canada: Cape Breton; Sydney Tar Ponds	Contaminated tar ponds	281 clones affiliated with D-C06 were reported	Koenig et al., 2009
HQ065902	Canada: Athabasca oil sand refine (Alberta)	Oil sand tailing pond		Ramos-Padron et al., 2010
HQ845189	China: Shengli oil field	Methanogenic hexadecane-enrichment from a terrestrial oil reservoir (1600 m below surface)		Cheng et al., 2011
GU120489	Trinidad y Tobago: Pitch lake, asphalt lake	Liquid asphalts, oil and mud volcanoes	D-C06 classified as Tar ARC I group. They represent more than 50% of the archaeal community in the oil wells	Schulze-Makuch et al., 2011
HM041907	Japan: Niiboli oilfield	Terrestrial oil reservoir (1050 m below surface)	Present in the crude-oil fraction	Kobayashi et al., 2012
AB899898	Egypt:Suez Gulf, Elzaiteya site	Petroleum-contaminated marine sediment (20 m below surface)		Elsaied, 2014
JF947128	China: Shengli oil field	Methanogenic hexadecane-degrading enrichment at 35°C	D-C06 represents around 20-40% of the archaeal community.	Cheng et al., 2014
JF947151	China: Shengli oil field	Methanogenic hexadecane-degrading enrichment at 55°C	D-C06 represents between 10-30% of the archaeal community	Cheng et al., 2014
KC442804	China: Xinjian Luliang Oil Field	Water samples from terrestrial oil well		Gao et al., 2015
AY996927		Hydrocarbon-containing wastewater		Kapley et al., unpublished
HQ133153	China: Shengli oil field	Crude-oil contaminated soil		Cheng and Lu, unpublished
KU025251		Oil field		Song, unpublished

Table 4. Thermodynamic calculations for the degradation of hexadecane under different conditions: complete oxidation, oxidation to acetate and coupled to methane production.

Reaction	**$\Delta G°'_{pH=7}$ (kJ per mol alkane)**
Hexadecane degradation	
$C_{16}H_{34} + 32\ H_2O \rightarrow 16\ CO_2 + 49\ H_2$	1365.1
$C_{16}H_{34} + 16\ H_2O \rightarrow 8\ C_2H_3O_2^- + 17\ H_2 + 8\ H^+$	471.8
$4\ C_{16}H_{34} + 30\ H_2O \rightarrow 49\ CH_4 + 15\ CO_2$	-339.2

References

Adam PS, Borrel G, Brochier-Armanet C and Gribaldo S (2017) The growing tree of Archaea: new perspectives on their diversity, evolution and ecology. *The ISME journal* **11**: 2407.

Amann RI, Krumholz L and Stahl DA (1990) Fluorescent-oligonucleotide probing of whole cells for determinative, phylogenetic, and evironmental studies in microbiology. *Journal of Bacteriology* **172**: 762-770.

Amann RI, Binder BJ, Olson RJ, Chisholm SW, Devereux R and Stahl DA (1990) Combination of 16S rRNA-targeted oligonucleotide probes with flow cytometry for analyzing mixed microbial populations. *Applied and environmental microbiology* **56**: 1919-1925.

Bankevich A, Nurk S, Antipov D, Gurevich AA, Dvorkin M, Kulikov AS, Lesin VM, Nikolenko SI, Pham S, Prjibelski AD, Pyshkin AV, Sirotkin AV, Vyahhi N, Tesler G, Alekseyeev MA and Pevzner PA (2012) SPAdes: A New Genome Assembly Algorithm and Its Applications to Single-Cell Sequencing. *Journal of Computational Biology* **19**: 455-477.

Beal EJ, House CH and Orphan VJ (2009) Manganese- and Iron-Dependent Marine Methane Oxidation. *Science* **325**: 184-187.

Boetius A, Ravenschlag K, Schubert CJ, Rickert D, Widdel F, Gieseke A, Amann R, Jørgensen BB, Witte U and Pfannkuche O (2000) A marine microbial consortium apparently mediating anaerobic oxidation of methane. *Nature* **407**: 623.

Bolger AM, Lohse M and Usadel B (2014) Trimmomatic: a flexible trimmer for Illumina sequence data. *Bioinformatics* **30**: 2114-2120.

Bushnell B (2016) *BBMap short read aligner*. University of California, Berkeley, California.

Cai C, Leu AO, Xie G-J, Guo J, Feng Y, Zhao J-X, Tyson G, Yuan Z and Hu S (2018) A methanotrophic archaeon couples anaerobic oxidation of methane to Fe(III) reduction. *The ISME journal*.

Cheng L, Dai L, Li X, Zhang H and Lu Y (2011) Isolation and Characterization of Methanothermobacter crinale sp. nov., a Novel Hydrogenotrophic Methanogen from the Shengli Oil Field. *Applied and environmental microbiology* **77**: 5212-5219.

Cheng L, Shi S, Li Q, Chen J, Zhang H and Lu Y (2014) Progressive Degradation of Crude Oil n-Alkanes Coupled to Methane Production under Mesophilic and Thermophilic Conditions. *PLoS One* **9**: e113253.

Daims H, Brühl A, Amann R and Schleifer KH (1999) The domain-specific probe EUB338 is insufficient for the detection of all Bacteria: Development and evaluation of a more comprehensive probe set. *Systematic and Applied Microbiology* **22**: 434-444.

Dolfing J, Larter SR and Head IM (2007) Thermodynamic constraints on methanogenic crude oil biodegradation. *The ISME journal* **2**: 442.

Dombrowski N, Seitz KW, Teske AP and Baker BJ (2017) Genomic insights into potential interdependencies in microbial hydrocarbon and nutrient cycling in hydrothermal sediments. *Microbiome* **5**: 106.

Edgar RC (2004) MUSCLE: multiple sequence alignment with high accuracy and high throughput. *Nucleic Acids Research* **32**: 1792-1797.

Ettwig KF, Zhu B, Speth D, Keltjens JT, Jetten MSM and Kartal B (2016) Archaea catalyze iron-dependent anaerobic oxidation of methane. *Proceedings of the National Academy of Sciences* **113**: 12792-12796.

Evans PN, Parks DH, Chadwick GL, Robbins SJ, Orphan VJ, Golding SD and Tyson GW (2015) Methane metabolism in the archaeal phylum Bathyarchaeota revealed by genome-centric metagenomics. *Science* **350**: 434-438.

Gihring TM, Moser DP, Lin LH, Davidson M, Onstott TC, Morgan L, Milleson M, Kieft TL, Trimarco E, Balkwill DL and Dollhopf ME (2006) The Distribution of Microbial Taxa in the Subsurface Water of the Kalahari Shield, South Africa. *Geomicrobiology Journal* **23**: 415-430.

Goris J, Konstantinidis KT, Klappenbach JA, Coenye T, Vandamme P and Tiedje JM (2007) DNA–DNA hybridization values and their relationship to whole-genome sequence similarities. *International Journal of Systematic and Evolutionary Microbiology* **57**: 81-91.

Gray ND, Sherry A, Grant RJ, Rowan AK, Hubert CRJ, Callbeck CM, Aitken CM, Jones DM, Adams JJ, Larter SR and Head IM (2011) The quantitative significance of *Syntrophaceae* and syntrophic partnerships in methanogenic degradation of crude oil alkanes. *Environmental microbiology* **13**: 2957-2975.

Hallam SJ, Putnam N, Preston CM, Detter JC, Rokhsar D, Richardson PM and DeLong EF (2004) Reverse Methanogenesis: Testing the Hypothesis with Environmental Genomics. *Science* **305**: 1457-1462.

Haroon MF, Hu S, Shi Y, Imelfort M, Keller J, Hugenholtz P, Yuan Z and Tyson GW (2013) Anaerobic oxidation of methane coupled to nitrate reduction in a novel archaeal lineage. *Nature* **500**: 567.

Harwood CS, Burchhardt G, Herrmann H and Fuchs G (1998) Anaerobic metabolism of aromatic compounds via the benzoyl-CoA pathway. *FEMS Microbiology Reviews* **22**: 439-458.

Holler T, Widdel F, Knittel K, Amann R, Kellermann MY, Hinrichs K-U, Teske A, Boetius A and Wegener G (2011) Thermophilic anaerobic oxidation of methane by marine microbial consortia. *The ISME journal* **5**: 1946.

IPPC (2014) *Report I: Anthropogenic and Natural Radiative Forcing*, pp. 659-740. Cambridge University Press, Cambridge.

Joye SB, Boetius A, Orcutt BN, Montoya JP, Schulz HN, Erickson MJ and Lugo SK (2004) The anaerobic oxidation of methane and sulfate reduction in sediments from Gulf of Mexico cold seeps. *Chemical Geology* **205**: 219-238.

Kallmeyer J, Ferdelman TG, Weber A, Fossing H and Jørgensen BB (2004) A cold chromium distillation procedure for radiolabeled sulfide applied to sulfate reduction measurements. *Limnology and Oceanography: Methods* **2**: 171-180.

Khelifi N, Grossi V, Hamdi M, Dolla A, Tholozan J-L, Ollivier B and Hirschler-Réa A (2010) Anaerobic Oxidation of Fatty Acids and Alkenes by the Hyperthermophilic Sulfate-Reducing Archaeon *Archaeoglobus fulgidus*. *Applied and environmental microbiology* **76**: 3057-3060.

Khelifi N, Amin Ali O, Roche P, Grossi V, Brochier-Armanet C, Valette O, Ollivier B, Dolla A and Hirschler-Réa A (2014) Anaerobic oxidation of long-chain *n*-alkanes by the hyperthermophilic sulfate-reducing archaeon, *Archaeoglobus fulgidus*. *The ISME journal* **8**: 2153.

Kleindienst S, Ramette A, Amann R and Knittel K (2012) Distribution and in situ abundance of sulfate-reducing bacteria in diverse marine hydrocarbon seep sediments. *Environmental microbiology* **14**: 2689-2710.

Kleindienst S, Herbst F-A, Stagars M, von Netzer F, von Bergen M, Seifert J, Peplies Jörg, Amann R, Musat F, Lueders T and Knittel K (2014) Diverse sulfate-reducing bacteria of the *Desulfosarcina/Desulfococcus* clade are the key alkane degraders at marine seeps. *The ISME journal* **8**: 2029.

Kniemeyer O, Musat F, Sievert SM, Knittel K, Wilkes H, Blumenberg M, Michaelis W, Classen A, Bolm C and Joye SB (2007) Anaerobic oxidation of short-chain hydrocarbons by marine sulphate-reducing bacteria. *Nature* **449**: 898.

Knittel K and Boetius A (2009) Anaerobic Oxidation of Methane: Progress with an Unknown Process. *Annual Review of Microbiology* **63**: 311-334.

Knittel K, Boetius A, Lemke A, Eilers H, Lochte K, Pfannkuche O, Linke P and Amann R (2003) Activity, Distribution, and Diversity of Sulfate Reducers and Other Bacteria in Sediments above Gas Hydrate (Cascadia Margin, Oregon). *Geomicrobiology Journal* **20**: 269-294.

Krukenberg V, Riedel D, Gruber-Vodicka HR, Buttigieg PL, Tegetmeyer HE, Boetius A and Wegener G (2018) Gene expression and ultrastructure of meso- and thermophilic methanotrophic consortia. *Environmental microbiology* **20**: 1651-1666.

Laso-Pérez R, Wegener G, Knittel K, Widdel F, Harding KJ, Krukenberg V, Meier DV, Richter M, Tegetmeyer HE, Riedel D, Richnow H-H, Adrian L, Reemtsma T, Lechtenfeld OJ and Musat F (2016) Thermophilic archaea activate butane via alkyl-coenzyme M formation. *Nature* **539**: 396.

Letunic I and Bork P (2016) Interactive tree of life (iTOL) v3: an online tool for the display and annotation of phylogenetic and other trees. *Nucleic Acids Research* **44**: W242-W245.

Ludwig W, Strunk O, Westram R, *et al.* (2004) ARB: a software environment for sequence data. *Nucleic Acids Research* **32**: 1363-1371.

MacDonald IR, Bohrmann G, Escobar E, Abegg F, Blanchon P, Blinova V, Brückmann W, Drews M, Eisenhauer A, Han X, Heeschen K, Meier F, Mortera C, Naehr T, Orcutt B, Bernard B, Brooks J

and de Faragó M (2004) Asphalt Volcanism and Chemosynthetic Life in the Campeche Knolls, Gulf of Mexico. *Science* **304**: 999-1002.

Mahé F, Rognes T, Quince C, de Vargas C and Dunthorn M (2014) Swarm: robust and fast clustering method for amplicon-based studies. *PeerJ* **2**: e593.

Marcon Y, Sahling H, MacDonald IR, Wintersteller P, dos Santos Ferreira C and Bohrmann G (2018) Slow volcanoes: The intriguing similarities between marine asphalt and basalt lavas. *Oceanography* **31**.

Mardanov AV, Ravin NV, Svetlitchnyi VA, Beletsky AV, Miroshnichenko ML, Bonch-Osmolovskaya EA and Skryabin KG (2009) Metabolic Versatility and Indigenous Origin of the Archaeon *Thermococcus sibiricus*, Isolated from a Siberian Oil Reservoir, as Revealed by Genome Analysis. *Applied and environmental microbiology* **75**: 4580-4588.

Martin M (2011) Cutadapt removes adapter sequences from high-throughput sequencing reads. *EMBnet. journal* **17**: pp. 10-12.

McGlynn SE, Chadwick GL, Kempes CP and Orphan VJ (2015) Single cell activity reveals direct electron transfer in methanotrophic consortia. *Nature* **526**: 531.

Meyerdierks A, Kube M, Kostadinov I, Teeling H, Glöckner FO, Reinhardt R and Amann R (2010) Metagenome and mRNA expression analyses of anaerobic methanotrophic archaea of the ANME-1 group. *Environmental microbiology* **12**: 422-439.

Nobu MK, Dodsworth JA, Murugapiran SK, Rinke C, Gies EA, Webster G, Schwientek P, Kille P, Parkes RJ, Sass H, Jørgensen BB, Weightman AJ, Liu W-T, Hallam SJ, Tsiamis G, Woyke T and Hedlund BP (2015) Phylogeny and physiology of candidate phylum '*Atribacteria*' (OP9/JS1) inferred from cultivation-independent genomics. *The ISME journal* **10**: 273.

Offre P, Spang A and Schleper C (2013) Archaea in Biogeochemical Cycles. *Annual Review of Microbiology* **67**: 437-457.

Orcutt BN, Joye SB, Kleindienst S, Knittel K, Ramette A, Reitz A, Samarkin V, Treude T and Boetius A (2010) Impact of natural oil and higher hydrocarbons on microbial diversity, distribution, and activity in Gulf of Mexico cold-seep sediments. *Deep Sea Research Part II: Topical Studies in Oceanography* **57**: 2008-2021.

Pachiadaki MG, Lykousis V, Stefanou EG and Kormas KA (2010) Prokaryotic community structure and diversity in the sediments of an active submarine mud volcano (Kazan mud volcano, East Mediterranean Sea). *FEMS Microbiology Ecology* **72**: 429-444.

Parks DH, Imelfort M, Skennerton CT, Hugenholtz P and Tyson GW (2015) CheckM: assessing the quality of microbial genomes recovered from isolates, single cells, and metagenomes. *Genome Research* **25**: 1043-1055.

Pedroni P, Volpe AD, Galli G, Mura GM, Pratesi C and Grandi G (1995) Characterization of the locus encoding the [Ni-Fe] sulfhydrogenase from the archaeon Pyrococcus furiosus: evidence for a relationship to bacterial sulfite reductases. *Microbiology* **141**: 449-458.

Pernthaler A, Pernthaler J and Amann R (2002) Fluorescence In Situ Hybridization and Catalyzed Reporter Deposition for the Identification of Marine Bacteria. *Applied and environmental microbiology* **68**: 3094-3101.

Peters JW, Schut GJ, Boyd ES, Mulder DW, Shepard EM, Broderick JB, King PW and Adams MWW (2015) [FeFe]- and [NiFe]-hydrogenase diversity, mechanism, and maturation. *Biochimica et Biophysica Acta (BBA) - Molecular Cell Research* **1853**: 1350-1369.

Pruesse E, Peplies J and Glöckner FO (2012) SINA: Accurate high-throughput multiple sequence alignment of ribosomal RNA genes. *Bioinformatics* **28**: 1823-1829.

Rabus R, Boll M, Heider J, *et al.* (2016) Anaerobic Microbial Degradation of Hydrocarbons: From Enzymatic Reactions to the Environment. *Journal of Molecular Microbiology and Biotechnology* **26**: 5-28.

Reeburgh WS (2007) Oceanic Methane Biogeochemistry. *Chemical Reviews* **107**: 486-513.

Ruff SE, Biddle JF, Teske AP, Knittel K, Boetius A and Ramette A (2015) Global dispersion and local diversification of the methane seep microbiome. *Proceedings of the National Academy of Sciences* **112**: 4015-4020.

Sahling H and Ohling G (2017) *R/V Meteor Cruise Report M114: Natural Hydrocarbon Seepage in the Southern Gulf of Mexico: Kingston-Kingston, 12 February-28 March 2015.* MARUM-Zentrum für Marine Umweltwissenschaften, Fachbereich Geowissenschaften, Universität Bremen.

Sahling H, Borowski C, Escobar-Briones E, Gaytán-Caballero A, Hsu C-W, Loher M, MacDonald I, Marcon Y, Pape T and Römer M (2016) Massive asphalt deposits, oil seepage, and gas venting support abundant chemosynthetic communities at the Campeche Knolls, southern Gulf of Mexico. *Biogeosciences* **13**: 4491-4512.

Sakai N, Kurisu F, Yagi O, Nakajima F and Yamamoto K (2009) Identification of putative benzene-degrading bacteria in methanogenic enrichment cultures. *Journal of Bioscience and Bioengineering* **108**: 501-507.

Schink B (1985) Degradation of unsaturated hydrocarbons by methanogenic enrichment cultures. *FEMS Microbiology Letters* **31**: 69-77.

Schmidt A, Müller N, Schink B and Schleheck D (2013) A Proteomic View at the Biochemistry of Syntrophic Butyrate Oxidation in Syntrophomonas wolfei. *PLoS One* **8**: e56905.

Schreiber L, Holler T, Knittel K, Meyerdierks A and Amann R (2010) Identification of the dominant sulfate-reducing bacterial partner of anaerobic methanotrophs of the ANME-2 clade. *Environmental microbiology* **12**: 2327-2340.

Schubotz F, Lipp JS, Elvert M, *et al.* (2011) Petroleum degradation and associated microbial signatures at the Chapopote asphalt volcano, Southern Gulf of Mexico. *Geochimica et Cosmochimica Acta* **75**: 4377-4398.

Schulze-Makuch D, Haque S, Antonio MRdS, Ali D, Hosein R, Song YC, Yang J, Zaikova E, Beckles DM, Guinan E, Lehto HJ and Hallam SJ (2011) Microbial Life in a Liquid Asphalt Desert. *Astrobiology* **11**: 241-258.

Schut G, Nixon W, Lipscomb G, Scott R and Adams M (2012) Mutational Analyses of the Enzymes Involved in the Metabolism of Hydrogen by the Hyperthermophilic Archaeon *Pyrococcus furiosus*. *Frontiers in microbiology* **3**.

Siddique T, Fedorak PM and Foght JM (2006) Biodegradation of Short-Chain *n*-Alkanes in Oil Sands Tailings under Methanogenic Conditions. *Environmental Science and Technology* **40**: 5459-5464.

Stagars MH, Ruff SE, Amann R and Knittel K (2016) High Diversity of Anaerobic Alkane-Degrading Microbial Communities in Marine Seep Sediments Based on (1-methylalkyl)succinate Synthase Genes. *Frontiers in microbiology* **6**.

Stahl DA and Amann R (1991) Development and application of nucleic acid probes in bacterial systematics. *Nucleic acid techniques in bacterial systematics,* Stackebrandt E and Goodfellow M, eds., pp. 205-248. John Wiley and Sons Ltd., Chichester, England.

Stamatakis A (2014) RAxML version 8: a tool for phylogenetic analysis and post-analysis of large phylogenies. *Bioinformatics* **30**: 1312-1313.

Stepanauskas R, Fergusson EA, Brown J, Poulton NJ, Tupper B, Labonté JM, Becraft ED, Brown JM, Pachiadaki MG, Povilaitis T, Thompson BP, Mascena CJ, Bellows WK and Lubys A (2017) Improved genome recovery and integrated cell-size analyses of individual uncultured microbial cells and viral particles. *Nature Communications* **8**: 84.

Stokke R, Roalkvam I, Lanzen A, Haflidason H and Steen IH (2012) Integrated metagenomic and metaproteomic analyses of an ANME-1-dominated community in marine cold seep sediments. *Environmental microbiology* **14**: 1333-1346.

Strous M, Kraft B, Bisdorf R and Tegetmeyer H (2012) The Binning of Metagenomic Contigs for Microbial Physiology of Mixed Cultures. *Frontiers in microbiology* **3**.

Tissot B and Welte D (2012) *Petroleum formation and occurrence: a new approach to oil and gas exploration*. Springer Science and Business Media.

Treude T, Boetius A, Knittel K, Wallmann K and Jorgensen BB (2003) Anaerobic oxidation of methane above gas hydrates at Hydrate Ridge, NE Pacific Ocean. *Marine Ecology Progress Series* **264**: 1-14.

von Netzer F, Kuntze K, Vogt C, Richnow HH, Boll M and Lueders T (2016) Functional Gene Markers for Fumarate-Adding and Dearomatizing Key Enzymes in Anaerobic Aromatic Hydrocarbon Degradation in Terrestrial Environments. *Journal of Molecular Microbiology and Biotechnology* **26**: 180-194.

Wang F-P, Zhang Y, Chen Y, He Y, Qi L, Hinrichs K-U, Zhang X-X, Xiao X and Boon N (2013) Methanotrophic archaea possessing diverging methane-oxidizing and electron-transporting pathways. *The ISME journal* **8**: 1069.

Wegener G, Krukenberg V, Riedel D, Tegetmeyer HE and Boetius A (2015) Intercellular wiring enables electron transfer between methanotrophic archaea and bacteria. *Nature* **526**: 587.

Widdel F, Knittel K and Galushko A (2010) Anaerobic Hydrocarbon-Degrading Microorganisms: An Overview. *Handbook of Hydrocarbon and Lipid Microbiology,*(Timmis KN, eds.), pp. 1997-2021. Springer Berlin Heidelberg, Berlin, Heidelberg.

Wu M, Chatterji S and Eisen JA (2012) Accounting For Alignment Uncertainty in Phylogenomics. *PLoS One* **7**: e30288.

Zengler K, Richnow HH, Rosselló-Mora R, Michaelis W and Widdel F (1999) Methane formation from long-chain alkanes by anaerobic microorganisms. *Nature* **401**: 266.

Zhang J, Kobert K, Flouri T and Stamatakis A (2014) PEAR: a fast and accurate Illumina Paired-End reAd mergeR. *Bioinformatics* **30**: 614-620.

Zhou J, Bruns MA and Tiedje JM (1996) DNA recovery from soils of diverse composition. *Applied and environmental microbiology* **62**: 316-322.

Supplementary Information

Supplementary Figures and Tables

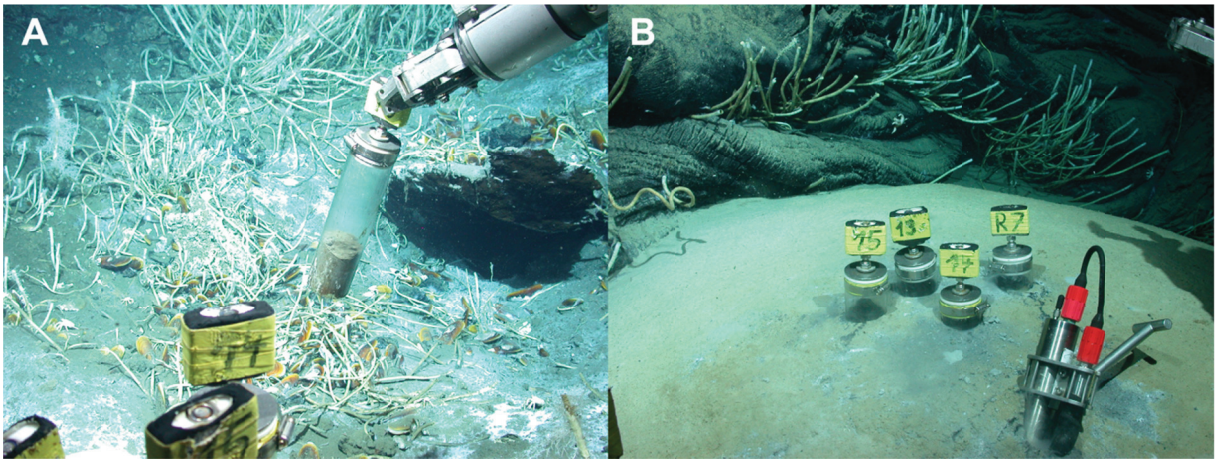

Supplementary Figure 1. Image of sampling sites at the Chapopote asphalt volcano. **A)** Oily sediments. Push core sampling (GeoB 19351-14) in a field covered by microbial mats, tube worms and mussels in the vicinity of gas hydrates (not seen). **B)** Ambient sediments. Sediment elevation covered with bacterial mat and tube worm bushes rooting in massive asphalt layers close-by.

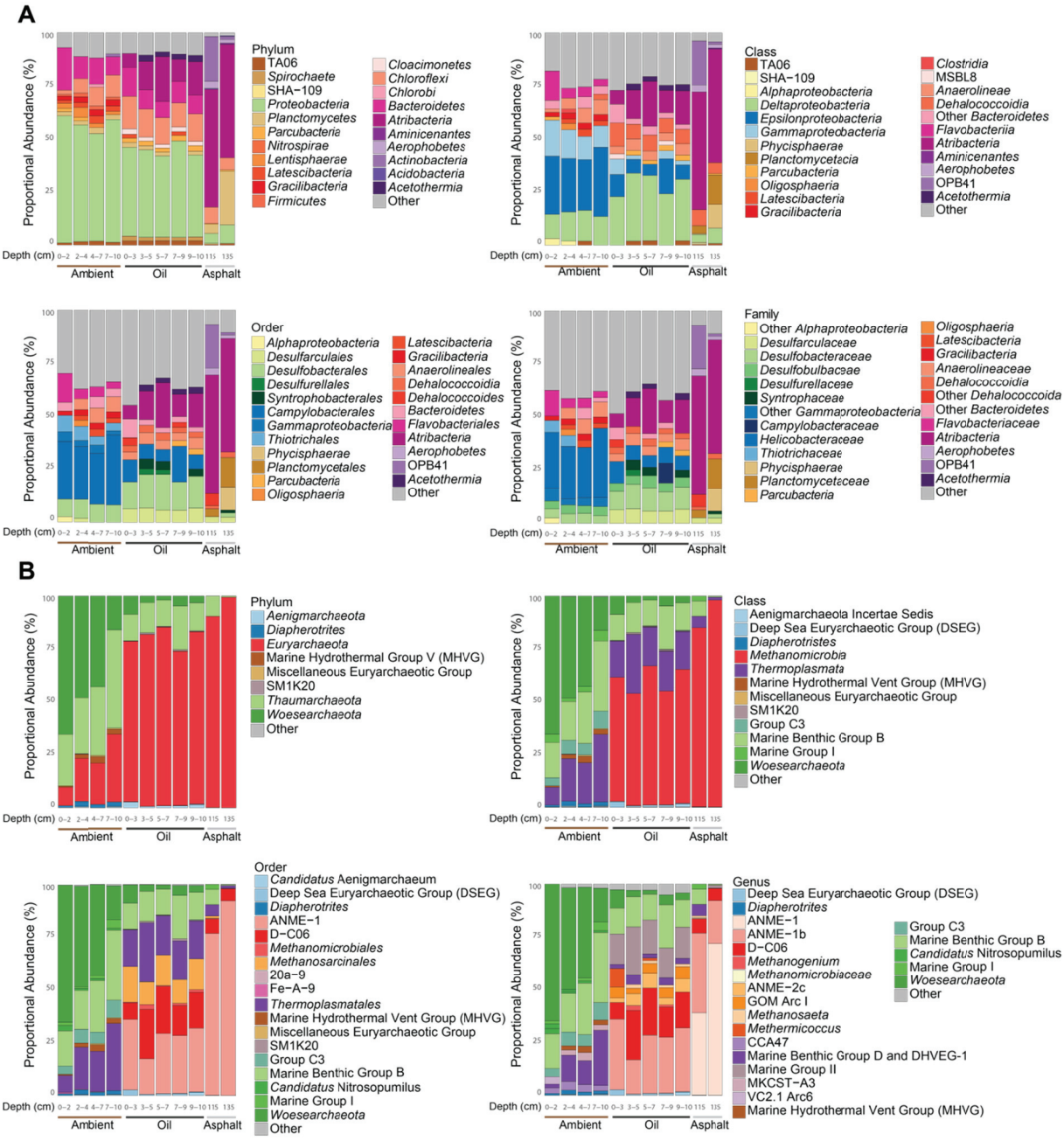

Supplementary Figure 2. Bacterial (A) and archaeal (B) 16S rRNA gene tags analysis at different taxonomic levels. Relative abundance of the 16S rRNA gene tags of the 10 most abundant clades are shown for each sample site (ambient, oil and asphalt) and depth. Phylum, class, order and family levels are shown for bacteria, while phylum, class, order and genus levels are shown in archaea.

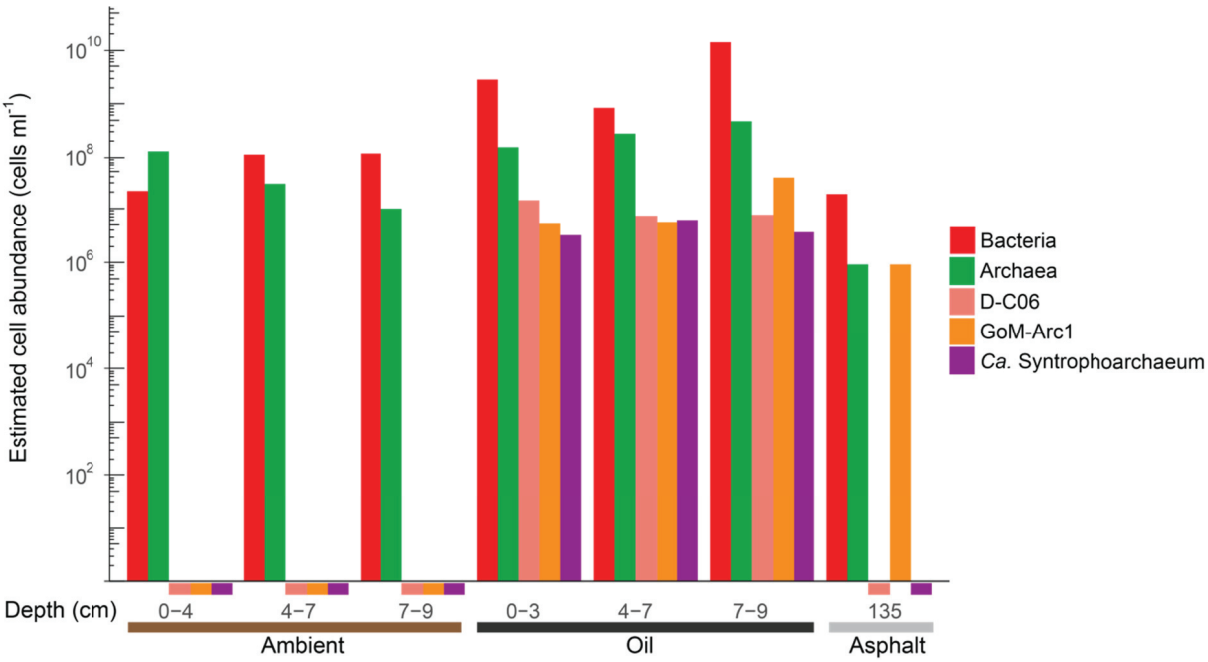

Supplementary Figure 3. Estimated cell abundances based on CARD-FISH counts. Estimated cell abundances for *Bacteria* and *Archaea,* as well as for the clades D-C06, GoM-Arc1 and *Ca.* Syntrophoarchaeum. Cell abundances are shown on a logarithmic scale. Bars below the axis indicate that no cells were found in the sample.

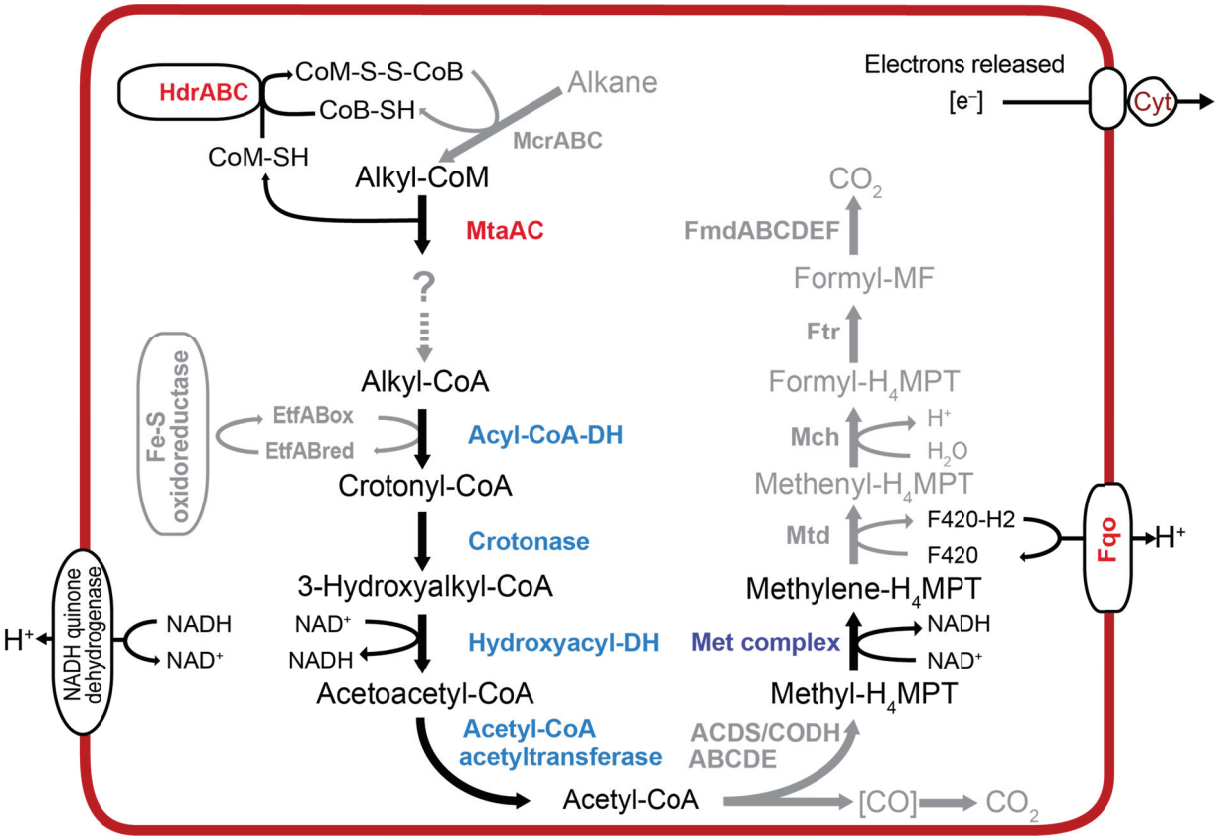

Supplementary Figure 4. Genes present in the Syntropho_SAG based on the metabolic model of *Ca.* Syntrophoarchaeum (Laso-Pérez, *et al.*, 2016). The genes encoding the corresponding enzymes are shown in color: red for alkane activation/methanogenesis, blue for the fatty acid oxidation pathway and purple for the Met complex. In grey, steps of the metabolic model of *Ca.* Syntrophoarchaeum, for which no gene was found in the Syntropho_SAG. The metabolic potential is largely similar to previously published MAGs of *Ca.* Syntrophoarchaeum, although not all genes are found for alkane degradation, which is likely due to its low completeness. For instance, operons with *mcrABG* are missing, yet other genes essential for the alkane-based catabolism were present including *mcrC*, *metFV*, heterodisulfide reductases complexes and divergent cobalamin methyltransferases (**Supplementary Figure 5**). Moreover, the Syntropho_SAG encodes for a complete fatty acid oxidation including several copies encoding some of the steps, what was proposed as a sign of potential degradation of different multi-carbon compounds.

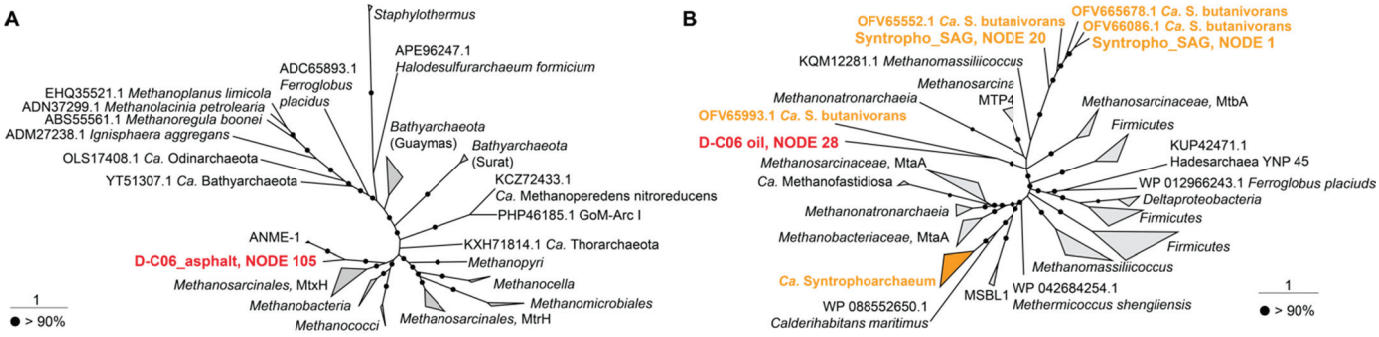

Supplementary Figure 5. Phylogenetic affiliations of the amino acid sequence of the *mtrH* (A) and *mta* (B) genes present in the D-C06 and *Ca.* Syntrophoarchaeum bins. A) Phylogenetic tree of the amino acid sequence of the *mtrH* gene. In red, the sequence present in the D-C06_asphalt MAG. A *mtrH* gene was found neither in D-C06_oil nor in the Syntropho_SAG. **B)** Phylogenetic tree of the amino acid sequence of the *mta* genes. In red, the sequence present in D-C06_oil. In orange, *Ca.* Syntrophoarchaeum sequences including those found in the Syntropho_SAG and in previous studies. For both trees, scale bars represent the number of amino acid substitutions per site and black circles bootstrap values over 90%.

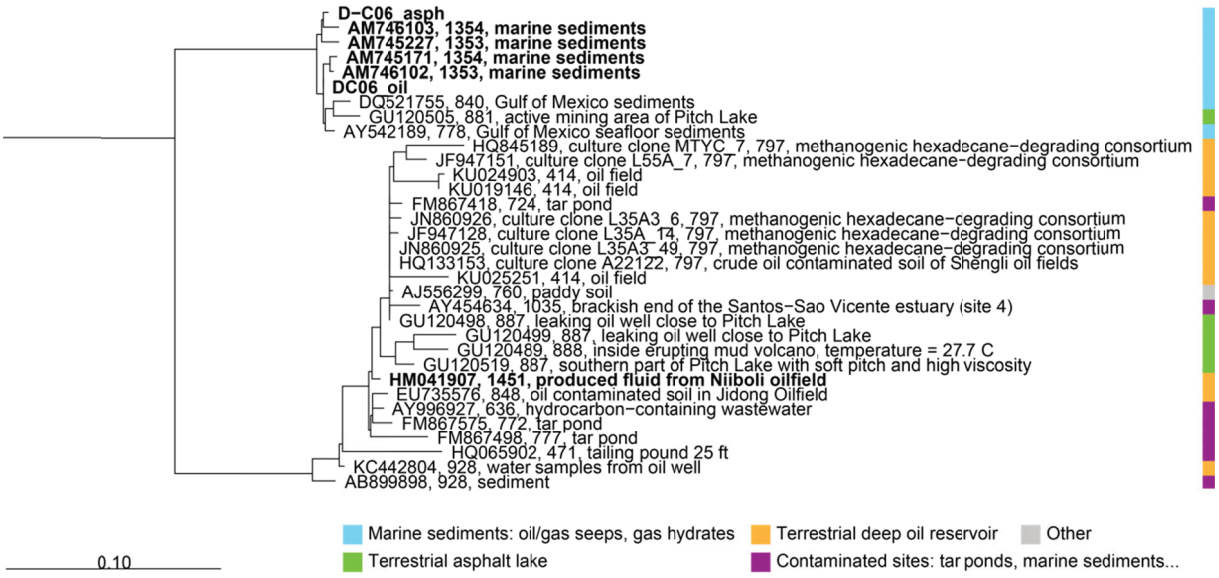

Supplementary Figure 6. D-C06 clade 16S rRNA gene phylogeny. This phylogeny includes the full-length sequences (in bold) as well as representatives short sequences from all the studies that have detected D-C06 present in the SILVA database v132. The tags refer: accession number, clone when applicable, length and isolation origin. On the right, classification of the sequences according to their environmental origin. Scale bars represent the number of nucleotide substitutions per site.

Supplementary Table 1. CARD-FISH probes applied in this study.

Name	Sequence 5'⇒ 3'	Specificity	FA %	Reference
EUB338 I	GCTGCCTCCCGTAGGAGT	Bacteria	35	Amann, *et al.* (1990)
EUB338 II	GCAGCCACCCGTAGGTGT	supplement to EUB338	35	Daims, *et al.* (1999)
EUB338 III	GCTGCCACCCGTAGGTGT	supplement to EUB338	35	Daims, *et al.* (1999)
ARCH915	GTGCTCCCCCGCCAATTCCT	Archaea	35	Stahl and Amann (1991)
GOM-ARCI-660	AGTACCTCCTACCTCTCCC	most GoM-Arc1, *Methanocellaceae*	35	This study
c1GOM-ARCI-660	AGTACCTCCCACCTCTCCC	most ANME-2d		This study
c2GOM-ARCI-660	AGTACCTCCAACCTCTCCC	*Methanosaetaceae* and *Methanobacteriales*		This study
c3GOM-ARCI-660	AGTACCTCCGACCTCTCCC	Diverse archaeal groups		This study
GOMARCII735	CGAACCTGTTCTAACTAG	D-C06	10	This study
SYNA666	CCTGAAGTACCTCCAACC	*Ca.* Syntrophoarchaeum clade	25	This study
c1SYNA666	CCTGAAGTACCTCAAACC	Marine Benthic Group E		This study
h1SYNA666	AGACCCGTTCCAGTTGGA			This study
h2SYNA666	AGACCCGTCCCAGTTGGA			This study
h3SYNA666	CCCAGGGATCACAGGATT			This study

Supplementary Table 2. Information from the metagenomic libraries used for the assembly of D-C06 bins.

Library name	Sampling site	Sequencing platform	Read length (bp)	Insert size (bp)	Read number (PE)
TSf_CH14_9-10_350a	Oily sediments	MiSeq	2×300	350	2,034,558
TSf_CH14_9-10_350b	Oily sediments	MiSeq	2×300	350	1,338,251
TSf_CH14_9-10_400a	Oily sediments	HiSeq	2×250	400	41,204,810
TSf_CH14_9-10_400b	Oily sediments	HiSeq	2×250	400	59,942,642
TSf_CH14_9-10_430	Oily sediments	HiSeq	2×250	430	19,480,273
TSf_CH14_9-10_750	Oily sediments	HiSeq	2×250	750	2,194,219
GoMasph_12	Asphalt sediments	MiSeq	2×300	550-600	2,354,296

Supplementary Table 3. Pairwise whole genome identity comparison between D-C06 MAGs and between the Syntropho_SAG and the genomes of the two *Ca.* Syntrophoarchaeum strains: S. butanivorans and S. caldarius.

	Average Nucleotide Identity (Blast)	Average Nucleotide Identity (MUMmer)	Tetranucleotide frequency
D-C06_oil/D-C06_asphalt	93.46	94.94	99.46
D-C06_asphalt/D-C06_oil	93.13	94.93	99.46
Syntropho_SAG/S.butanivorans	73.94	83.8	0.86
Syntropho_SAG/S.caldarius	75.95	84.37	0.94
S.butanivorans/Syntropho_SAG	73.66	83.7	0.86
S.caldarius/Syntropho_SAG	76.11	84.38	0.94

Supplementary Table 4. Overview of the genes involved in alkane degradation present in the MAGs of D-C06. The locus tags are provided for both MAGs. The pathway to which genes belong according to the model of **Figure 5** is indicated by different colors: alkane activation and conversion to a CoA-bound fatty acid (red), fatty acid oxidation (yellow), methanogenesis (blue) and electron cycling (green).

	Gene	D-C06_oil	D-C06_asph
Alkane activation	Alkane-degr.*mcrA*	694	Truncated
	Alkane-degr *mcrB*	696	1969
	Alkane-deg. *mcrC*	695	1970
	mtbA	1505	818, 819
	mttB	496,497	
	mttC	495	
	Alcohol dehydrogenase	1227, 1658	183, 654
	Aldehyde dehydrogenase	1914, 1955	166, 529, 650, 656
	fadD	265, 270, 311, 1598, 1674, 1675, 1676, 1848, 2025, 2030	181, 214, 446, 502, 742, 1051, 1494, 1667, 1678, 1748, 1851, 1856
Fatty acid degradation	*bcd/acd*	438, 1361, 1435, 1534, 1874, 1928, 1975, 2041	180, 349, 505, 506, 507, 784, 1000, 10001, 1815, 1837
	crt	106, 439, 703, 882, 1996, 2017, 2094	436, 606, 785, 1002, 1127, 1226, 1530
	hbd	440, 1694, 1860	1126
	thl	402, 442, 1921, 2043, 2059, 2111	350, 351, 356, 1005, 1124, 1555, 1669
	acs	33, 1342, 1451	668, 1343
	acds/codhA	1636	1627
	acds/codhB	1197	
	acds/codhC	1192	
	acds/codhD	1193	
	acds/codhE	1635	1626
Methanogenesis	*mcrA*	63	248
	mcrB	67	244
	mcrC	65	246
	mcrD	66	245
	mcrG	64	247
	mtrA		1334/35
	mtrB		1336
	mtrC		1337

	Gene	D-C06_oil	D-C06_asph
Methanogenesis	*mtrD*	1236	1338
	mtrE	1237	1339
	mtrF		
	mtrG		1333
	mtrH		1332
	mer	1171	3, 1828, 2117
	hmd	743	1802
	mch	537, 928	1441
	ftr	235	554
	fmdD		915
	fmdB	1855	916
	fmdA		917
	fmdC	312	918
Electron cycling	*hyhB*	245	1764
	hyhG	244	1765
	hyhD	243	
	hdrA	163, 252, 532, 1286	401, 434, 751, 1656
	hdrB	1284	749, 1602
	hdrC	1285	750
	rnfA	1241	958
	rnfB	1240	957
	rnfC	1245	962
	rnfD	1244	961
	rnfE	1242	959
	rnfG	1243	960
	etfA	1287	752, 385
	etfB	1288	386
	cytochrome c	1635	985, 1288

Supplementary Table 5. Primers used for the PCR sequencing of the 16S rRNA gene prior to Illumina sequencing.

ID name	Name in probeBase database	Sequence
Arch 349F	S-D-Arch-0349-a-S-17	5'- GYG CAS CAG KCG MGA AW -3'
Arch915R	S-D-Arch-0915-a-A-20	5'- GTG CTC CCC CGC CAA TTC CT -3'
Bact 341F	S-D-Bact-0341-b-S-17	5'- CCT ACG GGN GGC WGC AG -3'
Bact 785R	S-D-Bact-0785-a-A-21	5'- GAC TAC HVG GGT ATC TAA TCC -3'

Chapter IV

Substrates and gene expression patterns of different alkane-degrading strains of *Ca.* Syntrophoarchaeum

Rafael Laso-Pérez[1,2], David Benito Merino[1,2], Pier Luigi Buttigieg[2], Halina E. Tegetmeyer[2,3], Antje Boetius[1,2,4], Gunter Wegener[1,2,4]

[1]Max-Planck Institute for Marine Microbiology, 28359 Bremen, Germany.
[2]Alfred Wegener Institute Helmholtz Center for Polar and Marine Research, 27570 Bremerhaven, Germany.
[3]Center for Biotechnology, Bielefeld University, 33615 Bielefeld, Germany.
[4] MARUM, Center for Marine Environmental Sciences, University Bremen, 28359 Bremen, Germany.

Manuscript in preparation

Running title: *Substrates and gene expression of* Ca. *Syntrophoarchaeum*

Abstract

Recently, two archaeal strains of the genus *Candidatus* Syntrophoarchaeum have been described to degrade butane under anoxic conditions. They activate butane using a novel divergent type of methyl-coenzyme M reductase (MCR), which is encoded in four gene sets. The CoM-bound intermediate is subsequently degraded via the fatty acid oxidation pathway, the Wood-Ljungdahl pathway and the downstream components of the methanogenesis. Reducing equivalents are transferred to sulfate-reducing partner bacteria. Here we study the physiology of the two *Ca.* Syntrophoarchaeum strains in relation to their substrate specificity, temperature growth range and gene expression patterns during growth on different substrates. Incubations with different short-chain alkanes (C_1-C_6) showed that *Ca.* Syntrophoarchaeum grew only on butane and propane. Surprisingly, only one strain, *Candidatus* Syntrophoarchaeum caldarius was detected in the incubations with propane. This strain was also present in the incubations with butane, yet it was less abundant than *Ca.* Syntrophoarchaeum butanivorans. Analysis of the gene expression of *Ca.* S. caldarius showed that the expression of most genes is independent of the supplied substrate. Yet some genes were differentially expressed, foremost some *mcr* genes were preferentially transcribed depending on the provided substrate, butane or propane. This suggests that the different MCRs of *Ca.* Syntrophoarchaeum have different defined substrate range, most likely governed by the alkane chain length. Considering the recent discovery of many different divergent MCRs, it is likely this enzyme class can activate a yet uncovered variety of different alkanes.

Introduction

The anaerobic oxidation of hydrocarbons was first described in toluene-degrading bacteria (Dolfing*, et al.*, 1990, Lovley and Lonergan, 1990). Since then, many other bacteria have been reported to utilize several mechanisms to metabolize hydrocarbons (Widdel and Rabus, 2001). Anaerobic alkane degradation is typically attributed to some members of the *Deltaproteobacteria*, which use the fumarate addition pathway to activate alkanes (Kniemeyer*, et al.*, 2007, Kleindienst*, et al.*, 2014). In this pathway, a fumarate molecule is added to the substrate forming a succinate derivative that is oxidized further. The enzymes involved, (methyl)alkylsuccinate synthases (Mas and Ass), belong to the pyruvate-formate lyase family (Callaghan, 2013). Two archaea, *Archaeoglobus fulgidus* and *Thermococcus sibiricus,* have been described as anaerobic alkane degraders as well. They grow on hexadecane and use enzymes of the pyruvate-formate lyase family which have been presumably acquired from bacteria (Mardanov*, et al.*, 2009, Khelifi*, et al.*, 2014). Archaea play also a major role in the anaerobic oxidation of methane (AOM), which is performed by anaerobic methanotrophic archaea (ANME) of the class *Euryarchaeota*. They use a reversal of the methanogenesis pathway to degrade methane that has methyl-coenzyme M reductase (MCR) as the key enzyme, which catalyzes the activation of methane to methyl-CoM. Most ANME form consortia with syntrophic partner bacteria,

which use the reducing equivalents released during methane oxidation to perform sulfate reduction (Wegener*, et al.*, 2015, McGlynn*, et al.*, 2018).

However, some studies have indicated that archaea play a more prominent role in alkane degradation than previously thought. For instance, it was shown that some anaerobic alkane-degrading enrichments contain a considerable proportion of *Archaeoglobi* and *Methanomicrobia* (Adams*, et al.*, 2013). Additionally, two novel strains, *Candidatus* Syntrophoarchaeum butanivorans and *Candidatus* Syntrophoarchaeum caldarius, have been described as alkane-degrading archaea (Laso-Pérez*, et al.*, 2016). They activate propane and butane using specific types of MCR enzymes producing the corresponding alkyl-CoM as intermediate. The CoM-bound alkyl units are fully oxidized via the fatty acid oxidation pathway, the Wood-Ljungdahl pathway and the downstream part of the methanogenesis. Similar to ANME, reducing equivalents are transferred to sulfate-reducing partner bacterium affiliated with *Candidatus* Desulfofervidus auxilii (HotSeep-1 clade) (Krukenberg*, et al.*, 2016). Strikingly, both strains of *Ca.* Syntrophoarchaeum contain four sets of *mcr* genes, a hitherto unobserved phenomenon (Laso-Pérez*, et al.*, 2016). The phylogeny of these MCRs shows that they are highly divergent from the canonical MCRs of ANME and methanogens, which may suggest the need of a different molecular conformation to accommodate molecules larger than methane. The eight MCRs cluster in subgroups, each one containing a copy of each strain. Moreover, they are closely related to other MCRs recently discovered by metagenomics studies in *Bathyarchaeota* and the clade GoM-Arc1, what could indicate the capacity of these groups to metabolize alkanes with this new mechanism (Evans*, et al.*, 2015, Dombrowski*, et al.*, 2017).

The multiple threads of evidence noted above suggest that the role of MCR-harboring archaea in non-methane alkane degradation has been underestimated. Nonetheless, little is known about the physiology of these organisms and how this mechanism proceeds, as study has been limited to the enrichment Butane-50, which contains *Ca.* Syntrophoarchaeum archaea along with their syntrophic partner bacteria. This culture was established from hydrothermally-heated sediments from the Guaymas Basin, although related 16S rRNA gene sequences have been found in other locations like oil/gas seeps, mud volcanoes and oil-affected sediments under a wide range of temperatures (4 °C-80°C) (Orcutt*, et al.*, 2010, Biddle*, et al.*, 2011, Lazar*, et al.*, 2011, McKay*, et al.*, 2016). Transcriptomic analyses have shown that the four *mcr* gene sets are differently expressed in both strains during growth on butane (Laso-Pérez*, et al.*, 2016). This suggests that *Ca.* Syntrophoarchaeum archaea could have different MCR enzymes specialized in the activation of different substrates.

The aim of this study is to investigate the physiology of *Ca.* Syntrophoarchaeum in relation to three aspects: 1) examine the substrate range of *Ca.* Syntrophoarchaeum, 2) define the temperature optimum and growth range of *Ca.* Syntrophoarchaeum and 3) analyze the expression of genes in relation to the use of specific substrates.

Material and methods

Cultivation

Establishment of the Butane-50 enrichment culture was described in (Laso-Pérez*, et al.*, 2016). Enrichment cultures were incubated and maintained as described before for anaerobic hydrocarbon-degrading enrichments (Laso-Pérez*, et al.*, 2018). In short, they were incubated at 50 °C in anoxic synthetic seawater medium with butane as sole growth substrate and sulfate as unique electron acceptor. When sulfide concentrations exceed 15 mM, enrichment cultures were diluted (1:5) in fresh anoxic synthetic seawater. Metabolic activity was tracked based on sulfide concentration by measuring colloidal copper sulfide photometrically at 480 nm according to the Cord-Ruwisch method (Cord-Ruwisch, 1985, Laso-Pérez*, et al.*, 2018).

To test different alkanes as substrates duplicate incubations of the active culture were established with methane, ethane and propane headspace (2 atm). Additionally duplicates with liquid alkanes were prepared by exchanging the butane headspace with N_2/CO_2 (80:20, 1 atm). As substrates, pentane or butane (10 mM final concentration) were added dissolved in 4 ml of 2,2,4,4,6,8,8-heptamethylnonane, which acted as carrier phase to avoid toxic effects of the provided alkanes. Enrichment cultures were incubated at 50°C and microbial activity was monitored as described above by measuring the sulfide concentration. After the establishment of a propane-growing enrichment (hereafter Propane-50), the enrichment was maintained as described above for Butane-50.

Determination of activity optimum

Subcultures of Butane- and Propane-50 were established using 20 ml of synthetic anoxic mineral medium and 25 ml of inoculum and with a gas phase of butane or propane (1 atm). The established enrichments were incubated at 9 different temperatures: 28, 37, 45, 50, 55, 60, 65, 70 and 75 °C. Three replicates were established per temperature and treatment. Growth was monitored by measuring sulfide production weekly for 35 days as described above. Sulfide concentrations were plotted against time and used to calculate average sulfate reduction rates for the 35 days period.

RNA extraction and sequencing

Three replicates of Butane- and Propane-50 enrichments were established for gene expression analyses. They were sampled when sulfide concentrations reached values above 10 mM. Sampling, RNA extraction, DNA removal and purification were performed as previously described (Laso-Pérez*, et al.*, 2016, Laso-Pérez*, et al.*, 2018). In short, enrichment cultures were incubated in a water bath at the *in situ* temperature of 50°C. Medium was removed avoiding the biological material. Afterwards, samples were fixed with pre-heated RNAlater (Sigma-Aldrich, Darmstadt, Germany) and incubated for one hour. Fixed samples were filtered through 0.22 μm membrane filters (Whatman Nuclepore Track-Etched Membrane, Sigma-Aldrich). RNA was extracted from filters using glass beads and 600 μL of RNA Lysis Buffer in a bead-beating machine (2 cycles of 6 m/s for 20 s), followed by extraction

with the Quick-RNA MiniPrep Kit (Zymoresearch, Irvine, CA, USA). A subsequent DNA-removal step was applied to the RNA sample with DNase I. Finally, RNeasy MinElute Cleanup Kit (QIAGEN, Hilden, Germany) was used to purify the RNA. The total extracted RNA was in the range of 180-355 ng for the propane samples and of 935-2025 ng for the butane ones.

For strand-specific transcriptome sequencing, 80 ng of each purified RNA extract were used for Illumina library preparation, following the protocol for mRNA library preparation as described in the TruSeq®Stranded mRNA Sample Preparation Guide, with the modification of using purified total RNA instead of purified mRNA as input material. The generated RNA libraries were sequenced at the CeBiTec (Bielefeld, Germany) on an Illumina HiSeq instrument in a 1x150b single end run (Rapid SBS v2 chemistry).

Transcriptomics analysis

Sequenced libraries were processed to remove adaptors and contaminants and to perform quality trimming to a Q10 value using bbduk v34 from the BBMAP package (Bushnell, 2016). Trimmed reads were sorted using SortMeRNA (v2.0) to filter rRNA from tRNA and mRNA (Kopylova*, et al.*, 2012). Filtered rRNA reads were used to study the community composition with the phyloFlash package v2.0 (https://github.com/HRGV/phyloFlash) with a read input limit of 100000 reads and the SILVA database 119 as a reference. tRNA and mRNA reads were mapped with an identity threshold of 0.98 to the reference genomes of *Ca.* Syntrophoarchaeum butanivorans (PRJNA318983) and *Ca.* Syntrophoarchaeum caldarius (PRJNA319143) present in NCBI as well as to the genome of the *Ca.* D. auxilii strain present in the Butane-50 enrichment (Laso-Pérez*, et al.*, 2016). Afterwards the reads mapped to each organism were analyzed individually by applying two methods: fragment per kilobase of transcript per million mapped reads (FPKM) (Trapnell*, et al.*, 2010) and centered-log ratio (CLR) transformation (Fernandes*, et al.*, 2014). Read recruitment for the *mcr* genes was visualized using Tablet (Milne*, et al.*, 2010). Moreover, a dissimilarity analysis and a differential expression analysis were carried out comparing butane and propane treatment for the organisms present in both treatments (*Ca.* S. caldarius and *Ca.* D. auxilii). For the differential expression analysis, ALDEx2 R package (Fernandes*, et al.*, 2014) was used to calculate the P-values for the Welch's t-test, the Benjamini Hochberg corrected P-values, the effect size and the fold change.

Results and discussion

***Ca.* Syntrophoarchaeum can grow on butane and propane**

Duplicate cultures were established at 50°C with short-chain alkanes (C_1-C_6) using aliquots of Butane-50 as inoculum. Immediate activity (quantified as increase of sulfide concentration) was only detected in the cultures incubated with butane. Using propane as substrate, sulfide production slowly established in only one replicate after a lag-phase of 2 months. After two successful transfers of this

culture with propane as substrate, the culture Propane-50 was established. Similarly to Butane-50, the culture contained consortia formed by *Ca.* Syntrophoarchaeum archaea and partner bacteria.

After 334 days, substrate-dependent sulfide production was also detected in cultures with methane and ethane. The methane culture did not contain Ca. Syntrophoarchaeum but was dominated by consortia of ANME-1 archaea, which might be residual members from the original AOM culture. The ethane culture was dominated by not yet identified bacteria. Incubations with pentane and hexane did not show substrate-induced sulfide production or growth of microorganisms.

Ca. Syntrophoarchaeum can grow in a wider temperature range

To evaluate the temperature range of *Ca.* Syntrophoarchaeum and their associated partner bacteria, triplicate bottles of Butane- and Propane-50 were incubated for 40 days at 9 different temperatures (28, 37, 45, 50, 55, 60, 65, 70 and 75°C; **Figure 1A**). Measurements of sulfide concentration over time were used to calculate a sulfide production rate at each temperature (**Figure 1B**). Based on these calculations, both Butane- and Propane-50 show measureable sulfide production activity between 37°C and 60°C with an activity optimum around 50-55°C.

These cultures were established from hydrothermally heated sediments from the Guaymas Basin. The original sediment exhibited a temperature range from 4°C at the top of the sediment to 85°C at 45 cm depth (Holler*, et al.*, 2011), but the cultures were established from sediment derived from the 14-25 cm horizon with temperatures around 30-60°C matching the observed temperature growth range. The temperature optimum around 50-55°C could be expected considering that Butane-50 has been maintained at 50°C for more than 6 years and Propane-50 was established from it. Therefore, this has favoured the selection of strains especially adapted to these conditions. However, the wide range of temperatures in the sediment could create niches for other *Ca.* Syntrophoarchaeum strains as it was shown for ANME-1 organisms in Guaymas Basin, where strains growing at 37 and 50°C are reported (Holler*, et al.*, 2011, Krukenberg*, et al.*, 2016). *Ca.* Syntrophoarchaeum was first described from 16S rRNA gene sequences obtained from oil seeps of the Gulf of Mexico at 4°C (Orcutt*, et al.*, 2010). More recently, microscopy observations have confirmed their presence in consortia with bacteria in cold oil seeps of the Gulf of Mexico, what suggest the existence of psychrophilic species of *Ca.* Syntrophoarchaeum (Chapter III), implying a much wider temperature range for this clade.

The sulfide production in Propane-50 was lower than in Butane-50 (maximum rate of 0.07 mM day^{-1} vs. 0.26 mM day^{-1}; **Figure 1B**). This might be explained by the lower energy yield per molecule of propane compared to butane (equations 1 and 2, **Table 1**) in conjunction with the initial inoculum.

$2\ C_3H_8 + 5\ SO_4^{2-} + 4H^+ \rightarrow 6\ HCO_3^- + 5\ H_2S + 2\ H_2O$ (Equation 1)

$\Delta G_{323K,\ pH=7}$ = -118.18 kJ or -59.09 kJ per mole of propane

$4\ C_4H_{10} + 13\ SO_4^{2-} + 10H^+ \rightarrow 16\ HCO_3^- + 13\ H_2S + 4\ H_2O$ (Equation 2)

$\Delta G_{323K,\ pH=7}$ = -351.35 kJ or -87.84 kJ per mole of butane

The free energy of Gibbs per molecule of butane is around -88 kJ, while per molecule of propane is -59 kJ. Propane-50 was established from Butane-50 after a months-long lag phase. Transcriptomics analyses have shown that in Propane-50 only one archaeal strain is present, *Ca.* S. caldarius (see below, **Supplementary Table 1**), which was low in abundance in the Butane-50 culture. This means that the initial inoculum from Butane-50, employed to establish Propane-50, contained just a small fraction of archaea able to grow on propane (*Ca.* S. caldarius). Consequently, the relative low sulfide production rate during growth on propane might be caused due to the lower number of propane-degrading archaea in the propane culture as evidenced by the lower RNA yields from this culture. However, ongoing lower biomass in the propane culture would argue for in general lower growth yields for the propane culture. This hypothesis should be considered in future cultivation of Propane-50.

Gene expression shows differences in the community composition of Butane- and Propane-50

RNA libraries were sequenced from triplicates cultures of Butane- and Propane-50 and after quality trimming, reads were classified in two fractions: rRNA or mRNA and tRNA. Most of the reads (90.5-92%) belong to rRNA and only 8-9.5% corresponds to mRNA and tRNA (**Supplementary Table 1**). The rRNA fraction was used to analyse the phylogenetic composition of the active community based on the 16S rRNA gene transcripts. Most of them were assigned to *Ca.* Syntrophoarchaeum in both treatments, although the proportion was higher for propane than for butane (on average 81% vs 67% of 16S rRNA gene transcripts; **Figure 2**). Interestingly, almost all the reads assigned to *Ca.* Syntrophoarchaeum in the treatment with propane belonged to the strain *Ca.* S. caldarius. In contrast, *Ca.* S. butanivorans was the dominant but not exclusive archaeon during growth on butane (56% of the total 16S rRNA gene fragments; **Supplementary Table 1**).

Another large portion of the 16S rRNA gene transcripts were assigned to the *Ca.* D. auxilii strain, the partner bacterium in these cultures, which was more proportionally dominant in the samples with butane than in the propane ones (23% vs 11%, **Figure 2**). Around 7.5-10% of the 16S rRNA transcripts were classified to minor community members bacteria and archaea mostly *Syntrophobacteraceae* bacteria (1.4 - 4.1%) and *Methermicoccus* archaea (0.7 – 2.3 %). The low proportions of *Methermicoccus* may be explained by a missannotation of *Ca.* Syntrophoarchaeum reads in SILVA, as both organisms are closely related. Members of the *Syntrophobacteraceae* are known to degrade diverse substrates including some alkanes (C_6-C_{12}) and a variety of fatty acids (Davidova*, et al.*, 2006, Kuever*, et al.*, 2015). Thus, it might be possible that these bacteria are thriving on butane or on by-products of alkane degradation. If *Syntrophobacteraceae* are thriving on butane or propane in the studied cultures, the question about competition between archaea and bacteria in anaerobic alkane degradation arises. So far, studies have shown that bacteria tend to dominate alkane degradation in marine oil cold seeps (Kleindienst*, et al.*, 2014); however the dominance of *Ca.* Syntrophoarchaeum in our enrichments could indicate that archaea can also dominate niches

determined by alkane degradation. The specific conditions that might allow this predominance are still unknown. Temperature might offer an explanation, as it has been shown that archaea dominate environments at high temperatures, which might be linked with their membrane stability (van de Vossenberg*, et al.*, 1998, Siliakus*, et al.*, 2017). Nevertheless, bacterial alkane degraders have also been shown to grow at high temperatures (Kniemeyer*, et al.*, 2007). Future research should address this question in more detail.

mRNA and tRNA were mapped to the genomes of *Ca.* S. butanivorans, *Ca.* S. caldarius and *Ca.* D. auxilii. Around 36-67% of these reads mapped to *Ca.* Syntrophoarchaeum archaea or *Ca.* D. auxilii for both treatments (**Supplementary Table 1**). Transcripts mapped to features of *Ca.* S. caldarius and *Ca.* D. auxilii in both treatments, while for *Ca.* S. butanivorans, gene expression was only detected in the treatment with butane corroborating the rRNA results. This indicates that *Ca.* S. butanivorans is able to grow on butane but not on propane. Thus, a comparative analysis of this strain's response to different substrates could not be performed. In contrast, *Ca.* S. caldarius can degrade butane and propane, although proportionally it is much less abundant than *Ca.* S. butanivorans in the incubations with butane. The reasons why *Ca.* S. butanivorans is more dominant than *Ca.* S. caldarius are unknown, but it might be that under certain growth conditions *Ca.* S. caldarius is less efficient. *Ca.* D. auxilii is the sulfate-reducing partner bacterium during both treatments.

Differences in the gene expression pattern of Ca. S. caldarius and its partner bacterium during growth on propane and butane

To study the gene expression of mRNA and tRNA, raw expression data was transformed in two ways: FPKM (fragment per kilobase of transcript per million mapped reads) and using the centered-log ratio (CLR) transformation. FPKM transformation normalizes the gene expression based on gene length and total gene expression for an organism. The CLR transformation attempts to reduce the effect of compositionality in data derived from the nucleic acid samples, converting counts into fold changes above or below the geometric mean read count in each organism (Fernandes*, et al.*, 2014). Unless otherwise indicated, high or low expression is used to describe similar results in both transformations, although the proper terms for the description of the results obtained from the CLR transformation are "enrichment" or "depletion".

A dissimilatory analysis using the CLR-transformed data was performed to study the gene expression patterns in *Ca.* S. caldarius and *Ca.* D. auxilii between the butane and propane treatments. *Ca.* D. auxilii shows highly similar expression patterns within replicates (only 2-3% dissimilarity) and between treatments (5% dissimilarity, visualized with hierarchical cluster analysis in **Figure 3**). This low dissimilarity between treatments is probably attributable to the *Ca.* D. auxilii's identical role as syntrophic sulfate reducer in both treatments. In fact, an additional differential expression analysis with ALDEx2 showed no significant differences in the expression of any gene of *Ca.* D. auxilii between treatments (data not shown).

For the alkane oxidizer *Ca.* S. caldarius, the dissimilarity analysis reveals comparable results for the expression patterns within replicates (2-3% dissimilarity), but higher dissimilarity values between them (over 11%, **Figure 3**). The dissimilarities in the expression pattern of *Ca.* S. caldarius between both treatments could be due to compositional effects. *Ca.* S. caldarius represents a minor member of the Butane-50 community and therefore the absolute number of transcripts is much lower than in the treatment with propane. Although, the hierarchical cluster analysis was performed with CLR-transformed data, the high differences between the absolute expression levels between propane and butane treatments might have not been fully resolved with this transformation. Alternatively, this higher dissimilarity between treatments might be caused by different gene expression patterns to perform butane or propane degradation.

Ca. S. caldarius may need different enzymes during the metabolism of butane or propane, especially specific MCR types might be required in the initial activation step. This hypothesis is supported by the high substrate specificity of MCR. For instance, the MCR of methanogens were shown to be extremely less efficient in the formation of ethane than methane as shown in enzymatic essays (Ahn*, et al.*, 1991, Scheller*, et al.*, 2013). Furthermore, none of the divergent MCR types of *Ca.* Syntrophoarchaeum is able to generate methyl-CoM, as shown in methane incubation of the Butane-50 culture where methyl-CoM was not detected (Laso-Pérez*, et al.*, 2016). In fact, a differential expression analysis of the gene expression of *Ca.* S. caldarius using ALDEx2 revealed significant differences between butane and propane for two *mcrA* genes (**Supplementary Table 2**). Additionally, other 41 genes were differentially expressed between both treatments. Many of these genes encode transcriptional regulators such as ArsR family transcriptional regulator (SCAL_000545) and HTH transcriptional regulator archaea (SCAL_000831), which could be important to change the expression levels of certain genes and to adapt the protein contents depending on the substrate. Other genes that are differently expressed are directly related to the general metabolism of the cell like subunits of the ATPase complex indicating that *Ca.* S. caldarius is more active during growth on propane. Several other genes encode for hypothetical proteins without functional description.

The ALDEx2 analyses revealed that a relative low number of genes are differentially transcribed between both conditions. A plausible reason is that only a relative number of genes must change their expression pattern to adapt to the new substrate, most likely the ones responsible of their activation. Additionally, the original environmental conditions might also explain this expression pattern. *Ca.* S. caldarius inhabits sediments where different alkanes are present at the same time-Therefore it is likely that the basal status of *Ca.* S. caldarius is to express the machinery needed for the degradation of several alkanes and lacks fine mechanisms to regulate expression during growth on just one alkane.

Mcr expression during incubation with different substrates

Two *mcrA* genes of *Ca.* S. caldarius were differentially expressed between treatments according to ALDEx2. We decided to have a closer look in the expression patterns of all their *mcr* gene sets to see if there are connections between *mcr* expression and substrate. Both *Ca.* Syntrophoarchaeum strains have 4 *mcr* gene sets structured in operons except for the gene set SBU_000314/SBU_001009-1010 in *Ca.* S. butanivorans in which the *mcrA* is not located next to the *mcrBG*. All the *mcr* genes of *Ca.* Syntrophoarchaeum are highly divergent from the canonical MCRs, what has been interpreted as the need of conformational changes to accommodate larger substrates (Laso-Pérez*, et al.*, 2016). Three of the McrA subunits are related between both strains forming three clusters, while the remaining fourth McrA subunits (SBU_000314, SCAL_000352) are highly divergent being SBU_000314 close to the *Bathyarchaeaota* McrA and SCAL_000352 close to the McrA of GoM-Arc1 (**Figure 4**). Based on their phylogenetic relationships, we classified the MCR gene sets in four groups (**Table 2**). The corresponding MCR-1 enzymes of both strains are not monophyletic but they cluster together for simplicity and considering that both are highly divergent from the rest.

For *Ca.* S. caldarius, the *mcrA* genes of the sets MCR-1 and MCR-2 were differentially expressed (**Supplementary Table 2**). The alpha subunit gene of the MCR-1 was more enriched during growth on butane, while for MCR-2 it was more enriched in the treatment with propane (**Figure 5A**). However, there were notable differences in the expression levels of both considering the FPKM values (**Figure 5B**): the alpha subunit gene of the MCR-1 showed low levels of expression with propane (around 19), but quite high values with butane (270). In contrast, the expression levels of the alpha subunit gene of MCR-2 were considerably lower in both treatments. Strikingly, the *mcrBG* genes of both operons were not differentially expressed. For MCR-1, both *mcrBG* genes were highly expressed during incubations with butane and propane and have an opposite trend to the *mcrA* during growth on propane. Nonetheless, a visualization of the RNA read recruitment to the different MCR genes suggests that the expression levels of the corresponding *mcrBG* subunits might be overestimated (**Figure 6**). In both treatments, some gene regions were highly covered, whereas for other regions the read recruitment is much lower. This lacking uniformity is a hint that the read mapping was not always correct. The over-recruited regions corresponded to areas with the PFAM domains of the MCR enzyme, except for the highly transcribed region of the alpha subunit during growth on propane. In this case, the region only showed homology to the *mcrA* gene of GoM-Arc1 in the NCBI database. Thus, it might be possible that the real expression levels of *mcrBG* of the MCR-1 during growth on propane were more similar to those shown by the *mcrA* gene.

The other two *mcr* operons of *Ca.* S. caldarius did not show significant differential expression between treatments; however, there was higher enrichment during growth on propane than on butane especially for the MCR-4 (**Figure 5A**). This operon was the only one that shows considerable higher expression for all the subunits in propane than in butane and the corresponding FPKM expression values were also the highest of all operons (**Figure 5B**). The MCR-3 was the only MCR with

depletion during growth on butane and has in both treatments the lowest levels of expression compared to all *mcr* genes (**Figure 5**).

Hypothesis about substrate specificity of the MCRs

As shown, all 4 *mcr* operons of *Ca.* S. caldarius showed certain transcription during growth on butane and propane. All the *mcr* operons of *Ca.* S. butanivorans were also expressed during growth on butane (**Figure 5**). This suggests that independently of the substrate certain basal expression exist for all the *mcr* genes in both organisms. An explanation of this phenomenon might be the environmental conditions as previously mentioned. The niches of these organisms are not characterized by the presence of just one substrate but rather a mixture of different alkanes with different concentrations. However, for some *mcr* operons in both organisms the expression levels were higher with specific substrates and this could reveal links to certain substrates. Establishing an unambiguous connection between enzyme and substrate is still not possible, partly because *Ca.* S. butanivorans only grew on butane preventing the analysis of their *mcr* operons with a different substrate like propane. Based on the differential expression for *Ca.* S. caldarius, we propose that the MCR-1 enzyme is the candidate for butane activation, while the MCR-4 is likely responsible for propane degradation.

MCR-1 of *Ca.* S. caldarius is the candidate for butane activation since it was more expressed during growth on this substrate (**Figure 5**), after excluding the probably expression artefact for *mcrGB* (**Figure 6**). Similar results were found for the MCR-1 of *Ca.* S. butanivorans, which had the highest expression levels of all the *mcr* operons during growth on butane (**Figure 5**), especially for the *mcrA* gene which was separated from the *mcrBG* (**Figure 6**). The MCR-1 enzymes of both strains are not forming a monophyletic cluster (**Figure 4**), but both are highly divergent from the rest suggesting the need of more amino acid changes for their function. Interestingly, nearby genes to the MCR-1 operons showed similar high expression levels during growth on butane (**Figure 6**). Actually, the corresponding consecutive genes (SCAL_000353-355) of the MCR-1 of *Ca.* S. caldarius were also differently expressed with higher enrichment in the butane treatment (**Supplementary Table 2**). All these genes encode hypothetical proteins with low identity (below 40%) to any entry of the NCBI database, which are mostly uncharacterized or hypothetical proteins themselves. The role of the corresponding encoded proteins must be studied in the future since they could be important to regulate the MCR.

We suggest that in *Ca.* S. caldarius, the MCR-4 enzyme is responsible for the activation of propane, since its three subunit genes showed the highest levels of expression during growth of propane compared to any other *mcr* gene (**Figure 5**). A possible drawback for this hypothesis is that *Ca.* S. butanivorans did not thrive on propane, albeit it contains and expresses genes encoding a highly similar MCR-4 during growth on butane (**Figure 5**). Given that both enzymes are so closely related, it is reasonable to consider that they activate the same substrate. Consequently, it is still not understood why *Ca.* S. butanivorans did not grow on propane if it has the potential enzyme for propane activation.

The other MCRs operons (MCR-2 and -3) could not be assigned to a specific substrate, although the alpha subunit gene of the MCR-2 was differentially enriched during propane activation. However, the low expression levels of the MCR-2 and -3 genes for *Ca.* S. caldarius in both treatments are too low to suggest that the encoded enzymes were catalysing the activation of butane or propane, as transcriptomic analyses of ANME archaea have shown that *mcr* is usually a highly expressed gene (Haroon*, et al.*, 2013, Krukenberg*, et al.*, 2018). An alternative possibility is that these MCRs are in charge of the activation of a different unknown substrate. Another hypothesis would be that these MCRs have a different affinity to butane and propane and they catalyse their activation at different concentrations. In this way, *Ca.* Syntrophoarchaeum could adapt quickly to different substrate concentrations in the environment.

Further degradation of alkyl-CoM

After the activation by MCR, it was proposed that butyl-CoM is transformed to butyryl-CoA in a yet unresolved pathway. Then, butyryl-CoA is subsequently degraded via the fatty acid oxidation pathway, the Wood-Ljungdahl pathway and the downstream part of the methanogenesis (Laso-Pérez*, et al.*, 2016). The produced reducing equivalents are then transferred through conductive pili with the help of cytochromes to the bacteria *Ca.* D. auxilii that uses them for sulfate reduction. Genes encoding the responsible enzymes were considerably expressed for both organisms during growth on butane. Similarly, they were also expressed in *Ca.* S. caldarius during the treatment with propane indicating that propyl-CoM was further degraded in a similar pathway to butyl-CoM (**Supplementary Figure 1**). For the partner bacterium, the genes involved in sulfate oxidation or encoding cytochromes were highly expressed.

Some of the genes of *Ca.* S. caldarius were among those with differential expression between both treatments (**Supplementary Table 2**). Interestingly, several gene copies exist for these genes, what could indicate substrate specificity as proposed for the MCR. For instance, SCAL_000622 and SCAL_001545 were significantly more enriched in the propane incubations. They encode for methylcobalamin:CoM methyltransferases (Mta), likely involved in the conversion of the alkyl-CoM to a CoA-bound fatty acid. Likewise, SCAL_001203, which encodes a 3-hydroxyacyl-CoA dehydrogenase of the fatty acid oxidation pathway, was also significantly more enriched during growth on propane. A similar behaviour was shown for the gene SCAL_001080 encoding a cytochrome C and significantly more enriched in the propane treatment. This higher expression of cytochromes C genes in *C.* S. caldarius could be attributed that it is more active and that in Propane-50 is the only archaeon active. Thus, it probably has to build more conductive structures to transfer the electrons to the partner bacteria.

Summary and outlook

This study has investigated the physiology of *Ca.* Syntrophoarchaeum, showing that they can grow in a temperature range of 37-60 °C using butane and propane. No growth was detected in other short-chain alkanes. Transcriptomic analysis revealed that only the strain *Ca.* S. caldarius could grow on propane, while during incubations with butane two strains were present: *Ca.* S. caldarius and *Ca.* S. butanivorans, the dominant archaeon. The gene expression of the sulfate-reducing partner bacterium *Ca.* D. auxilii was not affected by the substrate change.

Ca. Syntrophoarchaeum caldarius metabolizes butane and propane using the same pathways according to the expression data, although specific MCRs enzymes might be responsible of the activation of butane or propane. This supports the idea that some of the highly divergent MCRs of *Ca.* Syntrophoarchaeum are specialized in the activation of different substrates. Future experiments like the crystallization of these MCRs could help to shed light in this question. This will also contribute to understand the functioning of other similar MCRs recently found in other archaea (Evans*, et al.*, 2015, Dombrowski*, et al.*, 2017). Furthermore, cultivation of *Ca.* Syntrophoarchaeum with additional substrates should be attempted to address the substrate range of this clade and their MCRs. For that, new samples potentially containing *Ca.* Syntrophoarchaeum should be retrieved, as the current cultured *Ca.* Syntrophoarchaeum have only shown growth on propane and butane.

Acknowledgments

We thank M. Meiners and S. Menger for assistance and support during cultivation and other laboratory work. We are indebted to A. Teske and the shipboard party, the crew and pilots of research expedition AT15-16 Research Vessel Atlantis and Research Submersible Alvin (NSF Grant OCE-0647633). This research project was funded by the DFG Leibniz Grant of the Deutsche Forschungsgemeinschaft (DFG) to Antje Boetius, and the DFG Research Center and Cluster of Excellence MARUM, the University of Bremen, the Max Planck Society and the Helmholtz Society.

Figures and Tables

Figure 1. Growth of Butane- and Propane-50 enrichments at different temperatures. A) Sulfide production over time for Butane-50 (butane) and Propane-50 (propane). Temperature regimes are indicated in the legend. B) Sulfide production rate per temperature during growth on butane and propane. In both panels, each point represents the average value of triplicate data. Bars indicate the standard error.

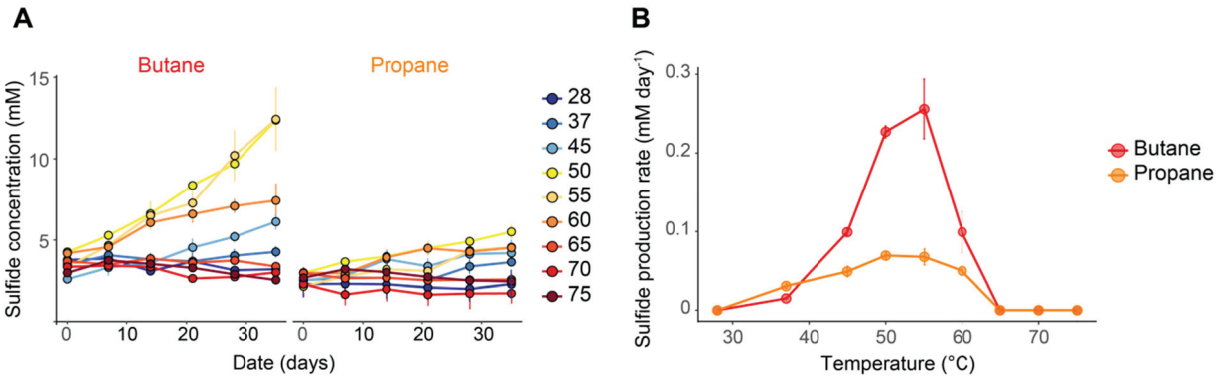

Figure 2. Community composition of the transcriptomes according to proportional abundance of 16S rRNA gene transcripts. Proportional abundances were calculated using the software phyloFlash, which mapped the 16S rRNA fragments to the SILVA 119 database. Prop refers to the transcriptomes originated from the triplicate Propane-50 cultures, while But refers to the Butane-50 ones. PhyloFlash classification of the *Ca.* Syntrophoarchaeum 16S rRNA fragments was limited to the genus level and therefore both *Ca.* Syntrophoarchaeum strains are merged in this graph.

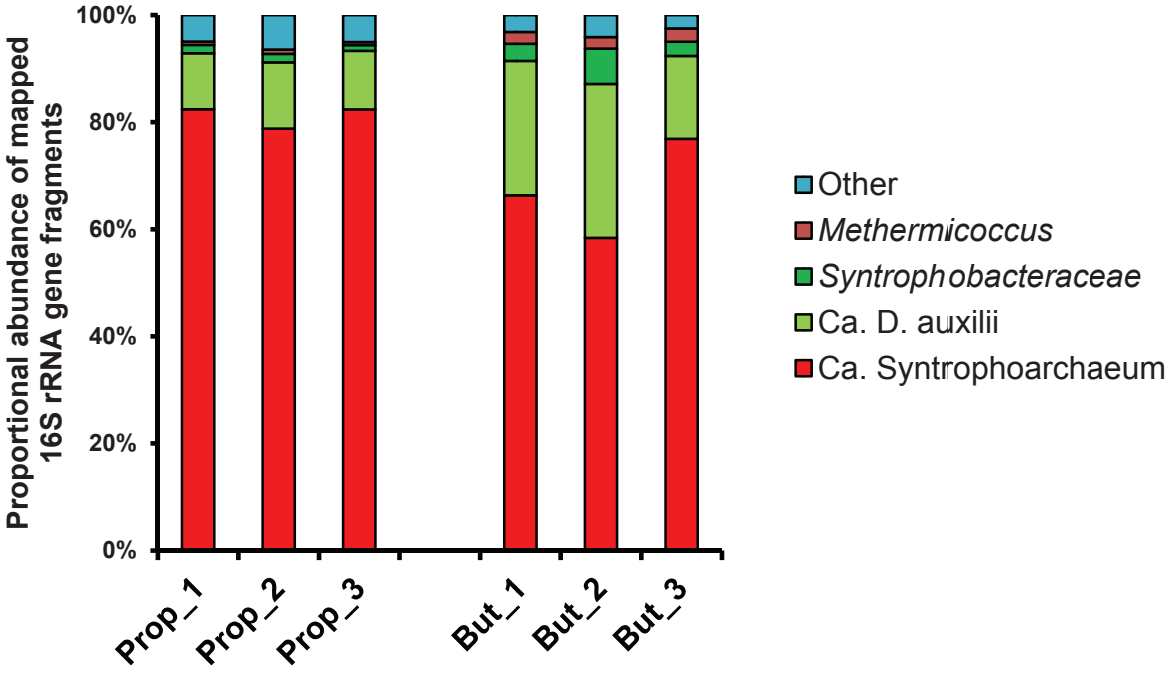

Figure 3. Hierarchical cluster dendrogram visualizing the dissimilarities in the gene expression of *Ca.* S. caldarius and *Ca.* D. auxilii during growth on butane and propane. The analysis includes the mRNA and tRNA reads mapping to the genomes during growth on both treatments.

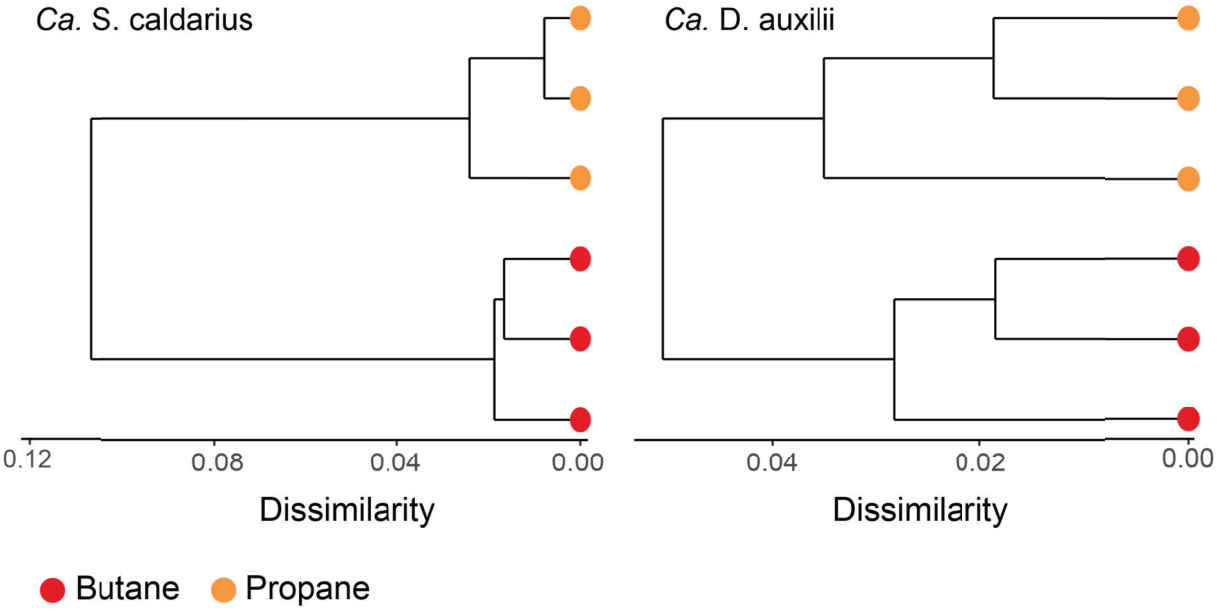

Figure 4. Phylogenetic tree of the amino acid sequence of the *Ca.* Syntrophoarchaeum *mcrA* genes. The colour of the labels indicates if the gene belongs to *Ca.* S. butanivorans (red) or *Ca.* S. caldarius (orange). The label includes the gene locus_tag, the MCR cluster (**Table 2**) and the NCBI protein accession number. The tree was calculated using a maximum likelihood algorithm using more than 500 amino acid positions. Bootstraps values >90% are shown with filled circles. The scale bar indicates the number of amino acid substitutions per site.

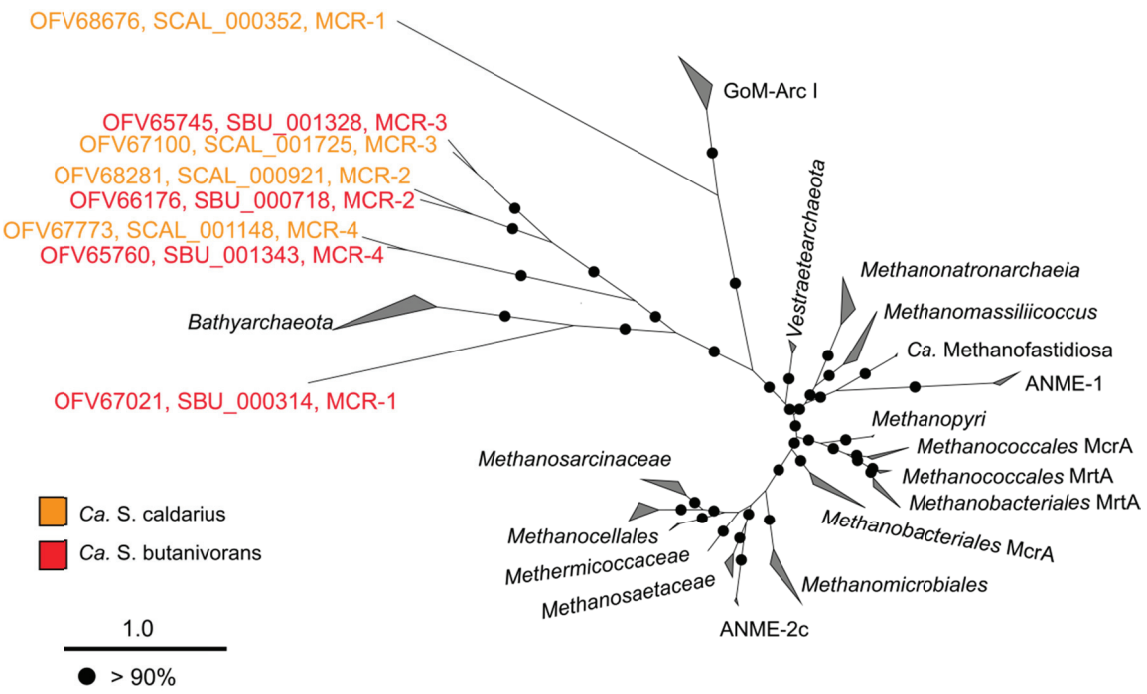

Figure 5. Expression of the *mcr* operons of *Ca.* Syntrophoarchaeum during growth on butane and propane. The 4 *mcr* operons are numbered based on their phylogenetic relationships (see **Figure 4** and **Table 2**). For each operon, the expression of the three subunits is indicated in the following order: alpha, beta gamma. The upper panel shows the centered log transformation value for each *mcr* gene, while the lower panel shows the corresponding FPKM value (fragment per kilobase of transcript per million mapped reads). Legend indicates organism and treatment by shape and colour. Bars indicate the range values for the triplicates in each treatment.

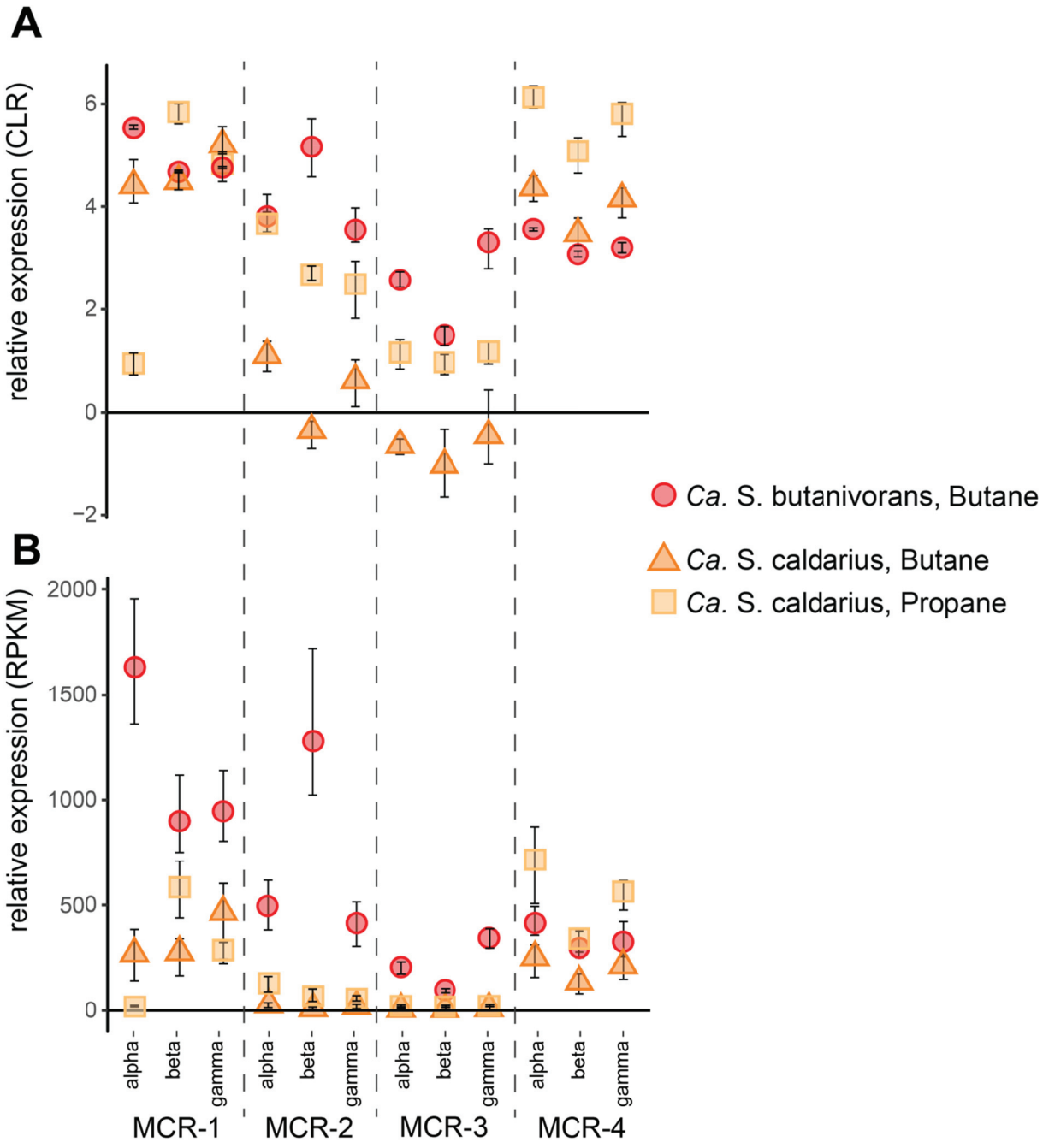

Figure 6. mRNA read recruitment to the *mcr* operons of *Ca.* Syntrophoarchaeum for both treatments (butane and propane). The genomic regions close to the *mcr* operons linked to butane (MCR-1) and propane (MCR-4) are depicted including the respective gene locus_tags for the *mcr* genes and the contig position. The annotation of nearby genes of interest is indicated in the legend. Below the operon depiction, total read coverage compared to the whole genome is shown in blue. Underneath the coverage, the reads recruited for that gene region are depicted (cutoff at 175 reads). Strain and treatments are indicated in the left side.

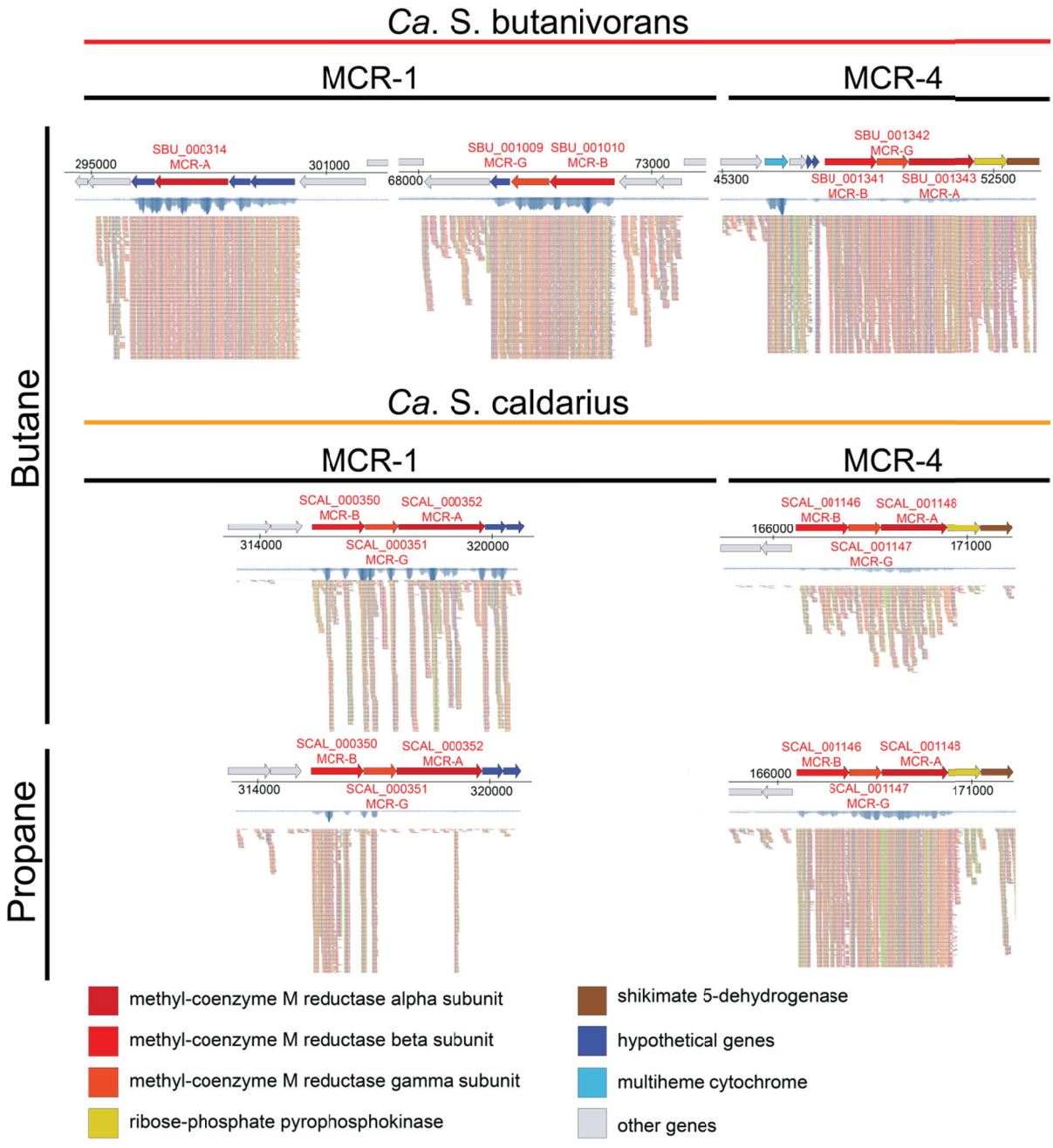

Table 1. Data used for thermodynamic calculations Gibbs energy were obtained from Thauer*, et al.*, 1977. Activity/fugacity was considered 1 for butane, propane and water. For the rest of compounds, activity values were based on the concentration in the culture medium at the first day of sulfide measurement. Calculations were done considering a temperature of 50°C (298 K) and with the assumption that ΔH and ΔS are the same at the lower and higher temperature (see Supplementary Discussion of **Chapter II**).

Compound	$\Delta_f G°_{298K}$ (kJ mol^{-1})	$\Delta_f H°_{298K}$ (kJ mol^{-1})	Activity/fugacity
n-C_4H_{10} (g)	-17.2	-125.6	1
C_3H_8 (g)	-23.4	-103.8	1
SO_4^{2-} (aq)	-744.6	-909.3	0.028
H^+ (aq, pH = 7)	-39.87	0	10^{-7}
HCO_3^- (aq)	-586.85	-691.1	0.03
H_2S (aq)	-27.87	-39.8	0.0025
H_2O (lq)	-237.18	-285.83	1

Table 2. MCR clusters of *Ca*. S. butanivorans and *Ca.* S. caldarius. They represent groups of the closely related operons of both strains based on the phylogenetic relationships of the *mcrA* genes.

MCR cluster	Subunit	*Ca.* S. butanivorans		*Ca.* S. caldarius	
		Gene locus_tag	NCBI accession number	Gene locus_tag	NCBI accession number
MCR-1	alpha	SBU_000314	OFV67021.1	SCAL_000352	OFV68676.1
	beta	SBU_001010	OFV66073.1	SCAL_000350	OFV68674.1
	gamma	SBU_001009	OFV66072.1	SCAL_000351	OFV68675.1
MCR-2	alpha	SBU_000718	OFV66176.1	SCAL_000921	OFV68281.1
	beta	SBU_000719	OFV66177.1	SCAL_000922	OFV68282.1
	gamma	SBU_000717	OFV66175.1	SCAL_000920	OFV86280.1
MCR-3	alpha	SBU_001328	OFV65745.1	SCAL_001725	OFV67100.1
	beta	SBU_001329	OFV65746.1	SCAL_001724	OFV67099.1
	gamma	SBU_001327	OFV65744.1	SCAL_001726	OFV67101.1
MCR-4	alpha	SBU_001343	OFV65760.1	SCAL_001148	OFV67773.1
	beta	SBU_001341	OFV65758.1	SCAL_001146	OFV67771.1
	gamma	SBU_001342	OFV65759.1	SCAL_001147	OFV67772.1

References

Adams M, Hoarfrost A, Bose A, Joye S and Girguis P (2013) Anaerobic oxidation of short-chain alkanes in hydrothermal sediments: potential influences on sulfur cycling and microbial diversity. *Frontiers in microbiology* **4**.

Ahn Y, Krzycki JA and Floss HG (1991) Steric course of the reduction of ethyl coenzyme M to ethane catalyzed by methyl coenzyme M reductase from *Methanosarcina barkeri*. *Journal of the American Chemical Society* **113**: 4700-4701.

Biddle JF, Cardman Z, Mendlovitz H, Albert DB, Lloyd KG, Boetius A and Teske A (2011) Anaerobic oxidation of methane at different temperature regimes in Guaymas Basin hydrothermal sediments. *The ISME journal* **6**: 1018.

Bushnell B (2016) *BBMap short read aligner*. University of California, Berkeley, California.

Callaghan A (2013) Enzymes involved in the anaerobic oxidation of *n*-alkanes: from methane to long-chain paraffins. *Frontiers in microbiology* **4**.

Cord-Ruwisch R (1985) A quick method for the determination of dissolved and precipitated sulfides in cultures of sulfate-reducing bacteria. *Journal of Microbiological Methods* **4**: 33-36.

Davidova IA, Duncan KE, Choi OK and Suflita JM (2006) *Desulfoglaeba alkanexedens* gen. nov., sp. nov., an *n*-alkane-degrading, sulfate-reducing bacterium. *International Journal of Systematic and Evolutionary Microbiology* **56**: 2737-2742.

Dolfing J, Zeyer J, Binder-Eicher P and Schwarzenbach RP (1990) Isolation and characterization of a bacterium that mineralizes toluene in the absence of molecular oxygen. *Archives of Microbiology* **154**: 336-341.

Dombrowski N, Seitz KW, Teske AP and Baker BJ (2017) Genomic insights into potential interdependencies in microbial hydrocarbon and nutrient cycling in hydrothermal sediments. *Microbiome* **5**: 106.

Evans PN, Parks DH, Chadwick GL, Robbins SJ, Orphan VJ, Golding SD and Tyson GW (2015) Methane metabolism in the archaeal phylum *Bathyarchaeota* revealed by genome-centric metagenomics. *Science* **350**: 434-438.

Fernandes AD, Reid JN, Macklaim JM, McMurrough TA, Edgell DR and Gloor GB (2014) Unifying the analysis of high-throughput sequencing datasets: characterizing RNA-seq, 16S rRNA gene sequencing and selective growth experiments by compositional data analysis. *Microbiome* **2**: 15.

Haroon MF, Hu S, Shi Y, Imelfort M, Keller J, Hugenholtz P, Yuan Z and Tyson GW (2013) Anaerobic oxidation of methane coupled to nitrate reduction in a novel archaeal lineage. *Nature* **500**: 567.

Holler T, Widdel F, Knittel K, Amann R, Kellermann MY, Hinrichs K-U, Teske A, Boetius A and Wegener G (2011) Thermophilic anaerobic oxidation of methane by marine microbial consortia. *The ISME journal* **5**: 1946.

Khelifi N, Amin Ali O, Roche P, Grossi V, Brochier-Armanet C, Valette O, Ollivier B, Dolla A and Hirschler-Réa A (2014) Anaerobic oxidation of long-chain *n*-alkanes by the hyperthermophilic sulfate-reducing archaeon, *Archaeoglobus fulgidus*. *The ISME journal* **8**: 2153.

Kleindienst S, Herbst F-A, Stagars M, von Netzer F, von Bergen M, Seifert J, Peplies Jörg, Amann R, Musat F, Lueders T and Knittel K (2014) Diverse sulfate-reducing bacteria of the *Desulfosarcina/Desulfococcus* clade are the key alkane degraders at marine seeps. *The ISME journal* **8**: 2029.

Kniemeyer O, Musat F, Sievert SM, Knittel K, Wilkes H, Blumenberg M, Michaelis W, Classen A, Bolm C and Joye SB (2007) Anaerobic oxidation of short-chain hydrocarbons by marine sulphate-reducing bacteria. *Nature* **449**: 898.

Kopylova E, Noé L and Touzet H (2012) SortMeRNA: Fast and accurate filtering of ribosomal RNAs in metatranscriptomic data. *Bioinformatics* **28**: 3211-3217.

Krukenberg V, Riedel D, Gruber-Vodicka HR, Buttigieg PL, Tegetmeyer HE, Boetius A and Wegener G (2018) Gene expression and ultrastructure of meso- and thermophilic methanotrophic consortia. *Environmental microbiology* **20**: 1651-1666.

Krukenberg V, Harding K, Richter M, Glöckner-Vodicka HR, Adam Birgit, Berg JS, Knittel K, Tegetmeyer HE and Botius A (2016) *Candidatus* Desulfofervidus auxilii, a hydrogenotrophic sulfate-reducing bacterium involved in the thermophilic anaerobic oxidation of methane. *Environmental microbiology* **18**: 3073-3091.

Kuever J, Rainey FA and Widdel F (2015) *Syntrophobacteraceae* fam. nov. *Bergey's Manual of Systematics of Archaea and Bacteria* 1-2.

Laso-Pérez R, Wegener G, Knittel K, Widdel F, Harding KJ, Krukenberg V, Meier DV, Richter M, Tegetmeyer HE, Riedel D, Richnow H-H, Adrian L, Reemtsma T, Lechtenfeld OJ and Musat F (2016) Thermophilic archaea activate butane via alkyl-coenzyme M formation. *Nature* **539**: 396.

Laso-Pérez R, Krukenberg V, Musat F and Wegener G (2018) Establishing anaerobic hydrocarbon-degrading enrichment cultures of microorganisms under strictly anoxic conditions. *Nature Protocols* **13**: 1310.

Lazar CS, L'Haridon S, Pignet P and Toffin L (2011) Archaeal Populations in Hypersaline Sediments Underlying Orange Microbial Mats in the Napoli Mud Volcano. *Applied and environmental microbiology* **77**: 3120-3131.

Lovley DR and Lonergan DJ (1990) Anaerobic Oxidation of Toluene, Phenol, and *p*-Cresol by the Dissimilatory Iron-Reducing Organism, GS-15. *Applied and environmental microbiology* **56**: 1858-1864.

Mardanov AV, Ravin NV, Svetlitchnyi VA, Beletsky AV, Miroshnichenko ML, Bonch-Osmolovskaya EA and Skryabin KG (2009) Metabolic Versatility and Indigenous Origin of the Archaeon *Thermococcus sibiricus*, Isolated from a Siberian Oil Reservoir, as Revealed by Genome Analysis. *Applied and environmental microbiology* **75**: 4580-4588.

McGlynn SE, Chadwick GL, O'Neill A, Mackey M, Thor A, Deerinck TJ, Ellisman MH and Orphan VJ (2018) Subgroup characteristics of marine methane-oxidizing ANME-2 archaea and their syntrophic partners revealed by integrated multimodal analytical microscopy. *Applied and environmental microbiology* AEM. 00399-00318.

McKay L, Klokman VW, Mendlovitz HP, LaRowe DE, Hoer DR, Albert D, Amend JP and Teske A (2016) Thermal and geochemical influences on microbial biogeography in the hydrothermal sediments of Guaymas Basin, Gulf of California. *Environmental Microbiology Reports* **8**: 150-161.

Milne I, Bayer M, Cardle L, Shaw P, Stephen G, Wright F and Marshall D (2010) Tablet—next generation sequence assembly visualization. *Bioinformatics* **26**: 401-402.

Orcutt BN, Joye SB, Kleindienst S, Knittel K, Ramette A, Reitz A, Samarkin V, Treude T and Boetius A (2010) Impact of natural oil and higher hydrocarbons on microbial diversity, distribution, and activity in Gulf of Mexico cold-seep sediments. *Deep Sea Research Part II: Topical Studies in Oceanography* **57**: 2008-2021.

Scheller S, Goenrich M, Thauer RK and Jaun B (2013) Methyl-Coenzyme M Reductase from Methanogenic Archaea: Isotope Effects on Label Exchange and Ethane Formation with the Homologous Substrate Ethyl-Coenzyme M. *Journal of the American Chemical Society* **135**: 14985-14995.

Siliakus MF, van der Oost J and Kengen SWM (2017) Adaptations of archaeal and bacterial membranes to variations in temperature, pH and pressure. *Extremophiles* **21**: 651-670.

Thauer RK, Jungermann K and Decker K (1977) Energy conservation in chemotrophic anaerobic bacteria. *Bacteriological Reviews* **41**: 100-180.

Trapnell C, Williams BA, Pertea G,Mortazavi A, Kwan G, van Baren MJ, Salzberg SL, Wold BJ and Pachter L (2010) Transcript assembly and quantification by RNA-Seq reveals unannotated transcripts and isoform switching during cell differentiation. *Nature biotechnology* **28**: 511-515.

van de Vossenberg JLCM, Driessen AJM and Konings WN (1998) The essence of being extremophilic: the role of the unique archaeal membrane lipids. *Extremophiles* **2**: 163-170.

Wegener G, Krukenberg V, Riedel D, Tegetmeyer HE and Boetius A (2015) Intercellular wiring enables electron transfer between methanotrophic archaea and bacteria. *Nature* **526**: 587.

Widdel F and Rabus R (2001) Anaerobic biodegradation of saturated and aromatic hydrocarbons. *Current Opinion in Biotechnology* **12**: 259-276.

Supplementary Information

Supplementary Figures and Tables

Supplementary Figure 1. Gene expression of enzymes involved in the alkane degradation in *Ca.* Syntrophoarchaeum and *Ca.* S. auxilii. The x-axis shows metabolic genes. Upper panel represents the clr values for each gene, while lower panels show the FPKM values. In the FPKM panel, note the different scales. Color circles indicate the different organisms. Color backgrounds indicate different pathways: red for methanogenesis, blue for fatty acid oxidation and Wood-Ljungdahl pathway, purple for electron cycling in *Ca.* Syntrophoarchaeum and green for the partner bacteria.

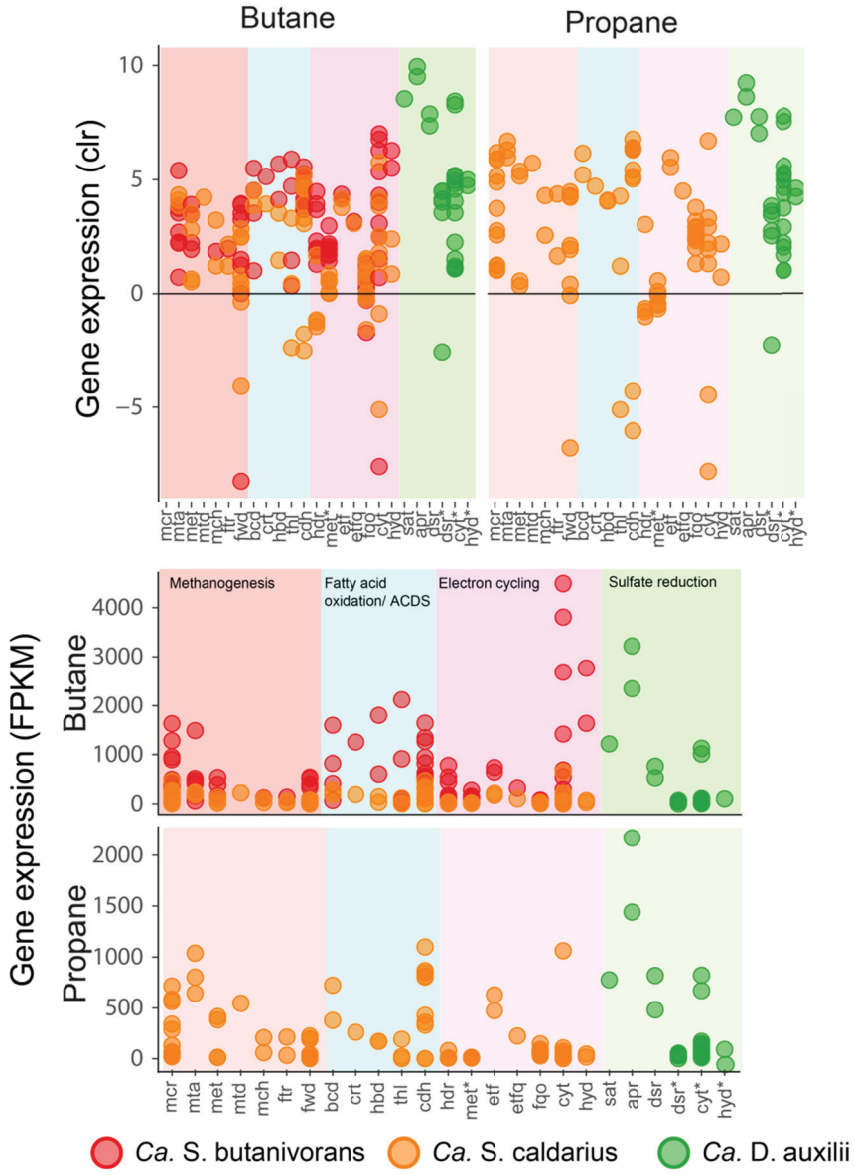

mcr = methyl CoM reductase; mta = methyltransferase corrionid protein; met = 5,10-methylenetetrahydrofolate reductase; mtd = methylenetetrahydromethanopterin dehydrogenase; mch = methylenetetrahydromethanopterin cyclohydrolase; ftr = formylmethanofuran--tetrahydromethanopterin formyltransferase; fwd = formylmethanofuran dehydrogenase; bcd = acyl-CoA dehydrogenase; crt = crotonase; hbd = 3-hydroxyacyl-CoA dehydrogenase; thl = acetyl-CoA acetyltransferase; acds = acetyl-CoA decarbonylase/synthase complex; hdr = heterodisulfide reductase; met* = associated complex to met; etf = electron transfer flavoprotein; etfq = Fe-S oxidoreductase associated to etf; fqo = $F_{420}H_2$:quinone oxidoreductase; cyt = *Ca.* Syntrophoarchaeum cytochrome; hyd = *Ca.* Syntrophoarchaeum hydrogenase; sat = sulfate adenylyltransferase; apr = adenylylsulfate reductase; dsr = dissimilatory sulfite reductase; dsr* = sulfite reduction-associated complex; cyt* = *Ca.* D. axuilii cytochrome; hyd* = *Ca.* D. auxilii hydrogenase.

Supplementary Table 1. Information about the triplicate transcriptomes of both treatments: butane and propane. The total number of raw reads and reads after quality trimming are shown in the first two rows. Then, total number of RNA reads assigned to rRNA or non-rRNA (mRNA and tRNA) by sortme software is indicated. From each of the RNA groups, the mapped reads to *Ca.* Syntrophoarchaeum organisms and *Ca.* D. auxilii are specified. For rRNA reads, the mapped reads were calculated based on the results of phyloFlash software. For *Ca.* Syntrophoarchaeum, phyloFlash could only resolve until genus levels. The assigned mapped counts are based on mapping performed by bbmap from the reads mapped to *Ca.* Syntrophoarchaeum. For the non-rRNA reads, the reads were mapped using bbmap to the genomes and then the mapped reads were assigned to features by Featurecounts. The percentages refer to the corresponding section, for instance in the Propane 1 sample 93.4% of the quality trimmed reads were classified as rRNA and 6.6% as nonRNA. From the 93.4% rRNA reads, 41.4% were mapped and 58.6% did not map.

	Propane 1		**Propane 2**		**Propane 3**		***Propane average***		**Butane 1**		**Butane 2**		**Butane 3**		***Butane average***	
	Reads	%	Reads	%	Reads	%	Reads	%	Reads	%	Reads	%	Reads	%	Reads	%
Total read number	60937181	100	61002912	100	52650435	100	58196843	100	56253985	100	58045289	100	53968393	100	56089222	100
After quality trimming	60889410	99.9	60940230	99.9	52600260	99.9	58143300	99.9	56208393	99.9	57998038	99.9	53913312	99.9	56039914	99.9
rRNA	56881785	93.4	52883025	86.8	48002675	91.3	52589162	90.5	51907495	92.3	53062993	91.5	49696944	92.2	51555811	92.0
mapped to	23545936	41.4	20973190	39.7	19691433	41.0	21403520	40.7	20260877	39.0	21408235	40.3	20416432	41.1	20695182	40.2
Ca. S. butanivorans	1789	< 0.1	2036	< 0.1	1848	< 0.1	1891	< 0.1	11116873	54.9	11120872	51.9	12476091	61.1	11571279	56.0
Ca. S. caldarius	19404125	82.4	16524022	78.8	16219043	82.4	17382397	81.2	2324342	11.5	1382907	6.5	3221225	15.8	2309491	11.2
Ca. D. auxilii	2461100	10.5	2594441	12.4	2154412	10.9	2403318	11.3	5085366	25.1	6153260	28.7	3157778	15.5	4798801	23.1
other organisms	1678923	7.1	1852691	8.8	1316130	6.7	1615915	7.5	1734296	8.6	2751196	12.9	1561337	7.6	2015610	9.7
unmapped	33335849	58.6	31909835	60.3	28311242	59.0	31185642	59.3	31646618	61.0	31654757	59.7	29280512	58.9	30860629	59.8
non rRNA	4007625	6.6	8057205	13.2	4597585	8.7	5554138	9.5	4300898	7.7	4935045	8.5	4216368	7.8	4484104	8.0
mapped	1419454	35.4	3010904	37.4	1637373	35.6	2022577	36.1	2680349	62.3	3089588	62.6	2693747	63.9	2821228	62.9
assigned to features from	1003514	70.7	2036807	67.6	1199508	73.3	1413276	70.5	1953909	72.9	2329694	75.4	1814784	67.4	2032796	71.9
Ca. S. butanivorans	723	0.1	995	0.0	871	0.1	863	0.1	1482558	75.9	1858511	79.8	1491963	82.2	1611011	79.3
Ca. S. caldarius	819467	81.7	1600401	78.6	1006477	83.9	1142115	81.4	120888	6.2	76998	3.3	99617	5.5	99168	5.0
Ca. D. auxilii	183324	18.3	435411	21.4	192160	16.0	270298	18.6	350463	17.9	394185	16.9	223204	12.3	322617	15.7
unmapped	2588171	64.6	5046301	62.6	2960212	64.4	3531561	63.9	1620549	37.7	1845457	37.4	1522621	36.1	1662876	37.1

Supplementary Table 2. Genes of *Ca.* S. caldarius with significant (<0.1) differential expression based on a pairwise comparison of incubations with butane vs. with propane. The locus_tag and gene annotations are provided as well as the median clr value for each gene in all samples for both treatments (rab.win). The asterisk in locus_tag indicates genes involved in the oxidation of butane. The median difference between the two groups (diff.btw), the effect and the expected (we.ep) and corrected (we.eBH) P values of Welch's test are also indicated.

Locus_tag	Gene annotation	rab.win (butane)	rab.win (propane)	diff.btw	effect	we.ep	we.eBH
SCAL_000353	hypothetical protein	4.62	-3.30	-7.96	-14.77	0.000428	0.03144
SCAL_000633	Fibronectin type III domain protein	5.71	2.30	-3.42	-12.11	0.000339	0.040591
SCAL_001354	transcriptional regulator	3.51	0.30	-3.17	-9.01	0.000689	0.048038
SCAL_001355	glycosyltransferase family 2	3.01	0.63	-2.40	-8.84	0.000746	0.046311
SCAL_000493	repeat domain protein	1.95	-3.07	-5.03	-8.40	0.002685	0.069784
SCAL_000545	ArsR family transcriptional regulator	2.88	-1.43	-4.35	-8.06	0.001974	0.068288
SCAL_000357	hypothetical protein	2.52	-4.10	-6.74	-7.94	0.003235	0.071869
SCAL_000352*	methyl coenzyme M reductase subunit alpha	4.32	0.39	-4.08	-7.76	0.000325	0.041113
SCAL_000354	hypothetical protein	2.30	-4.35	-6.48	-7.45	0.004743	0.075748
SCAL_001723*	5,10-methylenetetrahydrofolate reductase	2.82	4.60	1.74	7.43	0.003239	0.071111
SCAL_000895	protein containing von Willebrand factor type A	6.94	4.80	-2.06	-7.33	0.000396	0.045845
SCAL_001160	hypothetical protein	5.09	3.83	-1.28	-7.10	0.001161	0.055746
SCAL_000671	6-phospho 3-hexuloisomerase	0.38	2.66	2.26	6.52	0.004663	0.079012
SCAL_000831	HTH transcriptional regulator archaea	2.67	3.81	1.14	6.36	0.004465	0.075634
SCAL_000125	glycosyl transferase	3.89	2.42	-1.44	-6.28	0.002927	0.072452
SCAL_001124	threonine synthase	3.62	4.75	1.14	6.21	0.006404	0.09031
SCAL_001203*	3-hydroxyacyl-CoA dehydrogenase	1.44	3.48	1.96	6.07	0.006431	0.086811
SCAL_001257	nitrogen fixation protein NifU	6.06	4.38	-1.62	-5.83	0.001702	0.068074
SCAL_000622*	methylcobalamin:CoM methyltransferase	3.84	5.37	1.49	5.52	0.004546	0.085737
SCAL_001721	PP-loop domain-containing protein	2.61	-2.09	-4.63	-5.49	0.001336	0.063746
SCAL_000252	fructose 1,6-bisphosphatase	4.80	4.19	-0.61	-5.45	0.004879	0.081577
SCAL_001105	CRISPR-associated protein Cas1	1.69	0.17	-1.53	-5.36	0.005079	0.082498
SCAL_001198	Flagellin archaea	0.99	-1.84	-2.82	-5.36	0.007662	0.094725
SCAL_001253	DtxR family iron (metal) dependent repressor	3.40	1.63	-1.74	-5.00	0.002283	0.073213
SCAL_000701	transcriptional regulator	2.81	1.49	-1.32	-4.92	0.006318	0.089848
SCAL_001189	ATPase V1/A1 complex subunit E	3.13	4.75	1.54	4.83	0.002705	0.076685
SCAL_001787	hypothetical protein	4.15	-9.10	-13.02	-4.72	0.00966	0.096105
SCAL_001080*	cytochrome C	3.73	6.19	2.22	4.71	0.001604	0.069221
SCAL_000968*	formylmethanofuran-H4MPT formyltransferase	2.19	3.82	1.61	4.65	0.005434	0.089352
SCAL_000216	flavodoxin	3.46	2.02	-1.49	-4.64	0.003262	0.081297
SCAL_001254	(4Fe-4S)-binding protein	3.05	1.31	-1.79	-4.63	0.003565	0.084266
SCAL_000355	hypothetical protein	1.63	-5.29	-7.31	-4.56	0.007263	0.094739
SCAL_001364	methyl-CoM reductase system component A2	3.87	6.22	2.19	4.50	0.001723	0.071573
SCAL_000500	hypothetical protein	4.25	2.13	-2.11	-4.41	0.003116	0.082964
SCAL_000921*	methyl coenzyme M reductase subunit alpha	1.13	3.11	1.95	4.38	0.004372	0.085367
SCAL_001644	peptidase	4.64	3.93	-0.69	-4.37	0.004666	0.088214
SCAL_000632	conserved hypothetical protein%2C secreted	4.25	2.78	-1.48	-4.35	0.004949	0.091664
SCAL_001588*	ACDS complex gamma subunit	3.09	4.57	1.45	4.20	0.003718	0.087202
SCAL_000673	ArsR family transcriptional regulator	1.59	-0.31	-1.91	-4.05	0.005462	0.092033
SCAL_001504*	ACDS alpha subunit	4.58	5.87	1.18	4.05	0.003913	0.090226
SCAL_001256	Uncharacterized protein family UPF0066	4.75	3.12	-1.91	-4.02	0.003688	0.089063
SCAL_001545*	corrinoid methyltransferase	4.43	6.25	1.77	3.65	0.004345	0.094243
SCAL_000551	ATPase V0/A0 complex subunit C/D	3.81	5.83	1.77	3.31	0.004599	0.096453

Chapter V

Establishing anaerobic hydrocarbon-degrading enrichment cultures under strictly anoxic conditions

Rafael Laso-Pérez[1,2], Viola Krukenberg[1,2], Florin Musat[3] and Gunter Wegener[1,2,4]

[1]Max-Planck Institute for Marine Microbiology, 28359 Bremen, Germany.

[2]Alfred Wegener Institute Helmholtz Center for Polar and Marine Research, 27570 Bremerhaven, Germany.

[3]Helmholtz Centre for Environmental Research - UFZ, 04318 Leipzig, Germany.

[4]MARUM, Center for Marine Environmental Sciences, University Bremen, 28359 Bremen, Germany.

Nature Protocols ***13****: 1310-1330*

Published online 17 May 2018

Correspondence should be addressed to gwegener@mpi-bremen.de

https://www.nature.com/articles/nprot.2018.030

DOI: 10.1038/nprot.2018.030

Running title: *Cultivation of anaerobic hydrocarbon-degrading enrichments*

Abstract

Traditionally, the description of microorganisms starts with their isolation from an environmental sample. Many environmentally relevant anaerobic microorganisms grow very slowly, and often they rely on syntrophic interactions with other microorganisms. This impedes their isolation and characterization by classic microbiological techniques. We developed and applied an approach for the successive enrichment of syntrophic hydrocarbon-degrading microorganisms from environmental samples. We collected samples from microbial mat-covered hydrothermally heated hydrocarbon-rich sediments of the Guaymas Basin and mixed them with synthetic mineral medium to obtain sediment slurries. Supplementation with defined substrates (i.e., methane or butane), incubation at specific temperatures, and a regular maintenance procedure that included the measurement of metabolic products and stepwise dilutions enabled us to establish highly active, virtually sediment-free enrichment cultures of actively hydrocarbon-degrading communities in a 6-months to several-years' effort. Using methane as sole electron donor shifted the originally highly diverse microbial communities toward defined mixed cultures dominated by syntrophic consortia consisting of anaerobic methane-oxidizing archaea (ANME) and different sulfate-reducing bacteria. Cultivation with butane at 50 °C yielded consortia of archaea belonging to *Candidatus* Syntrophoarchaeum and *Candidatus* Desulfofervidus auxilii partner bacteria. This protocol also describes sampling for further molecular characterization of enrichment cultures by fluorescence *in situ* hybridization (FISH), and transcriptomics and metabolite analyses, which can provide insights into the functioning of hydrocarbon metabolism in archaea and resolve important mechanisms that enable electron transfer to their sulfate-reducing partner bacteria.

Introduction

The emergence of massive parallel sequencing of phylogenetic marker genes and environmental metagenomics has dramatically increased the known microbial diversity, yet most of the discovered organisms remain uncultured. The isolation of a microorganism from its environment is often precluded by notoriously slow growth, low abundance and complex interspecies dependencies. Thus, the metabolic potential and function of microbial communities is often assessed directly in environmental samples using culture-independent approaches[1]. However, resolving the physiology and environmental role of a microorganism, demands its accessibility for laboratory-based experiments under defined conditions. Classically, a target microorganism is isolated from the environment on a specific substrate using techniques such as dilution to extinction and streaking, thereby attempting to yield a clonal strain for physiological analysis[2]. Although this is often successful for rapidly growing microorganisms (e.g. doubling times of minutes to hours), it becomes difficult for those with lower growth rates or impossible for those demanding a syntrophic partner. Therefore, the establishment of microbial enrichment cultures dominated by a few species offers an alternative approach to study organisms not isolated in axenic cultures[3]. Circumventing the need for isolation, enriched

microorganisms can be studied by culture-dependent microbiological techniques combined with culture-independent approaches[4,5].

The concept of microbial enrichment cultures dates back more than a century ago to the work of Sergei Winogradsky and Martinus Beijerinck[6,7]. To establish a microbial enrichment culture, an environmental sample is incubated under conditions chosen to select microorganisms with defined physiological traits[8]. For instance, microorganisms performing a certain process such as the anaerobic degradation of hydrocarbons can be enriched by diluting a suitable environmental sample in defined growth medium and providing the model hydrocarbon as the sole substrate[9]. Tracking the consumption of the supplied substrates and/or the electron acceptor (e.g. nitrate, nitrite, sulfate or dissolved inorganic carbon), or the accumulation of reduced products, enables monitoring metabolic activity, which serves as proxy for the progress of enriching microorganisms with the desired metabolism. Steadily increasing substrate turnover rates and decreasing microbial diversity characterize a successful enrichment process. Enrichment cultures, as opposed to pure cultures (*i.e.* isolates), contain a multi-species community that is not necessarily stable in its composition over time[10], hence regular controls on of community compositions are important. However, very often the enrichment of a microorganism is the initial step towards its eventual isolation[11].

Marine and terrestrial subsurface sediments host large amounts of hydrocarbons that are biologically produced or result from the thermal decay of organic matter in sediments[12]. Gaseous hydrocarbons such as methane migrate via diffusion into sulfate-rich sediment layers. Here microorganisms oxidize methane with sulfate as electron acceptor, resulting in defined sulfate–methane interfaces[13]. Cold seeps and hot vents are submarine geological structures that emit fluids from the subsurface into the water column. These fluids are strongly reduced and often carry large amounts of hydrocarbons[14–16]. In the sediments, hydrocarbon seepage fuels vital microbial communities that thrive on the oxidation of methane and other hydrocarbons coupled to the reduction of sulfate[17–19]. The *in vitro* enrichment of anaerobic hydrocarbon oxidizers and their subsequent molecular characterization have been essential to the understanding of the microbial degradation of hydrocarbons in anoxic environments[5,19-26]. In general, isolation of anaerobic hydrocarbon degraders in pure culture is challenging due to slow growth, poor hydrocarbon solubility in water leading to mass transfer limitations, and trophic dependencies. For the anaerobic oxidation of methane, which is carried out by archaea that are strictly dependent on metabolic interactions with sulfate-reducing bacteria[5,18,27], isolation of the responsible organisms into pure culture has so far not been achieved. Therefore advancement in the field was largely dependent on the successful establishment of enrichment cultures. Investigations of enrichment cultures have also been key in understanding the anaerobic bacterial or archaeal oxidation of short-chain gaseous alkanes (C_2 to C_4)[19,28-30]. Anaerobic hydrocarbon oxidizers that metabolise medium to long chain *n*-alkanes, cycloalkanes or aromatic hydrocarbons have been enriched by growing them in media containing each of these substrates[31]. Even though in many cases successful enrichment led to isolation of hydrocarbon-degrading strains,

substantial strides in understanding the diversity, phylogeny, physiology and biochemistry of hydrocarbon degraders had already been achieved using mixed cultures[22,32-34].

Although numerous anaerobic hydrocarbon oxidizers have been isolated[31] anaerobic oxidizers of short-chain (C_1 to C_4) hydrocarbons grow particularly slowly, and to date only one representative has been isolated, *Desulfosarcina* sp. strain BuS5 (ref. 30). Moreover, all archaeal short-chain alkane oxidizers known so far are strictly dependent on metabolic interactions with bacteria[5,18,19,27]. Consequently, unravelling the basis of archaeal hydrocarbon metabolism largely depends on establishing and studying enrichment cultures of these organisms.

Here, we describe a protocol for establishing cultures from anoxic marine sediment samples that are enriched in consortia performing anaerobic hydrocarbon-degradation coupled to sulfate reduction (*i.e.* hydrocarbon-oxidizing archaea and sulfate-reducing bacteria) at elevated temperatures. Primarily we have used this protocol to enrich thermophilic organisms since they grow faster than their low-temperature adapted analogues. Furthermore, cultivation of short-chain hydrocarbon degraders at low temperatures led to the enrichment of free-living hydrocarbon-degrading bacteria[35], which were not the scope of our research. . However, our protocol would be also suitable for cultivating these organisms. We successfully used our approach to enrich for anaerobic methane-oxidizing communities thriving under meso- and thermophilic conditions. The resulting cultures were dominated by anaerobic methanotrophic archaea (ANME-1 clade) and Seep-SRB2 (mesophilic conditions) or ANME-1 and *Ca*. Desulfofervidus auxilii (HotSeep-1 clade)(thermophilic conditions)[36,37], and thermophilic butane-oxidizing consortia consisting of *Ca.* Syntrophoarchaeum (GoM-Arch87 clade) and *Ca*. Desulfofervidus auxilii[19]. In principle, this protocol can be used to establish enrichment cultures not only with gaseous alkanes, but any other model hydrocarbon (e.g. medium and long chain linear or branched alkanes, cycloalkanes, mono- or polycyclic aromatic hydrocarbons, alkylaromatic hydrocarbons), hydrocarbon mixtures, crude oil or crude oil refined products (e.g. gasoline, kerosene). Specific considerations regarding the addition of different hydrocarbons or hydrocarbon mixtures are discussed. Moreover, by modification of only the medium composition this protocol can be adapted to enrich for organisms that couple degradation of long-chain hydrocarbons to methane formation[21,38].

Our protocol describes 1) the preparation of growth medium, 2) the dilution of sediment samples, 3) the maintenance of enrichment cultures, including addition of hydrocarbon substrates, incubation and activity monitoring, 4) the propagation of enrichment cultures through regular transfer or dilution and 5) the collection and preservation of subsamples for subsequent molecular analysis including FISH analysis, DNA/RNA sequencing and metabolite analysis. The details for the molecular approaches are beyond the scope of this article. However, some recommendations for further analysis are included. Based on our experience, highly-enriched hydrocarbon-degrading enrichment cultures are obtained in a several months to over one year effort depending on the substrate, initial abundance of hydrocarbon degraders in the environmental sample and selection of suitable incubation

temperature. Once established the enrichment cultures allow assessing the identity and physiology of hydrocarbon-degrading microorganisms circumventing their isolation.

Selection of sediment samples as inoculate. The successful enrichment of slow-growing marine anaerobic hydrocarbon degraders from environmental samples in reasonable time frames requires careful selection of the source material. So far all successful enrichment of sulfate-dependent methane and short-chain hydrocarbon degraders used source material from site that have a long history of hydrocarbon exposure, are actively percolated by natural gas or crude oil (e.g. sediments around hydrocarbon seepage) and show elevated concentrations of sulfide as well as inorganic carbon (i.e. the products of sulfate-dependent hydrocarbon oxidation)[19,30,35,39,40].

For the cultivation of thermophilic hydrocarbon-oxidizers naturally heated gas- and oil-rich sediments are recommended. These prerequisites are best fulfilled by hydrothermal vents in the proximity of land and rivers that cause high sedimentation rates. We established our thermophilic hydrocarbon-degrading enrichment cultures from sediments of the Guaymas Basin, Gulf of California. In the Guaymas Basin subsurface magma intrusions heat the surrounding sediments, causing the thermogenic decay of organic matter to simple hydrocarbons, and the convection-driven venting of gas- and oil-rich fluids towards the water column[41]. We selected sites with steep vertical temperature gradients (*i.e.* from 4°C to 60°C in the uppermost 20 cm), which were highly sulfidic and rich in a complex mixture of gaseous and liquid hydrocarbons[42]. Other hydrothermal vents with substantial hydrocarbon seepage and at least partial sediment coverage are described: Juan de Fuca Ridge (*i.e.* Middle Valley Chowder Hill; 48°27.44' N,128°42.51'W[43]), Northern Mid Atlantic Ridge (*i.e.* Grimsey hydrothermal field; 66°35.50'N, 17°39.30'W[44]) and Loki's Castle (73° 30′ N, 8° 09′ E(ref. 45)). At all these sites widespread mats of sulfide-oxidizing bacteria indicate sulfide flux from below caused by intense hydrocarbon-dependent sulfate reduction. An updated list of vents is provided on the InterRigde Vents Database (https://vents-data.interridge.org/).

For the cultivation of meso- and psychrophilic hydrocarbon oxidizers sediments from cold seeps and mud volcanoes proved suitable. These seafloor structures are abundant at the continental shelf and margins. Compilations of global and regional seeps and vents are found elsewhere[16,46]. We performed successful enrichment from different sites[37] such as cold seeps at Hydrate Ridge, Cascadia Margin, Oregon[47], Mediterranean Mud Volcanoes and sites rich in short-chain hydrocarbons such as the seep sites in the Northern and Southern Gulf of Mexico. Above several of the North Sea gas fields and at seeps off the Mediterranean Island Elba anaerobic methanotrophy appears in coastal sands[48,49]. Here and potentially in other sandy seeps, sediment-depleted highly active microbial cell material could be gained by gravimetrical separation from the coarse sediment matrix[49]. Other sample sources may include crude oil and formation water from low-temperature oil reservoirs, contaminated anoxic aquifers, wastewater plants and soils.

Incubation conditions and expected microbial composition of produced enrichment cultures. The protocol presented here has been successfully used to enrich archaeal-bacterial consortia or single bacteria that couple the anaerobic oxidation of methane or specific short-chain hydrocarbons to the reduction of sulfate in a temperature range between 12 to 60°C[5,37,39,50]. Generally, to enrich for environmentally relevant clades, the incubation temperature should be chosen close to the *in situ* temperature at the sampling site. Our enrichment cultures initiated with material from cold seep environments (*in situ* temperatures 4 to 12°C) were successful when incubated between 12 to 20°C, while those initiated with material from hydrothermally-heated environments with steep temperature gradients developed hydrocarbon dependent sulfate reduction at elevated temperatures between 37 to 60°C. As our sediment samples were taken from marine environments, the growth medium used in the enrichment procedure was based on synthetic seawater with marine salinity and a pH adjusted to 7.1. For this sample type the medium should be carbonate-buffered and supplemented with phosphate, ammonium as well as essential vitamins and trace metals according to ref [31]. A single hydrocarbon compound should be added as energy source and sulfate serves as the sole provided electron acceptor. Enrichment cultures that grow under these selective conditions experience a successive decline in community complexity. This process is dynamic and relatively stable communities are achieved after several cycles of dilution in fresh medium. Throughout the enrichment process the development of the microbial community is monitored using 16S rRNA gene amplicon sequencing or metagenomics. Further, fluorescence *in situ* hybridisation is applied to enumerate clades of interest and to reveal spatial associations such as cell aggregates. The microbial composition of successful enrichment cultures predominantly depends on the source material, the supplied substrate and the incubation temperature. For instance, the enrichment of anaerobic methane oxidizers under sulfate-reducing conditions at meso- and thermophilic temperatures yielded communities dominated by ANME-1 archaea and sulfate-reducing bacteria of the Seep-SRB2 (37°C) or *Ca.* Desulfofervidus auxilii (50-60°C) clade[36,37,50] . In contrast, the anaerobic methane-oxidizing enrichment cultures obtained at lower temperatures (12°C to room temperature; 20 to 25°C) were repeatedly dominated by ANME-2 archaea and sulfate-reducing bacteria of the Seep-SRB2 or Seep-SRB1 clades, whereas the originally present ANME-1 where not enriched at low temperatures[37,39,51-53].

Thermophilic enrichments with butane selected for the novel archaeal hydrocarbon degrader *Ca.* Syntrophoarchaeum, which like ANME forms consortia with the sulfate reducer *Ca.* Desulfofervidus auxilii[19]. The *in vitro* enrichment of archaeal short-chain hydrocarbon degraders at lower temperatures has not been successful yet, although 16S rRNA gene sequences closely related to *Ca.* Syntrophoarchaeum have been retrieved from cold seep sediments[54]. Instead using the short-chain hydrocarbons propane or butane as substrate and moderate incubation temperatures, different hydrocarbon-degrading sulfate-reducing bacteria related to *Desulfosarcina* sp. were enriched[28,30,35].

Although only single substrates are supplied the enrichment cultures still contain considerable side communities: relative sequence abundance data from clone libraries, metagenomes and

metatranscriptomes the indicate that the hydrocarbon-degrading archaea and their partner bacteria account for about 60 to 90% established enrichments[19,37,50]. The side communities include bacteria affiliated with *Spirochaetes*, *Chloroflexi* (*Anaerolineaceae)* and several other clades without cultivated representatives (Candidate divisions OP3, KB1), and archaea affiliated with *Thermoplasmata*[19,37,50]. These organisms may thrive on cell exudates or organic compounds released from lysed cells. Other contaminants are even lower in abundance but they may quickly increase in number when non-hydrocarbon substrates are provided. For instance, mesophilic anaerobic methane-oxidizing enrichment cultures contain methylotrophic methanogens (*i.e. Methermicoccus* spp., *Methanococcoides* spp., and *Methanohalophilus* spp.) that likely thrive on methylated compounds released by the ANME archaea during methane oxidation[37]. Furthermore, in these enrichment cultures sulfur-disproportionating bacteria (e.g. GB-DISP1; *Desulfocapsa* related strains[37]) may thrive on minor amounts of zero-valent sulfur likely produced during medium preparation or medium exchange. Hence side communities need to be considered when conducting and interpreting physiological experiments, as well as in all downstream molecular analyses.

Scope and extended applications of the protocol. In its presented form, this protocol has been successfully applied to enrich for methane and short-chain hydrocarbon-oxidizing microorganisms in batch cultures. With minor adjustments, this protocol can also be used to enrich for marine degraders of higher hydrocarbons including medium- and long-chain alkanes, aromatic or polycyclic hydrocarbons (PAH). In such cases, different aspects need to be considered. Liquid hydrocarbons with relatively high water solubility (e.g. *n*-hexane, benzene) could have a pronounced toxic effect[55]. We recommend to add such compounds dissolved in the inert carrier phase 2,2,4,4,6,8,8-heptamethylnonane as described before[31]. By contrast, long-chain alkanes (e.g. *n*-hexadecane and higher alkanes) or PAH (e.g. phenanthrene) with very low water solubility should be added directly to the culture media, as liquid or crystals. A carrier phase should be avoided for this type of hydrocarbons as it may lead to low substrate availability in the water phase limiting the growth rates of microorganisms (for specific solubilities see ref. 56). Further details regarding the cultivation with liquid or solid hydrocarbons are found elsewhere[31]. In general, care must be taken to avoid contact between the rubber stoppers and the organic phase, which will eventually lead to swelling and dissolution of the stoppers. We recommend incubating the bottles upside down, with the stoppers below the medium-organic phase interface. The use of Teflon-based valve systems (i.e. Mininert, Sigma-Aldrich) has been established as alterative to this method. As these valves are not fully gas tight, experiments using these systems should be performed in anoxic chambers[57]. Other applications of the protocol described here include enrichment and cultivation of anaerobic microorganisms with soluble substrates (e.g. organic acids, alcohols). The preparation of stock solutions and the procedures for the addition of soluble substrates can be found elsewhere[58].

In addition, the current protocol can be adapted to enrich microorganisms from freshwater or brackish habitats by adjusting the salinity of the medium according to the environmental parameters.

Further, as organisms from such environments often show a limited tolerance to sulfide, the medium should be exchanged at low sulfide concentrations (e.g., 5 mM). For details and further considerations regarding freshwater medium compositions see refs. 31,58.

In addition, if sulfate is omitted from the medium (i.e. magnesium sulfate replaced by an equimolar amount of magnesium chloride), the protocol can be used to enrich and cultivate methanogenic archaea. As methanogenic microbial communities are highly sensitive to free sulfide or dithionite, amorphous ferrous iron has been successfully applied as alternative reductant in the medium[57,59]. The metabolic activity in methanogenic enrichment cultures is usually monitored by tracking the development of methane concentrations using gas chromatography[38].

Alternative approaches for enriching marine anaerobic methane-oxidizing consortia include the utilization of pressurized vessels[60], flow-through systems operated at ambient[61] or high pressures[51-53,62,63]. Most of these studies used media with similar composition to the one described here. However, the use of these highly expensive and laborious techniques could not substantially increase the biomass yields or growth rates of these microorganisms. Hence, these techniques rather suit specific applications, such as to yield *in situ* pressures or to simulate temperature gradients[64].

Experimental design. Here we describe the step-by-step procedure for the substrate-specific enrichment of hydrocarbon-degrading microorganisms and the retrieval of enrichment subsamples to monitor the cultivation progress. While we focus on describing the establishment of methane- and short-chain hydrocarbon-degrading enrichment cultures, we note the minor modifications necessary to adapt this protocol for the enrichment of degraders of other hydrocarbons (see above). The protocol suits for the production of initially 10 replicate enrichment cultures (100 ml) from approximately 100 ml wet surface sediment suspended in 1000 ml medium. This sediment density proved optimal to establish a vigorous hydrocarbon-degrading community from our sediment samples (i.e. Guaymas Basin sediments; see above). In practical terms, this setup leaves sufficient clear medium for chemical measurements once sediment particles settled. This protocol describes the procedure for cultivation in 156 ml bottles with 100 ml of culture. The remaining 56 ml headspace allows providing the gaseous hydrocarbon substrate in excess (2 mmol at 100 kPa). This set up is easily adaptable to other culture volumes. Care should be taken to keep a headspace to medium ratio of not less than 1:2 to ensure the supply of sufficient amounts of gaseous substrates and larger bottles should be constantly slowly agitated to avoid diffusion limitation. To test for the activity on endogenous substrates, replicate enrichment cultures without hydrocarbon addition (i.e. sediment slurry only) should be prepared and maintained. The regular measurement of sulfide allows the rapid determination of the activity and, hence, monitor the enrichment progress. The growth medium of the enrichment cultures should be exchanged when sulfide concentrations reach approximately 15 mM. At this stage culture material (i.e. biomass and remaining sediment) can be diluted to achieve sediment-free enrichment cultures over time. Due to the enrichment process, cultivation may be accompanied by severe community shifts.

Hence, several dilution and enrichment cycles should be performed to describe the community responsible for the turnover of a specific substrate. Our protocol describes also the necessary sampling steps to perform culture-independent methods on the produced enrichment cultures.

To reduce potential inhibitory effects by contaminants, we recommend working under sterile conditions even when setting up initial incubations for enrichment. General good microbiological practice should be followed. This includes sterile work next to a flame when critical. Once replicate enrichment cultures on different substrates are set up, cross-contaminations should be avoided by using new disposable material (e.g. needles and syringes) for every enrichment culture, while non-disposable material (e.g. metallic tweezers) should be sterilized.

We start with the preparation and handling of culture medium (step 1; **Fig. 1**) and the establishment of enrichment cultures of thermophilic hydrocarbon-degrading microorganisms from marine sediments (step 2-17; **Fig. 2**), monitoring of the produced enrichment and sampling of produced cultures for downstream analysis (step 18-23; **Fig. 2** and **3**). Our protocol also provides the modifications for alternative lab equipment.

Preparation of replicate enrichment cultures from an environmental sediment sample. The preparation of the sediment sample is carried out in an anoxic chamber to prevent exposure to oxygen. The preparation of inoculates without an anoxic chamber can be achieved by working under a constant stream of anoxic gas, preferentially a N_2:CO_2 mixture. However, this approach is more difficult and involves the risk to toxify highly sensitive organisms with oxygen. The source sediment is diluted (~ 1:10) in anoxic medium. The resulting slurry is evenly distributed to designated serum bottles (i.e. 156 ml serum bottles) filled approximately to 2/3 (100 ml). To increase the rate of success, we recommend preparing replicate incubations for each setup (*i.e.* hydrocarbon substrate and temperature). To achieve even sediment content in replicates the sediment slurry should be kept homogenous through continuous stirring during the distribution into serum bottles. Samples for dry weight determination and molecular analyses (such as tag sequencing, FISH or metagenomic analysis) should be collected at this stage to describe the source material. Bottles are sealed with gas-tight butyl rubber stoppers and aluminium crimp caps. All bottles prepared in anoxic chambers operated with partial hydrogen atmosphere need to be flushed with N_2:CO_2 (i.e. for at least 3 minutes) to remove this potential energy source.

Addition of hydrocarbon substrates to culture bottles. The kinetics of hydrocarbon degradation largely depends on the substrate concentrations; hence gaseous substrates are supplied with high partial pressures. Here we used 250 kPa methane or 100 kPa butane.

Incubation of enrichment cultures. Enrichment cultures are incubated in temperature-controlled, incubators in the dark. The contact of cells to their substrate is important, however constant shaking of samples has often shown negative effects in the cultures, but samples should be agitated weekly.

Tracking metabolic activity in the enrichment cultures. Well-growing enrichment cultures should show exponentially increasing cell numbers or an exponential accumulation of reaction product(s) in the medium. A convenient method to track the metabolic activity of sulfate-reducing microorganisms is to determine sulfide concentrations using a simple photometric assay[65,66]. Alternatively, sulfate or hydrocarbon (i.e. methane, butane) concentrations can be determined using ion or gas chromatography, respectively.

Maintenance and dilution of the enrichment cultures. When sulfide concentrations reach inhibitory or even potentially toxic levels (~ 15 mM), the medium should be exchanged. At this stage the enrichment culture is usually diluted. For instance, anaerobic methane-oxidizing enrichment cultures with a doubling time of 60 days and an activity causing a critical sulfide level (15 mM) in 90 days should be diluted 1:2. For faster growing enrichment cultures, such as the butane-oxidizing enrichment cultures, dilutions of 1:5 are suitable. We define an enrichment culture as established once it has been successfully subjected to at least three consecutive dilution steps.

Collection and preservation of enrichment material for subsequent analysis. Once an enrichment culture has been established it may be characterized by various molecular approaches. The collection and preservation of enrichment material differs depending on the desired analysis. Some approaches may require using a whole culture bottle while others only require subsamples. We provide an overview for the material collection and preservation for a selection of subsequent analyses that we consider most important based on the experience with our enrichment cultures. This includes FISH, amplicon-sequencing, metagenomics and transcriptomics. For metabolomic analyses we describe the preparation of samples for high resolution mass spectrometry (i.e. Fourier transform ion cyclotron resonance MS or Orbitrap-based MS) based on direct sample infusion. This approach avoids additional processing steps (e.g. chemical derivatization), which are usually demanding high amounts of sample.

MATERIALS

REAGENTS

Original sample

Here we describe the enrichment procedure for marine samples recovered after visual inspection of the sampling site. For rapid enrichment process intact sediment material (*i.e.* collected by push coring with 6 cm diameter cores) from defined hydrocarbon-rich, sulfidic spots should be selected. Avoid drained cores as microbial activity might be strongly affected by inflow of oxygen. A collection of comprehensive metadata, including exact position, temperature range and, if possible porewater chemistry (i.e. hydrocarbon concentrations, sulfate, sulfide, inorganic carbon, from replicate samples) is important to describe the original sample. Core sections of interest for cultivation are transferred

into sterile glass bottles (i.e. GL 45 glass bottles). Avoid air pockets in the sample and close bottle with gas-tight butyl rubber stoppers. If bottles are not completely filled with sediment, headspace should be exchanged with anoxic gas (i.e. N_2, Argon). Alternatively fill bottles completely with anoxic reduced medium prepared as described below. Samples collected to produce thermophilic enrichments can be stored at room temperature; if enrichments at lower temperatures are planned a storage temperature of 4°C is recommended. In this way samples can be stored for at least two months without losing substantial microbial activity, as tested for the enrichment of meso- and thermophilic anaerobic methane-oxidizing archaea. To maximize the cultivation success, we recommend starting the cultivation procedure as soon as possible (within weeks) after sampling. However, also after longer times (more than 6 months) many organisms (in particular those performing the anaerobic oxidation of methane) can be enriched from anoxic sediment samples. For each enrichment culture (156 ml bottle) 5 to 20 ml of the original sediment sample should be used. Enrichment attempts with higher dilutions may not be successful when targeting rare processes and organisms.

Gases

CRITICAL Hydrocarbon substrates should be selected according to planned enrichments. Specifications for gas containers, gas purity and gas regulators including their fittings differ regionally. This protocol uses EU specifications, for other regions ask your local supplier for similar purities.

! CAUTION High safety standards are required for handling pressurized and flammable gases. Wear safety googles. If not used store gas bottles in ventilated storage place. When handling pressurized gases use appropriate gas pressure reducers and connectors. Do not pressurize rubber tubing with more than 2 atm overpressure. During medium preparation in large bottles always use low-pressure line regulators (<0.1 atm). Do not use sterilization flame and other flammable gases (methane, other hydrocarbon gases) at the same time.

- CH_4 (i.e. ≥ 99.9995 mol % N55, Air Liquide, cat. no. P0716S10R2A001)
- CH_4:CO_2 (90:10; i.e. ≥ 99.9995 % Air Liquide, custom order)
- *n*-Butane (i.e. ≥ 99.95 Vol.% N35, Air Liquide, cat. no. P0645S10R0A001)
- CO_2 (i.e. ≥ 99.9995 mol % N55 Air Liquide, cat. no. P1725S10R0A001)
- N_2 (>99.999 mol% (Air Liquide, cat. no. P0272L50R2A001)
- N_2:CO_2 (90:10) gas mixture (i.e. ≥ 99.995 mol % N45 Air Liquide, custom order)

Chemicals

- Pure water (i.e., Milli-Q grade)
- KBr (Sigma-Aldrich, cat. no. P0838)
- KCl (Sigma-Aldrich, cat. no. P9333)
- $CaCl_2 \cdot 2H_2O$ (Sigma-Aldrich, cat. no. C3306)
- $MgCl_2 \cdot 6H_2O$ (Sigma-Aldrich, cat. no. M2670)
- $MgSO_4 \cdot 7H2O$ (Sigma-Aldrich, cat. no. 63138)
- NaCl (Sigma-Aldrich, cat. no. S7653)
- $CuSO_4 \cdot 5\ H_2O$ (Sigma-Aldrich, cat. no. C8027)
- Hydrochloric acid (HCl; 36.5–38.0% (wt/wt); Sigma-Aldrich, cat. no. H1758)
- $Na_2HPO_4 \cdot 2H_2O$ (Sigma-Aldrich, cat. no. S5136)
- $NaH_2PO_4 \cdot H_2O$ (Sigma-Aldrich, cat. no. S3522)
- NaOH pellets (Sigma-Aldrich, cat. no. S8045)

- $NaHCO_3$ (Sigma-Aldrich, cat. no. S5761)
- Na_2CO_3 (Sigma-Aldrich, cat. no. S7795)
- NH_4Cl (Sigma-Aldirch, cat. no. A9434)
- KH_2PO_4 (Sigma-Aldrich, cat. no. P9791)
- $FeSO_4 \cdot 7H_2O$ (Sigma-Aldrich, cat. no. F8633)
- H_3BO_3 (Sigma-Aldrich, cat. no. B6768)
- $MnCl_2 \cdot 4H_2O$ (Sigma-Aldrich, cat. no. M5005)
- $CoCl_2 \cdot 6H_2O$ (Sigma-Aldrich, cat. no. C8661)
- $NiCl_2 \cdot 6H_2O$ (Sigma-Aldrich, cat. no. N6136)
- $CuCl_2 \cdot 2H_2O$ (Sigma-Aldrich, cat. no. C3279)
- $ZnSO_4 \cdot 7H_2O$ (Sigma-Aldrich, cat. no. Z0251)
- $Na_2MoO_4 \cdot 2H_2O$ (Sigma-Aldrich, cat. no. M1651)
- Folic acid (Sigma-Aldrich, cat. no. F8758)
- Lipoic acid (Sigma-Aldrich, cat. no 07039)
- 4-Aminobenzoic acid (Sigma-Aldrich, cat. no. 06930)
- D(+)-Biotin (Sigma-Aldrich, cat. no. B4639)
- Nicotinic acid (Sigma-Aldrich, cat. no. N0761)
- Ca-D(+)-Pantothenate (Sigma-Aldrich, cat. no. 21210)
- Pyridoxine dihydrochloride (Sigma-Aldrich, cat. no. P9158)
- (−)-Riboflavin (Sigma-Aldrich, cat. no. R9504)
- Thiamine hydrochloride (Sigma-Aldrich, cat. no. T1270)
- Cyanocobalamin (Sigma-Aldrich, cat. no. V6629)
- $Na_2SeO_3 \cdot 5H_2O$ (Sigma-Aldrich, cat. no. S89771)
- $Na_2WO_4 \cdot 2H_2O$ (Sigma-Aldrich, cat. no. 72069)
- Resazurin sodium salt (Sigma-Aldrich, cat. no. R7017)
- Sodium sulfide nonahydrate crystals (Fisher Scientific, cat. no. S425-500)
- Hydrogen peroxide solution (H2O2; 30% (wt/wt); Sigma-Aldrich, cat. no. H1009)
- Sodium dithionite (EMD Millipore, cat. no. 106505)
- RNAlater (Sigma-Aldrich, cat. no. R0901) **CRITICAL** Reagent: alternative RNA fixation reagents might require different procedures).
- Diethyl pyrocarbonate (Sigma-Aldrich, cat. no. D5758)
- RNaseZAP (Sigma-Aldrich, cat. no. R2020)
- RNase-free water (Sigma-Aldrich, cat. no. 9601)
- Quick-RNA Miniprep Kit (Zymo Research, cat. no. R1050)
- Formaldehyde solution (36.5–38.0% in water; Sigma-Aldrich, cat. no. F8775)
- Ethanol (absolute; EMD Millipore, cat. no. 100983)
- Ammonium bicarbonate (EMD Millipore, cat. no. 533005)
- Acetonitrile (EMD Millipore, cat. no. 113212)
- Methanol (EMD Millipore, cat. no. 106002)

EQUIPMENT

- Gas controllers for the different gases and connectors (Air Liquide, custom order) to tubing (Norprene laboratory tubing (1/8-inch diameter; Sigma-Aldrich, cat. no. Z279900)) and Luer male adapters (1/8-inch diameter, Cole-Parmer, cat. no. GZ-30800-24)
- Low-pressure line regulator (GasTech, model no. Omega I 1SSLFDR-2)
- Anoxic chamber operated with N_2:CO_2, 90:10 atmosphere to keep the pH of the medium constant (UNIlab Pro Glove Box Workstation (MBraun) equipped with gas purifier (MBraun, model no. MB-20-G; ask supplier for best configuration)) **CRITICAL** Transfers in anoxic chambers operated with partial H_2 atmosphere require subsequent exchange of the enrichment culture's headspace with N_2:CO_2, 90:10 to reduce the risk of enriching hydrogen-oxidizing microorganisms.
- Duran glass bottle (1 liter, GL 45 opening; Omnilab, cat. no. 5072016)
- Medium preparation bottle ('Widdel flask') with bottle-filling system
- (Glasgerätebau Ochs, cat. no. 110011, or custom-order from a local manufacturer)
- Duran glass bottle (1 liter, GL 45 top opening and GL 25 side opening with screw caps (produced on request by glassware manufacturer, e.g., Glasgerätebau Ochs or a local manufacturer))
- Caps for Duran laboratory bottles (GL 25, Sigma-Aldrich, cat. no. Z232343; GL 45, Sigma-Aldrich, cat. no. Z153958)
- Serum bottles (150 ml; Glasgerätebau Ochs, cat. no. 102046; or Wheaton, cat. no. 223950)

- Butyl rubber stoppers (Glasgerätebau Ochs, cat. nos. 102049 and 102054) and aluminum crimp caps (Glasgerätebau Ochs, cat. no. 102050; or Bellco Glass, cat. no. 2048-11020)
- Capping and decapping tongs for serum bottles (Wheaton, cat. nos. W225303 and 224373)
- Tea strainer (plastic)
- All-glass syringe (Sigma-Aldrich, cat. no. Z314560)
- Graduated glass pipettes (5 ml, dry sterilized; Fisher Scientific, cat. no. 13-665-3K)
- Hoffman clamps (Fisher Scientific, cat. no. 05-871B)
- Pinchcock clamps (Fisher Scientific, cat. nos. 05-850A and 05-850B)
- Laboratory spoon that fits into GL 45 opening of Duran glass bottles (e.g., Sigma-Aldrich, cat. no. Z177911)
- Diverse spatulas (e.g., Sigma-Aldrich. cat. no. Z648299)
- Magnetic cylindrical and cell-preserving H-shape magnetic stirring bars (38 mm, VWR Spinbar, cat. no. 58948-150; 32 mm, VWR Circulus, cat. no. 102095-498)
- Magnetic stirrer (IKA, cat. no. 0025004601)
- Steam autoclave (SanoClav, cat. no. 01039)
- Brown-glass flasks for vitamin solutions (Thermo Fisher, cat. no. 149-0125)
- Glass flasks with aluminum caps for trace element solutions (Glasgerätebau Ochs, cat. no. 118100)
- Dry autoclave oven to sterilize glassware and metal (Steriliser SN series; Memmert)
- Serological plastic pipettes (sterile, individually wrapped, 10 ml; Sigma-Aldrich, cat. no. CLS4488) for use in anoxic chamber
- Pipette controller (Powerpette Pro; VWR, cat. no. 612-3870) for use with serological pipettes
- Pipettes (Finnpipette F1, 10 ml, 1 ml, 200 µl; Thermo Fisher, cat. nos. 4641120N; 4641100N and 4641080N) with fitting tips
- Centrifuge tubes (2 ml, 15 ml, 50 ml; Sarstedt, cat. nos. 72.694.406, 62.554.002, 62.547.004) for subsample collection (e.g., for dry weight determination and DNA or FISH analysis)
- Centrifuges for 50- and 15-ml tubes (Eppendorf, model no. 5810R) and for 2-ml tubes (Eppendorf, model no. 5427R)
- Sensitive laboratory balance (sensitivity ~1 mg; Sigma-Aldrich, cat. no. Z662941)
- Medical syringes (1 ml, Injekt F-SOLO, B. Braun, cat. no. 9166017V; 5 ml, B. Braun, cat. no. 4616057V; 50 ml, Omnifix Solo, B. Braun, cat. no. 4616502F)
- Single-use needles (Sterican single-use needles, 23-gauge × 1 1/4-inch, B. Braun, cat. no. 4657640; 20-gauge × 1 1/2-inch, B. Braun, cat. no. 4657519; 21-gauge × 4 3/4-inch, B. Braun, cat. no. 4665643; 26-gauge × 1-inch, B. Braun, cat. no. 4657683)
- Photometer (UV-visible spectrophotometer; Shimadzu, cat. no. UV-1280) (The photometer is calibrated as described in Box 1.)
- Test tubes (glass) with holding volumes of 5–10 ml (for copper sulfate assay and pH measurements; Sigma-Aldrich, cat. no. Z653500)
- Single-use cuvettes (2.5 ml; Sigma-Aldrich, cat. no. Z330388)
- Sterile membrane syringe filters with male Luer lock outlet (Sartorius, cat. no. 16532)
- Sterile surgical disposable scalpels (B. Braun, cat. no. BA825SU)
- Disposable cell scraper (Sarstedt, cat. no. 83.1832)
- Graduated cylinders for volumes of 100 ml and 1,000 ml (Sigma-Aldrich, cat. nos. Z131040 and Z131121)
- Volumetric flask with plastic lid for volumes of 1,000 ml (Sigma-Aldrich, cat. no. Z740783)
- Parafilm M (Sigma-Aldrich, cat. no. P7793)
- Aluminum foil (Sigma-Aldrich, cat. no. Z185140)
- Bunsen burner (Sigma-Aldrich, cat. no. Z270288)
- Incubator (Memmert, cat. no. IN750)
- pH-electrode setup (SevenCompact pH Meter with InLab Routine (Mettler Toledo) and Go-SIM pH electrode (Mettler Toledo))
- Bead-beating machine (MP Biomedicals, cat. no. 116004500)
- Lysing Matrix E (2-ml tube; MP Biomedicals, cat. no. 116914100)
- Heating bath (ICC basic; IKA)
- Sterile PVC male Luer-Lock tubing (Cole-Parmer, cat. no. GZ-30600-62)
- Stopcock with Luer connections (one-way; Cole Parmer, cat. no. GZ-30600-00)
- Stopcock with Luer connections (three-way; Cole Parmer, cat. no. GZ-30600-02)
- Tweezers (sterilized; Sigma-Aldrich, cat. no. F4517)
- 500-ml Beaker (Sigma-Aldrich, cat. no. BR87616)

- Membrane filter (Whatman Nuclepore Track-Etched Membrane, diameter = 47 mm, pore size = 0.2 µm; Sigma-Aldrich, cat. no. 111106-47)
- Cellulose nitrate membrane filter (diameter = 47 mm, pore size = 0.45 µm; Sartorius, cat. no. 11306-47)
- Nalgene polysulfone reusable bottle-top filter (Thermo Fisher, cat. no. DS0320-5045)
- Glass Petri dishes, sterilized (Sigma-Aldrich, cat. no. CLS70165101)
- Light microscope (Axio Scope A1; Zeiss, cat. no. 490035-0002-000) with standard oculars
- Microscope slides (Sigma-Aldrich, cat. no. S8400)
- Cover glasses (Sigma-Aldrich, cat. no. C9056-1CS)
- Benchtop bead-based homogenizer (Mo Bio Laboratories, model no. PowerLyzer 24)
- Glass beads (0.1-mm diameter, sterilized; Roth, cat. no. N029.1)
- 2-ml Glass vials (Zinsser NA, cat. no. 3088102) with Teflon-lined screw caps (Zinsser NA, cat. no. 3088933)

REAGENT SETUP

PBS (1× PBS/10× PBS; pH 7.4). Prepare 1× PBS from a 10× concentrated solution (10× PBS; pH 7.4) by dilution in MilliQ water. For 1 l of 1× PBS, add to a 1 l volumetric flask 100 ml of 10× PBS and 900 ml MilliQ water. Always filter sterilize 1× PBS aliquots before use. To prepare 10× PBS, add to a graduated cylinder 80 g NaCl, 2 g KCl, 26.8 g $Na_2HPO_4 \cdot 7H_2O$, 2.4 g KH_2PO_4 and fill up to 800 ml with MilliQ water. Adjust pH to 7.4 with NaOH solution (1 M) or HCl and fill up to 1000 ml with MilliQ water. Transfer the solution to a 1 l volumetric flask and autoclave (121°C, 25 min) it. This solution can be stored at room temperature for years.

HCl solution (1 M/0.1 M). Prepare a 1 M HCl solution in a glass flask by adding 20 ml of 37% (12 M) HCl into 220 ml MilliQ water. Prepare a 0.1 M HCl solution by diluting 10 ml 1 M HCl in 90 ml MilliQ water. Filter-sterilize before use. A filter-sterilized solution stored at room temperature can be used for several years. **! CAUTION** Always add the acid to the water in order to prevent vigorous exothermic reactions.

NaOH solution (1 M). Prepare a 1 M NaOH solution in a glass flask by adding 40 g of NaOH pellets to 1 liter of MilliQ water while mixing on a magnetic stirrer. Filter-sterilize before use. This solution can be stored at room temperature for years. **! CAUTION** Add the NaOH slowly since its dissolution in water releases considerable heat.

Sodium carbonate (Na_2CO_3) solution (1 M). To a volumetric flask, add 800 ml of Milli-Q water and a magnetic stirring bar. While mixing on a magnetic stirrer, add 142.019 g of Na_2CO_3. Close the volumetric flask with the lid and stir until salts are dissolved. Fill up with Milli-Q water to 1,000 ml. Transfer 100-ml aliquots to serum bottles (156 ml). Close the serum bottles with butyl rubber stoppers plus aluminum crimp caps and exchange the headspace with CO_2 gas. Autoclave the serum bottles for 20 min at 121 °C and store them at room temperature. Solutions last at least 6 months. Discard if carbonates precipitate.

Ammonium phosphate ($NH_4Cl + KH_2PO_4$) solution. To a graduated cylinder, add 900 ml of Milli-Q water and a magnetic stirring bar. While mixing on a magnetic stirrer, add 15.71 g of NH_4Cl and 8.00 g of KH_2PO_4. Fill up with Milli-Q water to 1,000 ml and stir until salts are dissolved. Transfer 25-ml aliquots to serum bottles (100 ml), close the serum bottles with butyl rubber stoppers plus aluminum

crimp caps and flush with N_2 gas (gentle gas stream, ~5 min). Autoclave for 20 min at 121 °C. Solutions stored at room temperature last for at least 1 year.

Sodium bicarbonate ($NaHCO_3$) solution (1 M). To a volumetric flask, add 800 ml of Milli-Q water and a magnetic stirring bar. While mixing on a magnetic stirrer, add 84.01 g of $NaHCO_3$. Close the volumetric flask with the lid and stir until salts are dissolved. Fill up with Milli-Q water to 1,000 ml. Transfer 30-ml aliquots to serum bottles (100 ml). Close the serum bottles with butyl rubber stoppers plus aluminum crimp caps and exchange headspace with CO_2 by purging for 5 min. Add a CO_2 headspace to 130 kPa. Autoclave the serum bottles in a dedicated rack for 20 min at 121 °C and store them at room temperature. Solutions last at least 6 months. Discard if carbonates precipitate.

Non-chelated trace element mixture. The non-chelated trace element mixture is prepared according to ref. 31. To a graduated cylinder, add 50 ml of Milli-Q water and a magnetic stirring bar. While mixing on a magnetic stirrer, add 2.1 g (7.5 mmol) $FeSO_4 \cdot 7H_2O$ and 8.8 ml of fuming HCl (37%). Allow mixing by slight stirring for a few minutes before adding 900 ml of Milli-Q water, 60 mg of H_3BO_3, 1 g of $MnCl_2 \cdot 4H_2O$, 380 mg of CoCl2 $\cdot 6H_2O$, 240 mg of $NiCl_2 \cdot 6H_2O$, 2 mg of $CuCl_2 \cdot 2H_2O$, 288 mg of $ZnSO_4 \cdot 7H_2O$ and 72 mg of $Na_2MoO_4 \cdot 2H_2O$. Fill up with Milli-Q water to 1,000 ml and keep stirring until salts are dissolved. Transfer 50-ml aliquots to glass flasks and close with aluminum screw caps. Autoclave solutions at 121 °C for 20 min, allow cooling to room temperature and store them at 4 °C. If refrigerated, solution can be used for at least 1 year.

Vitamin mixture. The vitamin mixture is prepared according to ref. 31. Prepare two autoclaved (20 min, 121 °C) brown-glass flasks (~50 ml) and aluminum screw caps. To a graduated cylinder, add 100 ml of a $NaH_2PO_4 \cdot H_2O$ solution (10 mM, pH 7.1) and a magnetic stirring bar. While mixing on a magnetic stirrer, add 4 mg of 4-aminobenzoic acid, 1 mg of D(+)-Biotin, 10 mg of nicotinic acid, 5 mg of Ca-D(+)-pantothenate, 15 mg of pyridoxine dihydrochloride, 4 mg of folic acid and 1.5 mg of lipoic acid. Keep stirring until the salts are dissolved. Transfer 50-ml aliquots to the autoclaved glass flasks by filter-sterilizing the solution through a 0.2-µm-pore-size syringe-driven filter. Close flasks with autoclaved aluminum screw caps and store them at 4 °C. If stored refrigerated, solutions can be used for at least 1 year. **CRITICAL** Work next to flame and under sterile conditions.

Riboflavin solution. Riboflavin solution is prepared according to ref. 31. Prepare two autoclaved (20 min, 121 °C) brown-glass flasks (~50 ml) and aluminum screw caps. To a graduated cylinder, add 100 ml of a $NaH_2PO_4 \cdot H_2O$ solution (25 mM, pH 3.2) and a magnetic stirring bar. While mixing on a magnetic stirrer, add 2.5 mg of riboflavin and keep stirring until it is dissolved. Transfer 50-ml aliquots to the autoclaved glass flasks by filter-sterilizing the solution through a 0.2-µm-pore-size syringe-driven filter. Close flasks with autoclaved aluminum screw caps and store them at 4 °C. If stored refrigerated, solutions can be used for at least 1 year. **CRITICAL** Work next to flame and under sterile conditions.

Thiamine solution. Thiamine solution is prepared according to ref. 31. Prepare two autoclaved (20 min, 121 °C) brown-glass flasks (~50 ml) and aluminum screw caps. To a graduated cylinder, add 100

ml of a $NaH_2PO_4 \cdot H_2O$ solution (25 mM, pH 3.4) and a magnetic stirring bar. While mixing on a magnetic stirrer, add 10 mg of thiamine hydrochloride and keep stirring until complete dissolution. Transfer 50-ml aliquots to the autoclaved glass flasks by filter-sterilizing the solution through a 0.2-µm-pore-size syringe-driven filter. Close flasks with autoclaved aluminum screw caps and store them at 4 °C. If stored refrigerated, solutions can be used for at least 1 year. **CRITICAL** Work next to flame and under sterile conditions.

Vitamin B_{12} solution. Vitamin B_{12} solution is prepared according to ref. 31. Prepare two autoclaved (20 min, 121 °C) brown-glass flasks (~50 ml) and aluminum screw caps. To a graduated cylinder, add 100 ml of Milli-Q water and a magnetic stirring bar. While mixing on a magnetic stirrer, add 5 mg of cyanocobalamin and keep stirring until it is dissolved. Transfer 50-ml aliquots to the autoclaved glass flasks by filter-sterilizing the solution through a 0.2-µm-pore-size syringe-driven filter. Close the flasks with autoclaved aluminum screw caps and store them at 4 °C. If stored refrigerated, the solution can be used for at least 1 year. **CRITICAL** Work next to flame and under sterile conditions.

Selenite-tungstate solution. Selenite-tungstate solution is prepared according to ref. 31. Prepare two autoclaved (20 min, 121 °C) glass flasks (~50 ml) and aluminum screw caps. To a graduated cylinder, add 1,000 ml of Milli-Q water and a magnetic stirring bar. While mixing on a magnetic stirrer, add 400 mg of NaOH pellets, 6 mg of $Na_2SeO_3 \cdot 5H_2O$, 8 mg of $Na_2WO_4 \cdot 2H_2O$ and keep stirring until the salts are dissolved. Transfer 50-ml aliquots to the autoclaved glass flasks by filter-sterilizing the solution through a 0.2-µm-pore-size syringe-driven filter. Close the flasks with autoclaved aluminum screw caps and store them at 4 °C. If stored refrigerated, solution can be used for at least 1 year. **CRITICAL** Work next to flame and under sterile conditions.

Resazurin solution. Prepare two autoclaved (20 min, 121 °C) glass flasks (~50 ml) and aluminum screw caps. To a graduated cylinder, add 100 ml of Milli-Q water and a magnetic stirring bar. While mixing on a magnetic stirrer, add 0.5 g of resazurin sodium salt and keep stirring until it is dissolved. Transfer 50-ml aliquots to autoclaved serum flasks by filter-sterilizing the solution through a 0.2-µm-pore-size syringe-driven filter. Close the flasks with autoclaved aluminum caps and store them at 4 °C. This solution can be used for at least 1 year if stored refrigerated. **CRITICAL** Work next to flame and under sterile conditions.

Sodium sulfide (Na_2S) solution (1 M) as medium reducing agent. To a small volumetric flask, add 150 ml of Milli-Q water and a magnetic stirring bar. While mixing on a magnetic stirrer, submerge a long needle (21-gauge × 4 3/4-inches) connected to N_2 gas and flush the Milli-Q water with N_2 gas (gentle gas stream). Using a plastic spatula, add 14 g of large sodium sulfide nonahydrate crystals to a tea strainer. Rinse the Na_2S crystals with a bit of Milli-Q water to remove the oxidized top layer. Cleaned Na_2S crystals should be clear. Dry the Na_2S crystals with paper tissue and add to the N_2-flushed Milli-Q water. Close the volumetric flask with a butyl rubber stopper, allowing the needle to stay submerged in the solution. Keep stirring and flushing the solution with N_2 gas until the Na_2S is dissolved. Flush an empty serum bottle with N_2 gas (~1 bar, 2 min) to remove oxygen and fill ~2/3 of

the serum bottle volume with Na_2S solution. Close the bottle with an autoclaved butyl rubber stopper and an aluminum crimp cap. Flush the headspace with N_2 gas (gentle gas stream) for 5 min and autoclave the serum bottle at 121 °C for 20 min. This Na_2S solution can be used for at least 1 year, if stored refrigerated. **! CAUTION** Na_2S solution is toxic and volatile; work in a fume hood. **CRITICAL** Make sure that 12 g of Na_2S crystals is left after the washing procedure.

Sulfide standards for calibration of photometer. Prepare sodium sulfide (N_2S) stock solution (1 M) as described above. The exact concentrations of sulfide should be determined iodometrically as described before[66–68]. Prepare anoxic Milli-Q water by adding 1 liter of Milli-Q water to a 1-liter Duran glass bottle with a side opening. After adding a magnetic stirring bar, close the top opening (GL 45 thread) with a butyl rubber stopper plus a screw cap and close the side opening loosely with a screw cap. Steam autoclave the bottle but do not close the steam outlet valve before the autoclave reaches 95 °C. After autoclaving, purge the bottle with N_2 gas as described for medium preparation (Box 2). Transfer sulfide stock solution, graduated cylinders, serum bottles, butyl rubber stoppers and anoxic water to an anoxic chamber. Prepare sulfide standards from mixtures of stock solution and anoxic water (i.e., 0–20 mM sulfide final conc.). Add standards to serum bottles and close with butyl rubber stoppers. Remove from anoxic chamber, close with aluminum crimps and add a small N_2 overpressure (50 kPa). These solutions can be used for calibration for at least 3 months if stored refrigerated (4 °C) in the dark.

Copper sulfate solution to measure sulfide concentrations. To prepare an acidified copper sulfate solution (5 mM) add 800 ml of Milli-Q water and a magnetic stirring bar to a 1-liter volumetric flask. While mixing on a magnetic stirrer, add 50 ml of 1 M HCl and 1.248 g of $CuSO_4 \cdot 5H_2O$. Fill up with Milli-Q water to 1,000 ml and stir until the crystals dissolve. Store the solution at room temperature; the solution can be used for at least 1 year.

DEPC water for RNA extraction. To a 1-liter volumetric flask, add 1 liter of Milli-Q water and a stirring bar. Add 1 ml of diethyl pyrocarbonate (DEPC) and mix thoroughly on a magnetic stirrer. Incubate this solution at 37 °C for at least 12 h. Autoclave the DEPC-treated water twice for 20 min at 121 °C to remove any residual DEPC. Store the solution at room temperature and use within 1 month. Alternatively, RNase-free water can be purchased (Sigma-Aldrich, cat. no. 9601).

Ammonium bicarbonate buffer solution (100 mM). To a volumetric flask, add 800 ml of Milli-Q water and a magnetic stirring bar. While mixing on a magnetic stirrer, add 7.91 g of ammonium bicarbonate and let the salt dissolve. Fill up with Milli-Q water to 1,000 ml. Transfer to a 1-liter Duran bottle and autoclave for 20 min at 121 °C. The solution can be stored at room temperature for at least 6 months.

Anoxic medium. Anoxic medium is prepared as described in Box 2.

Box 1: Photometer calibration for sulfide measurements TIMING 30-60 min

1. Pour 4 ml of copper sulfate solution into a test tube. Prepare as many test tubes as standards to be measured plus two test tubes for blank measurements.

2. Turn the photometer on and adjust the wavelength settings to 480 nm.

3. Make a blank measurement by filling a 2.5-ml cuvette with the copper sulfate reagent and placing it in the light beam of the photometer. Set as zero value.

4. With an N_2-flushed 1-ml syringe plus needle (26-gauge × 1-inch), sample ~0.3 ml of an anoxic sulfide standard and inject exactly 0.1 ml of the standard into the test tube filled with copper sulfate solution. A brown copper sulfide precipitate should form immediately. Quickly seal the test tube (e.g., with a piece of Parafilm), gently mix by inverting the tube two to three times and carefully pour the entire contents into a 2.5-ml cuvette, which holds up to 4 ml. Immediately measure the absorption by placing the cuvette in the light beam of the photometer.

5. Proceed with the next standard. Use a new syringe and needle for each standard.

6. Prepare a calibration curve (concentration versus measured absorption) and use it to determine the sulfide concentration.

Box 2: Preparation of anoxic medium TIMING 20 min

The preparation of anoxic medium requires a constant supply of an anoxic headspace, which is achieved by a continuous N_2 or N_2:CO_2 gas inflow. The setup to regulate this gas inflow differs between the Widdel flask and the Duran glass bottle with a sideward opening.

Medium preparation in a Widdel flask (Step 1A)

1. Place the autoclaved Widdel flask in a holder above a magnetic stirrer (**Fig. 1a**).

2. Attach a Luer one-way stopcock with an attached 0.2-µm-pore-size syringe filter to the inflow tube (gas inflow controller). **! CAUTION** Stopcock must be closed!

3. Remove the Hoffman clamp from the inflow tube.

4. During medium preparation, the Widdel flask's inflow and outflow are controlled as follows: to flush the headspace, the gas inflow controller is connected via the pressure regulator to a pressurized gas bottle (Step 1A(iv) and Step 1A(vi)) and then a side lid of the Widdel flask and the stopcock are opened.

5. To maintain a headspace on the Widdel flask (Step 1A(v)), the gas inflow controller is connected to the pressurized gas bottle through a pressure regulator (operated at 5 kPa), and then the side lid is closed and the stopcock is opened.

6. To distribute the medium into serum flasks (Step 1A(ix)), the gas inflow controller is set up as in step 5, the outflow tube is connected to the glass pipe of the bottle-filling system, the Hoffman clamp is removed, and the pinchcock clamp is used to control the medium outflow (i.e., releasing it allows medium outflow).

Medium preparation in a Duran glass bottle (Step 1B)

1. Place the autoclaved Duran flask on a magnetic stirrer (**Fig. 1b**).

2. Attach a Luer one-way stopcock with an attached 0.2-µm-pore-size syringe filter to a needle (20-gauge × 1 1/2-inch; gas inflow controller). **! CAUTION** Stopcock must be closed!

3. Introduce the needle attached to the inflow controller through the stopper of the Duran flask.
4. During medium preparation, the gas inflow to the Duran flask is controlled as follows: to flush the headspace, the gas inflow controller is connected via the pressure regulator to the pressurized gas bottle (Step 1B(iv) and Step 1B(vi)), and the side lid of the Duran flask and the stopcock are opened.
5. To maintain a headspace on the Duran flask (Step 1B(v)): the gas inflow controller is connected to the pressurized gas bottle through a pressure regulator (operated at 5 kPa), and the side lid is closed and the stopcock is opened.

EQUIPMENT SETUP

General advice for lab ware in contact with samples. All glass ware, stirring bars and metallic equipment should be machine-washed, rinsed with MilliQ water and sterilized at 160°C for 6 hours. New stoppers should be at least three times boiled in deionized water to remove excess of flexibilizers or other potential toxic compounds introduced during the production process. Plastic and rubber material is autoclaved at 121°C for 25 minutes.

Anoxic chamber. The anoxic chamber should be charged with an N_2:CO_2 gas mixture and, oxygen levels should be monitored. We operate our anoxic chamber with oxygen content below 0.3 p.p.m. To prevent the introduction of oxygen, all material (i.e. samples and equipment) is passed into the anoxic chamber through an airlock which is three times evacuated and flushed with anoxic gas (here N_2:CO_2). The headspace of bottles containing enrichment cultures or sediment samples is flushed with N_2:CO_2 gas prior to their transfer into the anoxic chamber. This reduces the introduction of hydrocarbon substrates into the anoxic chamber and thus decreases the risk of cross-contaminating enrichment cultures with different substrates. **CRITICAL** If the anaerobic chamber is operated with low amounts of hydrogen gas (i.e. 1 to 5 vol. %) as reductant, samples and enrichment cultures need to be purged for 2 minutes with N_2:CO_2 to remove hydrogen, which could act as alternative energy source .

PROCEDURE

Preparation of anoxic medium TIMING 4 h hands-on over 2 days

1 *Preparation of basal mineral medium:* To a measuring cylinder, add 900 ml of Milli-Q water and a magnetic stirring bar. While stirring, add 0.09 g of KBr, 0.6 g of KCl, 1.47 g of $CaCl_2 \cdot 2H_2O$, 5.67 g of $MgCl_2 \cdot 6H_2O$, 6.8 g of $MgSO_4 \cdot 7H_2O$ and 26.37 g of NaCl. When the salts have dissolved, fill up to 1,000 ml with Milli-Q water. The anoxic medium may be prepared in a Widdel flask (option A) or a Duran glass bottle with a GL 45 thread and an additional sideward opening (hereafter referred to as a Duran flask; option B). Prepare the medium in a Widdel flask (option A; see also **Supplementary Video 1** and **Fig. 1a**) and distribute it, using anaerobic working technique, into sterile serum bottles (e.g., for culture transfers outside an anoxic chamber; see Step 18B). If the medium is handled in an anoxic chamber (e.g., to set up, maintain or dilute culture; see Steps 2–5 and Step 17A), prepare the medium in a Duran flask (option B; see also **Fig. 1b** and **Supplementary Video 2**). We recommend preparation of medium in a Widdel flask

and performing the following transfers next to a flame when sterility is most important (i.e., isolation attempts). The preparation of medium in a Duran flask and culture transfers in the anoxic chamber are recommended for early enrichments with high sediment content and to guarantee strictly anoxic conditions even throughout the transfer.

A Preparation of anoxic medium in a Widdel flask

(i) *Setup of the Widdel flask for autoclaving.* Pour the basal mineral medium into the Widdel flask. Close the gas inflow tube with a Hoffman clamp and the outflow tube with a pinchcock clamp and a Hoffman clamp; cover tube openings with aluminum foil. Also cover the bottle-filling system with aluminum foil. Close the sideward openings with screw caps, but leave one of them loose.

(ii) Autoclave the Widdel flask and the bottle-filling system for 20 min at 121 °C. Autoclave serum bottles and butyl rubber stoppers as well. If possible, close the autoclave valve once the autoclave has been heated to ~95 °C; otherwise, increase flushing time with N_2 in Step 1A(iii).

(iii) *Setup of the Widdel flask for headspace exchange with N_2.* Remove the Widdel flask from the autoclave when the temperature is ~80 °C, close the side cap and place the flask in a holder above a magnetic stirrer (Widdel flask setup is also described in Box 2 and depicted in **Fig. 1a**).

(iv) Remove the aluminum foil from the end of the gas inflow tube and connect it to the N_2 gas source through a pressure regulator. Adjust the pressure to ~5 kPa and remove the Hoffman clamp from the gas inflow tube. **! CAUTION** After autoclaving, the tubing might stick together where the clamps were attached. Make sure that the tube is permeable where the clamp was attached. Loosen one side cap of the Widdel flask and open the stopcock of the gas inflow controller. Flush the Widdel flask headspace with N_2 gas (5 kPa) for 5 min while stirring.

(v) Close all lids and allow the solution to cool to room temperature while being stirred.

(vi) *Setup of Widdel flask for headspace exchange with N_2:CO_2.* Loosen one side lid of the Widdel flask. Exchange the gas inflow connection to N_2:CO_2 (90:10; ~5 kPa). Flush the Widdel flask for 5 min and then close the side lid.

(vii) Supplement the medium through a side opening of the Widdel flask. Take care to use sterile technique and work next to a flame when opening stock solutions and the side lid of the Widdel flask to supplement the medium. Open the sodium bicarbonate (1 M) and ammonium phosphate stock solutions using the decapping tongs and pour or pipette 30 ml of $NaHCO_3$ (30 mM final concentration) and 25 ml of ammonium phosphate stock solution (4.67 mM NH_4Cl and 1.47 mM KH_2PO_4 final concentration) through the side lid into the Widdel flask. With sterile glass pipettes and a pipette controller, add from stock solutions: 1 ml each of 7-vitamin mixture, riboflavin solution, thiamine solution, vitamin

B_{12} solution, selenite–tungstate solution, trace element solution and resazurin solution. Using a syringe and a short needle (23-gauge × 1 1/4-inch), add 0.5 ml of Na_2S solution. With a sterile spatula, add a small amount (~10 mg) of sodium dithionite.

(viii) Wait for the medium to change color from blue to brownish-clear. Check the pH by retrieving a 3-ml medium sample through the side opening using a sterile glass pipette and pipette controller. Transfer the aliquot to a test tube and immediately measure the pH with a pH electrode. The pH should be 7.1 ± 0.2. If necessary, adjust the pH with HCl (1 M) or Na_2CO_3 (1 M).

(ix) *Setup of Widdel flask for medium distribution.* Close all lids and keep stirring. Remove the Hoffman clamp from the outflow tube. **CRITICAL STEP** After autoclaving, the tubing might stick together. Make sure that the tube is permeable where the clamp was attached.

(x) Remove the aluminum foil cover from the bottle-filling system. Position the bottle-filling system with a clamp system in proximity to the outflow tube of the Widdel flask.

(xi) Remove the aluminum foil cover from the bottle-filling system and connect it to the outflow tube of the Widdel flask.

(xii) *Distribution of medium into serum bottles.* Work with sterile technique and next to a flame. Flush the serum bottle with N_2 gas (gentle gas stream, 2–3 min) using a cotton-filled glass syringe with a metal needle. **CRITICAL STEP** Flame the needle to sterilize it before inserting it into the bottle.

(xiii) Add medium from the Widdel flask to the sterile serum bottle by opening the pinchcock clamp of the outflow tube. When the desired volume is reached (e.g., at the marking on the serum vial), close the clamp and flush the serum bottle headspace with N_2:CO_2 gas (90/10; ~0.5 min, gentle gas stream) using the cotton-filled glass syringe with flame-sterilized metal needle.

(xiv) Close the serum bottle with a butyl rubber stopper and an aluminum crimp cap. Handle stoppers with flame-sterilized tweezers.

(xv) Flush for an additional 1–3 min with N_2:CO_2 (90:10; 100 kPa) gas by introducing short needles (26-gauge × 1-inch) for gas inflow and outflow through the stopper.

(xvi) Set an N_2:CO_2 (90:10) headspace pressure (100 kPa) by removing the outflow needle and allowing the pressure to build up before removing the inflow needle. Store the medium-filled serum bottle refrigerated (4 °C) in the dark. Medium can be used for at least 3 months.

? TROUBLESHOOTING

B Preparation of anoxic medium in a Duran flask

(i) Transfer basal mineral medium to a Duran flask with a side opening.

(ii) Close top opening of the Duran flask with a butyl rubber stopper and GL 45 open screw cap. Close the sideward opening with a screw cap, but leave the cap loose.

(iii) Autoclave the Duran flask for 20 min at 121 °C. To deplete the oxygen in the autoclave, close the autoclave valve once it has been heated to ~95 °C; otherwise, increase flushing time with N_2 to 15 min in Step 1B(iv).

(iv) Remove the Duran flask from the autoclave when the temperature is ~80 °C, close the side cap and place the flask on a magnetic stirrer. Inject the needle of the tubing coming from the gas inflow controller (as described in Box 2, "Medium preparation in a Duran glass bottle" and depicted in **Fig. 1b**) through the stopper and connect to the N_2 gas source. Adjust the pressure regulator to ~5 kPa and flush the Duran flask for 5 min while stirring.

(v) Close the side lid tightly and allow the solution to cool to room temperature while being stirred.

(vi) Loosen the side lid of the Duran flask. Switch the gas inflow connection to the N_2:CO_2 (90:10; 5 kPa) gas source via a pressure regulator. Flush the Duran flask for 5 min and then close the lid.

(vii) Supplement the medium through the side opening of the Duran flask. Work with sterile technique and next to a flame. Add 30 ml of $NaHCO_3$ (30 mM final concentration) and 25 ml of ammonium phosphate stock solution (4.67 mM NH_4Cl and 1.47 mM KH_2PO_4 final concentrations) after opening the stock bottles and pouring the contents into the Duran flask.

(viii) With sterile glass pipettes and a pipette controller, add from stock solutions through the side opening: 1 ml each of 7-vitamin mixture, riboflavin solution, thiamine solution, vitamin B_{12} solution, selenite–tungstate solution and trace element mixture, as well as 0.5 ml of resazurin solution.

(ix) With a disposable syringe and a short needle (23-gauge × 1 1/4-inch), add 0.5 ml of Na_2S solution.

(x) With a sterile spatula, add a small amount (~10 mg) of sodium dithionite.

(xi) Allow the color of the medium to change from blue/pink to brownish-clear. Check the pH by retrieving a 3-ml sample of medium through the side opening using a sterile pipette. Transfer the aliquot to a test tube and immediately measure the pH with a pH electrode. The pH should be 7.1 ± 0.2. If necessary, adjust the pH with HCl (1 M) or Na_2CO_3 (1 M).

(xii) Continue working in the anoxic chamber for the following steps. Refer to Step 1B(xiii–xvi) for the medium transfer into serum bottles, Steps 2–7 for preparation of replicate inoculates from an environmental sample, and Step 17A for medium exchange or dilution inside an anoxic chamber.

(xiii) Transfer the following material to the anoxic chamber: the anoxic medium in a Duran flask, sterile serum bottles (e.g., 156 ml), sterile butyl rubber stoppers, pipette controller and sterile plastic pipettes, sterile tweezers and some paper towels. **CRITICAL STEP** When transferring Duran flasks to the anoxic chamber, always ensure that the side cap is

loose; if the cap is tight, it is possible that the flask will break during evacuation of the airlock.

(xiv) Transfer the desired volume from the Duran flask to sterile serum bottles using a plastic pipette and a pipette controller. Close the bottles with sterile butyl rubber stoppers. Handle the stoppers with sterile tweezers.

(xv) Once the medium is distributed, remove all the material from the anoxic chamber and seal the serum bottles with aluminum crimp caps, using a capping tool.

(xvi) Set an N_2:CO_2 (90:10) headspace pressure (100 kPa) in the serum bottles by piercing the septum with a short needle (26-gauge × 1-inch) connected to the gas source, allowing pressure to build up. If medium was prepared and/or distributed under partial hydrogen atmosphere, the vials must be purged with N_2:CO_2 for several minutes (see above). Store the medium-filled serum bottles refrigerated (4 °C) in the dark. Medium can be used for at least 3 months.

? TROUBLESHOOTING

Preparation of replicate inoculates from an environmental sediment sample TIMING 5 hours for ten bottles

2 Transfer the following material to an anoxic chamber: the anoxic medium in a Duran flask, an environmental sediment sample stored in a gas-tight bottle (e.g., 1,000-ml Duran bottle), pre-weighted centrifuge tubes to collect subsamples for dry weight determination, centrifuge tubes (of 15- and 50-ml volume) to collect subsamples for molecular analysis, a lab spoon, a sterile H-shaped magnetic stirring bar, a sterile empty 1,000-ml Duran bottle, sterile serum bottles (e.g., 156 ml), sterile butyl stoppers, pipette controller and sterile plastic pipettes, sterile tweezers and some paper towels. **CRITICAL STEP** When transferring Duran flasks to the anoxic chamber, always ensure that the side cap is loose; if the cap is tight, it is possible that the flask will break during evacuation of the airlock.

3 Transfer the sediment sample (~100 ml) into the empty Duran bottle and prepare a slurry by adding ~600 ml of anoxic medium.

4 Add the magnetic stir bar and homogenize the slurry by constant stirring (~500 r.p.m.). Distribute the homogeneous slurry stepwise (i.e., 4 × 25 ml) into the serum bottles. For that, use a disposable plastic pipette and pipette controller until the desired volume is reached (i.e., 100 ml). During this procedure, take subsamples for molecular analysis (i.e., DNA extraction, FISH analysis) and dry weight determination of the produced sediment slurry (T_0 sampling). Using a disposable plastic pipette and pipette controller, transfer 25–50 ml of sediment slurry for DNA analysis to a centrifuge tube and 5–10 ml of sediment slurry for FISH analysis. For dry weight determination, see Steps 18 and 19. Close the serum bottle tightly with a butyl rubber stopper. Remove culture bottles, subsamples and all equipment from the anoxic chamber.

5 Remove culture bottles, subsamples and all equipment from the anoxic chamber.

6 Preserve samples for molecular analysis according to Step 23A(ii) for DNA samples and Step 23B(ii) for FISH analysis. These samples are required to determine the original microbial community composition of the sample. To determine the dry weight of subsamples, continue with Steps 20 and 21.

7 Seal the culture bottles with aluminium crimp caps using the capping tongs.

? TROUBLESHOOTING

Addition of hydrocarbon substrates to culture bottles TIMING 1 hour for ten bottles

! CAUTION Work with highly flammable, explosive gases is performed in the following steps. Follow safety instructions given above (see MATERIALS section) and do not work with open flames when working hydrocarbon gases

8 Set up the gas bottle with pressure regulator and tubing, and connect to a Luer-one-way stopcock and a sterile 0.2-µm-pore-size syringe filter. CH_4:CO_2 gas mixtures can be applied in flow-through (option A). Pure hydrocarbon gases such as butane should be added on top of the N_2:CO_2 headspace (option B) to avoid pH change by CO_2 loss. See **Supplementary Video 3**.

A. Flow-through method

(i) Attach a 26-gauge× 1-inch needle to the syringe filter of the gas source.

(ii) Adjust pressure regulator to 150 kPa, open main gas flow (CH_4:CO_2) to purge the system.

(iii) Inject the needle through the sterilised stopper of the culture bottle and open the stopcock to allow gas inflow.

(iv) To flush the headspace, inject a second needle (26-gauge × 1-inch) for gas outflow.

(v) Flush the headspace for 1-3 min, remove outflow needle and allow pressure to build up before closing the stopcock and removing the inflow needle.

B. Head space filling

(i) Attach a Luer-three-way-stopcock to the syringe filter of the gas source

(ii) Attach a 60-ml disposable syringe to the second port of the three-way stopcock

(iii) Attach a needle (26-gauge × 1-inch) to the third (male) port of the stopcock.

(iv) Adjust the gas flow to ~0.2 bar and flush the syringe with the hydrocarbon gases at least three times by filling the complete volume of the syringe and discarding the gas through the attached needle. Therefore, fill the syringe with gas by adjusting the stopcock to allow the gas flow from the gas source into the syringe. Discard the gas volume by adjusting the stopcock to allow gas to move out of the syringe via the needle and press the syringe plunger.

(v) Sterilize the stopper of the culture bottle

(vi) Then fill the syringe with the defined gas volume (i.e., 56 ml for 100-kPa gas pressure in a 156-ml bottles filled with 100 ml of liquid phase and a 56-ml headspace) and adjust the valve of the three-way stopcock to allow gas flow between the syringe and the needle. Now inject the needle through the stopper and press the gas into the culture bottle.

CRITICAL STEP Before addition of hydrocarbon gas, we recommended releasing overpressure from the bottles by introducing a short needle (20-gauge × 1 1/2-inch or 23-gauge × 1 1/4-inch) through the stopper to make this step easier

Incubation of culture bottles

9 Transfer the culture bottles to an incubator. Shake the bottles by hand for 5-10 seconds once a week by hand to avoid compaction of slurry and to equilibrate the medium and the headspace. **CRITICAL STEP** If possible set a shutdown-temperature 5°C above the incubation temperature at the incubator to avoid loss of enrichment cultures in case of a thermostat malfunction.

Tracking metabolic activity in the enrichment cultures TIMING 1 hour for 10 samples

CRITICAL STEP Sulfide concentrations (Steps 10-16) should be determined at the start of the incubation, and at intervals of 2–4 weeks, depending on the initial sulfide production and its development over time. Shake all culture bottles gently 6–15 h before measurement and keep culture bottles in the incubator until measurements are performed. The settling time can be reduced after cultures no longer contain large amounts of sediment particles.

10 Transfer 4 ml of copper sulfate solution into a test tube. Prepare as many test tubes as samples to be measured, plus one for a blank measurement.

11 Turn on the photometer that has been calibrated with sulfide standards; make sure to set it to 480 nm and perform a zero-point calibration with 4 ml copper sulfate solution in a 2.5-ml cuvette (it holds all 4 ml).

12 Remove the culture bottles from the incubator, avoid shaking (in particular when they still contain sediment particles) and place them next to the photometer. Sterilize the stopper surface by igniting a drop of ethanol (96% (vol/vol)) on it. **! CAUTION** When working with flammable elements, use protective googles and avoid wearing gloves.

13 Inject a short needle (26-gauge × 1-inch) attached to a 1-ml syringe through one side of the stopper. Tilt the culture bottle to quickly withdraw ~300 µl of medium and pull out the syringe containing the sample.

14 Quickly remove any bubbles and inject exactly 100 µl sample into the test tube.

15 Quickly seal the test tube (e.g. with a piece of Parafilm), mix by inverting the tube once and decant the content into a 2.5 ml cuvette (it holds all 4 ml). Immediately measure the sample in the photometer. Discard the sample (i.e. pour it into a bottle for dissolved metal waste).

? TROUBLESHOOTING

16 To proceed with the next culture bottle repeat steps 14 to 16 using a new syringe, needle and test tube.

Maintenance and dilution of enrichment cultures (when sulfide concentrations are exceeding maximum value)

17 The procedure for maintenance and continuation of enrichment cultures should be carried out when sulfide concentrations exceed 15 mM or sulfide production rates start to decline because of product inhibition. This is done by exchanging the enrichment medium and optionally diluting the enrichment material (i.e., biomass and/or sediment particles) within an anoxic chamber (option A) or by transferring a portion of the enrichment material to serum bottles with fresh anoxic medium (option B; see also **Supplementary Video 4**). Option A is preferable when the culture bottles still contain substantial amounts of sediment or when large consortia are formed, because then the sample cannot be evenly distributed using option B. Option B does not require the use of an anoxic chamber and should be chosen when there is little sediment remaining in the culture. Moreover, option B reduces the risk of cross-contamination. The amount of transferred enrichment material depends on the growth rates/doubling times of the culture (i.e., very slow-growing methanotrophic cultures should be diluted by a factor of 2–4). **CRITICAL** To reduce the risk of losing a complete sample set, always work with a subset of your samples and store remaining samples from earlier dilutions in bottles under anoxic conditions at room temperature. Enrichments can be restarted from these samples after months.

A. Enrichment medium exchange and dilution within an anoxic chamber. TIMING 3 hours for ten samples

CRITICAL Step 17A(i–v) is only required if medium is exchanged while keeping the complete biomass in the bottle. The sulfidic medium can be removed in the chamber, but by removing the supernatant outside of the chamber, the amount of sulfide transferred to the chamber is reduced. Prepare anoxic medium in Duran flasks with side opening (Step 1B).

(i) Let the enrichment material settle for ~12 h before starting the procedure (i.e., do not shake the culture bottles during this time). Connect a long needle (21-gauge × 4 3/4-inches) to a Luer one-way stopcock with attached tube. Use forceps to inject the needle through the stopper of the culture bottle. Submerge the needle until it is slightly above the surface of the enrichment material (i.e., sediment particles, biomass, inorganic precipitates).

(ii) Open the stopcock and collect the outflowing medium in a dedicated waste beaker. While the culture bottle is under pressure, the medium will flow out.

(iii) Once no overpressure is left, inject a short needle (20-gauge × 1 1/2-inch) connected via a stopcock plus tubing to a N_2:CO_2 gas source. Set the pressure regulator to 100 kPa and open the stopcock to allow gas inflow into the culture bottle. Do not use pressures higher than 200 kPa in order to reduce the risk of breaking the glass bottles. **! CAUTION** The removed medium is strongly sulfidic and therefore toxic when inhaled. Work under a fume hood.

(iv) When the desired medium volume is removed, purge the headspace for additional 2 min to remove hydrocarbon gases and excess sulfide to avoid their accumulation in the anoxic chamber.

(v) Keep the medium waste under a fume hood until the contained sulfide is oxidized. To rapidly oxidize sulfide, add hydrogen peroxide (30%, 10 ml per liter medium). Once oxidized (i.e., the color has changed to yellow or pinkish), dispose of the medium waste in the sink.

(vi) Transfer the following material to an anoxic chamber: anoxic medium in a Duran flask, culture bottles, autoclaved butyl rubber stoppers, disposable plastic pipettes and pipette controller, decapping tongs, sterile serum bottles (if dilution of the enrichment culture is to be performed) and disposable scrapers. **! CAUTION** Always loosen the side cap of the Duran flask for the transfer to the anoxic chamber.

(vii) Use the decapping tongs to open the culture bottles. (Optional) If the enrichment material (i.e., the biomass) attaches to the glass of the culture bottle, use a sterile disposable scraper to detach it.

(viii) If the enrichment material needs to be diluted, transfer equal volumes to fresh bottles (e.g., for a 1:1 dilution, split into two bottles) using a sterile pipette plus a pipette controller and fill up with medium to the desired volume (e.g., 100 ml). If no dilution is required, fill up the culture bottle with fresh medium to the desired volume.

(ix) Close the culture bottles with sterile butyl rubber stoppers. Handle the stoppers with sterile tweezers.

(x) Remove the culture bottles and all equipment from the anoxic chamber. Cap the culture bottles with aluminum crimp caps using capping tongs. Add substrate to the culture bottles according to Step 8 and continue with incubation (Step 9).

? TROUBLESHOOTING

B. Enrichment culture transfer without anoxic chamber. TIMING 4 hours for ten samples

(i) Prepare serum bottles prefilled with medium (Step 1A(i–xvi) or Step 1B(i–xvi)). Release overpressure from these bottles by introducing a short needle (20-gauge × 1 1/2-inchor 23-gauge × 1 1/4-inch) through the stopper.

(ii) (Optional) Often the cells in enrichment cultures attach to the bottle walls and need to be detached before the transfer of the enrichment material. To detach the cells, remove overpressure from the culture bottle by piercing the stopper with a short needle, opening the bottle using the decapping tool under sterile conditions (e.g., next to the flame) and immediately introducing a needle (20-gauge × 1 1/2-inch) connected via stopcock plus tubing to an anoxic gas (N_2:CO_2) source. Open stopcock for gas inflow to prevent oxygen influx during the handling of the open culture bottle. **! CAUTION** Work under a fume hood while handling strongly sulfidic liquids.

(iii) (Optional) Detach the biomass from the bottom and the walls of the culture bottle using a sterile disposable scraper. Seal the culture bottle with a sterile butyl rubber stopper and an aluminum crimp cap. Connect a needle (20-gauge × 1 1/2-inch) via stopcock plus tubing to an anoxic gas (N_2:CO_2) source with 150-kPa gas pressure. Inject the needle into the bottle to create overpressure. **! CAUTION** Do not exceed a gas pressure of 200 kPa in order to avoid breaking the glass bottles. This overpressure allows easier sampling in the next step and avoids oxygen penetration.

(iv) Mix the culture bottle well and sterilize the stopper surface before retrieving a subsample. Using a plastic syringe with a Luer-Lock tip plus a thick needle (20-gauge × 1 1/2-inch or 23-gauge × 1 1/3-inch), withdraw the desired enrichment volume (e.g., 20 ml) and transfer it to a serum bottle filled with fresh anoxic medium (e.g., 80 ml).

(v) Add substrates to the culture bottles (Step 8) and continue incubation (Step 9).

Dry weight determination of initial slurry TIMING 2 hours over 2 days

18 Weigh three appropriate centrifuge tubes (50 ml).

19 Transfer the same amount of the initial slurry (Step 4) to each of pre-weighed tubes. **! CAUTION** the volume of the subsample must be defined exactly (i.e. 25 ml).

20 Centrifuge the subsample (i.e., 2,000*g*, 10 min, room temperature), decant the supernatant and dry the pellet in an oven (60 °C) until the weight remains constant (e.g., for ~3 d).

21 Weigh the tube with the pellet and determine the dry weight of the pellet. The determined dry weight can be used to normalize all measurements and compare metabolic activity of early enrichment cultures (i.e. sulfate reduction per g_{dry_weight} sediment)

Calculation of activity doubling from sulfide production rates TIMING 1 hours

22 Use a spreadsheet program such as Excel to plot in a semi-logarithmic manner the sulfide concentrations [HS^-] from at least six time points measured in the culture (ln[HS^-] versus sampling time). Use the statistical tools of the program to calculate the exponential function of their relation representing the function $[HS^-]_{(t)} = [HS^-]_{(0)} \times e^{K \times t}$, where K is the slope of the logarithmic relationship and represents the change of sulfide concentration over time. From this slope, the time of activity doubling (T_d) can be inferred based on the function $T_d = \ln(2)/K$. The time of activity doubling meets the doubling times of the hydrocarbon-oxidizing community members

Collection and preservation of enrichment material for subsequent analysis

23 The procedure for collecting material from the enrichment culture and its preservation depends on the desired downstream analysis. Proceed as follows to collect and preserve samples for DNA extraction (option A), FISH (option B), RNA extraction (option C) or metabolomics analysis

(option D). The required volume of material depends on the activity, expected biomass and stage of the enrichment (e.g., sediment-containing or sediment-free), as well as on the approach desired for analysis. As a general recommendation, if possible, material should be sampled from well-growing, active enrichment cultures. We recommend comparing the microbial compositions of the initial slurry (T_0, see Step 4) with those of the well-established cultures (minimum three successful transfers). However, intermediate analysis can be performed in order to monitor and study the development of the culture.

RNA extraction (option C; **Supplementary Video 5**) should be done on active enrichment cultures during the exponential growth phase (enrichment cultures should show a sulfide production ≥0.1 mmol per liter per day, and sulfide concentrations should be <12 mM, to ensure sampling during the exponential growth phase). For RNA extraction, autoclave all material with direct sample contact (i.e., filtration system, glass Petri dishes, pipette tips and metallic tweezers) at 121 °C for 40 min. Clean lab space and instruments with RNaseZAP.

A Collection and preservation of material for DNA extraction TIMING **1 hour for four samples**

(i) Mix the culture bottle well and sterilize the stopper surface before retrieving a subsample. Using a plastic syringe with Luer-Lock tip plus a thick needle (20-gauge × 1 1/2-inch or 23-gauge × 1 1/4-inch), withdraw the desired enrichment volume (e.g., 50 ml) and transfer it to a sterile tube (e.g., a 50-ml Falcon tube).

(ii) Close tube and centrifuge the subsample down (i.e., 5,000*g*, 4 °C, 10 min).

(iii) Discard supernatant and remove the residual liquid with a pipette.

(iv) Store the pellet at −20 °C. Frozen material for DNA extraction can be stored for years.

B Collection and preservation of material for FISH TIMING **2-3 hours**

(i) Mix the culture bottle well and sterilize the stopper surface before retrieving a subsample. Using a plastic syringe with a Luer-Lock tip plus a thick needle (20-gauge × 1 1/2-inch or 23-gauge × 1 1/4-inch), withdraw the desired enrichment volume (e.g., 2 ml) and transfer it to a sterile tube (e.g., 2-ml Eppendorf tube).

(ii) Add 37% formaldehyde solution to achieve a final formaldehyde concentration of 2% (e.g. to a 2 ml subsample add 108 µl of 37% formaldehyde solution).

(iii) Mix well and incubate for 1 h at room temperature or overnight (12 h) at 4°C. **CRITICAL STEP** Prolonged incubation will lead to an over fixation and thus reduced accessibility of cells for oligonucleotide probes.

(iv) Centrifuge the subsample (e.g., 8,000*g*, 4 °C, 5 min), decant the supernatant, add 1× PBS (e.g., 2 ml of 1× PBS to a pellet from a 2-ml subsample) and resuspend the pellet. Repeat this washing procedure twice.

(v) Centrifuge the subsample (e.g., 8,000*g*, 4 °C, 5 min), decant the supernatant, add a 1:1 mixture of 1× PBS:99% (vol/vol) ethanol (e.g., 2 ml of 1× PBS:EtOH to a pellet from a 2-

ml subsample) to achieve a final concentration of 50% (vol/vol) ethanol in 1× PBS, and resuspend the pellet.

(vi) Store the subsample in PBS:EtOH solution at −20 °C. Samples can be stored for years.

? TROUBLESHOOTING

C Collection and preservation of material for RNA extraction using RNAlater TIMING 2-3 hours

(i) Fill a sterile 50 ml syringe with 50 ml RNAlater and heat it to the enrichment's incubation temperature (e.g. by placing it in an incubation oven).

(ii) Fill a water bath and heat the water to the temperature used for incubation of the enrichment culture. **! CAUTION** Cultures contain large amounts of toxic sulfide. Work under a fume hood when performing Step 23C(iii–x).

(iii) Place the culture bottle in the water bath (**Fig. 3**). Make sure that ~2/3 of the bottle is submerged but do not submerge the bottle completely. Sterilize the stopper surface. Let the biomass and any inorganic precipitates or sediment particles settle. **CRITICAL STEP** Move the bottle as little as possible during the rest of the procedure to avoid resuspension of the settled material.

(iv) Connect a Luer one-way stopcock plus a needle (20-gauge × 1 1/2-inch) to a CO_2:N_2 (90:10) gas source adjusted to 100 kPa. Connect the culture bottle to the gas source by injecting the needle through the stopper and then open the stopcock for gas inflow. Attach a long needle (21-gauge × 4 3/4-inches) to a Luer one-way stopcock connected to sterile PVC male Luer-Lock tubing. Ensure the stopcock is closed and use sterile forceps to inject the long needle through the stopper of the culture bottle. Keep the needle tip close to the surface of the medium.

(v) Open the stopcock in front of the long needle to withdraw the medium using the overpressure created by the gas inflow. Collect the outflowing medium in a beaker. While the medium flows out, make sure to continuously move the long needle down to keep it submerged but close to the medium surface in order to limit disturbance of the settled material. Remove ~90–95% of the medium volume, but avoid removal of the cell material. **! CAUTION** The supernatant has high sulfide concentrations. Collect and treat supernatant as described above (Step 17A(v)).

(vi) Move the long needle to a position above the remaining medium and immediately inject the pre-warmed RNAlater with a short, thick needle (20-gauge × 1 1/2-inch). Remove the long needle and allow the pressure to build up before closing the inflow stopcock and removing the short needle.

(vii) Incubate the bottles in the water bath for 30 min. **PAUSE POINT** Samples can be stored at −20 °C for months if necessary.

(viii) *Setup of filtration system*. Place the vacuum filtration device on a Duran bottle. Moisten both sides of a support filter (47-mm diameter, 0.45-µm pore size) by submerging it in a Petri dish filled with DEPC water. Place the moistened filter on the vacuum filtration device. Using sterile tweezers, place a polycarbonate filter (47-mm diameter, 0.2-µm pore size) on top of the support filter. Avoid wrinkling of the filters. Connect the filtration device to a vacuum system and screw in the funnel of the filter device.

(ix) Release overpressure from the bottle using a short needle (20-gauge × 1 1/2-inch or 23-gauge × 1 1/4-inch) and open the bottle using decapping tongs. Resuspend the material in the culture bottle by mixing or by using a sterile cell scraper.

(x) Turn on the vacuum system. Pour the bottle contents slowly onto the filter so the material is deposited on it. Once the liquid is completely removed, transfer the polycarbonate filter to a sterile Petri dish using sterile tweezers. Cut the filter into four pieces using a sterile disposable scalpel. Collect and treat the filtered medium as described above (Step 17A(v)).

(xi) Use sterile tweezers to combine all filter pieces in a Lysis Matrix E tube pre-filled with 600 µl of RNA lysis buffer from the Quick-RNA Miniprep Kit. Keep the sample tube on ice.

(xii) Lyse the sample in a bead-beating machine, applying two cycles of 6 m/s for 20 s. **! CAUTION** To ensure safe use of the bead-beating machine, follow the manufacturer's instructions; i.e., to avoid overheating, the described instrument needs to cool for at least 5 min between the two cycles.

(xiii) For RNA extraction, we recommend continuing extraction as detailed in the Quick-RNA MiniPrep Kit instructions.

? TROUBLESHOOTING

D Collection and lysis of cells for metabolome analysis TIMING 2-3 hours

CRITICAL Samples for metabolome analysis should be taken from a dense enrichment culture during the exponential growth phase; sulfide concentration should not be higher than 12–15 mM. The enrichment culture should be kept at the incubation temperature during the sampling procedure. All steps should be performed rapidly. Avoid breaks.

(i) Mix the culture bottle well and sterilize the stopper surface before retrieving a subsample. Using a plastic syringe with a Luer-Lock tip plus a thick needle (20-gauge × 1 1/2-inch), withdraw the desired enrichment volume (minimum = 20 ml) and transfer it to a sterile 50-ml centrifuge tube. **! CAUTION** Sulfide will flush out; work under a fume hood. Alternatively, release the overpressure in the culture bottle by inserting a needle through the stopper. Remove the rubber stopper of the culture bottle, and, under a gentle stream of N_2:CO_2 (90:10) or in an anoxic chamber, collect a 20-ml culture volume using a 10-ml pipette with a wide tip (i.e., cut the tip of a normal pipette tip).

(ii) Centrifuge for 10 min at 16,000*g* and 4°C

(iii) Remove supernatant with a pipette plus pipette controller. **! CAUTION** Supernatant has high sulfide concentrations. Work in a fume hood. Collect and treat supernatant as described above (Step 17A(v)).

(iv) Wash the cells with 1 ml of 100 mM ammonium bicarbonate buffer and gently resuspend the cells in the buffer by slow up-and-down pipetting. **CRITICAL STEP** It is essential that the integrity of the cells is maintained until planned lysis in the solvent mix; otherwise metabolites will be released and discarded in the following steps.

(v) Transfer in 2-ml centrifuge tubes. Verify the cells for signs of lysis under a light microscope. If needed, adjust the concentration of the buffer, or test other buffers recommended for electrospray ionization (e.g., ammonium acetate).

(vi) Centrifuge for 10 min at 16,000*g* and 4 °C. Discard the buffer and repeat the washing twice.

(vii) Add 1 ml of solvent mix (acetonitrile:methanol:water 40:40:20 (vol/vol/vol)). Here the cell lysis starts. Vortex briefly to resuspend the cells. Add 0.3–0.5 g of glass beads per tube.

(viii) Lyse the cells in a bench-top bead-based homogenizer using five cycles of 2,000 r.p.m. for 50 seconds, with a 15-s pause between cycles.

(ix) Remove the tubes from the homogenizer and allow the beads to settle. Collect the liquid in a clean tube.

(x) To remove cell debris and residual glass beads, centrifuge for 10 min at 16,000*g* at 4 °C. Collect the clear supernatant in 2-ml Zinsser NA glass vials and close with Teflon-lined screw caps. Place the samples at −20 °C until analysis. At this temperature, samples can be stored indefinitely.

? TROUBLESHOOTING

? TROUBLESHOOTING

Troubleshooting advice can be found in **Table 1** (see **Fig. 4**).

TIMING

Reagent setup for medium preparation: 2 d

Step 1, medium preparation: 1 d

Steps 2–9, setup of initial incubations and substrate addition: 1 d for ten enrichment cultures

Steps 10–16, measurement of sulfide concentrations: 1 h for ten samples

Step 17, transfer/dilution of enrichment cultures: 3–4 h for ten samples

Steps 18–21, dry weight determination and doubling time calculation: 2 h hands-on over 2 d

Step 22, calculation of activity doubling from sulfide production rates: 1 h

Step 23A, collection and sample preservation for DNA extraction: 1 h for four samples

Step 23B, collection and sample preservation for FISH: 2–3 h

Step 23C, collection and sample preservation for RNA extraction: 2–3 h per sample

Step 23D, collection and lysis of cells for metabolome analysis: 2–3 h per sample

Box 1, photometer calibration for sulfide measurements: 30–60 min

Box 2, preparation of anoxic medium: 20 min

ANTICIPATED RESULTS

This protocol enables the enrichment of anaerobic hydrocarbon-degrading microorganisms from hydrocarbon-rich sulfidic sediments in a cost-efficient and low-maintenance batch-cultivation approach. Using a suitable inoculum activity, doubling times below those obtainable using flow-through reactors can be achieved (**Table 2**). This protocol describes the procedure to enrich microorganisms responsible for the anaerobic oxidation of specific gaseous hydrocarbons. The successful establishment of such enrichment cultures depends on (i) the selection of suitable sediment material (i.e., sediments harboring a microbial community with metabolic potential to degrade hydrocarbons) and (ii) the selection of enrichment conditions (i.e., hydrocarbon substrate and incubation temperature selected according to *in situ* data from the sampling site). Using hydrothermally heated sediments from the Guaymas Basin, we established sediment-free enrichment cultures within 1 year (**Fig. 5**). The provided hydrocarbon (i.e., methane or butane) and the incubation temperature (i.e., 37–60 °C) determined which organisms were predominantly enriched. Enrichment cultures supplied with methane are dominated by consortia of ANME-1/*Ca*. Desulfofervidus auxilii at 60 °C or ANME-1/Seep-SRB2 at 37 °C, and enrichment cultures provided with butane at 50 °C are dominated by consortia of *Ca*. Syntrophoarchaeum/*Ca*. Desulfofervidus auxilii. The high relative abundance of syntrophic hydrocarbon-degrading consortia in these enrichment cultures facilitated their extensive molecular and physiological characterization using culture-dependent and culture-independent approaches. For RNA sampling, the optimized anoxic fixation procedure at cultivation temperatures yielded much higher amounts and quality of RNA than in previously described standard procedures.

ACKNOWLEDGMENTS We thank F. Widdel for his advice and guidance in regard to cultivation and the development of this protocol. We are indebted to R. Appel, S. Menger and T. Holler for their contributions to the maintenance of the enrichment cultures and their suggestions for further improvement of our protocol. This protocol was tested with samples collected during Guaymas expedition AT15/45 in December 2016, Chief Scientist A. Teske, NSF grant BIO-OCE 1357238. This work was supported by the DFG Excellence Cluster MARUM and a Leibniz Grant to A. Boetius.

AUTHOR CONTRIBUTIONS R.L.-P., V.K., F.M. and G.W. contributed equally to the design, validation and optimization of this protocol. R.L.-P., V.K. and G.W. prepared the figures; R.L.-P. and G.W. prepared the supplementary videos. R.L.-P., V.K., F.M. and G.W. cooperatively wrote and edited the manuscript.

COMPETING FINANCIAL INTERESTS The authors declare no competing financial interests.

REFERENCES

1. Handelsman, J. Metagenomics: application of genomics to uncultured microorganisms. *Microbiol. Mol. Biol. Rev.* **68**, 669–685 (2004).
2. Edwards, T. & McBride, B. New method for the isolation and identification of methanogenic bacteria. *Appl. Microbiol.* **29**, 540–545 (1975).
3. Gieg, L.M., Davidova, I.A., Duncan, K.E. & Suflita, J.M. Methanogenesis, sulfate reduction and crude oil biodegradation in hot Alaskan oilfields. *Environ. Microbiol.* **12**, 3074–3086 (2010).
4. Strous, M., Heijnen, J., Kuenen, J.G. & Jetten, M. The sequencing batch reactor as a powerful tool for the study of slowly growing anaerobic ammonium-oxidizing microorganisms. *Appl. Microbiol. Biotechnol.* **50**, 589–596 (1998).
5. Wegener, G., Krukenberg, V., Riedel, D., Tegetmeyer, H.E. & Boetius, A. Intercellular wiring enables electron transfer between methanotrophic archaea and bacteria. *Nature* **526**, 587–590 (2015).
6. Winogradsky, S. Sur les organismes de la nitrification. *Comptes Rendus Acad. Sci.* **110**, 1013–1016 (1890).
7. Beijerinck, M.W. Anhaufungsversuche mit Ureumbakterien. *Centralblatt f. Bakteriologie II* **7**, 33–61 (1901).
8. Harder, W., Kuenen, J. & Matin, A. Microbial selection in continuous culture. *J. Appl. Micobiol.* **43**, 1–24 (1977).
9. Johnsen, A.R., Wick, L.Y. & Harms, H. Principles of microbial PAH-degradation in soil. *Environ. Pollut.* **133**, 71–84 (2005).
10. Wittebolle, L., Vervaeren, H., Verstraete, W. & Boon, N. Quantifying community dynamics of nitrifiers in functionally stable reactors. *Appl. Environ. Microbiol.* **74**, 286–293 (2008).
11. Whittenbury, R., Phillips, K. & Wilkinson, J. Enrichment, isolation and some properties of methane-utilizing bacteria. *Microbiology* **61**, 205–218 (1970).
12. Whiticar, M.J. Carbon and hydrogen isotope systematics of bacterial formation and oxidation of methane. *Chem. Geol.* **161**, 291–314 (1999).
13. Reeburgh, W.S. & Heggie, D.T. Microbial methane consumption reactions and their effect on methane distributions in freshwater and marine environments. *Limnol. Oceanogr.* **22**, 1–9 (1977).
14. Welhan, J.A. & Lupton, J.E. Light hydrocarbon gases in Guaymas Basin hydrothermal fluids: thermogenic versus abiogenic origin. *AAPG Bull.* **71**, 215–223 (1987).
15. Proskurowski, G. *et al.* Abiogenic hydrocarbon production at lost city hydrothermal field. *Science* **319**, 604–607 (2008).
16. Boetius, A. & Wenzhofer, F. Seafloor oxygen consumption fuelled by methane from cold seeps. *Nat. Geosci.* **6**, 725–734 (2013).
17. Rueter, P. *et al.* Anaerobic oxidation of hydrocarbons in crude oil by new types of sulphate-reducing bacteria. *Nature* **372**, 455–458 (1994).

18. Boetius, A. *et al.* A marine microbial consortium apparently mediating anaerobic oxidation of methane. *Nature* **407**, 623–626 (2000).

19. Laso-Pérez, R. *et al.* Thermophilic archaea activate butane via alkyl-coenzyme M formation. *Nature* **539**, 396–401 (2016).

20. Rabus, R., Fukui, M., Wilkes, H. & Widdle, F. Degradative capacities and 16S rRNA-targeted whole-cell hybridization of sulfate-reducing bacteria in an anaerobic enrichment culture utilizing alkylbenzenes from crude oil. *Appl. Environ. Microbiol.* **62**, 3605–3613 (1996).

21. Zengler, K., Richnow, H.H., Rossello-Mora, R., Michaelis, W. & Widdel, F. Methane formation from long-chain alkanes by anaerobic microorganisms. *Nature* **401**, 266–269 (1999).

22. Meckenstock, R.U., Annweiler, E., Michaelis, W., Richnow, H.H. & Schink, B. Anaerobic naphthalene degradation by a sulfate-reducing enrichment culture. *Appl. Environ. Microbiol.* **66**, 2743–2747 (2000).

23. Wang, L.-Y. *et al.* Characterization of an alkane-degrading methanogenic enrichment culture from production water of an oil reservoir after 274 days of incubation. *Int. Biodeterior. Biodegrad.* **65**, 444–450 (2011).

24. Schink, B. Degradation of unsaturated hydrocarbons by methanogenic enrichment cultures. *FEMS Microbiol. Ecol.* **1**, 69–77 (1985).

25. Rios-Hernandez, L.A., Gieg, L.M. & Suflita, J.M. Biodegradation of an alicyclic hydrocarbon by a sulfate-reducing enrichment from a gas condensate-contaminated aquifer. *Appl. Environ. Microbiol.* **69**, 434–443 (2003).

26. Raghoebarsing, A.A. *et al.* A microbial consortium couples anaerobic methane oxidation to denitrification. *Nature* **440**, 918–921 (2006).

27. McGlynn, S.E., Chadwick, G.L., Kempes, C.P. & Orphan, V.J. Single cell activity reveals direct electron transfer in methanotrophic consortia. *Nature* **526**, 531–535 (2015).

28. Jaekel, U. *et al.* Anaerobic degradation of propane and butane by sulfate-reducing bacteria enriched from marine hydrocarbon cold seeps. *ISME J.* **7**, 885–895 (2013).

29. Jaekel, U., Vogt, C., Fischer, A., Richnow, H.-H. & Musat, F. Carbon and hydrogen stable isotope fractionation associated with the anaerobic degradation of propane and butane by marine sulfate-reducing bacteria. *Environ. Microbiol.* **16**, 130–140 (2014).

30. Kniemeyer, O. *et al.* Anaerobic oxidation of short-chain hydrocarbons by marine sulphate-reducing bacteria. *Nature* **449**, 898–901 (2007).

31. Widdel, F. in *Handbook of Hydrocarbon and Lipid Microbiology* (ed. Timmis, K.N.) 3787–3798 (Springer, 2010).

32. Musat, F. & Widdel, F. Anaerobic degradation of benzene by a marine sulfate-reducing enrichment culture, and cell hybridization of the dominant phylotype. *Environ. Microbiol.* **10**, 10–19 (2008).

33. Tan, B. *et al.* Comparative analysis of metagenomes from three methanogenic hydrocarbon-degrading enrichment cultures with 41 environmental samples. *ISME J.* **9**, 2028–2045 (2015).
34. Jaekel, U., Zedelius, J., Wilkes, H. & Musat, F. Anaerobic degradation of cyclohexane by sulfate-reducing bacteria from hydrocarbon-contaminated marine sediments. *Front. Microbiol.* **6**, 116 (2015).
35. Kleindienst, S. *et al.* Diverse sulfate-reducing bacteria of the *Desulfosarcina*/*Desulfococcus* clade are the key alkane degraders at marine seeps. *ISME J.* **8**, 2029–2044 (2014).
36. Krukenberg, V. *et al. Candidatus desulfofervidus auxilii*, a hydrogenotrophic sulfate-reducing bacterium of the HotSeep-1 cluster involved in the thermophilic anaerobic oxidation of methane. *Environ. Microbiol.* **18**, 3073–3091 (2016).
37. Wegener, G., Krukenberg, V., Ruff, S.E., Kellermann, M.Y. & Knittel, K. Metabolic capabilities of microorganisms involved in and associated with the anaerobic oxidation of methane. *Front. Microbiol.* **7**, 46 (2016).
38. Gieg, L.M., Duncan, K.E. & Suflita, J.M. Bioenergy production via microbial conversion of residual oil to natural gas. *Appl. Environ. Microbiol.* **74**, 3022–3029 (2008).
39. Holler, T. *et al.* Substantial $^{13}C/^{12}C$ and D/H fractionation during anaerobic oxidation of methane by marine consortia enriched *in vitro*. *Environ. Microbiol. Rep.* **1**, 370–376 (2009).
40. Meulepas, R.J. *et al.* Enrichment of anaerobic methanotrophs in sulfate-reducing membrane bioreactors. *Biotechnol. Bioeng.* **104**, 458–470 (2009).
41. Simoneit, B.R.T., Kawka, O.E. & Brault, M. Origin of gases and condensates in the Guaymas Basin hydrothermal system (Gulf of California). *Chem. Geol.* **71**, 169–182 (1988).
42. Teske, A. *et al.* The Guaymas Basin hiking guide to hydrothermal mounds, chimneys, and microbial mats: complex seafloor expressions of subsurface hydrothermal circulation. *Front. Microbiol.* **7**, 75 (2016).
43. Cruse, A.M. & Seewald, J.S. Low-molecular weight hydrocarbons in vent fluids from the Main Endeavour Field, northern Juan de Fuca Ridge. *Geochim. Cosmochim. Acta* **74**, 6126–6140 (2010).
44. Riedel, C., Schmidt, M., Botz, R. & Theilen, F. The Grimsey hydrothermal field offshore North Iceland: crustal structure, faulting and related gas venting. *Earth Planet. Sci. Lett.* **193**, 409–421 (2001).
45. Jaeschke, A. *et al.* Biosignatures in chimney structures and sediment from the Loki's Castle low-temperature hydrothermal vent field at the Arctic Mid-Ocean Ridge. *Extremophiles* **18**, 545–560 (2014).
46. Baker, E.T. & German, C.R. On the global distribution of hydrothermal vent fields. in *Mid-Ocean Ridges* (eds. German, C.R., Lin, J. & Parson, L.M.) 245–266 (Wiley, 2004).
47. Nauhaus, K., Boetius, A., Krüger, M. & Widdel, F. *In vitro* demonstration of anaerobic oxidation of methane coupled to sulphate reduction in sediments from a marine gas hydrate area. *Environ. Microbiol.* **4**, 296–305 (2002).

48. Wegener, G. *et al.* Biogeochemical processes and microbial diversity of the Gullfaks and Tommeliten methane seeps (Northern North Sea). *Biogeosciences* **5**, 1127–1144 (2008).

49. Ruff, E.S. *et al.* Methane seep in shallow-water permeable sediment harbors high diversity of anaerobic methanotrophic communities, Elba, Italy. *Front. Microbiol.* **7**, 374 (2016).

50. Holler, T. *et al.* Thermophilic anaerobic oxidation of methane by marine microbial consortia. *ISME J.* **5**, 1946–1956 (2011).

51. Girguis, P.R., Cozen, A.E. & DeLong, E.F. Growth and population dynamics of anaerobic methane-oxidizing archaea and sulfate-reducing bacteria in a continuous-flow bioreactor. *Appl. Environ. Microbiol.* **71**, 3725–3733 (2005).

52. Jagersma, G.C. *et al.* Microbial diversity and community structure of a highly active anaerobic methane-oxidizing sulfate-reducing enrichment. *Environ. Microbiol.* **11**, 3223–3232 (2009).

53. Aoki, M. *et al.* A long-term cultivation of an anaerobic methane-oxidizing microbial community from deep-sea methane-seep sediment using a continuous-flow bioreactor. *PLoS One* **9**, e105356 (2014).

54. Orcutt, B.N. *et al.* Impact of natural oil and higher hydrocarbons on microbial diversity, distribution, and activity in Gulf of Mexico cold-seep sediments. *Deep Sea Res. Part II Top. Stud. Oceanogr.* **57**, 2008–2021 (2010).

55. Sikkema, J., De Bont, J. & Poolman, B. Mechanisms of membrane toxicity of hydrocarbons. *Microbiol. Rev.* **59**, 201–222 (1995).

56. McAuliffe, C. Solubility in water of paraffin, cycloparaffin, olefin, acetylene, cycloolefin, and aromatic hydrocarbons1. *J. Phys. Chem.* **70**, 1267–1275 (1966).

57. Edwards, E.A. & Grbic´-Galic´, D. Complete mineralization of benzene by aquifer microorganisms under strictly anaerobic conditions. *Appl. Environ. Microbiol.* **58**, 2663–2666 (1992).

58. Widdel, F. & Bak, F. in *The Prokaryotes* Vol. 4 (eds. Trüper H.G., Balows A., Dworkin M., Harder W. & Schleifer K.H.) 3352–3378 (Springer, 1992).

59. Brock, T.D. & Od'ea, K. Amorphous ferrous sulfide as a reducing agent for culture of anaerobes. *Appl. Environ. Microbiol.* **33**, 254–256 (1977).

60. Nauhaus, K., Albrecht, M., Elvert, M., Boetius, A. & Widdel, F. *In vitro* cell growth of marine archaeal-bacterial consortia during anaerobic oxidation of methane with sulfate. *Environ. Microbiol.* **9**, 187–196 (2007).

61. Wegener, G. & Boetius, A. An experimental study on short-term changes in the anaerobic oxidation of methane in response to varying methane and sulfate fluxes. *Biogeosciences* **6**, 867–876 (2009).

62. Deusner, C., Meyer, V. & Ferdelman, T.G. High-pressure systems for gas-phase free continuous incubation of enriched marine microbial communities performing anaerobic oxidation of methane. *Biotechnol. Bioeng.* **105**, 524–533 (2010).

63. Zhang, Y., Henriet, J.-P., Bursens, J. & Boon, N. Stimulation of *in vitro* anaerobic oxidation of methane rate in a continuous high-pressure bioreactor. *Bioresour. Technol.* **101**, 3132–3138 (2010).
64. Wankel, S.D. *et al.* Anaerobic methane oxidation in metalliferous hydrothermal sediments: influence on carbon flux and decoupling from sulfate reduction. *Environ. Microbiol.* **14**, 2726–2740 (2012).
65. Cord-Ruwisch, R. A quick method for the determination of dissolved and precipitated sulfides in cultures of sulfate-reducing bacteria. *Microbiol. Methods* **4**, 33–36 (1985).
66. Aeckersberg, F., Bak, F. & Widdel, F. Anaerobic oxidation of saturated hydrocarbons to CO_2 by a new type of sulfate-reducing bacterium. *Arch. Microbiol.* **156**, 5–14 (1991).
67. Pawlak, Z. & Pawlak, A.S. Modification of iodometric determination of total and reactive sulfide in environmental samples. *Talanta* **48**, 347–353 (1999).
68. Grasshoff, K., Kremling, K. & Ehrhardt, M. *Methods of Seawater Analysis* (Wiley, 2009).

Figures and Tables

Figures

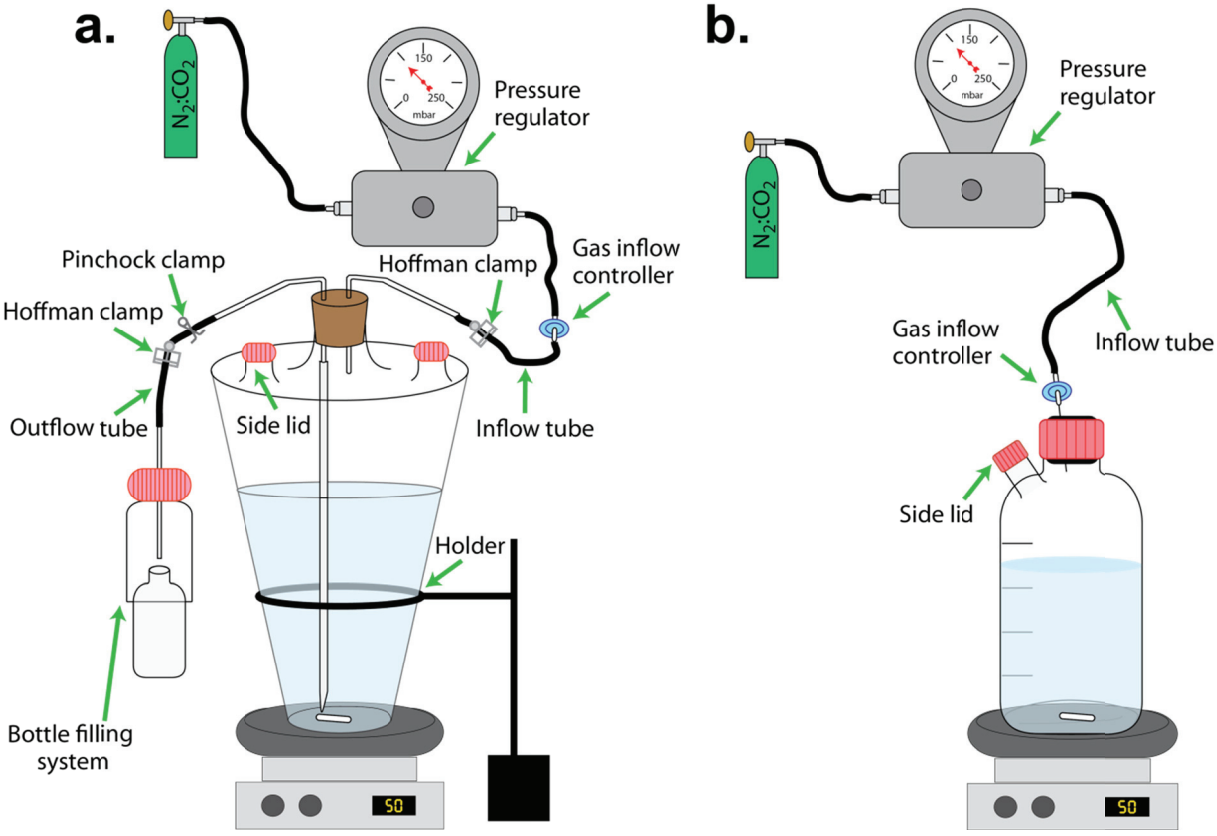

Figure 1. Setups for the production of anaerobic medium (Step 1). (**a,b**) Setups using a Widdel flask for the filling of serum vials (**a**) or a Duran flask manufactured with a sideward opening for medium transfers inside the anoxic chamber (**b**). The gas inflow controller consists of a 0.2-µm-pore-size filter and a Luer one-way stopcock.

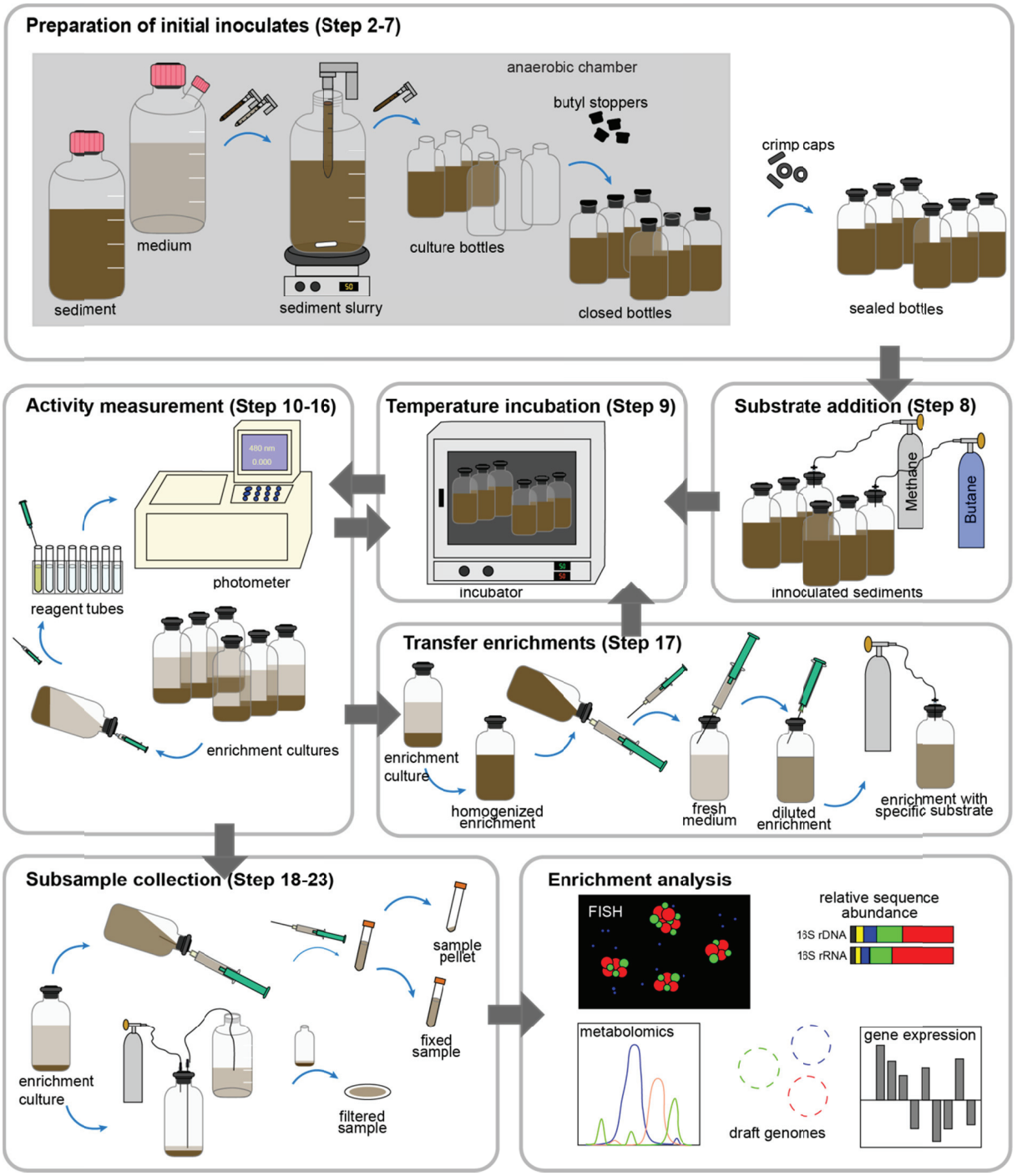

Figure 2. Scheme illustrating the preparation of initial inoculates, the incubation and dilution of enrichment cultures, activity measurements, and subsampling for downstream analyses.

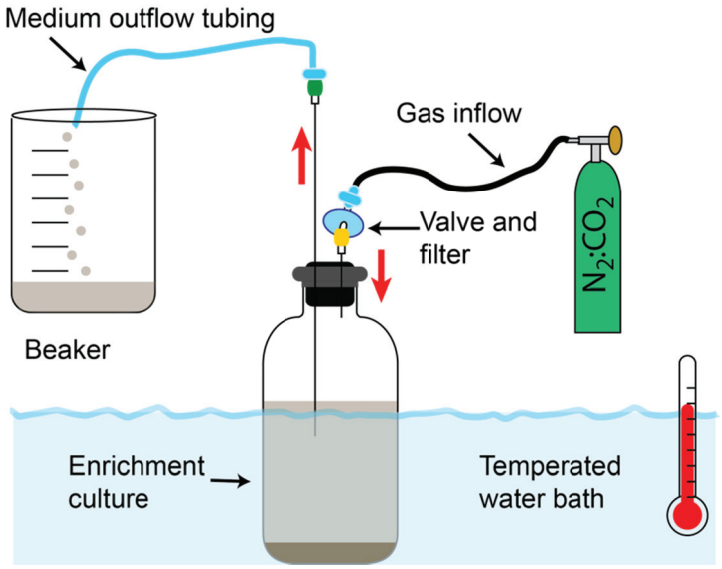

Figure 3. Setup for the temperature-controlled fixation of cell material for transcriptome analysis (Step 23C(ii–vi)). The enrichment culture is kept at constant temperature using a heated water bath. The gas bottle is connected to the culture bottle. A long needle connected to a PVC Luer tube is injected into the culture bottle. The inflowing gas replaces the medium. After the medium is removed, RNAlater is added to preserve the RNA.

Figure 4. The culture medium in serum bottles. (Left) Medium prepared under strictly anoxic conditions appears colorless with small black precipitates. (Middle) Yellowish medium indicates formation of elemental sulfur in the culture medium due to minor oxygen contamination. (Right) Medium has turned pink due to an increase of redox potential by contamination with more oxygen.

Figure 5. Appearance of enrichment cultures during cultivation. (Left) The freshly incubated sediment slurry is dark brown. (Middle) After two dilution steps/transfers, sediment content is strongly reduced. (Right) After five or more transfers, enrichment cultures appear sediment-free, and clumps of microbial consortia become visible to the eye.

VIDEOS (available at the online version of the paper)

Video 1. Step 1 A. Preparation of anoxic medium in Widdel flask (29.1 MB, Download)

Video 2. Step 1 B. Preparation of anoxic medium in Duran bottle (28.7 MB, Download)

Video 3. Step 8. Addition of hydrocarbon substrates to culture bottles (12.3 MB, Download)

Video 4. Step 17 B. Enrichment culture transfer without an anoxic chamber (19.7 MB, Download)

Video 5. Step 23 C. Collection and preservation of material for RNA extraction using RNAlater (24.8 MB, Download)

Table 1. Troubleshooting table.

Step	Problem	Possible reason	Solution
Step 1A(viii), 1B(xi)	Medium cannot be reduced, as indicated by a pinkish color (**Fig. 4**)	Influx of oxygen	Add a small amount of dithionite to reduce the medium; check the gas inflow and ensure that the medium is supplied with an anoxic headspace (i.e., when connected to the pressure regulator, check that overpressure builds up when all openings of the bottle are closed); prepare new medium and check the setup of the Widdel flask or Duran bottle (i.e., glass openings are not cracked, stoppers seal properly, clamps seal tubing tightly)
	Medium turns yellow (**Fig. 4**)	Formation of elemental sulfur due to oxygen influx	Irreversible; prepare new medium. Ensure that the medium is supplied with an oxygen-free headspace (i.e., N_2 or N_2:CO_2 gas) and that all openings can be properly sealed (e.g., glass openings are not cracked)
	Precipitation of gray crystals in the medium and/or formation of a grayish surface layer (black precipitates/metal sulfide precipitation is normal with time)	pH might be too high or CO_2 is missing from the gas phase	Irreversible; prepare new medium. Ensure that the medium is supplied with a CO_2-containing (e.g., N_2:CO_2 gas) headspace once the bicarbonate buffer has been added
Step 7	Medium in initial incubation turns pink	Very little/no sulfide production; stoppers are not gas-tight	Reduce the medium with small amounts of freshly prepared sodium dithionite solution; ensure stoppers are made of gas-tight material (e.g., butyl rubber); check quality of the stoppers (i.e., no fissures in the rubber material); replace the stoppers with new ones
Step 15	No sulfide formation in the freshly incubated sediment	Microorganisms with the required metabolism are low in abundance or even absent in the source material	Prolong the incubation (i.e., check for activity every few months) or use an alternative source material
	No/decreased sulfide production in the culture after medium exchange/dilution	Composition or pH of the medium is incorrect; insufficient time to detect activity; hydrocarbon substrate has not been supplied or has been completely consumed; stoppers are not tight and sulfide or hydrocarbon substrates leaked out	Check pH; prolong the incubation; exchange medium, supply (more) hydrocarbon substrate; check quality of the stoppers and, if necessary, replace the stoppers
Step 17A(x), 17B(v)	No or little growth after transfer	Most cells attached to the walls of the incubation bottle, therefore only little biomass was transferred	Before transfer, open the culture bottle and scratch the cells from the walls using a sterile disposable scraper. Work under anoxic conditions Use the stored bottles from earlier enrichment stages to repeat the culture transfer procedure
Step 23B(vi)	Filters appear milky under the microscope	Formation of carbonate precipitates in the subsample	Incubate a subsample with 10 mM HCl (final conc.) for 1–5 min before filtration to dissolve carbonate crystals

Table 1. Troubleshooting table (continuation).

Step	Problem	Possible reason	Solution
Step 23C(xiii)	Recovery of no/little or highly degraded RNA	Equipment might be contaminated with RNases; the amount of material sampled was insufficient	Repeat RNA extraction. If possible, increase the amount of material sampled for RNA extraction. This might be particularly important when the enrichment culture has only low activity. Ensure that all equipment has been cleaned with RNaseZAP and autoclaved for 45 min at 121 °C. Prepare fresh DEPC-treated water
Step 23D(x)	No/insufficient amounts of metabolites for analysis	The amount of material was insufficient; cells lysed during washing steps	Use more/more-concentrated cells; harvest at a later stage; test other washing buffers

Table 2. Comparison of published approaches for the enrichment of anaerobic methanotrophic archaea

	Unpressured flow-through reactor	Pressurized flow-through reactors	Pressurized batch incubation	Low-pressure batch incubation
Reference	61	51	60	50
Activity/doubling times	No growth observed	Down to 2-month doubling time; strongly increased as compared with other low-temperature systems	Doubling time = 7 months; growth rates are comparable to low-temperature, low-pressure incubations	Doubling time down to 50 days
Maintenance effort	High	Very high	Medium	Low
Cost of the setup	Medium	Very high costs for high-pressure pumps and setup	High costs for pressure vessels and pumps	Low
Disadvantages	Vulnerability to technical malfunctions, high maintenance	Vulnerability to technical malfunctions, high costs, high maintenance	Decompression effects during sampling, changes in reactant and product concentrations	Changes in product and reactant concentrations during incubation
Cultivation success	Activity kept constant over 180 d	Strong increase in activity possible	Ten times increased rates, within >2 years	Sediment-free cultures reached within ~1 year
Enriched archaea	Not assessed	ANME-2	ANME-2	≤20 °C: ANME-2 37–60 °C: ANME-1
Suggested application	Physiological tests	Physiological tests, optimization of growth yields	Biomass increase, physiological tests, piezophilic organisms	Enrichment to sediment-free state, enrichment of specific strains, multiple substrate tests

Chapter VI

Discussion and perspectives

At the time of the start of my thesis, the anaerobic degradation of non-methane hydrocarbons was solely attributed to bacteria with the exception of three archaea. Several pathways have been described for the activation of these compounds with fumarate addition as the most studied and widespread one. The only genuine archaeal pathway for hydrocarbon degradation was the reverse methanogenesis responsible of the anaerobic oxidation of methane. In this chapter, I will discuss the outcome of my research projects on thermophilic butane- and propane-degrading microbial enrichments dominated by *Ca.* Syntrophoarchaeum archaea and on metagenome assembled genomes of archaea from the D-C06 clade. I was able to demonstrate the existence of a novel pathway for the anaerobic degradation of non-methane alkanes (from hereon simply referred to as alkanes) in archaea, which is based on elements of the methanogenesis pathway.

6.1. A novel archaeal pathway for the degradation of hydrocarbons via CoM activation

Novel divergent MCRs catalyse the activation of butane and propane in *Ca.* Syntrophoarchaeum

In my thesis research, I discover a novel archaeal pathway to degrade propane and butane anaerobically (**Chapter II**). This pathway was discovered in two archaeal strains of the *Ca.* Syntrophoarchaeum clade, which is closely related to ANME-1 and the order *Methanosarcinaceae*. Therefore, it is not surprising that the pathway is based on a similar mechanism to the reverse methanogenesis with modifications for the oxidation of multi-carbon compounds. The key enzymes are modified versions of the methyl-coenzyme M reductase. Previously, it was considered that MCR exclusively catalysed reactions involving methane, an assumption based on the high selectivity of the active site, though MCRs from methanogens were shown to reduce *in vitro* ethyl-CoM to ethane with extremely low efficiency (Ahn*, et al.*, 1991, Scheller*, et al.*, 2013). We demonstrated for the first time that some MCRs activate *in vivo* alkanes different from methane. These MCRs catalyse the first step in the oxidation of butane and propane, forming the corresponding alkyl-CoM. Phylogenetic analyses revealed that these MCRs are highly divergent from the canonical MCRs of methanogens and methanotrophs, with numerous amino acid changes in their structure. These changes probably confer a different molecular conformation that allows to accommodate substrates larger than methane.

Surprisingly, four MCRs were present in each *Ca.* Syntrophoarchaeum strain (*Candidatus* Syntrophoarchaeum butanivorans and *Candidatus* Syntrophoarchaeum caldarius). In contrast, most methanogens and ANME archaea have only a single MCR with the exception of methanogens from the *Methanococcales* and *Methanobacteriales*, which contain two MCRs (Steigerwald*, et al.*, 1993, Pihl*, et al.*, 1994, Friedrich, 2005). A possible explanation for multiple MCRs in *Ca.* Syntrophoarchaeum could be different substrate specificities of each MCR. The results from transcriptomic analysis and substrate experiments support this idea (**Chapter IV**). They showed that the strain *Ca.* S. butanivorans was the dominant archaeon during growth on butane, but it was absent in enrichments growing on propane. In contrast, *Ca.* S. caldarius was a minor member of the microbial community during incubations with butane, but it was also present during incubations on propane, where it was the only alkane-degrading archaeon. Analyses of the expression levels of the *mcr* genes showed certain correlations linking different MCRs to specific substrates. The most divergent MCR of both strains (MCR-1) was most expressed during butane oxidation and, hence, MCR-1 could be responsible for the butane activation. During growth on propane, the MCR-4 of *Ca.* S. caldarius was mostly expressed, what suggest that MCR-4 of *Ca.* S. caldarius is likely catalysing the activation of propane (see Figure 5 of **Chapter IV**). However, these links are not unequivocal, because all MCRs of both strains showed a certain level of expression independent of the growth substrate. A possible reason would be the lack of precise mechanisms for the transcriptional regulation of the *mcr* genes. These *Ca.* Syntrophoarchaeum inhabit hydrothermal sediments, where fluids carry diverse substrates and gas bubbles with highly variable alkane concentrations. Therefore, it may be advantageous to

express basal levels of all MCRs, what allows them to utilize at any moment any available substrate. Additionally, different MCRs might activate the same substrate but have different affinity, as it has also been described for other proteins like transporters. This could help the organisms to use any possible alkane regardless of concentration changes, which can result from ascending gas bubbles or advection processes. Finally, different MCRs could be regulated by different unknown environmental factors, similarly to the two aerobic methane-oxidizing enzymes (pMMO and MMO), which are expressed depending on the concentration of copper ions (Stanley*, et al.*, 1983, Prior and Dalton, 1985, Murrell*, et al.*, 2000).

How are the CoM-bound alkyl units further oxidized?

After CoM activation, *Ca.* Syntrophoarchaeum fully oxidizes the corresponding alkyl-CoM units using the fatty acid oxidation pathway, enzymes of the Wood-Ljungdahl pathway and the downstream part of the methanogenesis pathway (**Chapter II** and **IV**). Then, the reducing equivalents are transferred to the sulfate-reducing bacterial partner, with which they are forming consortia. Still, the activation of butane is not fully resolved. Two possible intermediates 1-butyl-CoM and 2-butyl-CoM, were detected in the cultures (**Chapter II**). We propose that either both compounds represent genuine intermediates or that one of the intermediates is a by-product that does not undergo further reactions. Likewise, the conversion from alkyl-CoM to the corresponding CoA-ligated fatty acids, which enter into the fatty acid oxidation pathway, is also unresolved.

This conversion requires the oxidation of the alkyl group to an acid and the exchange of the CoM by CoA, yet both reactions are unprecedented and await experimental verification. One possibility for this process would be substrate cleavage from the CoM forming free alcohols followed by stepwise oxidation to a fatty acid, to which a CoA must be ligated. For butane, the corresponding intermediates would be butanol, butanal, butyrate and butyryl-CoA. Genes encoding alcohol and aldehyde dehydrogenases are present but very poorly expressed, whereas the genes of the subsequent fatty acid oxidation pathway are highly transcribed (**Chapter II**). Moreover, genes encoding potential CoA-ligases were not identified in *Ca.* Syntrophoarchaeum.

Based on the molecular information of *Ca.* Syntrophoarchaeum and discussions with leading biochemists including Dr. Steven Mansoorabadi (Auburn University, Alabama, USA), I propose an alternative pathway for the conversion of both possible alkyl-CoM isomers to the CoA bound fatty acid (**Figure 1**). First, the butyl group would be split from CoM and transferred to a corrinoid protein. This step could be catalysed by a modified methylcobalamin:coenzyme M methyltransferase (MtaAC). Mta is present in some methanogens, where it consists of three subunits (MtaABC) and works in the reverse direction catalysing the conversion of methanol to methyl-CoM. MtaB is responsible of the reduction of methanol to a methyl radical bound to the MtaC and then the methyl groups is transferred from MtaC to CoM by MtaA. In *Ca.* Syntrophoarchaeum, MtaA would be

responsible of transferring the alkyl group from CoM to the corrinoid protein (MtaC). In *Ca.* Syntrophoarchaeum, the *mtaB* gene is absent, indicating that the corrinoid-bound alkyl could not be released as a free alcohol. Instead, the corrinoid-alkyl unit might be ligated to CoA and simultaneously carboxylated by an acetyl-CoA decarbonylase:synthase (ACDS) complex.

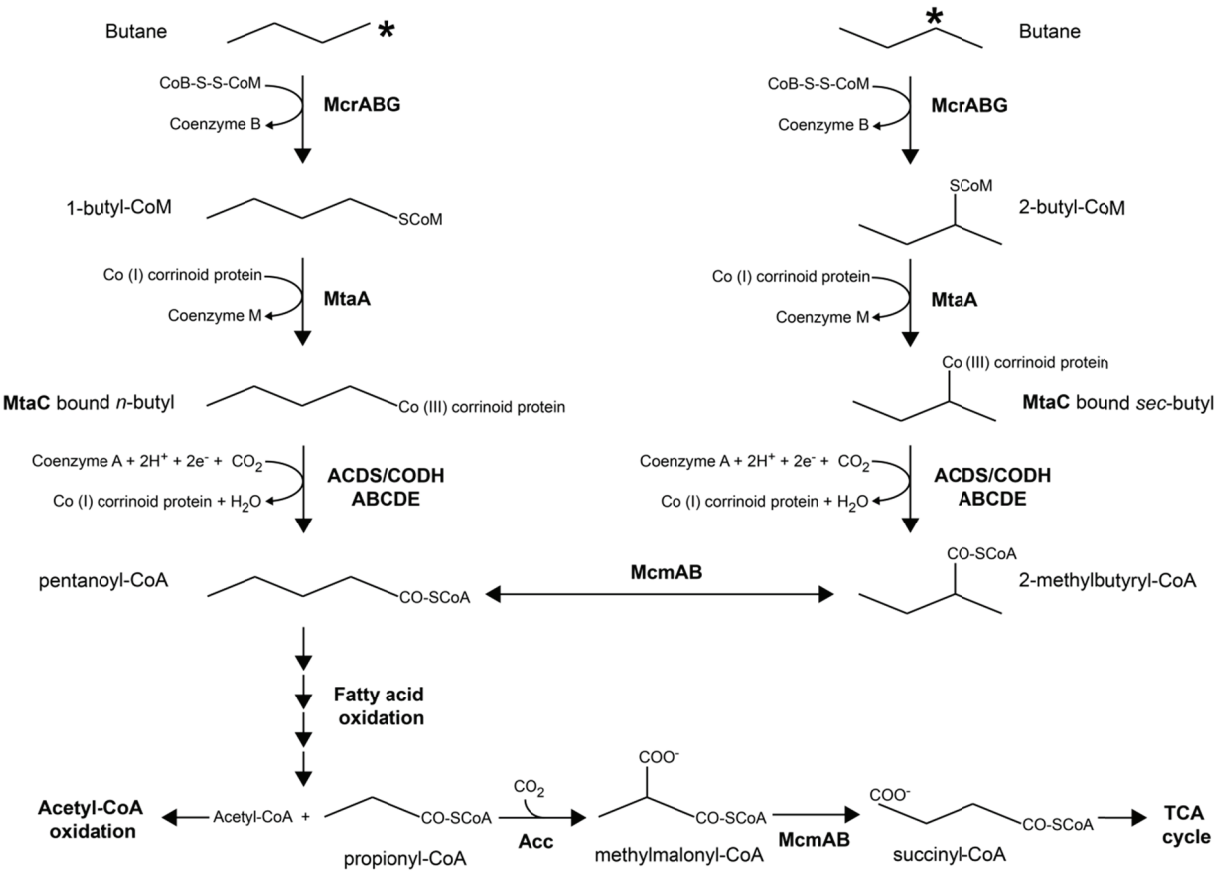

Figure 1. Proposed pathway for the conversion of alkyl-CoM to acyl-CoA in *Ca.* Syntrophoarchaeum. The model describes the case of butane oxidation considering that both, 1-butyl-CoM and 2-butyl-CoM, are genuine intermediates. The asterisk indicates the potential site for butane activation. Afterwards, the alkyl moiety is first transferred to a corrinoid (MtaC) protein by MtaA and later to CoA with a simultaneous carboxylation by ACDS. A five carbon molecule bound to CoA is formed. This molecule enters the fatty acid oxidation pathway, where it is split into acetyl-CoA and propionyl-CoA. Acetyl-CoA is further oxidized and propionyl-CoA can re-enter the central metabolism through the tricarboxylic acid cycle (TCA cycle). Mcr=methyl-CoM reductase; Mta=methylcobalamin:CoM methyltransferase; ACDS/CODH=acetyl-CoA decarbonylase:synthase/CO dehydrogenase; Mcm=methylmalonyl-CoA mutase; Acc=acetyl-CoA carboxylase. *sec*-butyl stands for secondary butyl, since the activation happened in the secondary carbon.

ACDS usually catalyses the oxidation of acetyl-CoA to CO_2 and methyl-H_4MPT or the respective reverse reaction. Strikingly, both *Ca.* Syntrophoarchaeum MAGs contain two highly expressed operons encoding ACDS complexes. According to phylogenetic analysis, one of its ACDS complexes clusters with those of ANME-1 and hence it likely performs the conventional acetyl-CoA oxidation. Interestingly, the second ACDS complex is highly divergent from any known ACDS sequences (Adam*, et al.*, 2018). This points out that this ACDS might have a still unknown substrate specificity, similarly to the divergent MCRs of *Ca.* Syntrophoarchaeum. I suggest that this ACDS is

used to carboxylate the alkyl units received from the Mta. As a result of the CoA-carboxylation of the divergent ACDS, an acyl-CoA with an additional carbon would be produced.

Considering the production of two isomers of butyl-CoM in the initial activation, the carboxylation would also generate two different isoforms with a five carbon chain (**Figure 1**). Before entering the fatty acid degradation pathway, the branched isomer (2-methylbutyryl-CoA) would need to be converted into a linear CoA-bound fatty acid (acyl-CoA). This reaction might be catalysed by a methylmalonyl-CoA mutase (MCM). MCM enzymes are B_{12}-mutases in charge of the conversion of methylmalonyl-CoA to succinyl-CoA. Both *Ca.* Syntrophoarchaeum MAGs harbour a remarkable high number of *mcm* genes, which are highly expressed. Afterwards, the linear acyl-CoA would be degraded in the fatty acid oxidation pathway. For propane, the CoA-bound fatty acid entering this pathway will be butyryl-CoA, which will be metabolized to two acetyl-CoA molecules, whereas for butane the CoA-fatty acid would be pentanoyl-CoA resulting in acetyl-CoA and propionyl-CoA after the degradation (**Figure 1**). This propionyl-CoA could then re-enter the central metabolism through carboxylation by an acetyl-coenzyme A carboxylase (Acc) and carbon rearrangement by one of the other MCM enzymes. A first support for this hypothesis is the highly transcription levels of all the genes involved in the conversion. The verification of this proposal will require additional experiments including isotope labelling and metabolomics.

6.2 Hydrocarbon degradation via CoM activation is present in additional archaeal linages

This novel mechanism to degrade alkanes is not restricted to *Ca.* Syntrophoarchaeum. Divergent *mcr* genes related to those of *Ca.* Syntrophoarchaeum have recently been found in MAGs affiliated to *Bathyarchaeota* (Evans*, et al.*, 2015) and the euryarchaeotal clades GoM-Arc1 (Dombrowski*, et al.*, 2017) and D-C06 (**Chapter III**). These MAGs also share many additional genomic features with *Ca.* Syntrophoarchaeum genomes. All of them derived from hydrocarbon-rich environments, although genomic and ecological information points towards important differences in lifestyles (**Table 1**).

D-C06 is a novel archaeal clade that couples hydrocarbon degradation to methanogenesis

Before this thesis, D-C06 archaea represented an unknown clade within *Methanomicrobia*. In **Chapter III**, we showed that this clade has the potential to couple hydrocarbon degradation to methane formation based on two MAGs derived from oil seeps of the Gulf of Mexico. Both MAGs contained one divergent *mcr* related to those of *Ca.* Syntrophoarchaeum and a second *mcr* close to those of methanogens and methanotrophs. They also harboured genes encoding a mechanism for the CoM-CoA transformation, a fatty acid oxidation pathway, an ACDS complex and a complete methanogenesis pathway. Considering the thermodynamic restrictions and the genomic and environmental evidences, it is unlikely that the canonical MCR is used for methane oxidation. Based

on this genomic evidence as well as the lack of bacterial partners, we propose that D-C06 archaea disproportionate hydrocarbons producing methane and CO_2. Previously, the coupling of hydrocarbon degradation to methanogenesis was only described as a syntrophic interaction between hydrocarbon-degrading bacteria and methanogenic archaea (Zengler*, et al.*, 1999, Gieg*, et al.*, 2014). In the here described case, D-C06 would be the first described organism performing methanogenic hydrocarbon degradation in a single cell.

Beyond the alkane activation mechanisms, D-C06 shares many genomic features with *Ca.* Syntrophoarchaeum such as the presence of a fatty acid oxidation pathway, the ACDS complex and the putatively oxidative C_1-branch (see Figure 5 in **Chapter III**). Nonetheless, the conversion of alkyl-CoM to acyl-CoA may proceed on a different pathway as suggested for *Ca.* Syntrophoarchaeum, since D-C06 lack a divergent ACDS and have additional encoded enzymes. We suggest that the alkyl is fist released from the CoM as a free alcohol. This hypothesis is supported by the presence of genes encoding a complete methyltransferase (MtbA/MttBC), unlike *Ca.* Syntrophoarchaeum that missed the subunit in charge of the alcohol formation. Then, the produced alcohol would be stepwise oxidized to an aldehyde and a fatty acid, which would be ligated to CoA before entering into the fatty acid degradation pathway. Genes encoding the corresponding enzymes (alcohol and aldehyde dehydrogenases, and CoA-transferases) were present in both D-C06 MAGs. The fate of the reducing equivalents is also different. As D-C06 lack a dissimilatory sulfate reduction pathway and syntrophic partner bacteria, they likely use the electrons for methanogenesis. For that, D-C06 contain a complete methanogenesis pathway, unlike *Ca.* Syntrophoarchaeum which lack genes for the Mtr and a canonical MCR. Based on this evidence, D-C06 likely use the reducing equivalents generated during alkane oxidation to produce methane using the canonical methanogenesis pathway. As substrates for this pathway, D-C06 can use CO_2 or methyl-H_4MPT generated by the oxidation of acetyl-CoA by the ACDS complex.

Due to the lack of cultures for the groups, we can only speculate about the potential substrate(s) of D-C06 based on genomic and environmental information. The divergent *mcr* of D-C06 forms a different cluster than those of *Ca.* Syntrophoarchaeum, what could point towards different substrate specificities. We suggest that D-C06 archaea are able to degrade long-chain alkanes based on their preferential niche within the oil droplets and their exclusive presence in oil reservoirs, oil seeps and alkane lakes (Lloyd*, et al.*, 2006, Liu*, et al.*, 2009, Orcutt*, et al.*, 2010, Schulze-Makuch*, et al.*, 2011, Kobayashi*, et al.*, 2012). In fact, 16S rRNA gene clones of D-C06 have been observed twice in enrichment cultures established from oil reservoir sediments with hexadecane as substrate (Cheng*, et al.*, 2011, Cheng*, et al.*, 2014). In agreement with our hypothesis, the encoded CoA-ligases of D-C06 are classified as long-chain fatty-acid-CoA ligases. The presence of just one divergent *mcr* in D-C06 archaea might suggest that D-C06 are specialized on a single alkane substrate, though it would be surprising considering that crude oil consist of a diverse mixture of hydrocarbons including alkanes of

a wide length spectrum (Tissot and Welte, 1984). I hypothesize that the divergent MCR of D-C06 can activate several long-chain alkanes.

Based on my prior discussion about the MCR specificity in *Ca*. Syntrophoarchaeum, it seems contradictory to propose that D-C06 use a single MCR to activate many different substrates. Nevertheless, I propose that beyond a specific carbon number the alkane length may not be anymore crucial for the activation. The active centre of the MCR enzyme is located in a cavity, to which the substrates enter through a hydrophobic channel (Ermler*, et al.*, 1997). However, part of the chain of longer alkanes may not need to enter the reaction cavity. In this case, the reacting part would be one of the chain termini that would be placed in the vicinity of the active centre, while the other terminus might remain in the hydrophobic channel, or project out of the MCR enzyme. Contrary to this theory would be the current mechanism proposed for MCR, in which coenzyme B is blocking the hydrophobic channel during the catalysis (Ermler*, et al.*, 1997). Alternatively, slight changes in the active centre could open a new hydrophobic channel according to the current MCR models. The long-chain alkanes could then be projected to this new tunnel. This proposal needs future research for confirmation; in particular the crystal structure of this MCR needs to be obtained, which depends on the successful cultivation of D-C06.

Strikingly, D-C06 archaea might be able to degrade certain aromatic hydrocarbons as well. Both MAGs contained genes encoding for a benzoyl-CoA reductase (Bad) associated with methylmalonyl-CoA mutase and CoA-ligase genes. The Bad enzyme catalyses the dearomatization of benzoyl-CoA, a central metabolite in aromatic hydrocarbon degradation. Thus, D-C06 archaea might also be able to use aromatic hydrocarbons that are abundantly found in crude oil. However, the subunits of Bad resemble those of the 2-hydroxyglutaryl-CoA dehydratase from *Acidaminococcus fermentans,* which takes part in the fermentative degradation of L-glutamate (Schweiger*, et al.*, 1987, Müller and Buckel, 1995). Moreover, no genes encoding the activation or the subsequent degradation steps have been identified, although some are similar to those of the fatty acid degradation pathway. The potential for aromatic hydrocarbon degradation in D-C06 should be addressed in the future by cultivation-based approaches.

The potential of *Bathyarchaeota* for hydrocarbon degradation

The divergent MCR type was originally described in two MAGs affiliated to *Bathyarchaeota,* which derived from coal-bed well samples (Evans*, et al.*, 2015). It was the first time that *mcr* genes were detected in organisms that do not belong to the *Euryarchaeota.* Based on their metabolic potential, these members of the *Bathyarchaeota* were considered to be methylotrophic methanogens. In the light of my results, these organisms are more likely degrading alkanes via CoM activation using the divergent MCRs. Interestingly their *mcr* genes cluster together with the *mcr* sequence of D-C06 (**Chapter III**), what could indicate that they use long-chain alkanes as substrate. Nevertheless, these

Bathyarchaeota did not possess a full alkane degradation pathway as detected in *Ca.* Syntrophoarchaeum or D-C06. One MAG encoded a partial fatty acid degradation pathway and the other a complete methanogenesis pathway, but none of them encoded both. Consequently, the way alkane degradation proceeds in *Bathyarchaeota* remains unresolved. Moreover, it is still not understood how these organisms conserve energy, since no ATP synthase genes were detected (Evans*, et al.*, 2015). Besides, there was no evidence of coupling to sulfate reduction, neither in the genome, nor by syntrophic partners. The presence of genes encoding a hydrogenase and an acetate synthetase suggest that these organisms do not fully oxidize alkanes but produce hydrogen and acetate, which could be used by syntrophic acetoclastic methanogens. Indeed, recurrent reports of the co-occurrence of members of the *Bathyarchaeota* and *Methanomicrobia* could indicate biotic interactions between both groups (He*, et al.*, 2016, Xiang*, et al.*, 2017, Zhou*, et al.*, 2018).

Archaea of the GoM-Arc1 clade are likely syntrophic alkane degraders

Divergent *mcr* genes were also found in MAGs affiliated to the GoM-Arc1 clade obtained from hydrothermal sediment samples, yet they form a different cluster of divergent MCRs (Dombrowski*, et al.*, 2017). Further genes encoded for a complete methanogenesis pathway, but there was no indication of a fatty acid oxidation or a sulfate reduction pathway. Accordingly, the authors proposed that GoM-Arc1 archaea are metabolizing short-chain alkanes other than methane coupled to sulfate reduction by syntrophic partner bacteria. In **Chapter III**, we provide support for this hypothesis, as we could visualize consortia of GoM-Arc1 archaea and bacteria in samples from oil seeps of the Gulf of Mexico. These consortia were detected in horizons, where sulfate reduction and short-chain alkane oxidation were taking place. Moreover, molecular surveys have frequently detected GoM-Arc1 archaea in gas seeps (Lloyd*, et al.*, 2006, Orcutt*, et al.*, 2010, Pachiadaki*, et al.*, 2011, McKay*, et al.*, 2016). Forthcoming research should address the cultivation of GoM-Arc1 and their exact substrate range.

Hydrocarbon degradation via CoM activation might be present in additional archaeal lineages

Recent studies suggest that alkane degradation via CoM activation is not restricted to the abovementioned organisms. For instance, genomic information of some members of the *Hadesarchaea* revealed the presence of an almost complete methanogenesis pathway and of genes encoding an ACDS complex (Baker*, et al.*, 2016). Due to their occurrence in subsurface environments, the potential for hydrocarbon degradation via CoM activation seems likely, although no *mcr* genes have been found so far.

In line with this, a recent preprint deposited in the bioRxiv archive reports the presence of divergent *mcr* genes in MAGs affiliated to the euryarchaeotal class *Archaeoglobi* (Boyd*, et al.*, 2018),

obtained from subsurface fluid samples of the hydrothermal environments of the Juan de Fuca Ridge flank (Jungbluth, *et al.*, 2017). They contained two divergent MCRs operons, one affiliated to the MCRs of *Ca.* Syntrophoarchaeum and the second one related to the MCRs of *Bathyarchaeota* and D-C06. The *Archaeoglobi* class is currently consisting of three genera (*Archaeoglobus, Ferroglobus* and *Geoglobus*) and all its members are thermophiles. *Archaeoglobi* genomes encode for the fatty acid degradation and the Wood-Ljungdahl pathway (Vorholt, *et al.*, 1997, Klenk, *et al.*, 1998, Mardanov, *et al.*, 2009, Brileya and Reysenbach, 2014). Two members can degrade hydrocarbons anaerobically, but they presumably use enzymes of bacterial origin (Khelifi, *et al.*, 2010, Holmes, *et al.*, 2011, Khelifi, *et al.*, 2014). In contrast, the new study points out that some members of *Archaeoglobi* might metabolize hydrocarbons via CoM activation expanding this trait within the *Euryarchaeota* tree.

Table 1. Overview and main characteristics of organisms with features potentially allowing alkane metabolism. ANME archaea are generalized as one group. Some of the metabolisms, substrates, electron sinks and syntrophic partners have just been proposed and still need to be confirmed. RM = reverse methanogenesis, M = methanogenesis, FAO = fatty acid oxidation.

	ANME	***Ca.* Syntrophoarchaeum**	**D-C06**	**GoM-Arc1**	***Bathyarchaeota***	***Archaeoglobi***
Phylum	*Euryarchaeota*	*Euryarchaeota*	*Euryarchaeota*	*Euryarchaeota*	*Bathyarchaeota*	*Euryarchaeota*
Substrate	Methane	Butane and propane	Long-chain alkanes*	Short-chain alkanes*	Long-chain alkanes*	Unknown
MCR number	1 canonical MCR	4 divergent MCRs	1 divergent MCR/ 1 canonical MCR	1 divergent MCR	1 divergent MCR	2 divergent MCRs
Potential metabolism	RM	FAO, ACDS, RM (Mtr missing)	FAO, ACDS, M	RM, ACDS	RM/FAO, ACDS	FAO, ACDS, RM
Electron sink	Syntrophic sulfate reduction/NO_3^- and Fe^{3+} reduction	Syntrophic sulfate reduction	Methanogenesis*	Syntrophic sulfate reduction*	Syntrophic methanogenesis*	Nitrate and iron reduction
Syntrophic partners	Sulfate reducing bacteria (except ANME-2d)	Sulfate reducing bacteria	None	Bacteria	Methanogens*	Unknown
Environments	Gas seeps, mud volcanoes, SMTZ…	Gas/oil seeps, hydrothermal areas, mud volcanoes	Oil seeps, asphalt lakes, deep oil reservoirs	Gas/oil seeps, hydrothermal areas, mud volcanoes	Coal-bed well, hydrothermal areas	Hydrothermal areas

*hypothesised, awaits experimentally verification

6.3 Evolution and characteristics of the archaeal clades harbouring divergent *mcr* genes

The discovery of novel divergent *mcr* genes in multiple archaeal phyla opens the question concerning their evolutionary origin. They were originally detected in *Bathyarchaeota*, where they were assigned to methane metabolism and considered a sign of this trait in early archaeal lineages (Evans, *et al.*, 2015). My thesis work sheds a different a light on this topic. The divergent *mcr* types are mostly found

in alkane-degrading clades of the *Euryarchaeota.* Two of these clades, *Ca.* Syntrophoarchaeum and GoM-Arc1, share an evolutionary origin with methane-oxidizing archaea (ANME) according to 16S rRNA gene phylogenetic analyses (**Chapter III**). These analyses showed that *Ca.* Syntrophoarchaeum has probably the same ancestor as ANME-1 archaea, what was also confirmed by other phylogenetic analyses using concatenated unique marker genes (Adam*, et al.*, 2017). Moreover, both share several metabolic features like a fatty acid oxidation pathway and the substitution of the Mer enzyme, encoding a step of the methanogenesis, by the dimeric enzyme Met (Stokke*, et al.*, 2012, Krukenberg*, et al.*, 2018, **Chapter II**). The presence of several cytochromes, probably mediating the electron transfer to the corresponding sulfate-reducing bacteria, is also a common characteristic. Furthermore, ANME-1 and *Ca.* Syntrophoarchaeum share the same syntrophic partner, *Ca.* D. auxilii, in thermophilic enrichments derived from the Guaymas Basin (Krukenberg*, et al.*, 2016, **Chapter II**).

GoM-Arc1 archaea are closely related to ANME-2 archaea, in particular to the ANME-2d, currently named *Ca.* Methanoperedens. Besides, they share metabolic features like the absence of a fatty acid oxidation pathway and the presence of a complete reverse methanogenesis pathway (Haroon*, et al.*, 2013, Dombrowski*, et al.*, 2017). By contrast, GoM-Arc1 seems to have a different electron sink. While *Ca.* Methanoperedens possess the machinery for nitrate and iron reduction (Haroon*, et al.*, 2013, Ettwig*, et al.*, 2016, Cai*, et al.*, 2018), GoM-Arc1 seems to have a syntrophic lifestyle with bacteria, which are probably performing sulfate reduction (**Chapter III**).

The evolutionary relationships of D-C06 to other archaea are less clear. D-C06 likely form a deep-branching class within the *Euryarchaeota* related to *Archaeoglobi* (**Chapter III**). D-C06 is the first example of an archaeon that contains a canonical and a divergent MCR. The recently published *Archaeoglobi* MAG, with two divergent MCRs, might indicate certain shared evolutionary origin with D-C06 (Boyd*, et al.*, 2018). However, only one MCR of D-C06 belongs to the divergent alkane-degrading type close to the ones of *Bathyarchaeota,* whereas the other one is involved in methanogenesis and placed between the MCR lineages of *Methanomicrobia* and *Methanobacteriales* (**Chapter III**). In this regard, the presence of divergent *mcr* genes in *Bathyarchaeota* could be attributed to horizontal gene transfer from D-C06 or a related clade, implying that alkane-degrading MCRs have a euryarchaeotal origin. Support for this could be the fact that most *Bathyarchaeota* genomes do not encode for any MCR type (He*, et al.*, 2016).

Based on these arguments, I propose that organisms with divergent MCR types likely evolved from ANME clades; though for D-C06 the parental clade is still unknown. Firstly, genetic modification would change the metabolism from methanogenesis to methanotrophy. Later, new changes in the *mcr* genes (and probably in other genes) would enable alkane degradation. Likewise methanotrophy, this metabolism has evolved several times and the MCR tree shows polyphyletic cluster of divergent MCRs that indicates that similar modifications in the MCR structure are necessary in order to accommodate and activate larger substrates.

The study of the sequence and crystal structure of MCR enzymes from methanogens and methanotrophs have revealed numerous conserved residues. Crystal structures have revealed that some of these residues interact with different elements involved in the catalysis such as CoM, CoB, cofactor F_{430} or the methane itself. Moreover, many of these residues undergo different post-translational modifications (Ermler, *et al.*, 1997, Shima, *et al.*, 2011, Wagner, *et al.*, 2017). These modifications have been hypothesized to be important in the catalysis and stability of the MCR. Interestingly, the alkane-degrading MCRs sequences have numerous amino acid changes, some in conserved residues (**Figure 2**). These changes occur also in amino acid present in the active site, what provides clues about the hypothetical arrangements to accommodate larger substrates than methane. For instance, canonical MCRs usually have a tyrosine or a phenylalanine in the active site at position 444 (numbering of Ermler *et al.* (1997)). Phenylalanine has a large aromatic side chain that interacts with the CoM. This residue has been substituted by glycine or alanine in most alkane-degrading MCRs, probably because the side chain of these substitutes is smaller leaving space for larger substrates.

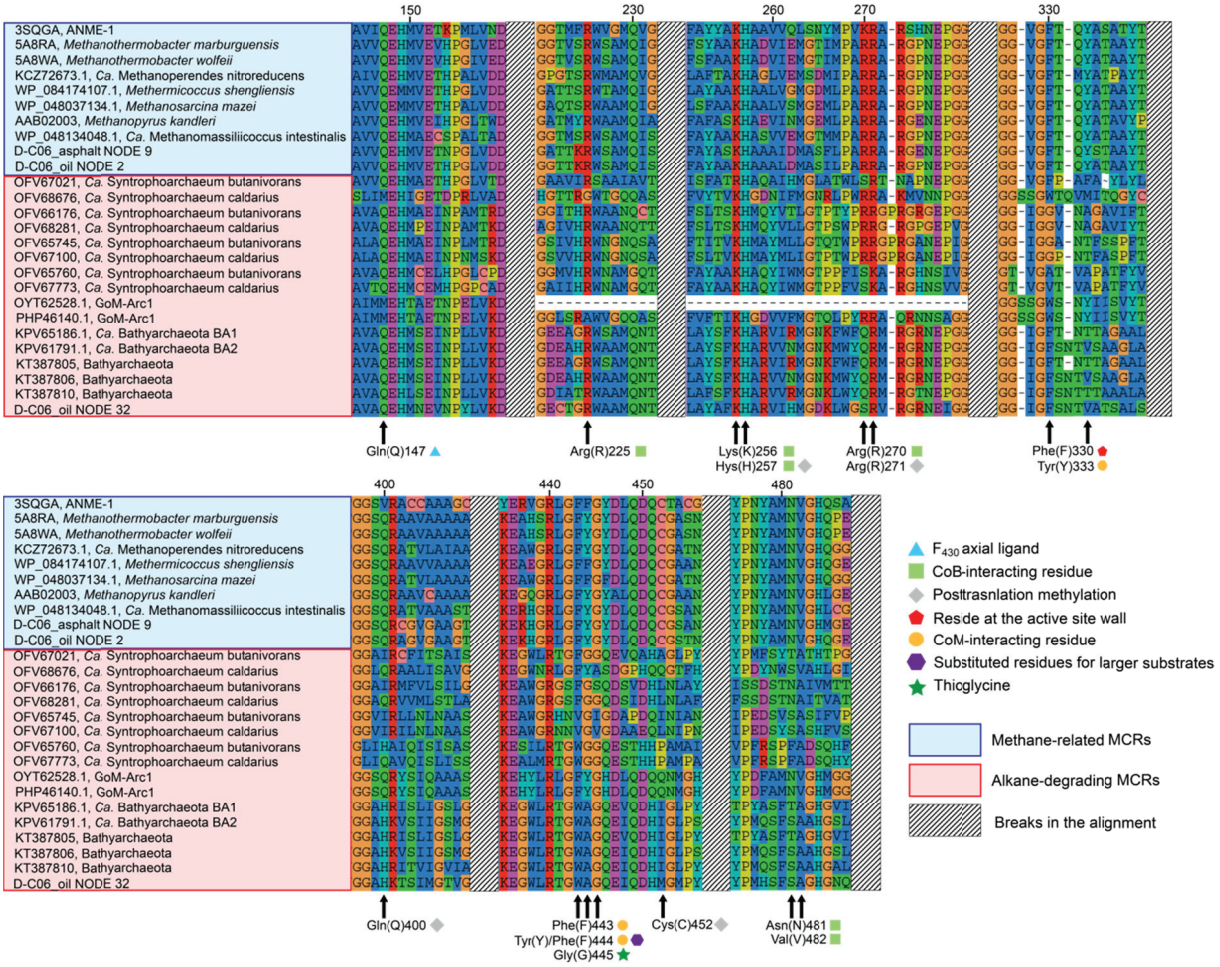

Figure 2. Alignment of MCR-A regions with catalytically relevant residues. Residues are numbered according to Emler et al. (1997). Amino acids are coloured based on their chemical features using the software Seaview (Gouy, *et al.*, 2010). All novel alkane-degrading MCRs (red box) are included in the alignment except those of *Archaeoglobi*. Selected MCRs of methanogens and ANME are in the blue box including the canonical MCRs of D-C06 archaea. Important residues interacting with elements of the catalysis or with post-translational modifications are indicated under the alignment. Additionally, a purple hexagon indicates the possible residue substitution in the active centre to accommodate larger substrates.

Another interesting amino acid interacting with the CoM is the tyrosine at position 333 (Ermler*, et al.*, 1997), which strikingly is not conserved in most alkane-degrading MCRs (**Figure 2**). More surprising is the substitution of the thioglyicine at position 445 in four MCRs of *Ca.* Syntrophoarchaeum. Thioglycine is produced by the post-translational thioamidation of a glycine (Ermler*, et al.*, 1997). It has been detected in all so far crystallized MCRs including those of methanotrophic archaea and all published MCR sequences encode for the precursor glycine. Thus, this thioglycine was considered to play a fundamental role in the catalysis of methane (Grabarse*, et al.*, 2001, Horng*, et al.*, 2001, Goenrich*, et al.*, 2005). The absence of the corresponding glycine in four MCRs of *Ca.* Syntrophoarchaeum challenges its proposed catalytic function.

Supporting this idea, a recent study has shown that this thioglycine is not necessary for the catalytic function of MCR (Nayak*, et al.*, 2017). The researchers were able to knock out the genes in charge of the glycine modification in *Methanosarcina acetivorans*. The mutants were still able to produce methane except at high temperatures. Therefore, Nayak and coworkers suggest that thioglycine confers stability to the active site of the MCR, especially at high temperatures. Consequently, new catalytic models of the MCR based on the thioglycine should include these findings. An arising question in this regard is why thioglycine is absent in some of the MCRs of the thermophilic *Ca.* Syntrophoarchaeum. One possibility is that novel post-translational modifications occur in amino acids different than glycine in these MCRs to substitute the stabilizing role of the thioglycine. Another possibility is that stability is achieved through other amino acids, while the absence of glycine provides a different conformation allowing the accommodation of certain substrates. Crystallization of these MCRs could help to address these questions in the future.

6.4 Ecological role of the novel hydrocarbon degrading archaea

Bacteria have been considered the main non-methane hydrocarbon degraders in anoxic environments. Nonetheless, this thesis revealed the existence of a novel archaeal pathway that was so far not considered for alkane degradation. The key genes of this pathway are divergent versions of the MCR. These *mcr* genes were previously not detected because primers used in molecular survey to search for *mcr* were not targeting the divergent *mcr* genes. Additional molecular surveys have unravelled an even greater diversity of *mcr* genes in hot springs by using newly developed primers targeting the divergent *mcr* (McKay*, et al.*, 2016). The archaeal clades harbouring the divergent MCRs are diverse and inhabit diverse niches with different lifestyles; therefore they might be important players in the cycling of hydrocarbons.

Future research should continue studying the role of these archaea in the environment, although I propose some hypotheses based on the current ecological information. Similar to *Ca.* Syntrophoarchaeum, GoM-Arc1 are likely short-chain alkane degraders that couple the process to sulfate reduction performed by syntrophic partner bacteria resembling the mechanisms and lifestyle of

ANME. GoM-Arc1 has been repeatedly found in cold gas seeps, mud volcanoes and hydrothermal vent sediments (Lloyd, *et al.*, 2006, Orcutt, *et al.*, 2010, Pachiadaki, *et al.*, 2011, Dombrowski, *et al.*, 2017). *Ca.* Syntrophoarchaeum has been detected in similar environments, but much less frequently (Orcutt, *et al.*, 2010, McKay, *et al.*, 2016), suggesting that they have different ecological niches and/or environmental ranges, probably due to different substrate specificity. Sulfate-reducing bacteria are considered the main anaerobic alkane degraders in cold seeps (Kleindienst, *et al.*, 2014), but both archaeal clades have been detected in these environments, pointing out that the syntrophic alkane degradation could be dominant under certain conditions as discussed in **Chapter IV**. For instance, thermophilic conditions might select for archaea of these two clades, given that archaeal membranes can be especially adapted to resist high temperatures (van de Vossenberg, *et al.*, 1998, Siliakus, *et al.*, 2017).

The methanogenic hydrocarbon degradation has been known for long time as a syntrophic process between hydrocarbon-degrading bacteria and methanogenic archaea (Zengler, *et al.*, 1999, Gieg, *et al.*, 2014). This view is expanded considering the potential metabolism of D-C06 and MCR-containing *Bathyarchaeota*. D-C06 archaea are likely the first described organisms able to metabolize hydrocarbons coupled to the production of methane in a single cell. According to 16S rRNA surveys, they inhabit environments with the presence of oil and little or no sulfate, such as deep reservoirs, asphalt lakes or oil seeps (Lloyd, *et al.*, 2006, Liu, *et al.*, 2009, Orcutt, *et al.*, 2010, Schulze-Makuch, *et al.*, 2011, Kobayashi, *et al.*, 2012). This supports a role as methanogenic long-chain alkane degraders. Especially relevant can be their involvement in oil degradation in deep reservoirs, where most of the 16S rRNA gene sequences have been found. Methanogenic crude oil degradation is observed in many different oil reservoirs and it might have an economic interest (Jones, *et al.*, 2007, Gieg, *et al.*, 2008). Despite the attribution of this process to associations of bacteria and archaea, there are indications that crude oil alkane activation does not proceed through the bacteria pathway of fumarate addition (Aitken, *et al.*, 2013). Therefore, D-C06 might be important players in crude oil degradation in deep reservoirs, a role that should be studied in the future.

Bathyarchaeota are probably the most widespread and abundant archaeal phylum in marine sediments. They are a diverse group of global generalists which reaches high abundances in anoxic sediments and have a fundamental contribution to the organic matter degradation (Kubo, *et al.*, 2012, He, *et al.*, 2016, Zhou, *et al.*, 2018). Only few members related to the subgroup MCG-G have been found to carry alkane-degrading *mcr* genes (Evans, *et al.*, 2015). *Bathyarchaeota* have been detected in different hydrocarbon-rich environments like the Hydrate Ridge, seeps from the Gulf of Mexico or Guaymas Basin (Kubo, *et al.*, 2012). They were reported to represent an important part of the archaeal community in seeps where sulfate depletion was detected deeper than 15 cm in the sediment (Kubo, *et al.*, 2012). In this case, *Bathyarchaeota* cells would live in the methanogenic zone and they could perform anaerobic degradation of hydrocarbons coupled to methanogenesis by syntrophic methanogenic archaea. This hypothesis receives support from studies reporting associations of

Bathyarchaeota and *Methanomicrobia* (He*, et al.*, 2016, Xiang*, et al.*, 2017, Zhou*, et al.*, 2018). Forthcoming research should address, if these relations are based on the methanogenic degradation of hydrocarbons.

The potential ecological role of *Archaeoglobi* in the hydrocarbon degradation is still not studied, but they are repeatedly detected in hydrothermal vents, hot springs and other hydrocarbon environments (Brileya and Reysenbach, 2014). It is of special interest that the MCR-containing *Archaeoglobi* MAG has the potential to use oxidized forms of sulfur, nitrate and iron as electron acceptors, expanding the ecological niches, where alkane degradation via CoM activation could take place (Boyd*, et al.*, 2018).

6.5 Future directions to unravel the nature of hydrocarbon-degrading archaea

This thesis unravelled novel divergent MCRs, which activate non-methane alkanes. In the future, one priority is to understand the catalytic mechanism of these MCR. For that, structural predictions relying only on the amino acid sequence may resolve poorly the real structural conformation of these MCRs, as they are based on the models predicted for canonical MCRs and cannot address the presence of post-translational modifications. Consequently, crystallization of these MCRs is of greatest interest, as the obtained protein structures will shed light on the way larger substrates are accommodated in the active centre and the role of post-translational modifications.

Several MCRs of methanogens have already been crystallized as well as an MCR of ANME-1 derived from dense microbial mats. Thus, the crystallization of the novel MCRs is a feasible task, though several challenges exist such as slow growth of the organisms of interest or presence of several MCR enzymes in the same organism. For *Ca.* Syntrophoarchaeum, we already attempted to detect MCR in protein extracts from several enrichment cultures, yet the MCR yield was much lower than for cultures of ANME-1, suggesting that larger amounts of culture will be required for successful enzyme crystallization. The effort for crystallizing MCRs should not be limited to a single organism, since the novel MCRs are quite diverse. So far, three clusters have been identified: *Bathyarchaeota/*D-C06, *Ca.* Syntrophoarchaeum and GoM-Arc1. Each cluster might be involved in the degradation of different substrates and, hence, they likely have quite different molecular conformations.

The crystallization of MCRs of these organisms would surely need of prior large-scale cultivation of the corresponding organisms. We already obtained enrichment cultures for *Ca.* Syntrophoarchaeum, while D-C06, GoM-Arc1 and *Bathyarchaeota* are yet not cultivated. Enrichment techniques are an adequate approach to start, since many of these organisms might live in syntrophy and have slow growth rates. Cultivation efforts should be firstly based on the proposed metabolisms: oxidation of long-chain alkanes coupled to methanogenesis for *Bathyarchaeota* and D-C06 and short-chain alkane oxidation coupled to sulfate-reduction for GoM-Arc1. The discovery of divergent MCRs in some members of the *Archaeoglobi* indicates that the clades mentioned in this thesis are likely not

the only ones with these MCRs. Therefore, cultivation should also target novel organisms and metabolisms like alkane oxidation coupled to nitrate reduction as it has been seen for AOM. Metagenomes from environmental samples could be a valuable resource to identify candidate organisms prior to the cultivation procedures. Additionally, the proposed metabolic pathways for further degradation of alkyl-CoM units must be confirmed. The current model is based on genomics, transcriptomics and proteomics data, but it includes unprecedented reactions and pathways like the proposed conversion of alkyl-CoM to acyl-CoA in *Ca.* Syntrophoarchaeum. Isotope labelling experiments and metabolomics will enable to elucidate the metabolic mechanisms of these organisms.

Future research should also focus on the ecological role of these organisms. First, researchers should investigate the global distribution of these clades with molecular surveys targeting the 16S rRNA gene and the novel *mcr* genes. Later, their environmental role should be studied, for instance by *in situ* incubations with stable isotope probing techniques. However, experiments like this would not be feasible in some cases like in deep oil reservoirs. Cultivation of samples of these sites could help the understanding of the process in these environments.

Finally, the appearance of novel *mcr* genes outside of the *Euryarchaeota,* like in *Bathyarchaeota* or in the novel clade *Verstraetearchaeota* (Vanwonterghem*, et al.*, 2016), has raised the possibility that the last archaeal ancestor was a methanogen harbouring MCR enzymes. The study of the novel MCRs from the evolutionary point of view will for sure contribute to comprehend the different phylogenetic relationships within archaea.

6.6 Concluding remarks

My thesis has focused on the study of hydrocarbon degradation by archaea. I have shown for the first time a novel archaeal pathway to degrade alkanes larger than methane via CoM activation. The enzymes responsible of the activation are modified versions of the MCR. The pathway has been demonstrated for butane and propane in enrichment cultures containing archaea of the *Ca.* Syntrophoarchaeum clade. After the CoM activation, they fully oxidized the alkanes using a combination of the fatty acid oxidation pathway, the Wood-Ljungdahl pathway and the downstream of the methanogenesis. The oxidation is coupled to sulfate reduction performed by syntrophic partner bacteria. Similar *mcr* genes were detected in MAGs affiliated to another archaeal cluster, D-C06. These archaea were detected within oil droplets in sediment samples from an oil seep of the Gulf of Mexico. According to their metabolic potential, D-C06 presumably degrade long-chain alkanes via CoM activation and the fatty acid oxidation pathway and they would couple the process to methanogenesis in the same cell, what would represent the first report of such a metabolism in a single organism. The finding of other divergent *mcr* genes in other clades like *Bathyarchaeota* and GoM-Arc1 indicates that this metabolism is more widespread and its potential role in the environment has been so far overlooked.

Bibliography

Abbasian F, Lockington R, Mallavarapu M and Naidu R (2015) A comprehensive review of aliphatic hydrocarbon biodegradation by bacteria. *Applied biochemistry and biotechnology* **176**: 670-699.

Abu Laban N, Selesi D, Rattei T, Tischler P and Meckenstock RU (2010) Identification of enzymes involved in anaerobic benzene degradation by a strictly anaerobic iron-reducing enrichment culture. *Environmental microbiology* **12**: 2783-2796.

Adam PS, Borrel G and Gribaldo S (2018) Evolutionary history of carbon monoxide dehydrogenase/acetyl-CoA synthase, one of the oldest enzymatic complexes. *Proceedings of the National Academy of Sciences* **115**: E1166-E1173.

Adam PS, Borrel G, Brochier-Armanet C and Gribaldo S (2017) The growing tree of Archaea: new perspectives on their diversity, evolution and ecology. *The ISME journal* **11**: 2407.

Adams M, Hoarfrost A, Bose A, Joye S and Girguis P (2013) Anaerobic oxidation of short-chain alkanes in hydrothermal sediments: potential influences on sulfur cycling and microbial diversity. *Frontiers in microbiology* **4**.

Aeckersberg F, Bak F and Widdel F (1991) Anaerobic oxidation of saturated hydrocarbons to CO_2 by a new type of sulfate-reducing bacterium. *Archives of Microbiology* **156**: 5-14.

Ahn Y, Krzycki JA and Floss HG (1991) Steric course of the reduction of ethyl coenzyme M to ethane catalyzed by methyl coenzyme M reductase from Methanosarcina barkeri. *Journal of the American Chemical Society* **113**: 4700-4701.

Aitken CM, Jones DM and Larter SR (2004) Anaerobic hydrocarbon biodegradation in deep subsurface oil reservoirs. *Nature* **431**: 291.

Aitken CM, Jones DM, Maguire MJ, Gray ND, Sherry A, Bowler BFJ, Ditchfield AK, Larter SR and Head IM (2013) Evidence that crude oil alkane activation proceeds by different mechanisms under sulfate-reducing and methanogenic conditions. *Geochimica et Cosmochimica Acta* **109**: 162-174.

Al-Mailem DM, Eliyas M and Radwan SS (2012) Enhanced haloarchaeal oil removal in hypersaline environments via organic nitrogen fertilization and illumination. *Extremophiles* **16**: 751-758.

Al-Mailem DM, Sorkhoh NA, Al-Awadhi H, Eliyas M and Radwan SS (2010) Biodegradation of crude oil and pure hydrocarbons by extreme halophilic archaea from hypersaline coasts of the Arabian Gulf. *Extremophiles* **14**: 321-328.

Alain K, Holler T, Musat F, Elvert M, Treude T and Krüger M (2006) Microbiological investigation of methane- and hydrocarbon-discharging mud volcanoes in the Carpathian Mountains, Romania. *Environmental microbiology* **8**: 574-590.

Amann R and Fuchs BM (2008) Single-cell identification in microbial communities by improved fluorescence in situ hybridization techniques. *Nature Reviews Microbiology* **6**: 339.

Amann RI, Binder BJ, Olson RJ, Chisholm SW, Devereux R and Stahl DA (1990) Combination of 16S rRNA-targeted oligonucleotide probes with flow cytometry for analyzing mixed microbial populations. *Applied and environmental microbiology* **56**: 1919-1925.

Anderson RT and Lovley DR (2000) Hexadecane decay by methanogenesis. *Nature* **404**: 722.

Annweiler E, Materna A, Safinowski M, Kappler A, Richnow HH, Michaelis W and Meckenstock RU (2000) Anaerobic Degradation of 2-Methylnaphthalene by a Sulfate-Reducing Enrichment Culture. *Applied and environmental microbiology* **66**: 5329-5333.

Asperger O, Naumann A and Kleber HP (1981) Occurrence of cytochrome P-450 in Acinetobacter strains after growth on n-hexadecane. *FEMS Microbiology Letters* **11**: 309-312.

Atlas RM and Bartha R (1972) Degradation and mineralization of petroleum in sea water: Limitation by nitrogen and phosphorous. *Biotechnology and Bioengineering* **14**: 309-318.

Baker BJ, Saw JH, Lind AE, Lazar CS, Hinrichs K-U, Teske AP and Ettema TJ (2016) Genomic inference of the metabolism of cosmopolitan subsurface Archaea, *Hadesarchaea*. *Nature Microbiology* **1**: 16002.

Ball HA, Johnson HA, Reinhard M and Spormann AM (1996) Initial reactions in anaerobic ethylbenzene oxidation by a denitrifying bacterium, strain EB1. *Journal of Bacteriology* **178**: 5755-5761.

Baptist JN, Gholson RK and Coon MJ (1963) Hydrocarbon oxidation by a bacterial enzyme system: I. Products of octane oxidation. *Biochimica et biophysica acta* **69**: 40-47.

Beal EJ, House CH and Orphan VJ (2009) Manganese- and Iron-Dependent Marine Methane Oxidation. *Science* **325**: 184-187.

Beller HR, Reinhard M and Grbić-Galić D (1992) Metabolic by-products of anaerobic toluene degradation by sulfate-reducing enrichment cultures. *Applied and environmental microbiology* **58**: 3192-3195.

Beller HR, Kane SR, Legler TC and Alvarez PJJ (2002) A Real-Time Polymerase Chain Reaction Method for Monitoring Anaerobic, Hydrocarbon-Degrading Bacteria Based on a Catabolic Gene. *Environmental Science and Technology* **36**: 3977-3984.

Beller HR, Kane SR, Legler TC, McKelvie JR, Sherwood Lollar B, Pearson F, Balser L and Mackay DM (2008) Comparative Assessments of Benzene, Toluene, and Xylene Natural Attenuation by Quantitative Polymerase Chain Reaction Analysis of a Catabolic Gene, Signature Metabolites, and Compound-Specific Isotope Analysis. *Environmental Science and Technology* **42**: 6065-6072.

Berdugo-Clavijo C and Gieg LM (2014) Conversion of crude oil to methane by a microbial consortium enriched from oil reservoir production waters. *Frontiers in microbiology* **5**.

Bergmann F, Selesi D, Weinmaier T, Tischler P, Rattei T and Meckenstock RU (2011) Genomic insights into the metabolic potential of the polycyclic aromatic hydrocarbon degrading sulfate-reducing Deltaproteobacterium N47. *Environmental microbiology* **13**: 1125-1137.

Bergmann FD, Selesi D and Meckenstock RU (2011) Identification of new enzymes potentially involved in anaerobic naphthalene degradation by the sulfate-reducing enrichment culture N47. *Archives of Microbiology* **193**: 241-250.

Bertrand JC, Almallah M, Acquaviva M and Mille G (1990) Biodegradation of hydrocarbons by an extremely halophilic archaebacterium. *Letters in Applied Microbiology* **11**: 260-263.

Boetius A, Ravenschlag K, Schubert CJ, Rickert D, Widdel F, Gieseke A, Amann R, Jørgensen BB, Witte U and Pfannkuche O (2000) A marine microbial consortium apparently mediating anaerobic oxidation of methane. *Nature* **407**: 623.

Botton S and Parsons JR (2007) Degradation of BTX by dissimilatory iron-reducing cultures. *Biodegradation* **18**: 371-381.

Boyd J, Jungbluth S, Leu A, Evans P, Woodcroft B, Chadwick G, Orphan V, Amend J, Rappe M and Tyson G (2018) Divergent methyl-coenzyme M reductase genes in a deep-subseafloor Archaeoglobi. *bioRxiv*.

Bregnard TP, Haner A, Hohener P and Zeyer J (1997) Anaerobic Degradation of Pristane in Nitrate-Reducing Microcosms and Enrichment Cultures. *Applied and environmental microbiology* **63**: 2077-2081.

Brileya K and Reysenbach A-L (2014) The Class Archaeoglobi. *The Prokaryotes: Other Major Lineages of Bacteria and The Archaea,*(Rosenberg E, DeLong EF, Lory S, Stackebrandt E and Thompson F, eds.), pp. 15-23. Springer Berlin Heidelberg, Berlin, Heidelberg.

Cai C, Leu AO, Xie G-J, Guo J, Feng Y, Zhao J-X, Tyson G, Yuan Z and Hu S (2018) A methanotrophic archaeon couples anaerobic oxidation of methane to Fe(III) reduction. *The ISME journal* **12**: 1929-1939.

Callaghan A (2013) Enzymes involved in the anaerobic oxidation of *n*-alkanes: from methane to long-chain paraffins. *Frontiers in microbiology* **4**.

Callaghan AV, Gieg LM, Kropp KG, Suflita JM and Young LY (2006) Comparison of Mechanisms of Alkane Metabolism under Sulfate-Reducing Conditions among Two Bacterial Isolates and a Bacterial Consortium. *Applied and environmental microbiology* **72**: 4274-4282.

Callaghan AV, Wawrik B, Ní Chadhain SM, Young LY and Zylstra GJ (2008) Anaerobic alkane-degrading strain AK-01 contains two alkylsuccinate synthase genes. *Biochemical and Biophysical Research Communications* **366**: 142-148.

Callaghan AV, Davidova IA, Savage-Ashlock K, Parisi VA, Gieg LM, Suflita JM, Kukor JJ and Wawrik B (2010) Diversity of Benzyl- and Alkylsuccinate Synthase Genes in Hydrocarbon-Impacted Environments and Enrichment Cultures. *Environmental Science and Technology* **44**: 7287-7294.

Canfield DE (1993) Organic Matter Oxidation in Marine Sediments. In: Wollast R, Mackenzie FT, Chou L (eds.) *Interactions of C, N, P and S Biogeochemical Cycles and Global Change.* NATO ASI Series (SeriesI: Global Environmental Change), vol 4. Springer, Berlin, Heidelberg.

Canfield DE and Thamdrup B (2009) Towards a consistent classification scheme for geochemical environments, or, why we wish the term 'suboxic' would go away. *Geobiology* **7**: 385-392.

Cao B, Nagarajan K and Loh K-C (2009) Biodegradation of aromatic compounds: current status and opportunities for biomolecular approaches. *Applied Microbiology and Biotechnology* **85**: 207-228.

Chan SI, Chen KHC, Yu SSF, Chen C-L and Kuo SSJ (2004) Toward Delineating the Structure and Function of the Particulate Methane Monooxygenase from Methanotrophic Bacteria. *Biochemistry* **43**: 4421-4430.

Chang W, Um Y and Holoman TRP (2006) Polycyclic Aromatic Hydrocarbon (PAH) Degradation Coupled to Methanogenesis. *Biotechnology Letters* **28**: 425-430.

Chang Y-H, Cheng T-W, Lai W-J, Tsai W-Y, Sun C-H, Lin L-H and Wang P-L (2012) Microbial methane cycling in a terrestrial mud volcano in eastern Taiwan. *Environmental microbiology* **14**: 895-908.

Cheng L, Dai L, Li X, Zhang H and Lu Y (2011) Isolation and Characterization of *Methanothermobacter crinale* sp. nov., a Novel Hydrogenotrophic Methanogen from the Shengli Oil Field. *Applied and environmental microbiology* **77**: 5212-5219.

Cheng L, Rui J, Li Q, Zhang H and Lu Y (2013) Enrichment and dynamics of novel syntrophs in a methanogenic hexadecane-degrading culture from a Chinese oilfield. *FEMS Microbiology Ecology* **83**: 757-766.

Cheng L, Shi S, Li Q, Chen J, Zhang H and Lu Y (2014) Progressive Degradation of Crude Oil *n*-Alkanes Coupled to Methane Production under Mesophilic and Thermophilic Conditions. *PLoS One* **9**: e113253.

Cheng Q, Thomas S and Rouvière P (2002) Biological conversion of cyclic alkanes and cyclic alcohols into dicarboxylic acids: biochemical and molecular basis. *Applied Microbiology and Biotechnology* **58**: 704-711.

Coates JD, Anderson RT, Woodward JC, Phillips EJP and Lovley DR (1996) Anaerobic Hydrocarbon Degradation in Petroleum-Contaminated Harbor Sediments under Sulfate-Reducing and Artificially Imposed Iron-Reducing Conditions. *Environmental Science and Technology* **30**: 2784-2789.

Coates JD, Chakraborty R, Lack JG, O'Connor SM, Cole KA, Bender KS and Achenbach LA (2001) Anaerobic benzene oxidation coupled to nitrate reduction in pure culture by two strains of *Dechloromonas*. *Nature* **411**: 1039.

Coon MJ (2005) Omega Oxygenases: Nonheme-iron enzymes and P450 cytochromes. *Biochemical and Biophysical Research Communications* **338**: 378-385.

Cord-Ruwisch R (1985) A quick method for the determination of dissolved and precipitated sulfides in cultures of sulfate-reducing bacteria. *Journal of Microbiological Methods* **4**: 33-36.

Cox GB, Young IG, McCann LM and Gibson F (1969) Biosynthesis of Ubiquinone in *Escherichia coli* K-12: Location of Genes Affecting the Metabolism of 3-Octaprenyl-4-hydroxybenzoic Acid and 2-Octaprenylphenol. *Journal of Bacteriology* **99**: 450-458.

Cravo-Laureau C, Matheron R, Cayol J-L, Joulian C and Hirschler-Réa A (2004) *Desulfatibacillum aliphaticivorans* gen. nov., sp. nov., an *n*-alkane- and *n*-alkene-degrading, sulfate-reducing bacterium. *International Journal of Systematic and Evolutionary Microbiology* **54**: 77-83.

Crowe SA, Katsev S, Leslie K, Sturm A, Magen C, Nomosatryo S, Pack MA, Kessler JD, Reeburgh WS, Roberts JA, Gonzaléz L, Douglas Haffner G, Mucci A, Sundby B and Fowle DA (2011) The methane cycle in ferruginous Lake Matano. *Geobiology* **9**: 61-78.

Curiale JA and Frolov EB (1998) Occurrence and origin of olefins in crude oils. A critical review. *Organic Geochemistry* **29**: 397-408.

Daims H, Brühl A, Amann R, Schleifer K-H and Wagner M (1999) The Domain-specific Probe EUB338 is Insufficient for the Detection of all Bacteria: Development and Evaluation of a more Comprehensive Probe Set. *Systematic and applied microbiology* **22**: 434-444.

Davidova IA, Duncan KE, Choi OK and Suflita JM (2006) *Desulfoglaeba alkanexedens* gen. nov., sp. nov., an *n*-alkane-degrading, sulfate-reducing bacterium. *International Journal of Systematic and Evolutionary Microbiology* **56**: 2737-2742.

Davidova IA, Gieg LM, Nanny M, Kropp KG and Suflita JM (2005) Stable Isotopic Studies of *n*-Alkane Metabolism by a Sulfate-Reducing Bacterial Enrichment Culture. *Applied and environmental microbiology* **71**: 8174-8182.

Deutzmann JS and Schink B (2011) Anaerobic Oxidation of Methane in Sediments of Lake Constance, an Oligotrophic Freshwater Lake. *Applied and environmental microbiology* **77**: 4429-4436.

DiDonato RJ, Jr., Young ND, Butler JE, Chin K-J, Hixson KK, Mouser P, Lipton MS, DeBoy R and Methé BA (2010) Genome Sequence of the Deltaproteobacterial Strain NaphS2 and Analysis of Differential Gene Expression during Anaerobic Growth on Naphthalene. *PLoS One* **5**: e14072.

Dolfing J, Larter SR and Head IM (2007) Thermodynamic constraints on methanogenic crude oil biodegradation. *The ISME journal* **2**: 442.

Dolfing J, Zeyer J, Binder-Eicher P and Schwarzenbach RP (1990) Isolation and characterization of a bacterium that mineralizes toluene in the absence of molecular oxygen. *Archives of Microbiology* **154**: 336-341.

Dombrowski N, Seitz KW, Teske AP and Baker BJ (2017) Genomic insights into potential interdependencies in microbial hydrocarbon and nutrient cycling in hydrothermal sediments. *Microbiome* **5**: 106.

Dowell F, Cardman Z, Dasarathy S, Kellermann MY, Lipp JS, Ruff SE, Biddle JF, McKay LJ, MacGregor BJ, Lloyd KG, Albert DB, Mendlovitz H, Hinrichs K-U and Teske A (2016) Microbial Communities in Methane- and Short Chain Alkane-Rich Hydrothermal Sediments of Guaymas Basin. *Frontiers in microbiology* **7**.

Duetz WA, Bouwmeester H, van Beilen JB and Witholt B (2003) Biotransformation of limonene by bacteria, fungi, yeasts, and plants. *Applied Microbiology and Biotechnology* **61**: 269-277.

Durisch-Kaiser E, Klauser L, Wehrli B and Schubert C (2005) Evidence of Intense Archaeal and Bacterial Methanotrophic Activity in the Black Sea Water Column. *Applied and environmental microbiology* **71**: 8099-8106.

Dyksterhouse SE, Gray JP, Herwig RP, Lara JC and Staley JT (1995) *Cycloclasticus pugetii* gen. nov., sp. nov., an aromatic hydrocarbon-degrading bacterium from marine sediments. *International Journal of Systematic and Evolutionary Microbiology* **45**: 116-123.

Edwards EA and Grbić-Galić D (1992) Complete mineralization of benzene by aquifer microorganisms under strictly anaerobic conditions. *Applied and environmental microbiology* **58**: 2663-2666.

Edwards EA and Grbić-Galić D (1994) Anaerobic degradation of toluene and *o*-xylene by a methanogenic consortium. *Applied and environmental microbiology* **60**: 313-322.

Ehrenreich P, Behrends A, Harder J and Widdel F (2000) Anaerobic oxidation of alkanes by newly isolated denitrifying bacteria. *Archives of Microbiology* **173**: 58-64.

Einsele G, Gieskes JM, Curray J, Moore DM, Aguayo E, Aubry M-P, Fornari D, Guerrero J, Kastner M, Kelts K, Lyle M, Matoba Y, Molina-Cruz A, Niemitz J, Rueda J, Saunders A, Schrader H, Simoneit B and Vacquier V (1980) Intrusion of basaltic sills into highly porous sediments, and resulting hydrothermal activity. *Nature* **283**: 441.

Elliott SJ, Zhu M, Tso L, Nguyen HHT, Yip JHK and Chan SI (1997) Regio- and Stereoselectivity of Particulate Methane Monooxygenase from *Methylococcus capsulatus* (Bath). *Journal of the American Chemical Society* **119**: 9949-9955.

Elsaied HE (2014) Genotyping of uncultured archaea in a polluted site of Suez Gulf, Egypt, based on 16S rRNA gene analyses. *The Egyptian Journal of Aquatic Research* **40**: 27-33.

Engelhardt MA, Daly K, Swannell RPJ and Head IM (2001) Isolation and characterization of a novel hydrocarbon-degrading, Gram-positive bacterium, isolated from intertidal beach sediment, and description of *Planococcus alkanoclasticus* sp. nov. *Journal of Applied Microbiology* **90**: 237-247.

Ermler U, Grabarse W, Shima S, Goubeaud M and Thauer RK (1997) Crystal Structure of Methyl-Coenzyme M Reductase: The Key Enzyme of Biological Methane Formation. *Science* **278**: 1457-1462.

Ettwig KF, Zhu B, Speth D, Keltjens JT, Jetten MSM and Kartal B (2016) Archaea catalyze iron-dependent anaerobic oxidation of methane. *Proceedings of the National Academy of Sciences* **113**: 12792-12796.

Ettwig KF, Butler MK, Le Paslier D, Pelletier E, Mangenot S, Kuypers MMM, Schreiber F, Dutilh BE, Zedelius J, de Beer D, Gloerich J, Wessels HJCT, van Alen T, Luesken F, Wu ML, van de Pas-Schoonen KT, Op den Camp HJM, Janssen-Megens EM, Francoijs KJ, Stunnenberg H, Weissenbach J, Jetten MSM and Strous M (2010) Nitrite-driven anaerobic methane oxidation by oxygenic bacteria. *Nature* **464**: 543.

Evans PJ, Ling W, Goldschmidt B, Ritter ER and Young LY (1992) Metabolites formed during anaerobic transformation of toluene and *o*-xylene and their proposed relationship to the initial steps of toluene mineralization. *Applied and environmental microbiology* **58**: 496-501.

Evans PN, Parks DH, Chadwick GL, Robbins SJ, Orphan VJ, Golding SD and Tyson GW (2015) Methane metabolism in the archaeal phylum Bathyarchaeota revealed by genome-centric metagenomics. *Science* **350**: 434-438.

Fathepure BZ (2014) Recent studies in microbial degradation of petroleum hydrocarbons in hypersaline environments. *Frontiers in microbiology* **5**.

Fernandes AD, Reid JN, Macklaim JM, McMurrough TA, Edgell DR and Gloor GB (2014) Unifying the analysis of high-throughput sequencing datasets: characterizing RNA-seq, 16S rRNA gene sequencing and selective growth experiments by compositional data analysis. *Microbiome* **2**: 15.

Forney FW and Markovetz AJ (1970) Subterminal Oxidation of Aliphatic Hydrocarbons. *Journal of Bacteriology* **102**: 281-282.

Foss S, Heyen U and Harder J (1998) *Alcaligenes defragrans* sp. nov., description of four strains isolated on alkenoic monoterpenes ((+)-menthene, α-pinene, 2-carene, and α-phellandrene) and nitrate. *Systematic and applied microbiology* **21**: 237-244.

Friedrich MW (2005) Methyl-Coenzyme M Reductase Genes: Unique Functional Markers for Methanogenic and Anaerobic Methane-Oxidizing Archaea. *Methods in Enzymology,* Vol. 397, pp. 428-442. Academic Press.

Fuchs G, Boll M and Heider J (2011) Microbial degradation of aromatic compounds — from one strategy to four. *Nature Reviews Microbiology* **9**: 803.

Funhoff EG, Bauer U, García-Rubio I, Witholt B and van Beilen JB (2006) CYP153A6, a Soluble P450 Oxygenase Catalyzing Terminal-Alkane Hydroxylation. *Journal of Bacteriology* **188**: 5220-5227.

Funk MA, Marsh ENG and Drennan CL (2015) Substrate-bound Structures of Benzylsuccinate Synthase Reveal How Toluene Is Activated in Anaerobic Hydrocarbon Degradation. *Journal of Biological Chemistry* **290**: 22398-22408.

Funk MA, Judd ET, Marsh ENG, Elliott SJ and Drennan CL (2014) Structures of benzylsuccinate synthase elucidate roles of accessory subunits in glycyl radical enzyme activation and activity. *Proceedings of the National Academy of Sciences* **111**: 10161-10166.

Geiselbrecht AD, Hedlund BP, Tichi MA and Staley JT (1998) Isolation of Marine Polycyclic Aromatic Hydrocarbon (PAH)-Degrading *Cycloclasticus* Strains from the Gulf of Mexico and Comparison of Their PAH Degradation Ability with That of Puget Sound *Cycloclasticus* Strains. *Applied and environmental microbiology* **64**: 4703-4710.

Gibson DT (1984) *Microbial degradation of organic compounds*. Marcel Dekker Inc.

Gieg LM, Duncan KE and Suflita JM (2008) Bioenergy Production via Microbial Conversion of Residual Oil to Natural Gas. *Applied and environmental microbiology* **74**: 3022-3029.

Gieg LM, Fowler SJ and Berdugo-Clavijo C (2014) Syntrophic biodegradation of hydrocarbon contaminants. *Current Opinion in Biotechnology* **27**: 21-29.

Gittel A, Donhauser J, Røy H, Girguis PR, Jørgensen BB and Kjeldsen KU (2015) Ubiquitous Presence and Novel Diversity of Anaerobic Alkane Degraders in Cold Marine Sediments. *Frontiers in microbiology* **6**: 1414.

Goenrich M, Duin EC, Mahlert F and Thauer RK (2005) Temperature dependence of methyl-coenzyme M reductase activity and of the formation of the methyl-coenzyme M reductase red2 state induced by coenzyme B. *JBIC Journal of Biological Inorganic Chemistry* **10**: 333-342.

Golyshin PN, Chernikova TN, Abraham W-R, Lünsdorf H, Timmis KN and Yakimov MM (2002) *Oleiphilaceae* fam. nov., to include *Oleiphilus messinensis* gen. nov., sp. nov., a novel marine bacterium that obligately utilizes hydrocarbons. *International Journal of Systematic and Evolutionary Microbiology* **52**: 901-911.

Gouy M, Guindon S and Gascuel O (2010) SeaView Version 4: A Multiplatform Graphical User Interface for Sequence Alignment and Phylogenetic Tree Building. *Molecular Biology and Evolution* **27**: 221-224.

Grabarse W, Mahlert F, Duin EC, Goubeaud M, Shima Seigo, Thauer RK, Lamzin V and Ermler U (2001) On the mechanism of biological methane formation: structural evidence for conformational changes in methyl-coenzyme M reductase upon substrate binding. Edited by R. Huber. *Journal of Molecular Biology* **309**: 315-330.

Gray ND, Sherry A, Grant RJ, Rowan AK, Hubert CRJ, Callbeck CM, Aitken CM, Jones DM, Adams JJ, Larter SR and Head IM (2011) The quantitative significance of *Syntrophaceae* and syntrophic partnerships in methanogenic degradation of crude oil alkanes. *Environmental microbiology* **13**: 2957-2975.

Grossi V, Cravo-Laureau C, Rontani J-F, Cros M and Hirschler-Réa A (2011) Anaerobic oxidation of n-alkenes by sulphate-reducing bacteria from the genus *Desulfatiferula*: *n*-Ketones as potential metabolites. *Research in Microbiology* **162**: 915-922.

Grossi V, Cravo-Laureau C, Méou A, Raphel D, Garzino F and Hirschler-Réa A (2007) Anaerobic 1-Alkene Metabolism by the Alkane- and Alkene-Degrading Sulfate Reducer *Desulfatibacillum aliphaticivorans* Strain CV2803(T). *Applied and environmental microbiology* **73**: 7882-7890.

Grossi V, Raphel D, Hirschler-Réa A, Gilewicz M, Mouzdahir A, Bertrand J-C and Rontani J-F (2000) Anaerobic biodegradation of pristane by a marine sedimentary bacterial and/or archaeal community. *Organic Geochemistry* **31**: 769-772.

Grossman EL, Cifuentes LA and Cozzarelli IM (2002) Anaerobic Methane Oxidation in a Landfill-Leachate Plume. *Environmental Science and Technology* **36**: 2436-2442.

Grundmann O, Behrends A, Rabus R, Amann J, Halder T, Heider J and Widdel F (2008) Genes encoding the candidate enzyme for anaerobic activation of n-alkanes in the denitrifying bacterium, strain HxN1. *Environmental microbiology* **10**: 376-385.

Gundersen JK, Jorgensen BB, Larsen E and Jannasch HW (1992) Mats of giant sulphur bacteria on deep-sea sediments due to fluctuating hydrothermal flow. *Nature* **360**: 454.

Gunsalus RP, Romesser JA and Wolfe RS (1978) Preparation of coenzyme M analogs and their activity in the methyl coenzyme M reductase system of Methanobacterium thermoautotrophicum. *Biochemistry* **17**: 2374-2377.

Hallam SJ, Putnam N, Preston CM, Detter JC, Rokhsar D, Richardson PM and DeLong EF (2004) Reverse Methanogenesis: Testing the Hypothesis with Environmental Genomics. *Science* **305**: 1457-1462.

Hanson RS and Hanson TE (1996) Methanotrophic bacteria. *Microbiological Reviews* **60**: 439-471.

Harms G, Zengler K, Rabus R, Aeckersberg F, Minz D, Rosselló-Mora R and Widdel F (1999) Anaerobic Oxidation of *o*-Xylene, *m*-Xylene, and Homologous Alkylbenzenes by New Types of Sulfate-Reducing Bacteria. *Applied and environmental microbiology* **65**: 999-1004.

Haroon MF, Hu S, Shi Y*,* Imelfort M, Keller J, Hugenholtz P, Yuan Z and Tyson GW (2013) Anaerobic oxidation of methane coupled to nitrate reduction in a novel archaeal lineage. *Nature* **500**: 567.

Harwood CS, Burchhardt G, Herrmann H and Fuchs G (1998) Anaerobic metabolism of aromatic compounds via the benzoyl-CoA pathway. *FEMS Microbiology Reviews* **22**: 439-458.

Hazen TC, Dubinsky EA, DeSantis TZ*, et al.* (2010) Deep-Sea Oil Plume Enriches Indigenous Oil-Degrading Bacteria. *Science* **330**: 204-208.

He Y, Li M, Perumal V*,* Feng X, Fang J, Xie J, Sievert SM and Wang F (2016) Genomic and enzymatic evidence for acetogenesis among multiple lineages of the archaeal phylum Bathyarchaeota widespread in marine sediments. *Nature Microbiology* **1**: 16035.

Head IM, Jones DM and Röling WFM (2006) Marine microorganisms make a meal of oil. *Nature Reviews Microbiology* **4**: 173.

Head IM, Larter SR, Gray ND*,* Sherry A, Adams JJ, Aitken CM, Jones DM, Rowan AK, Huang H and Röling WFM (2010) Hydrocarbon Degradation in Petroleum Reservoirs. *Handbook of Hydrocarbon and Lipid Microbiology,* Timmis KN, ed., pp. 3097-3109. Springer, Berlin, Heidelberg.

Hinrichs K-U and Boetius A (2003) The Anaerobic Oxidation of Methane: New Insights in Microbial Ecology and Biogeochemistry. *Ocean Margin Systems,* (Wefer G, Billett D, Hebbeln D, Jørgensen BB, Schlüter M and van Weering TCE, ed.), pp. 457-477. Springer, Berlin, Heidelberg.

Hinrichs K-U, Hayes JM, Sylva SP, Brewer PG and DeLong EF (1999) Methane-consuming archaebacteria in marine sediments. *Nature* **398**: 802.

Hippler B and Thauer RK (1999) The energy conserving methyltetrahydromethanopterin:coenzyme M methyltransferase complex from methanogenic archaea: function of the subunit MtrH. *FEBS Letters* **449**: 165-168.

Hoehler TM, Alperin MJ, Albert DB and Martens CS (1994) Field and laboratory studies of methane oxidation in an anoxic marine sediment: Evidence for a methanogen-sulfate reducer consortium. *Global Biogeochemical Cycles* **8**: 451-463.

Holler T, Widdel F, Knittel K, Amann R, Kellermann MY, Hinrichs K-U, Teske A, Boetius A, Wegener G (2011) Thermophilic anaerobic oxidation of methane by marine microbial consortia. *The ISME journal* **5**: 1946.

Holmes DE, Risso C, Smith JA and Lovley DR (2011) Anaerobic Oxidation of Benzene by the Hyperthermophilic Archaeon Ferroglobus placidus. *Applied and environmental microbiology* **77**: 5926-5933.

Horng Y-C, Becker DF and Ragsdale SW (2001) Mechanistic Studies of Methane Biogenesis by Methyl-Coenzyme M Reductase: Evidence that Coenzyme B Participates in Cleaving the C−S Bond of Methyl-Coenzyme M. *Biochemistry* **40**: 12875-12885.

Hu S, Zeng RJ, Haroon MF, Keller J, Lant PA, Tyson GW and Yuan Z (2015) A laboratory investigation of interactions between denitrifying anaerobic methane oxidation (DAMO) and anammox processes in anoxic environments. *Scientific Reports* **5**: 8706.

Iida T, Sumita T, Ohta A and Takagi M (2000) The cytochrome P450ALK multigene family of an n-alkane-assimilating yeast, *Yarrowia lipolytica*: cloning and characterization of genes coding for new CYP52 family members. *Yeast* **16**: 1077-1087.

IPCC (2014) *Report I: Anthropogenic and Natural Radiative Forcing*. Intergovernmental Panel on Climate Change, pp. 659-740. Cambridge University Press, Cambridge.

Iversen N and Jorgensen BB (1985) Anaerobic methane oxidation rates at the sulfate-methane transition in marine sediments from Kattegat and Skagerrak (Denmark). *Limnology and Oceanography* **30**: 944-955.

Iwabuchi N, Sunairi M, Urai M, Itoh C, Anzai H, Nakajima M and Harayama S (2002) Extracellular Polysaccharides of *Rhodococcus rhodochrous* S-2 Stimulate the Degradation of Aromatic Components in Crude Oil by Indigenous Marine Bacteria. *Applied and environmental microbiology* **68**: 2337-2343.

Jaekel U, Zedelius J, Wilkes H and Musat F (2015) Anaerobic degradation of cyclohexane by sulfate-reducing bacteria from hydrocarbon-contaminated marine sediments. *Frontiers in microbiology* **6**: 116.

Ji Y, Mao G, Wang Y and Bartlam M (2013) Structural insights into diversity and *n*-alkane biodegradation mechanisms of alkane hydroxylases. *Frontiers in microbiology* **4**.

Jobst B, Schühle K, Linne U and Heider J (2010) ATP-Dependent Carboxylation of Acetophenone by a Novel Type of Carboxylase. *Journal of Bacteriology* **192**: 1387-1394.

Johnson EL and Hyman MR (2006) Propane and *n*-butane oxidation by Pseudomonas putida GPo1. *Applied and environmental microbiology* **72**: 950-952.

Johnson JM, Wawrik B, Isom C, Boling WB and Callaghan AV (2015) Interrogation of Chesapeake Bay sediment microbial communities for intrinsic alkane-utilizing potential under anaerobic conditions. *FEMS Microbiology Ecology* **91**: 1-14.

Jones DM, Head IM, Gray ND, Adams JJ, Rowan AK, Aitken CM, Bennett B, Huang H, Brown A, Bowler BFJ, Oldenburg T, Erdmann M and Larter SR (2007) Crude-oil biodegradation via methanogenesis in subsurface petroleum reservoirs. *Nature* **451**: 176.

Joye SB, Boetius A, Orcutt BN, Montoya JP, Schulz HN, Erickson MJ and Lugo SK (2004) The anaerobic oxidation of methane and sulfate reduction in sediments from Gulf of Mexico cold seeps. *Chemical Geology* **205**: 219-238.

Jungbluth SP, Amend JP and Rappé MS (2017) Metagenome sequencing and 98 microbial genomes from Juan de Fuca Ridge flank subsurface fluids. *Scientific Data* **4**: 170037.

Kasai Y, Kishira H and Harayama S (2002) Bacteria Belonging to the Genus *Cycloclasticus* Play a Primary Role in the Degradation of Aromatic Hydrocarbons Released in a Marine Environment. *Applied and environmental microbiology* **68**: 5625-5633.

Kasai Y, Takahata Y, Hoaki T and Watanabe K (2005) Physiological and molecular characterization of a microbial community established in unsaturated, petroleum-contaminated soil. *Environmental microbiology* **7**: 806-818.

Kasai Y, Kishira H, Sasaki T, Syutsubo K, Watanabe K and Harayama S (2002) Predominant growth of *Alcanivorax* strains in oil-contaminated and nutrient-supplemented sea water. *Environmental microbiology* **4**: 141-147.

Kessler JD, Valentine DL, Redmond MC, Du M, Chan EW, Mendes SD, Quiroz EW, Villanueva CJ, Shusta SS, Werra LM, Yvon-Lewis SA and Weber TC (2011) A Persistent Oxygen Anomaly Reveals the Fate of Spilled Methane in the Deep Gulf of Mexico. *Science* **331**: 312-315.

Khelifi N, Grossi V, Hamdi M, Dolla A, Tholozan J-L, Ollivier B and Hirschler-Réa A (2010) Anaerobic Oxidation of Fatty Acids and Alkenes by the Hyperthermophilic Sulfate-Reducing Archaeon *Archaeoglobus fulgidus*. *Applied and environmental microbiology* **76**: 3057-3060.

Khelifi N, Amin Ali O, Roche P, Grossi V, Brochier-Armanet C, Valette O, Ollivier B, Dolla A, Hirschler-Réa A (2014) Anaerobic oxidation of long-chain *n*-alkanes by the hyperthermophilic sulfate-reducing archaeon, Archaeoglobus fulgidus. *The ISME journal* **8**: 2153.

Kim TJ, Lee EY, Kim YJ, Cho K-S and Ryu HW (2003) Degradation of polyaromatic hydrocarbons by *Burkholderia cepacia* 2A-12. *World Journal of Microbiology and Biotechnology* **19**: 411-417.

King G, Smith C, Tolar B and Hollibaugh J (2013) Analysis of Composition and Structure of Coastal to Mesopelagic Bacterioplankton Communities in the Northern Gulf of Mexico. *Frontiers in microbiology* **3**.

King GM, Kostka JE, Hazen TC and Sobecky PA (2015) Microbial Responses to the Deepwater Horizon Oil Spill: From Coastal Wetlands to the Deep Sea. *Annual Review of Marine Science* **7**: 377-401.

Kleindienst S (2012) *Hydrocarbon-degrading sulfate-reducing bacteria in marine hydrocarbon seep sediments.* PhD thesis, Universität Bremen, Bremen.

Kleindienst S, Ramette A, Amann R and Knittel K (2012) Distribution and in situ abundance of sulfate-reducing bacteria in diverse marine hydrocarbon seep sediments. *Environmental microbiology* **14**: 2689-2710.

Kleindienst S, Herbst F-A, Stagars M*,* von Netzer F, von Bergen M, Seifert J, Peplies J, Amann R, Musat F, Lueders T and Knittel K (2014) Diverse sulfate-reducing bacteria of the *Desulfosarcina/ Desulfococcus* clade are the key alkane degraders at marine seeps. *The ISME journal* **8**: 2029.

Klenk H-P, Clayton RA, Tomb J-F*, et al.* (1998) The complete genome sequence of the hyperthermophilic, sulphate-reducing archaeon *Archaeoglobus fulgidus*. *Nature* **394**: 101.

Kloer DP, Hagel C, Heider J and Schulz GE (2006) Crystal Structure of Ethylbenzene Dehydrogenase from Aromatoleum aromaticum. *Structure* **14**: 1377-1388.

Kniemeyer O and Heider J (2001) Ethylbenzene dehydrogenase, a novel hydrocarbon-oxidising molybdenum/iron-sulfur/heme enzyme. *Journal of Biological Chemistry*.

Kniemeyer O and Heider J (2001) (S)-1-Phenylethanol dehydrogenase of *Azoarcus* sp. strain EbN1, an enzyme of anaerobic ethylbenzene catabolism. *Archives of Microbiology* **176**: 129-135.

Kniemeyer O, Fischer T, Wilkes H, Glöckner FO and Widdel F (2003) Anaerobic Degradation of Ethylbenzene by a New Type of Marine Sulfate-Reducing Bacterium. *Applied and environmental microbiology* **69**: 760-768.

Kniemeyer O, Musat F, Sievert SM*,* Knittel K, Wilkes H, Blumenberg M, Michaelis W, Classen A, Bolm C and Joye SB (2007) Anaerobic oxidation of short-chain hydrocarbons by marine sulphate-reducing bacteria. *Nature* **449**: 898.

Knittel K and Boetius A (2009) Anaerobic Oxidation of Methane: Progress with an Unknown Process. *Annual Review of Microbiology* **63**: 311-334.

Knittel K, Lösekann T, Boetius A, Kort R and Amann R (2005) Diversity and Distribution of Methanotrophic Archaea at Cold Seeps. *Applied and environmental microbiology* **71**: 467-479.

Knittel K, Boetius A, Lemke A*,* Eilers H, Lochte K, Pfannkuche O, Linke P and Amann R (2003) Activity, Distribution, and Diversity of Sulfate Reducers and Other Bacteria in Sediments above Gas Hydrate (Cascadia Margin, Oregon). *Geomicrobiology Journal* **20**: 269-294.

Kobayashi H, Endo K, Sakata S*,* Mayumi D, Kawaguchi H, Ikarashi M, Miyagawa Y, Maeda H and Sato K (2012) Phylogenetic diversity of microbial communities associated with the crude-oil, large-insoluble-particle and formation-water components of the reservoir fluid from a non-flooded high-temperature petroleum reservoir. *Journal of Bioscience and Bioengineering* **113**: 204-210.

Koschinsky A (2014) Hydrothermal Vent Fluids (Seafloor). *Encyclopedia of Marine Geosciences,* (Harff J, Meschede M, Petersen S and Thiede J, eds.), pp. 1-8. Springer Netherlands, Dordrecht.

Kostichka K, Thomas SM, Gibson KJ, Nagarajan V and Cheng Q (2001) Cloning and Characterization of a Gene Cluster for Cyclododecanone Oxidation in Rhodococcus ruber SC1. *Journal of Bacteriology* **183**: 6478-6486.

Kostka JE, Prakash O, Overholt WA, Green SJ, Freyer G, Canion A, Delgardio J, Norton N, Hazen TC, and Huettel M (2011) Hydrocarbon-Degrading Bacteria and the Bacterial Community Response in Gulf of Mexico Beach Sands Impacted by the Deepwater Horizon Oil Spill. *Applied and environmental microbiology* **77**: 7962-7974.

Kotani T, Yamamoto T, Yurimoto H, Sakai Y and Kato N (2003) Propane Monooxygenase and NAD-Dependent Secondary Alcohol Dehydrogenase in Propane Metabolism by *Gordonia* sp. Strain. *Journal of Bacteriology* **185**: 7120-7128.

Krieger CJ, Beller HR, Reinhard M and Spormann AM (1999) Initial Reactions in Anaerobic Oxidation of *m*-Xylene by the Denitrifying Bacterium *Azoarcus* sp. Strain T. *Journal of Bacteriology* **181**: 6403-6410.

Kropp KG, Davidova IA and Suflita JM (2000) Anaerobic Oxidation of *n*-Dodecane by an Addition Reaction in a Sulfate-Reducing Bacterial Enrichment Culture. *Applied and environmental microbiology* **66**: 5393-5398.

Krüger M, Meyerdierks A, Glöckner FO, Amann R, Widdel F, Kube M, Reinhardt R, Kahnt J, Böcher R, Thauer RK and Shima S (2003) A conspicuous nickel protein in microbial mats that oxidize methane anaerobically. *Nature* **426**: 878.

Krukenberg V, Riedel D, Gruber-Vodicka HR, Buttigieg PL, Tegetmeyer HE, Boetius A and Wegener G (2018) Gene expression and ultrastructure of meso- and thermophilic methanotrophic consortia. *Environmental microbiology* **20**: 1651-1666.

Krukenberg V, Harding K, Richter M, Glöckner FO, Gruber-Vodicka HR, Adam B, Berg JS, Knittel K, Tegetmeyer HE and Boetius A (2016) *Candidatus* Desulfofervidus auxilii, a hydrogenotrophic sulfate-reducing bacterium involved in the thermophilic anaerobic oxidation of methane. *Environmental microbiology* **18**: 3073-3091.

Kubo K, Lloyd KG, F Biddle J, Amann R, Teske A and Knittel K (2012) Archaea of the Miscellaneous Crenarchaeotal Group are abundant, diverse and widespread in marine sediments. *The ISME journal* **6**: 1949.

Kuhn EP, Colberg PJ, Schnoor JL, Wanner O, Zehnder AJ and Schwarzenbach RP (1985) Microbial transformations of substituted benzenes during infiltration of river water to groundwater: laboratory column studies. *Environmental Science and Technology* **19**: 961-968.

Kvenvolden KA and Cooper CK (2003) Natural seepage of crude oil into the marine environment. *Geo-Marine Letters* **23**: 140-146.

Leuthner B and Heider J (2000) Anaerobic Toluene Catabolism of *Thauera aromatica*: the *bbs* Operon Codes for Enzymes of β Oxidation of the Intermediate Benzylsuccinate. *Journal of Bacteriology* **182**: 272-277.

Leuthner B, Leutwein C, Schulz H, Hörth P, Haehnel W, Schitz E, Schägger H and Heider J (1998) Biochemical and genetic characterization of benzylsuccinate synthase from *Thauera aromatica*: a new glycyl radical enzyme catalysing the first step in anaerobic toluene metabolism. *Molecular Microbiology* **28**: 615-628.

Li L, Liu X, Yang W, Xu F, Wang W, Feng L, Bartlman M, Wang L and Rao Z (2008) Crystal Structure of Long-Chain Alkane Monooxygenase (LadA) in Complex with Coenzyme FMN: Unveiling the Long-Chain Alkane Hydroxylase. *Journal of Molecular Biology* **376**: 453-465.

Liu R, Zhang Y, Ding R, Li D, Gao Y and Yang M (2009) Comparison of archaeal and bacterial community structures in heavily oil-contaminated and pristine soils. *Journal of Bioscience and Bioengineering* **108**: 400-407.

Lloyd KG, Lapham L and Teske A (2006) An Anaerobic Methane-Oxidizing Community of ANME-1b Archaea in Hypersaline Gulf of Mexico Sediments. *Applied and environmental microbiology* **72**: 7218-7230.

Lonsdale P and Becker K (1985) Hydrothermal plumes, hot springs, and conductive heat flow in the Southern Trough of Guaymas Basin. *Earth and Planetary Science Letters* **73**: 211-225.

Lovley DR and Lonergan DJ (1990) Anaerobic Oxidation of Toluene, Phenol, and *p*-Cresol by the Dissimilatory Iron-Reducing Organism, GS-15. *Applied and environmental microbiology* **56**: 1858-1864.

Lovley DR, Giovannoni SJ, White DC, Champine JE, Phillips EJP, Gorby YA and Goodwin S (1993) *Geobacter metallireducens* gen. nov. sp. nov., a microorganism capable of coupling the complete oxidation of organic compounds to the reduction of iron and other metals. *Archives of Microbiology* **159**: 336-344.

MacDonald IR, Bohrmann G, Escobar E, Abegg F, Blanchon P, Blinova V, Brückmann W, Drews M, Eisenhauer A, Han X, Heeschen K, Meier F, Mortera C, Naehr T, Orcutt B, Bernard B, Brooks J and de Faragó M (2004) Asphalt Volcanism and Chemosynthetic Life in the Campeche Knolls, Gulf of Mexico. *Science* **304**: 999-1002.

MacNaughton SJ, Stephen JR, Venosa AD, Davis GA, Chang Y-J and White DC (1999) Microbial Population Changes during Bioremediation of an Experimental Oil Spill. *Applied and environmental microbiology* **65**: 3566-3574.

Magoon LB, Hudson TL and Cook HE (2001) *AAPG Memoir 75*, Chapter 4: Pimienta-Tamabra (!)--A Giant Supercharged Petroleum System in the Southern Gulf of Mexico, Onshore and Offshore Mexico.

Mahé F, Rognes T, Quince C, de Vargas C and Dunthorn M (2014) Swarm: robust and fast clustering method for amplicon-based studies. *PeerJ* **2**: e593.

Maier T, Förster H-H, Asperger O and Hahn U (2001) Molecular Characterization of the 56-kDa CYP153 from *Acinetobacter* sp. EB104. *Biochemical and Biophysical Research Communications* **286**: 652-658.

Mardanov AV, Ravin NV, Svetlitchnyi VA, Beletsky AV, Miroshnichenko ML, Bonch-Osmolovskaya EA and Skryabin KG (2009) Metabolic Versatility and Indigenous Origin of the Archaeon *Thermococcus sibiricus*, Isolated from a Siberian Oil Reservoir, as Revealed by Genome Analysis. *Applied and environmental microbiology* **75**: 4580-4588.

Mason OU, Hazen TC, Borglin S, Chain PSG, Dubinsky EA, Fortney JL, Han J, Holman H-YN, Hultman J, Lamendella R, Mackelprang R, Malfatti S, Tom LM, Tringe SG, Woyke T, Zhou J, Rubin EM and Jansson JK (2012) Metagenome, metatranscriptome and single-cell sequencing reveal microbial response to Deepwater Horizon oil spill. *The ISME journal* **6**: 1715.

Mattison RG and Harayama S (2001) The predatory soil flagellate *Heteromita globosa* stimulates toluene biodegradation by a *Pseudomonas* sp. *FEMS Microbiology Letters* **194**: 39-45.

Mbadinga SM, Li K-P, Zhou L, Wang L-Y, Yang S-Z, Liu J-F, Gu J-D and Mu B-Z (2012) Analysis of alkane-dependent methanogenic community derived from production water of a high-temperature petroleum reservoir. *Applied Microbiology and Biotechnology* **96**: 531-542.

McGlynn SE, Chadwick GL, Kempes CP and Orphan VJ (2015) Single cell activity reveals direct electron transfer in methanotrophic consortia. *Nature* **526**: 531.

McKay L, Klokman VW, Mendlovitz HP, LaRowe DE, Hoer DR, Albert D, Amend JP and Teske A (2016) Thermal and geochemical influences on microbial biogeography in the hydrothermal sediments of Guaymas Basin, Gulf of California. *Environmental Microbiology Reports* **8**: 150-161.

Meckenstock RU, Annweiler E, Michaelis W, Richnow HH and Schink B (2000) Anaerobic Naphthalene Degradation by a Sulfate-Reducing Enrichment Culture. *Applied and environmental microbiology* **66**: 2743-2747.

Meckenstock RU, Boll M, Mouttaki H, Koelschbach JS, Cunha Tarouco P, Weyrauch P, Dong X and Himmelberg AM (2016) Anaerobic Degradation of Benzene and Polycyclic Aromatic Hydrocarbons. *Journal of Molecular Microbiology and Biotechnology* **26**: 92-118.

Meulepas RJW, Jagersma CG, Khadem AF, Stams AJM and Lens PNL (2010) Effect of methanogenic substrates on anaerobic oxidation of methane and sulfate reduction by an anaerobic methanotrophic enrichment. *Applied Microbiology and Biotechnology* **87**: 1499-1506.

Meyerdierks A, Kube M, Kostadinov I, Teeling H, Glöckner FO, Reinhardt R and Amann R (2010) Metagenome and mRNA expression analyses of anaerobic methanotrophic archaea of the ANME-1 group. *Environmental microbiology* **12**: 422-439.

Michaelis W, Seifert R, Nauhaus K, Treude T, Thiel V, Blumenberg M, Knittel K, Gieseke A, Peterknecht K, Pape T, Boetius A, Amann R, Jørgensen BB, Widdel F, Peckmann J, Pimenov NV, Gulin MB (2002) Microbial Reefs in the Black Sea Fueled by Anaerobic Oxidation of Methane. *Science* **297**: 1013-1015.

Mills HJ, Hodges C, Wilson K, MacDonald IR and Sobecky PA (2003) Microbial diversity in sediments associated with surface-breaching gas hydrate mounds in the Gulf of Mexico. *FEMS Microbiology Ecology* **46**: 39-52.

Milucka J, Ferdelman TG, Polerecky L, Franzke D, Wegener G, Schmid M, Lieberwirth I, Wagner M, Widdel F and Kuypers MMM (2012) Zero-valent sulphur is a key intermediate in marine methane oxidation. *Nature* **491**: 541.

Moran JJ, Beal EJ, Vrentas JM, Orphan VJ, Freeman KH and House CH (2008) Methyl sulfides as intermediates in the anaerobic oxidation of methane. *Environmental microbiology* **10**: 162-173.

Morasch B, Schink B, Tebbe CC and Meckenstock RU (2004) Degradation of *o*-xylene and *m*-xylene by a novel sulfate-reducer belonging to the genus *Desulfotomaculum*. *Archives of Microbiology* **181**: 407-417.

Morrison R and Boyd R (1992) *Organic Chemistry*, 6th. eds., Englewood Cliffs, NJ: Prentice Hall.

Mouttaki H, Johannes J and Meckenstock RU (2012) Identification of naphthalene carboxylase as a prototype for the anaerobic activation of non-substituted aromatic hydrocarbons. *Environmental microbiology* **14**: 2770-2774.

Muller FM (1957) On methane fermentation of higher alkanes. *Antonie van Leeuwenhoek* **23**: 369-384.

Müller U and Buckel W (1995) Activation of (*R*)-2-hydroxyglutaryl-CoA Dehydratase from *Acidaminococcus fermentans*. *European Journal of Biochemistry* **230**: 698-704.

Murrell JC, McDonald IR and Gilbert B (2000) Regulation of expression of methane monooxygenases by copper ions. *Trends in Microbiology* **8**: 221-225.

Murrell JC, Gilbert B and McDonald IR (2000) Molecular biology and regulation of methane monooxygenase. *Archives of Microbiology* **173**: 325-332.

Musat F, Wilkes H, Behrends A, Woebken D and Widdel F (2010) Microbial nitrate-dependent cyclohexane degradation coupled with anaerobic ammonium oxidation. *The ISME journal* **4**: 1290.

Nauhaus K, Boetius A, Krüger M and Widdel F (2002) In vitro demonstration of anaerobic oxidation of methane coupled to sulphate reduction in sediment from a marine gas hydrate area. *Environmental microbiology* **4**: 296-305.

Nauhaus K, Treude T, Boetius A and Krüger M (2005) Environmental regulation of the anaerobic oxidation of methane: a comparison of ANME-I and ANME-II communities. *Environmental microbiology* **7**: 98-106.

Nayak DD, Mahanta N, Mitchell DA and Metcalf WW (2017) Post-translational thioamidation of methyl-coenzyme M reductase, a key enzyme in methanogenic and methanotrophic Archaea. *Elife* **6**: e29218.

Nelson DC, Wirsen CO and Jannasch HW (1989) Characterization of Large, Autotrophic *Beggiatoa* spp. Abundant at Hydrothermal Vents of the Guaymas Basin. *Applied and environmental microbiology* **55**: 2909-2917.

Nhi-Cong LT, Mikolasch A, Klenk H-P and Schauer F (2009) Degradation of the multiple branched alkane 2,6,10,14-tetramethyl-pentadecane (pristane) in *Rhodococcus ruber* and *Mycobacterium neoaurum*. *International Biodeterioration and Biodegradation* **63**: 201-207.

Niemann H and Boetius A (2010) Mud Volcanoes. *Handbook of Hydrocarbon and Lipid Microbiology,* (Timmis KN, eds.), pp. 205-214. Springer, Berlin, Heidelberg.

Niemann H, Lösekann T, de Beer D*,* Elvert M, Nadalig T, Knittel K, Amann R, Sauter EJ, Schlüter M, Klages M, Foucher JP and Boetius A (2006) Novel microbial communities of the Haakon Mosby mud volcano and their role as a methane sink. *Nature* **443**: 854.

Noguchi M, Kurisu F, Kasuga I and Furumai H (2014) Time-Resolved DNA Stable Isotope Probing Links *Desulfobacterales*- and *Coriobacteriaceae*-Related Bacteria to Anaerobic Degradation of Benzene under Methanogenic Conditions. *Microbes and Environments* **29**: 191-199.

Omoregie EO, Mastalerz V, de Lange G*,* Straub KL, Krappler A, Røy H, Stadnitskaia A, Foucher J-P and Boetius A (2008) Biogeochemistry and Community Composition of Iron- and Sulfur-Precipitating Microbial Mats at the Chefren Mud Volcano (Nile Deep Sea Fan, Eastern Mediterranean). *Applied and environmental microbiology* **74**: 3198-3215.

Orcutt BN, Joye SB, Kleindienst S*,* Knittel K, Ramette A, Reitz A, Samarkin V, Treude T and Boetius A (2010) Impact of natural oil and higher hydrocarbons on microbial diversity, distribution, and activity in Gulf of Mexico cold-seep sediments. *Deep Sea Research Part II: Topical Studies in Oceanography* **57**: 2008-2021.

Oremland RS and Capone DG (1988) Use of "Specific" Inhibitors in Biogeochemistry and Microbial Ecology. *Advances in Microbial Ecology,*(Marshall KC, eds.), pp. 285-383. Springer US, Boston, MA.

Orphan VJ, House CH, Hinrichs K-U, McKeegan KD and DeLong EF (2002) Multiple archaeal groups mediate methane oxidation in anoxic cold seep sediments. *Proceedings of the National Academy of Sciences* **99**: 7663-7668.

Orphan VJ, Hinrichs KU, Ussler W*,* Paull CK, Taylor LT, Sylva SP, Hayes JM and Delong EF (2001) Comparative Analysis of Methane-Oxidizing Archaea and Sulfate-Reducing Bacteria in Anoxic Marine Sediments. *Applied and environmental microbiology* **67**: 1922-1934.

Osman OA, Gudasz C and Bertilsson S (2014) Diversity and abundance of aromatic catabolic genes in lake sediments in response to temperature change. *FEMS Microbiology Ecology* **88**: 468-481.

Pachiadaki MG, Kallionaki A, Dählmann A, De Lange GJ and Kormas KA (2011) Diversity and Spatial Distribution of Prokaryotic Communities Along A Sediment Vertical Profile of A Deep-Sea Mud Volcano. *Microbial Ecology* **62**: 655-668.

Pérez-Pantoja D, González B and Pieper DH (2016) Aerobic Degradation of Aromatic Hydrocarbons. *Aerobic Utilization of Hydrocarbons, Oils and Lipids,*(Rojo F, eds.), pp. 1-44. Springer International Publishing, Cham.

Pernthaler A, Pernthaler J and Amann R (2002) Fluorescence In Situ Hybridization and Catalyzed Reporter Deposition for the Identification of Marine Bacteria. *Applied and environmental microbiology* **68**: 3094-3101.

Pernthaler A, Dekas AE, Brown CT, Goffredi SK, Embaye T and Orphan VJ (2008) Diverse syntrophic partnerships from deep-sea methane vents revealed by direct cell capture and metagenomics. *Proceedings of the National Academy of Sciences of the United States of America* **105**: 7052-7057.

Pihl TD, Sharma S and Reeve JN (1994) Growth phase-dependent transcription of the genes that encode the two methyl coenzyme M reductase isoenzymes and N5-methyltetrahydromethanopterin:coenzyme M methyltransferase in *Methanobacterium thermoautotrophicum* delta H. *Journal of Bacteriology* **176**: 6384-6391.

Prior SD and Dalton H (1985) The Effect of Copper Ions on Membrane Content and Methane Monooxygenase Activity in Methanol-grown Cells of *Methylococcus capsulatus* (Bath). *Microbiology* **131**: 155-163.

Pruesse E, Peplies J and Glöckner FO (2012) SINA: Accurate high-throughput multiple sequence alignment of ribosomal RNA genes. *Bioinformatics* **28**: 1823-1829.

Pumphrey GM and Madsen EL (2007) Naphthalene metabolism and growth inhibition by naphthalene in *Polaromonas naphthalenivorans* strain CJ2. *Microbiology* **153**: 3730-3738.

Rabus R and Widdel F (1995) Anaerobic degradation of ethylbenzene and other aromatic hydrocarbons by new denitrifying bacteria. *Archives of Microbiology* **163**: 96-103.

Rabus R and Heider J (1998) Initial reactions of anaerobic metabolism of alkylbenzenes in denitrifying and sulfate-reducing bacteria. *Archives of Microbiology* **170**: 377-384.

Rabus R, Nordhaus R, Ludwig W and Widdel F (1993) Complete oxidation of toluene under strictly anoxic conditions by a new sulfate-reducing bacterium. *Applied and environmental microbiology* **59**: 1444-1451.

Rabus R, Kube M, Beck A, Widdel F and Reinhardt R (2002) Genes involved in the anaerobic degradation of ethylbenzene in a denitrifying bacterium, strain EbN1. *Archives of Microbiology* **178**: 506-516.

Rabus R, Boll M, Heider J*, et al.* (2016) Anaerobic Microbial Degradation of Hydrocarbons: From Enzymatic Reactions to the Environment. *Journal of Molecular Microbiology and Biotechnology* **26**: 5-28.

Raghoebarsing AA, Pol A, van de Pas-Schoonen KT*,* Smolders AJP, Ettwig KF, Rijpstra WIC, Schouten S, Damsté JSS, Op den Camp HJM, Jetten MSM and Strous M (2006) A microbial consortium couples anaerobic methane oxidation to denitrification. *Nature* **440**: 918.

Reeburgh WS (1980) Anaerobic methane oxidation: Rate depth distributions in Skan Bay sediments. *Earth and Planetary Science Letters* **47**: 345-352.

Reeburgh WS (2007) Oceanic Methane Biogeochemistry. *Chemical Reviews* **107**: 486-513.

Regnier P, Dale AW, Arndt S, LaRowe DE, Mogollón J and Van Cappellen P (2011) Quantitative analysis of anaerobic oxidation of methane (AOM) in marine sediments: A modeling perspective. *Earth-Science Reviews* **106**: 105-130.

Rios-Hernandez LA, Gieg LM and Suflita JM (2003) Biodegradation of an Alicyclic Hydrocarbon by a Sulfate-Reducing Enrichment from a Gas Condensate-Contaminated Aquifer. *Applied and environmental microbiology* **69**: 434-443.

Rockne KJ, Chee-Sanford JC, Sanford RA, Hedlund BP, Staley JT and Strand SE (2000) Anaerobic Naphthalene Degradation by Microbial Pure Cultures under Nitrate-Reducing Conditions. *Applied and environmental microbiology* **66**: 1595-1601.

Rojo F (2010) Enzymes for aerobic degradation of alkanes. *Handbook of hydrocarbon and lipid microbiology*, pp. 781-797. Springer.

Röling WFM, Couto de Brito IR, Swannell RPJ and Head IM (2004) Response of Archaeal Communities in Beach Sediments to Spilled Oil and Bioremediation. *Applied and environmental microbiology* **70**: 2614-2620.

Röling WFM, Milner MG, Jones DM, Lee K, Daniel F, Swannell RJP and Head IM (2002) Robust Hydrocarbon Degradation and Dynamics of Bacterial Communities during Nutrient-Enhanced Oil Spill Bioremediation. *Applied and environmental microbiology* **68**: 5537-5548.

Röling WFM, Milner MG, Jones DM, Fratepietro F, Swannell RPJ, Daniel F and Head IM (2004) Bacterial Community Dynamics and Hydrocarbon Degradation during a Field-Scale Evaluation of Bioremediation on a Mudflat Beach Contaminated with Buried Oil. *Applied and environmental microbiology* **70**: 2603-2613.

Rontani J-F, Mouzdahir A, Michotey V and Bonin P (2002) Aerobic and anaerobic metabolism of squalene by a denitrifying bacterium isolated from marine sediment. *Archives of Microbiology* **178**: 279-287.

Rubin-Blum M, Antony CP, Borowski C*,* Sayavedra L, Pape T, Sahling H, Bohrmann G, Kleiner M, Redmond MC, Valentine DL and Dubilier N (2017) Short-chain alkanes fuel mussel and sponge *Cycloclasticus* symbionts from deep-sea gas and oil seeps. *Nature Microbiology* **2**: 17093.

Ruff SE, Biddle JF, Teske AP, Knittel K, Boetius A and Ramette A (2015) Global dispersion and local diversification of the methane seep microbiome. *Proceedings of the National Academy of Sciences* **112**: 4015-4020.

Sahling H, Borowski C, Escobar-Briones E*,* Gaytán-Caballero A, Hsu C-W, Loher M, MacDonald I, Marcon Y, Pape T and Römer M (2016) Massive asphalt deposits, oil seepage, and gas venting support abundant chemosynthetic communities at the Campeche Knolls, southern Gulf of Mexico. *Biogeosciences* **13**: 4491-4512.

Sakai N, Kurisu F, Yagi O, Nakajima F and Yamamoto K (2009) Identification of putative benzene-degrading bacteria in methanogenic enrichment cultures. *Journal of Bioscience and Bioengineering* **108**: 501-507.

Sakai Y, Maeng HJ, Tani Y and Kato N (1994) Use of Long-chain *n*-Alkanes (C_{13}-C_{44}) by an Isolate, *Acinetobacter* sp. M-1. *Bioscience, Biotechnology, and Biochemistry* **58**: 2128-2130.

Sakai Y, Maeng JH, Kubota S, Tani A, Tani Y and Kato N (1996) A non-conventional dissimilation pathway for long chain *n*-alkanes in *Acinetobacter* sp. M-1 that starts with a dioxygenase reaction. *Journal of Fermentation and Bioengineering* **81**: 286-291.

Salinero KK, Keller K, Feil WS, Feil H, Trong S, Di Bartolo G and Lapidus A (2009) Metabolic analysis of the soil microbe *Dechloromonas aromatica* str. RCB: indications of a surprisingly complex life-style and cryptic anaerobic pathways for aromatic degradation. *BMC Genomics* **10**: 351.

Scheller S, Goenrich M, Thauer RK and Jaun B (2013) Methyl-Coenzyme M Reductase from Methanogenic Archaea: Isotope Effects on Label Exchange and Ethane Formation with the Homologous Substrate Ethyl-Coenzyme M. *Journal of the American Chemical Society* **135**: 14985-14995.

Scheller S, Yu H, Chadwick GL, McGlynn SE and Orphan VJ (2016) Artificial electron acceptors decouple archaeal methane oxidation from sulfate reduction. *Science* **351**: 703-707.

Schink B (1985) Degradation of unsaturated hydrocarbons by methanogenic enrichment cultures. *FEMS Microbiology Letters* **31**: 69-77.

Schink B (1985) Fermentation of acetylene by an obligate anaerobe, *Pelobacter acetylenicus* sp. nov. *Archives of Microbiology* **142**: 295-301.

Schirmer M, Ijaz UZ, D'Amore R, Hall N, Sloan WT and Quince C (2015) Insight into biases and sequencing errors for amplicon sequencing with the Illumina MiSeq platform. *Nucleic Acids Research* **43**: e37-e37.

Schmitz C, Goebel I, Wagner S, Vomberg A and Klinner U (2000) Competition between *n*-alkane-assimilating yeasts and bacteria during colonization of sandy soil microcosms. *Applied Microbiology and Biotechnology* **54**: 126-132.

Schubert CJ, Durisch-Kaiser E, Holzner CP, Klauser L, Wehrli B, Schmale O, Greinert J, McGinnis DF, De Batist M and Kipfer R (2006) Methanotrophic microbial communities associated with bubble plumes above gas seeps in the Black Sea. *Geochemistry, Geophysics, Geosystems* **7**.

Schulze-Makuch D, Haque S, Antonio MRdS, Ali D, Hosein R, Song YC, Yang J, Zaikova E, Beckles DM, Guinan E, Lehto HJ and Hallam SJ (2011) Microbial Life in a Liquid Asphalt Desert. *Astrobiology* **11**: 241-258.

Schweiger G, Dutscho R and Buckel W (1987) Purification of 2-hydroxyglutaryl-CoA dehydratase from *Acidaminococcus fermentans*. *European Journal of Biochemistry* **169**: 441-448.

Selesi D, Jehmlich N, von Bergen M, Schmidt F, Rattei T, Tischler P, Lueders T and Meckenstock RU (2010) Combined Genomic and Proteomic Approaches Identify Gene Clusters Involved in Anaerobic 2-Methylnaphthalene Degradation in the Sulfate-Reducing Enrichment Culture N47. *Journal of Bacteriology* **192**: 295-306.

Shima S, Krueger M, Weinert T, Demmer U, Kahnt J, Thauer RK and Ermler U (2011) Structure of a methyl-coenzyme M reductase from Black Sea mats that oxidize methane anaerobically. *Nature* **481**: 98.

Sibuet M and Olu K (1998) Biogeography, biodiversity and fluid dependence of deep-sea cold-seep communities at active and passive margins. *Deep Sea Research Part II: Topical Studies in Oceanography* **45**: 517-567.

Siliakus MF, van der Oost J and Kengen SWM (2017) Adaptations of archaeal and bacterial membranes to variations in temperature, pH and pressure. *Extremophiles* **21**: 651-670.

Simoneit BRT and Lonsdale PF (1982) Hydrothermal petroleum in mineralized mounds at the seabed of Guaymas Basin. *Nature* **295**: 198.

Simoneit BRT, Kawka OE and Brault M (1988) Origin of gases and condensates in the Guaymas Basin hydrothermal system (Gulf of California). *Chemical Geology* **71**: 169-182.

Simoneit BRT, Mazurek MA, Brenner S, Crisp PT and Kaplan IR (1979) Organic geochemistry of recent sediments from Guaymas Basin, Gulf of California. *Deep Sea Research Part A. Oceanographic Research Papers* **26**: 879-891.

Smith TJ (2009) Monooxygenases, bacterial: Oxidation of alkenes. *Encyclopedia of Industrial Biotechnology: Bioprocess, Bioseparation, and Cell Technology* 1-13.

So CM and Young LY (1999) Isolation and Characterization of a Sulfate-Reducing Bacterium That Anaerobically Degrades Alkanes. *Applied and environmental microbiology* **65**: 2969-2976.

So CM, Phelps CD and Young LY (2003) Anaerobic Transformation of Alkanes to Fatty Acids by a Sulfate-Reducing Bacterium, Strain Hxd3. *Applied and environmental microbiology* **69**: 3892-3900.

Söhngen N (1913) Benzin, petroleum, paraffinöl und paraffin als kohlenstoff-und energiequelle für mikroben. *Zentralblatt für Bakteriologie, Parasitenkunde und Infektionskrankheiten* **37**: 595-609.

Stagars MH, Ruff SE, Amann R and Knittel K (2016) High Diversity of Anaerobic Alkane-Degrading Microbial Communities in Marine Seep Sediments Based on (1-methylalkyl)succinate Synthase Genes. *Frontiers in microbiology* **6**.

Stagars MH, Mishra S, Treude T, Amann R and Knittel K (2017) Microbial Community Response to Simulated Petroleum Seepage in Caspian Sea Sediments. *Frontiers in microbiology* **8**.

Stahl DA and Amann R (1991) Development and application of nucleic acid probes in bacterial systematics. *Nucleic acid techniques in bacterial systematics,* Stackebrandt E and Goodfellow M, eds., pp. 205-248. John Wiley and Sons Ltd., Chichester, England.

Stanley SH, Prior SD, Leak DJ and Dalton H (1983) Copper stress underlies the fundamental change in intracellular location of methane mono-oxygenase in methane-oxidizing organisms: Studies in batch and continuous cultures. *Biotechnology Letters* **5**: 487-492.

Steigerwald V, Hennigan A, Pihl T and Reeve J (1993) Genes encoding the methyl viologen-reducing hydrogenase, polyferredoxin and methyl coenzyme M reductase II are adjacent in the genomes of

Methanobacterium thermoautotrophicum and *Methanothermus fervidus*. *Microbial growth on C* **1**: 181-191.

Stokke R, Roalkvam I, Lanzen A, Haflidason H and Steen IH (2012) Integrated metagenomic and metaproteomic analyses of an ANME-1-dominated community in marine cold seep sediments. *Environmental microbiology* **14**: 1333-1346.

Story S, Parker S, Hayasaka S, Riley M and Kline E (2001) Convergent and divergent points in catabolic pathways involved in utilization of fluoranthene, naphthalene, anthracene, and phenanthrene by *Sphingomonas paucimobilis* var. EPA505. *Journal of Industrial Microbiology and Biotechnology* **26**: 369-382.

Suess E (2010) Marine Cold Seeps. *Handbook of Hydrocarbon and Lipid Microbiology,* Timmis KN, eds., pp. 185-203. Springer, Berlin, Heidelberg.

Summers ZM, Fogarty HE, Leang C, Franks AE, Malvankar NS and Lovley DR (2010) Direct Exchange of Electrons Within Aggregates of an Evolved Syntrophic Coculture of Anaerobic Bacteria. *Science* **330**: 1413-1415.

Syutsubo K, Kishira H and Harayama S (2001) Development of specific oligonucleotide probes for the identification and in situ detection of hydrocarbon-degrading *Alcanivorax* strains. *Environmental microbiology* **3**: 371-379.

Tapilatu YH, Grossi V, Acquaviva M, Militon C, Bertrand J-C and Cuny P (2010) Isolation of hydrocarbon-degrading extremely halophilic archaea from an uncontaminated hypersaline pond (Camargue, France). *Extremophiles* **14**: 225-231.

Teske A, Hinrichs K-U, Edgcomb V*,* de Vera Gómez A, Kysela D, Sylva SP, Sogin ML and Jannasch HW (2002) Microbial Diversity of Hydrothermal Sediments in the Guaymas Basin: Evidence for Anaerobic Methanotrophic Communities. *Applied and environmental microbiology* **68**: 1994-2007.

Thauer RK and Shima S (2008) Methane as Fuel for Anaerobic Microorganisms. *Annals of the New York Academy of Sciences* **1125**: 158-170.

Throne-Holst M, Wentzel A, Ellingsen TE, Kotlar H-K and Zotchev SB (2007) Identification of Novel Genes Involved in Long-Chain *n*-Alkane Degradation by *Acinetobacter* sp. Strain DSM 17874. *Applied and environmental microbiology* **73**: 3327-3332.

Timmers PHA, Suarez-Zuluaga DA, van Rossem M, Diender M, Stams AJM and Plugge CM (2015) Anaerobic oxidation of methane associated with sulfate reduction in a natural freshwater gas source. *The ISME journal* **10**: 1400.

Tissot BP and Welte DH (1984) *Petroleum Formation and Occurrence*. Springer, Berlin.

Toda H, Imae R, Komio T and Itoh N (2012) Expression and characterization of styrene monooxygenases of *Rhodococcus* sp. ST-5 and ST-10 for synthesizing enantiopure (*S*)-epoxides. *Applied Microbiology and Biotechnology* **96**: 407-418.

Townsend GT, Prince RC and Suflita JM (2003) Anaerobic Oxidation of Crude Oil Hydrocarbons by the Resident Microorganisms of a Contaminated Anoxic Aquifer. *Environmental Science and Technology* **37**: 5213-5218.

Trapnell C, Williams BA, Pertea G, Mortazavi A, Kwan G, van Baren MJ, Salzberg SL, Wold BK and Pachter L (2010) Transcript assembly and quantification by RNA-Seq reveals unannotated transcripts and isoform switching during cell differentiation. *Nature biotechnology* **28**: 511-515.

Valentine DL and Reeburgh WS (2000) New perspectives on anaerobic methane oxidation. *Environmental microbiology* **2**: 477-484.

van Beilen JB, Kingma J and Witholt B (1994) Substrate specificity of the alkane hydroxylase system of *Pseudomonas oleovorans* GPo1. *Enzyme and Microbial Technology* **16**: 904-911.

van Beilen JB, Wubbolts MG and Witholt B (1994) Genetics of alkane oxidation by *Pseudomonas oleovorans*. *Biodegradation* **5**: 161-174.

Van Beilen JB, Marín MM, Smits THM, Röthlisberger M, Franchini AG, Witholt B and Rojo F (2004) Characterization of two alkane hydroxylase genes from the marine hydrocarbonoclastic bacterium *Alcanivorax borkumensis*. *Environmental microbiology* **6**: 264-273.

van de Vossenberg JLCM, Driessen AJM and Konings WN (1998) The essence of being extremophilic: the role of the unique archaeal membrane lipids. *Extremophiles* **2**: 163-170.

Van Dover C (2000) *The ecology of deep-sea hydrothermal vents*. Princeton University Press.

Van Hamme JD, Singh A and Ward OP (2003) Recent Advances in Petroleum Microbiology. *Microbiology and Molecular Biology Reviews* **67**: 503-549.

Vanwonterghem I, Evans PN, Parks DH, Jensen PD, Woodcroft BJ, Hugenholtz P and Tyson GW (2016) Methylotrophic methanogenesis discovered in the archaeal phylum *Verstraetearchaeota*. *Nature Microbiology* **1**: 16170.

Villatoro-Monzón WR, Morales-Ibarria MG, Velázquez EK, Ramírez-Saad H and Razo-Flores E (2008) Benzene Biodegradation under Anaerobic Conditions Coupled with Metal Oxides Reduction. *Water, Air, and Soil Pollution* **192**: 165-172.

von Netzer F, Pilloni G, Kleindienst S, Krüger M, Knittel K, Gründger F and Lueders T (2013) Enhanced Gene Detection Assays for Fumarate-Adding Enzymes Allow Uncovering of Anaerobic Hydrocarbon Degraders in Terrestrial and Marine Systems. *Applied and environmental microbiology* **79**: 543-552.

Vorholt JA, Hafenbradl D, Stetter KO and Thauer RK (1997) Pathways of autotrophic CO_2 fixation and of dissimilatory nitrate reduction to N_2O in *Ferroglobus placidus*. *Archives of Microbiology* **167**: 19-23.

Wagner T, Wegner C-E, Kahnt J, Ermler U and Shima S (2017) Phylogenetic and structural comparisons of the three types of methyl-coenzyme M reductase from *Methanococcales* and *Methanobacteriales*. *Journal of Bacteriology*.

Wang F-P, Zhang Y, Chen Y, He Y, Qi L, Hinrichs K-U, Zhang X-X, Xiao X and Boon N (2013) Methanotrophic archaea possessing diverging methane-oxidizing and electron-transporting pathways. *The ISME journal* **8**: 1069.

Wang L, Tang Y, Wang S, Liu R-L, Liu M-Z, Zhang Y, Liang F-L and Feng L (2006) Isolation and characterization of a novel thermophilic *Bacillus* strain degrading long-chain *n*-alkanes. *Extremophiles* **10**: 347.

Watkinson RJ and Morgan P (1991) Physiology of aliphatic hydrocarbon-degrading microorganisms. *Physiology of Biodegradative Microorganisms,*Ratledge C, eds., pp. 79-92. Springer Netherlands, Dordrecht.

Wegener G, Krukenberg V, Riedel D, Tegetmeyer HE and Boetius A (2015) Intercellular wiring enables electron transfer between methanotrophic archaea and bacteria. *Nature* **526**: 587.

Wegener G, Krukenberg V, Ruff SE, Kellermann MY and Knittel K (2016) Metabolic capabilities of microorganisms involved in and associated with the anaerobic oxidation of methane. *Frontiers in microbiology* **7**: 46.

Widdel F and Bak F (1992) Gram-Negative Mesophilic Sulfate-Reducing Bacteria. *The Prokaryotes: A Handbook on the Biology of Bacteria: Ecophysiology, Isolation, Identification, Applications,* Balows A, Trüper HG, Dworkin M, Harder W and Schleifer K-H, eds., pp. 3352-3378. Springer New York.

Widdel F and Rabus R (2001) Anaerobic biodegradation of saturated and aromatic hydrocarbons. *Current Opinion in Biotechnology* **12**: 259-276.

Widdel F, Knittel K and Galushko A (2010) Anaerobic Hydrocarbon-Degrading Microorganisms: An Overview. *Handbook of Hydrocarbon and Lipid Microbiology,* Timmis KN, eds., pp. 1997-2021. Springer, Berlin, Heidelberg.

Wilkes H and Schwarzbauer J (2010) Hydrocarbons: An Introduction to Structure, Physico-Chemical Properties and Natural Occurrence. *Handbook of Hydrocarbon and Lipid Microbiology,* Timmis KN, eds., pp. 1-48. Springer, Berlin, Heidelberg.

Wilkes H, Buckel W, Golding BT and Rabus R (2016) Metabolism of Hydrocarbons in *n*-Alkane-Utilizing Anaerobic Bacteria. *Journal of Molecular Microbiology and Biotechnology* **26**: 138-151.

Wilkes H, Rabus R, Fischer T, Armstroff A, Behrends A and Widdel F (2002) Anaerobic degradation of *n*-hexane in a denitrifying bacterium: Further degradation of the initial intermediate (1-methylpentyl)succinate via C-skeleton rearrangement. *Archives of Microbiology* **177**: 235-243.

Wilson BH, Smith GB and Rees JF (1986) Biotransformations of selected alkylbenzenes and halogenated aliphatic hydrocarbons in methanogenic aquifer material: a microcosm study. *Environmental Science and Technology* **20**: 997-1002.

Winderl C, Schaefer S and Lueders T (2007) Detection of anaerobic toluene and hydrocarbon degraders in contaminated aquifers using benzylsuccinate synthase (*bssA*) genes as a functional marker. *Environmental microbiology* **9**: 1035-1046.

Woese CR (1987) Bacterial evolution. *Microbiological Reviews* **51**: 221-271.

Wongnate T, Sliwa D, Ginovska B, Smith D, Wolf MW, Lehnert N, Raugei S and Ragsdale SW (2016) The radical mechanism of biological methane synthesis by methyl-coenzyme M reductase. *Science* **352**: 953-958.

World Energy Council (2016) *World Energy Resources 2016*

Xiang X, Wang R, Wang H, Gong L, Man B and Xu Y (2017) Distribution of Bathyarchaeota Communities Across Different Terrestrial Settings and Their Potential Ecological Functions. *Scientific Reports* **7**: 45028.

Yakimov MM, Timmis KN and Golyshin PN (2007) Obligate oil-degrading marine bacteria. *Current Opinion in Biotechnology* **18**: 257-266.

Yarza P, Yilmaz P, Pruesse E, Glöckner FO, Ludwig W, Schleifer K-H, Whitman WB, Euzéby J, Amann R and Rosselló-Móra R (2014) Uniting the classification of cultured and uncultured bacteria and archaea using 16S rRNA gene sequences. *Nature Reviews Microbiology* **12**: 635.

Zedelius J, Rabus R, Grundmann O, Werner I, Brodkorb D, Schreiber F, Ehrenreich P, Behrends A, Wilkes H, Kube M, Reinhardt Richard and Widdel F (2011) Alkane degradation under anoxic conditions by a nitrate-reducing bacterium with possible involvement of the electron acceptor in substrate activation. *Environmental Microbiology Reports* **3**: 125-135.

Zengler K, Heider J, Rosselló-Mora R and Widdel F (1999) Phototrophic utilization of toluene under anoxic conditions by a new strain of *Blastochloris sulfoviridis*. *Archives of Microbiology* **172**: 204-212.

Zengler K, Richnow HH, Rosselló-Mora R, Michaelis W and Widdel F (1999) Methane formation from long-chain alkanes by anaerobic microorganisms. *Nature* **401**: 266.

Zhang T, Tremblay P-L, Chaurasia AK, Smith JA, Bain TS and Lovley DR (2013) Anaerobic benzene oxidation via phenol in *Geobacter metallireducens*. *Applied and environmental microbiology*.

Zhang X and Young LY (1997) Carboxylation as an initial reaction in the anaerobic metabolism of naphthalene and phenanthrene by sulfidogenic consortia. *Applied and environmental microbiology* **63**: 4759-4764.

Zhou Z, Pan J, Wang F, Gu J-D and Li M (2018) Bathyarchaeota: globally distributed metabolic generalists in anoxic environments. *FEMS Microbiology Reviews* **42**: 639-655.

Zobell CE (1946) Action of microorganims on hydrocarbons. *Bacteriological Reviews* **10**: 1-49.

Zylstra GJ and Kim E (1997) Aromatic hydrocarbon degradation by *Sphingomonas yanoikuyae* B1. *Journal of Industrial Microbiology and Biotechnology* **19**: 408-414.

Acknowledgements

This thesis would have been impossible without the support and help from many people. Thank you all!

Many thanks to Prof. Dr. Antje Boetius for giving me this amazing opportunity and the support and comprehension during all my PhD activities. I have learned a lot from your way to look into “the big picture”.

Many thanks to all the members of my defense committee: Prof. Dr. Ida Helene Steen for being my second reviewer, Prof. Dr. Kai-Uwe Hinrichs, Dr. Tristan Wagner, Dr. Gunter Wegener and Marion Jespersen.

My greatest thanks to Gunter. It was been a huge privilege to be under your supervision. Thanks for convincing me to stay, for supporting me during all these years in all my scientific and non-scientific PhD life and for showing always this amazing and inspiring interest and desire for Science. Your passion for our topic is truly a model for any researcher.

Lots of thanks to all the teachers, supervisors and tutors that I had during my PhD, especially to Viola Krukenberg and Dimitri Meier. Thanks Viola for being always available, helpful and with a great smile. I have learned so much from you. Dimitri, thank you, for introducing me in the exciting world of metagenomics.

Special thanks for all collaborators during this time. Thanks to Halina Tegetmeyer for her impressive sequencing skills, which have contributed significantly to this PhD. Many thanks to Pier Luigi Buttigieg for his time and patience; talking with you gave me always new insights. I am also really grateful to other collaborators, especially to Florin Musat for our work in Butane-50. Great thanks to Prof. Dr. Friedrich Widdel for the amazing discussions in our Butane-50 paper. It is a pleasure to have collaborated with you. I am really greatful with Prof. Dr. Victoria Orphan for giving me the opportunity to work in her lab. Special thanks to Hank Yu, Grayson Chadwick and Elizabeth Trembath-Reichert for the help durint my stay in California. This PhD has opened new questions and therefore I am also really thankful with Tristan Wagner and Seigo Shima, you have discovered me a totally new tridimensional world. I am also really happy with the fruitful conversations with Prof. Dr. Steven Mansoorabadi. Your biochemistry knowledge left a huge impression on me.

Many thanks also to my Katrin Knittel and Pierre Offre for being my part of my thesis committees. Thanks Katrin for going with us in this hydrocarbon trip and thanks Pierre for all the advices concerning genomics.

This work would have impossible without the support and aid of many technicians. Thanks to all TAs from the Habitat group, especially to Susanne Menger. Thank you for all the care in the lab and being our “grandma” at work. Also many thanks to Ramona Appel for her support and advice in the Microbiology lab. I am also in debt with Mirja Meiners, Jakob Barz, Jana Bäger and Erika Weiz. Your work was a great help for my PhD.

Special thanks to Matthew Schechter, David Benito Merino, Josephine Rapp and Cedric Hahn for cheking my thesis. Ich bin auch ganz dankbar meiner Deutsch Lehrerin Annekatrin Gudat für ihre Korrektur meiner Zussamenfassung. Diesen Jahren habe ich so viel von Ihnen gelernt! Vielen Dank!

I am really thankful with my three lab rotation students: Iva Soža, David Benito Merino and Mara Maeke. It was a pleasure to have you during my PhD time.

Also great thanks to the Marmic program and to Christiane Glöckner for being always there to answer any question. Thanks to many MPI colleagues for the scientific and the life support: Burak, Miguel, Antonio, Nadine, Clara, Karen, the Gretas, Laura, Bram…

I am tremendously grateful for being part of the Habitat group. Thank all Habitat members (past and present) for making this group such a nice working environment: Mar, Massi, Christina, Mari, Mirja, Susanne, Pier, Pierre, Verena, Ralph, Josi (for the good and the “shade” moments)…. Great thanks to all my office mates: thanks to Gerd and Katy for making such a funny Christmas office with little hands; thanks Eddie for doing this PhD journey with me including an Arctic stop; thanks Claudia for feeding me during the writing period. Thanks also to my colleague in the topic, Cedric, you were always available and willing to help.

I am privileged because I had the opportunity to be in the PhDnet Steering Group during one year of my PhD. Thanks Leo, Jana, Lisa, Teresa and Gabriel for that great year and the amazing team work!

My PhD in Bremen would have not been possible without the support and company of great friends during these years. Thanks to my Marmic class, especially to Rahel (I loved our drama nights), Jen and Veronika. I don’t have words to thank my Bremen family who was always there during this time: Yannis for being always to party; Stan for creating a home in Bremen with candles and second-hand objects; Ivan for your scientific company during these years, we missed you a lot; Agustin for sharing those aerobics movements and many other student representatives stories; Ana for being my spiritual support and recommending so many movies, and Chema for every moment from the first coffee in Wohnzimmer to the last cake in Ana’s house.

Finally, thanks to my family. Gracias Juan y Pablo por ser mis hermanos mayores y mostrando lo orgullosos que estáis de mi. En la distancia me ayudáis a dar lo mejor. Muchísimas gracias papá y mamá: gracias por estar siempre cada domingo, gracias por cada abrazo en el aeropuerto. Ver vuestra sonrisa en cada viaje ha sido una de las mayores fuerzas en todos estos años.

Appendix

Additional co-author contributions

Diversity and metabolism of JTB255 bacteria (Gammaproteobacteria), global members of deep-sea sediment communities

Katy Hoffmann[1,2], Christina Bienhold[1,2], Pier Luigi Buttigieg[1,2], Katrin Knittel[3], Rafael Laso-Pérez[1], Josephine Z. Rapp[1,2], Antje Boetius[1,2,4], Pierre Offre[1,5]

[1]HGF-MPG Joint Research Group for Deep Sea Ecology and Technology, Max Planck Institute for Marine Microbiology, Bremen, Germany

[2]HGF-MPG Joint Research Group for Deep Sea Ecology and Technology, Alfred-Wegener-Institut Helmholtz-Zentrum für Polar- und Meeresforschung, Bremerhaven, Germany

[3]Department of Molecular Ecology, Max Planck Institute for Marine Microbiology, Bremen, Germany,

[4]MARUM University Bremen, Germany

[5]NIOZ Royal Netherlands Institute for Sea Research, Department of Marine Microbiology and Biogeochemistry, and Utrecht University, Den Burg, The Netherlands

Under review in ISME

Abstract

Surveys of 16S rRNA gene sequences derived from marine sediments have indicated that a widely distributed group of Gammaproteobacteria, named 'JTB255 Marine Benthic Group', accounts for 1-22% of the retrieved sequences. Despite their ubiquity in seafloor communities, little is known about their distribution and specific ecological niches in the deep sea, which constitutes the largest biome globally. Here, we characterized the phylogeny, environmental distribution patterns, abundance and metabolic potential of JTB255 bacteria with a focus on representatives from the deep sea. From a phylogenetic analysis of publicly available 16S rRNA gene sequences (≥1400 bp, n=994) we identified specific JTB255 lineages with greater prevalence in the deep sea than in coastal environments, a pattern corroborated by the distribution of 16S oligotypes recovered from 34 globally distributed sediment samples. Cell counts revealed that JTB255 bacteria accounted for 5 ± 2% of all microbial cells in deep-sea surface sediments at 23 globally distributed sites. Comparative analyses of a genome, metagenome bins and single-cell genomes suggested that the investigated clades of JTB255 bacteria are likely to grow on proteinaceous matter, potentially derived from detrital cell membranes, cell walls and other organic remnants in marine sediments.

Scientific cruises

2017 R/V Polarstern, PS107, HAUSGARTEN, Fram Strait, Arctic Ocean, Alfred Wegener Institute (Germany, 24/07/2017-18/08/2017)

Conferences

July-August 2016, GRS and GRC – Molecular Basis of C1 Metabolism, Waterville Valley, USA. "Novel archaeal-bacterial consortia use methanogenesis-type enzymes for butane oxidation" (oral presentation and poster)

May 2017, It MaTer(s) – 1st PhD Conference on Environmental Microbiology, Marburg, Germany. "Anaerobic degradation of propane and butane in archaeal-bacterial consortia" (oral presentation)

Sep. 2017, SAME15 , Zagreb, Croatia. "Novel archaeal-bacterial consortia use methanogenesis-type enzymes for butane oxidation" (poster)

July 2018, It MaTer(s) - 2nd PhD Conference on Environmental Microbiology, Bremen, Germany. "Genomic insights into archaea of the D-C06 clade" (oral presentation)

July-August 2018, GRS and GRC – Molecular Basis of C1 Metabolism, Newry, USA. "Genomic insights of the D-C06 clade: a potential hydrocarbon degrader with a methanogenesis pathway" (poster). Leader for panel discussion in "Mentorship Component: Beyond PhD: Scientific Career Opportunities"

August 2018, ISME17, Leipzig, Germany. "Abundant, novel, putative hydrocarbon-degrading archaea inhabit the asphalt volcanoes of the Southern Gulf of Mexico" (poster)

Versicherung an Eides Statt / *Affirmation in lieu of an oath*

gem. § 5 Abs. 5 der Promotionsordnung vom 18.06.2018 /
according to § 5 (5) of the Doctoral Degree Rules and Regulations of 18 June, 2018

Ich / I, _____
(Vorname / First *Name*, Name / *Name*, Anschrift / *Address*, ggf. Matr.-Nr. / *student ID no., if applicable)*

versichere an Eides Statt durch meine Unterschrift, dass ich die vorliegende Dissertation selbständig und ohne fremde Hilfe angefertigt und alle Stellen, die ich wörtlich dem Sinne nach aus Veröffentlichungen entnommen habe, als solche kenntlich gemacht habe, mich auch keiner anderen als der angegebenen Literatur oder sonstiger Hilfsmittel bedient habe und die zu Prüfungszwecken beigelegte elektronische Version (PDF) der Dissertation mit der abgegebenen gedruckten Version identisch ist. / *With my signature I affirm in lieu of an oath that I prepared the submitted dissertation independently and without illicit assistance from third parties that I appropriately referenced any text or content from other sources that I used only literature and resources listed in the dissertation, and that the electronic (PDF) and printed versions of the dissertation are identical.*

Ich versichere an Eides Statt, dass ich die vorgenannten Angaben nach bestem Wissen und Gewissen gemacht habe und dass die Angaben der Wahrheit entsprechen und ich nichts verschwiegen habe*. / I affirm in lieu of an oath that the information provided herein to the best of my knowledge is true and complete.*

Die Strafbarkeit einer falschen eidesstattlichen Versicherung ist mir bekannt, namentlich die Strafandrohung gemäß § 156 StGB bis zu drei Jahren Freiheitsstrafe oder Geldstrafe bei vorsätzlicher Begehung der Tat bzw. gemäß § 161 Abs. 1 StGB bis zu einem Jahr Freiheitsstrafe oder Geldstrafe bei fahrlässiger Begehung. / *I am aware that a false affidavit is a criminal offence which is punishable by law in accordance with § 156 of the German Criminal Code (StGB) with up to three years imprisonment or a fine in case of intention, or in accordance with § 161 (1) of the German Criminal Code with up to one year imprisonment or a fine in case of negligence.*

_____ _____
Ort / *Place*, Datum / *Date* Unterschrift / *Signature*

Name / Name: _____Datum / Date: _____

Anschrift / Address: _____

Erklärung gem. § 4 Abs. 1 Nr. 3 und 4
der Promotionsordnung vom 18.06.2018 /
Statement according to § 4 (1) no. 3 and 4
of the Doctoral Degree Rules and Regulations of 18.06.2018

Ich erkläre, dass ich mich weder einem Promotionsverfahren unterzogen noch ein solches beantragt habe. /
I affirm that I did not undergo a doctoral degree granting procedure, nor did I apply for the examination procedure elsewhere.

Mit einer Überprüfung der Dissertation mit qualifizierter Software zur Untersuchung von Plagiatsvorwürfen bin ich einverstanden. /
I accept scanning of the doctoral thesis with appropriate software for the detection of plagiarism.

_____

(Unterschrift Doktorand/in / Signature PhD student)